JPL D-33509

Earth Observing System (EOS)

Aura Microwave Limb Sounder (MLS)

Version 3.3 Level 2 data quality and description document.

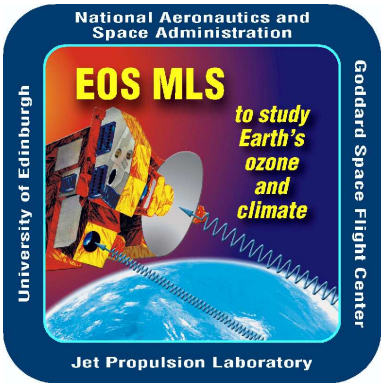

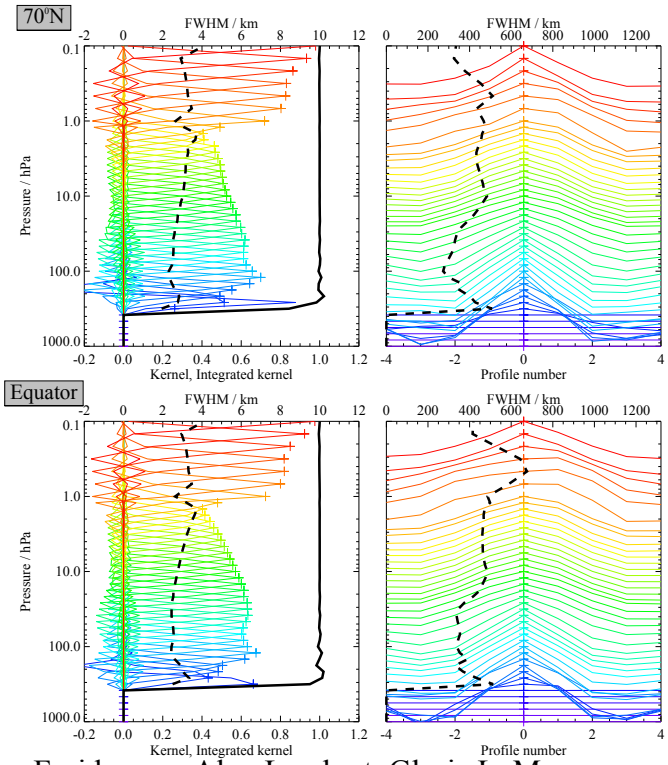

Nathaniel J. Livesey, William G. Read, Lucien Froidevaux, Alyn Lambert, Gloria L. Manney, Hugh C. Pumphrey, Michelle L. Santee, Michael J. Schwartz, Shuhui Wang, Richard E. Cofeld, David T. Cuddy, Ryan A Fuller, Robert F. Jarnot, Jonathan H. Jiang, Brian W. Knosp, Paul C. Stek, Paul A. Wagner, and Dong L. Wu.

Version 3.3x-1.0
January 18, 2011

Jet Propulsion Laboratory
California Institute of Technology
Pasadena, California, 91109-8099

Where to find answers to key questions

This document serves two purposes. Firstly, to summarize the quality of version 3.3 (v3.3) EOS MLS Level 2 data. Secondly, to convey important information on how to read and interpret the data to the scientific community.

The MLS science team strongly encourages users of MLS data to thoroughly read this document. Chapter 1 describes essential general information for all users. Chapter 2 is considered background material that may be of interest to data users. Chapter 3 discusses individual MLS data products in detail.

For convenience, this page provides information on how to quickly ascertain answers to anticipated key questions.

Where do I get v3.3 MLS Level 2 data?

All the MLS Level 2 data described here can be obtained from the NASA Goddard Space Flight Center Data and Information Services Center (GSFC-DISC, see `http://disc.gsfc.nasa.gov/`).

What format are MLS Level 2 data files in? How do I read them?

MLS Level 2 data are in HDF-EOS version 5 format. Details are given in section 1.5 (page 4).

Which MLS data points should be avoided? How much should I trust the remainder?

These issues are described in section 1.6 (starting on page 5), and on a product by product basis in chapter 3. The key rules are:

- Only data within the appropriate pressure range (described product by product in chapter 3) are to be used.
- Always consider the precision of the data, as reported in the `L2gpPrecision` field.
- Do not use any data points where the precision is set negative. This indicates poor information yield from MLS.
- Do not use data for any profile where the field `Status` is an odd number.
- Data for profiles where the `Status` field is non zero should be approached with caution. See section 1.6 on page 5, and the product by product description in chapter 3 for details on how to interpret the `Status` field.
- Do not use any data for profiles where the `Quality` field is *lower* than the threshold given in the section of chapter 3 describing your product of interest.
- Do not use any data for profiles where the `Convergence` field is *higher* than the threshold given in the section of chapter 3 describing your product of interest.
- Some products require additional screening to remove biases or outliers, as described in chapter 3.
- Information on the accuracy of each product is given in Chapter 3. Detailed MLS accuracy budgets are given in papers in the Aura Validation special issue of the Journal of Geophysical Research – Atmospheres. These papers describe the earlier (v2.2) MLS data, the accuracy budgets for which are expected to be similar to that of v3.3 described herein.
- Data users are strongly encouraged to contact the MLS science team to discuss their anticipated usage of the data, and are always welcome to ask further data quality questions.

Why do some species abundances show negative values, and how do I interpret these?

Some of the MLS measurements have a poor signal to noise ratio for individual profiles. Radiance noise can naturally lead to some negative values for these species. It is critical to consider such values in scientific study. Any analysis that involves taking some form of average will exhibit a high bias if the points with negative mixing ratios are ignored.

Contents

Acknowledgment

This research was carried out at the Jet Propulsion Laboratory, California Institute of Technology, under a contract with the National Aeronautics and Space Administration.

Chapter 1
Essential reading for users of MLS version 3.3 data

1.1 Scope and background for this document

This document describes the quality of the geophysical data products produced by version 3.3 (v3.3 hereafter) of the data processing algorithms for the EOS Microwave Limb Sounder (MLS) instrument on the Aura spacecraft. The intended audience is those wishing to make use of EOS MLS data for scientif c study. The geophysical products described in this document are all produced by the "Level 2" algorithms, and brief y summarized in Table 1.1.1.

The v3.3 MLS data are the third 'public release' of MLS data, the f rst being version 1.5 [Livesey et al., 2005], and the second version 2.2. The v2.2 data are described in a series of validation papers published in a special issue of the *Journal of Geophysical Research* in 2007/2008. This document updates f ndings from these papers for version 3.3, and gives more general information on the use of MLS data. As always, those wishing to use MLS data are strongly advised to consult the MLS science team concerning their intended use.

In addition to describing the data quality, this document gives a brief outline of the algorithms used to generate these "Level 2" data (geophysical products reported along the instrument track) from the input "Level 1" data (calibrated microwave radiance observations).

More information on the MLS instrument can be found in the document *An Overview of the EOS MLS Experiment* [Waters et al., 2004]. A more general discussion of the microwave limb sounding technique and an earlier MLS instrument is given in Waters et al. [1999]. The theoretical basis for the Level 2 software is described in Livesey and Snyder [2004]. A crucial component of the Level 2 algorithms is the "Forward Model", which is described in detail in Read et al. [2004] and Schwartz et al. [2004]. The document *EOS MLS Retrieved Geophysical Parameter Precision Estimates* [Filipiak et al., 2004] is a very useful source of information on the expected precision of the EOS MLS data, and should be regarded as a companion volume to this document. The impact of clouds on MLS measurements and the use of MLS data to infer cloud properties is described in Wu and Jiang [2004]. All the above documents and papers are available from the MLS web site (`http://mls.jpl.nasa.gov/`).

A subset of the information in these documents is also reported in the *IEEE Transactions on Geoscience and Remote Sensing*. An overview of MLS is given in Waters et al. [2006], the algorithms that produce the data described here are reviewed in Livesey et al. [2006]; Read et al. [2006]; Schwartz et al. [2006]; Wu et al. [2006]. Other papers describe the calibration and performance of the various aspects of the MLS instrument [Jarnot et al., 2006; Pickett, 2006; Cof eld and Stek, 2006] and the MLS ground data system [Cuddy et al., 2006]. The detailed validation of the MLS v2.2 dataset is described in a collection of papers in the 'Aura Validation' special issue of JGR-Atmospheres (papers published in 2007 and 2008). These are cited in the sections of Chapter 3 on a product-by-product basis.

Table 1.1.1: Summary of key information for each MLS standard product. Essential additional information is given in each product section of chapter 3.

Product name	Useful vertical range / hPa	Quality threshold [1]	Convergence threshold [2]	Notes	Contact name
BrO	10 – 3.2	1.3	1.05	A,D,N	Nathaniel Livesey
CH3Cl	147 – 4.6	1.3	1.05	N	Michelle Santee
CH3CN	46 – 1.0	1.4	1.05	E,N	Michelle Santee
ClO	147 – 1.0	1.3	1.05	B	Michelle Santee
CO	100 – 0.0046 215 – 146	0.2 1.1	1.4	C,O	Hugh Pumphrey Michael Schwartz
GPH	261 – 0.001	0.65	1.2	C	Michael Schwartz
H2O	83 – 0.002 316 – 100	1.3	2.0	– C	Alyn Lambert William Read
HCl	100 – 0.32	1.2	1.05	–	Lucien Froidevaux
HCN	10 – 0.1	0.2	2.0	A,E,N	Hugh Pumphrey
HNO3	215 – 1.5	See text	See text	C,O	Gloria Manney
HO2	22 – 0.046	N/A	1.1	D,N	Shuhui Wang
HOCl	10 – 2.2	1.2	1.05	N	Lucien Froidevaux
IWC	215 – 83	N/A	N/A	B	Alyn Lambert
IWP	N/A	N/A	N/A	B	Alyn Lambert
N2O	100 – 0.46	1.4	1.01	C	Alyn Lambert
O3 [3]	100 – 0.02 261 – 121	0.6	1.18	C,O	Lucien Froidevaux Michael Schwartz
OH	32 – 0.0032	N/A	1.1	D	Shuhui Wang
RHI [4]	316 – 0.002	See text	See text	C	William Read
SO2	215 – 10	0.6	1.8	E	William Read
Temperature [5]	261 – 0.001	0.65	1.2	C	Michael Schwartz

Notes:

A Users should consider using alternative versions of these products, produced (or planned to be produced) using different algorithms, as described in the text.

B This product contains significant biases in certain regions that may need to be accounted or corrected for in scientific studies. See text for details.

C Interference from clouds can affect this product at certain altitudes. See text for details.

D Biases in this product can be ameliorated (in selected conditions) by taking day/night differences. See text for details.

E At some altitudes, this product contains biases of a magnitude that render the product useful only for the study of 'enhancement events' (e.g., volcanic plumes, extreme fire pollution). See text for details.

N This is a 'noisy' product requiring significant averaging (e.g., monthly zonal mean). See text for details.

O This product contains significant outliers (e.g., spikes or oscillations) in some regions (typically related to clouds in the tropical upper troposphere). These should be screened out as detailed in the text.

[1] Only use profiles having 'Quality' *higher* than this value.

[2] Only use profiles having 'Convergence' *lower* than this value.

[3] File also contains two swaths giving column above the (MLS and GEOS-5 defined) tropopause.

[4] Relative humidity with respect to ice computed from the MLS H_2O and Temperature data.

[5] File also contains swaths giving estimates of tropopause. pressure (WMO definition) inferred from MLS and GEOS-5 temperatures.

1.2 Overview of v3.3 and this document

The remainder of this chapter reviews issues that are considered *essential reading* for users of the v3.3 dataset. Chapter 2 details relevant aspects of the MLS instrument design and operations and the theoretical basis for the v3.3 algorithms that are considered *background reading*.

Chapter 3 describes the data quality to be expected for "Standard" products from the MLS instrument for v3.3. These are observations of vertical profiles of the abundance of BrO, CH_3Cl (a new product on v3.3), CH_3CN, ClO, CO, H_2O, HCl, HCN, HNO_3, HO_2, HOCl, N_2O, O_3, and OH and SO_2, along with temperature, geopotential height, relative humidity (deduced from the H_2O and temperature data), and cloud ice water content, all described as functions of pressure. In v3.3 these profiles are mostly output on a grid that has a vertical spacing of six surfaces per decade change in pressure ($\sim$2.5 km), thinning out to three surfaces per decade above 0.1 hPa. Exceptions to this are water vapor, temperature, ozone and relative humidity which are on a finer 12 per decade grid from 1000 hPa to 1 hPa. Cloud ice water content is also reported on this fine grid, and profiles do not extend to the stratosphere and mesosphere. The OH product maintains a 6 per decade grid spacing into the upper mesosphere. Horizontally the profiles are spaced by 1.5° great-circle angle along the orbit, which corresponds to about 160 km. The true vertical and horizontal resolution of the products is typically somewhat coarser than the reporting grid described here. For some of the products, the signal to noise ratio is too low to yield scientifically useful data from a single MLS profile observation. In these cases, some form of averaging (e.g., weekly maps, monthly zonal means etc.) will be required to obtain more useful results.

In addition to these standard products, the algorithms also produce data for many "diagnostic" products. The bulk of these are similar to the standard products, in that they represent vertical profiles of retrieved species abundances. However, the information on these diagnostic products has typically been obtained from a different spectral region than that used for the standard products. These diagnostic products are not discussed in this document. Further information on these is available from the MLS science team.

At the time of writing, the current version of the data processing software is version 3.30, producing files labeled `v03-30`. Any minor 'bug fix' updates will be referred to as v3.31, v3.32, etc. This document is intended to be applicable to any v3.3*x* MLS data. Revisions that represent more than a minor 'bug fix' will not be known as v3.3*x* and will be accompanied by a revised version of this document.

1.3 MLS data validation status

As discussed above, a complete set of MLS validation papers describe the validation state of the earlier v2.2 data. The majority of the v2.2 MLS data products have, accordingly, completed 'Stage 3 Validation' defined[1] as:

> *Product accuracy has been assessed. Uncertainties in the product and its associated structure are well quantified from comparison with reference in situ or other suitable reference data. Uncertainties are characterized in a statistically robust way over multiple locations and time periods representing global conditions. Spatial and temporal consistency of the product and with similar products has been evaluated over globally representative locations and periods. Results are published in the peer-reviewed literature.*

Work, including that described in this document, is underway to re-validate the v3.3 data, and to further establish them as 'Stage 4' validated, defined as:

> *Validation results for stage 3 are systematically updated when new product versions are released and as the time-series expands.*

[1] See `http://science.nasa.gov/earth-science/earth-science-data/data-maturity-levels/`

1.4 Differences between MLS v3.3 data and earlier v2.2 data

All of the MLS data products have been updated from the earlier v2.2 algorithms. Significant updates are detailed below.

Changes to vertical grids: Most products are reported on a vertical grid spaced at 6 surfaces per decade change in pressure (∼2.5 km spacing), thinning out to 3 surfaces per decade at pressures less than 0.1 hPa. As with v2.2, selected products are reported on a higher resolution grid at lower altitudes, spaced at 12 surfaces per decade (∼1.3 km).

In v3.3, these 'high resolution' products transition back to the regular 6-surfaces-per-decade grid at 1.0 hPa (v2.2 transitioned at 22 hPa). As with v2.2, H_2O, Temperature, geopotential height, and relative humidity are reported on this grid. In addition, O_3 is now reported on this 'high resolution' grid in v3.3.

Amelioration of biases in upper tropospheric CO and HNO_3: Significant biases in these products at 215 hPa (and partly at 146 hPa) have been ameliorated. This has been accomplished by updates in spectroscopy, a change in the manner in which background radiance is modeled, and neglecting information from a small number of channels (in the 240-GHz spectral region) that were giving rise to retrieval problems.

Extension of the vertical range for O_3: In addition to being reported on a higher resolution vertical grid, the O_3 product now contains scientifically useful values at 261 hPa, in contrast to v2.2 where retrievals were useful only at pressures of 215 hPa or less.

Reduction of biases in ClO: Biases in lower stratospheric ClO observations have been significantly reduced, but still need to be accounted for as described in the ClO section.

New methyl chloride product: CH_3Cl is now retrieved from spectral signatures in the 640-GHz region (partly responsible for the lower stratosphere ClO bias).

In addition to these specific changes, changes in all products, including those not listed above, have resulted from updates to spectroscopy and instrument calibration knowledge, and in indirect response to the larger changes detailed above.

The improvements in the 240-GHz species (O_3, HNO_3, and CO in the upper troposphere and lower stratosphere) partly derive from changes in the modeling of background radiances (as described above). An unfortunate side effect of this change is that these measurements are more sensitive to clouds than in v2.2. Additional screening rules for these products must be considered, as described in chapter 3.

Also note that the threshold values of 'Quality' and 'Convergence' to be applied in data screening have been updated for all products.

1.5 EOS MLS file formats, contents, and first order quality information

All the MLS Level 2 data files described here are available from the NASA Goddard Space Flight Center Data and Information Services Center (GSFC-DISC, see `http://disc.gsfc.nasa.gov/`). The standard and diagnostic products are stored in the EOS MLS *Level 2 Geophysical Product* (L2GP) files. These are standard HDF-EOS (version 5) files containing swaths in the Aura-wide standard format. For more information on this format see Craig et al. [2003]. A sample reading function for the Interactive Data Language (IDL, version 7.1.1 or later required), known as `readl2gp.pro` may have been supplied with the data and is available from the *Open Channel Software Foundation* (`http://www.openchannelsoftware.org/`). A

reader for MATLAB (`readL2GP.m`) is also available at the same site, and one for python is planned to be added shortly.

The standard products are stored in files named according to the convention

```
MLS-Aura_L2GP-<product>_v03-30_<yyyy>d<ddd>.he5
```

where `<product>` is `BrO`, `O3`, `Temperature`, etc. The files are produced on a one-day granularity (midnight to midnight, universal time), and named according to the observation date where `<yyyy>` is the four digit calendar year and `<ddd>` is the day number in that year (`001` = 1 January). The files contain an HDF-EOS swath given the same name as the product. In addition, the standard O_3 product files also contain swaths describing column abundances, and the standard Temperature file contains additional swaths describing tropopause pressure. As some L2GP files contain multiple swaths, it is important to ensure that the correct swath in the `L2GP` files is requested from the file. In the case where the 'default' swath is requested (i.e., no swath name is supplied) most HDF software will access the one whose name falls earliest in ASCII order. This generally results in the desired result for all products. For example, "`O3`" comes before "`O3␣column-GEOS5`". Likewise, for temperature, the standard "`Temperature`" product will be read in preference to the "`WMOTPPressure-MLS`" or "`WMOTPPressure-GEOS5`" swaths that give tropopause pressures (note that, as with v2.2, these names are different from the equivalent products in v1.5).

Each swath contains data fields `L2gpValue` and `L2gpPrecision`, which describe the value and precision of the data, respectively. Data points for which `L2gpPrecision` is set negative *should not be used*, as this flags that the resulting precision is worse than 50% of the *a priori* precision, indicating that instrument and/or the algorithms have failed to provide enough useful information for that point. In addition to these fields, fields such as `latitude` etc. describe geolocation information. The field `time` describes time, in the EOS standard manner, as the number of seconds elapsed (including the 5 or 6 subsequent leap seconds to date) since midnight universal time on 1 January 1993.

1.6 Additional quality control information described in the 'Quality', 'Convergence' and 'Status' fields

In addition to the data and their estimated precisions, three quality metrics are output for every profile of each product. The first, called `Quality`, gives a measure of the quality of the product based on the fit achieved by the Level 2 algorithms to the relevant radiances. Larger values of `Quality` generally indicate good radiance fits and therefore trustworthy data. Values of `Quality` closer to zero indicate poorer radiance fits and therefore less trustworthy data. The value of `Quality` to be used as a "threshold" for rejecting data in scientific studies varies from product to product, and is given later in this document.

The second quality metric is called `Status`. This is a 32 bit integer that acts as a bit field containing several "flags". Figure 1.6.1 describes the interpretation of these flags in more detail. The first two bits (bits 0 and 1) are "flagging" bits. If the first bit is set it indicates that the profile *should not be used in any scientific study*. Accordingly, any profile for which `Status` is an odd number should not be used. The second bit indicates that data are considered questionable for some reason. Higher bits give more information on the reasons behind the setting of the first two bits. So, for example, a value of `Status` of `18` (2+16) indicates that the data are questionable ($2 \equiv$ bit 2) because of the possible presence of high altitude clouds ($16 \equiv$ bit 4).

The most commonly set information bits are the "high altitude cloud" and "low altitude cloud" bits. These indicate that the data have been marked as questionable because the Level 2 software believed that the measurements may have been affected by the presence of clouds (clouds alone will never cause a profile to be marked as not to be used). The implications of this vary from product to product and, more importantly, height to height. For example, situations of "low cloud" typically have very little impact on the quality of

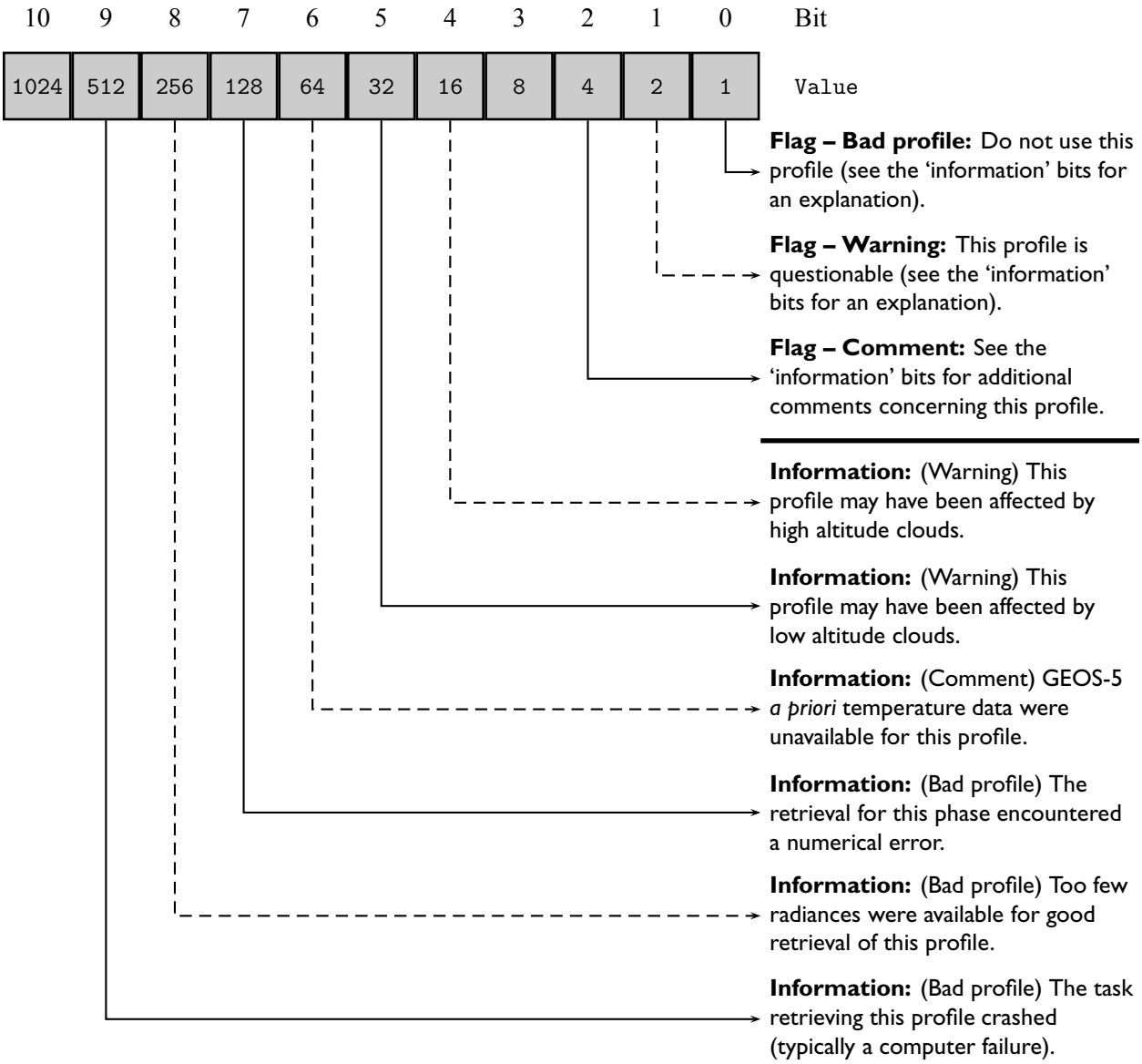

Figure 1.6.1: The meaning of the various bits in the `Status` field. The bits not labeled are not used in v3.3. Later versions may implement specific meanings for these bits. Note that bit 6 (GEOS-5 data) was not used in v1.5, and that the information in bits 7 and 8 were combined into bit 8 in versions 1.5 and 2.2.

stratospheric data. Further details of the implications of these flags are given later in this document on a product by product basis.

The third diagnostic field `Convergence` describes how the fit to the radiances achieved by the retrieval algorithms compared to the degree of fit to be expected. This is quantified as a ratio of an aggregate χ^2 value to that predicted based on the assumption of a linear system [Livesey et al., 2006]. Values around unity indicate good convergence, the threshold values above which profiles should not be used are given on a product by product basis later in this document.

1.7 An important note on negative values

Some of the MLS observations are 'noisy' in nature. A consequence of this is that negative values may often be reported for species mixing ratios. It is important that such values *not be ignored or masked*. Ignoring such values will automatically introduce a positive bias into any averages made of the data as part of scientif c analysis. Water vapor is retrieved using a logarithmic basis (both vertically and horizontally, as discussed in section 1.9). Accordingly, no negative water vapor abundances are produced by v3.3.

1.8 Averaging kernels for MLS v3.3 profiles

As is common for remote sounding instruments, consideration of the 'Averaging Kernel' [e.g., Rodgers, 2000] can be important in some scientif c studies. However, the relatively high vertical resolution of the MLS observations (compared, for example, to nadir sounding composition instruments) allows for many scientif cally useful studies to be undertaken without reference to the averaging kernels. This section reviews the role averaging kernels play in comparing MLS prof les to other observations and/or model prof les and describes how to obtain representative kernels for the v3.3 data.

The averaging kernel matrix $\mathbf{A}$ relates the retrieved MLS prof les (given by the vector $\hat{\mathbf{x}}$) to the 'true' atmospheric state (the vector $\mathbf{x}$) according to

$$\mathbf{A} = \frac{\partial \hat{\mathbf{x}}}{\partial \mathbf{x}}. \tag{1.1}$$

Rows of the $\mathbf{A}$ matrix accordingly describe the contributions of the true atmospheric prof le to the given level in the retrieved prof le. The f gures later in this document show these rows as individual colored lines.

Given an independent observation or model estimate of an atmospheric prof le $\mathbf{x}$, the averaging kernels, in combination with the MLS *a priori* prof le $\mathbf{x}_a$, can be used to compute the prof les that MLS would observe, were the true prof le to be in the state given by $\mathbf{x}$, according to

$$\hat{\mathbf{x}} = \mathbf{x}_a + \mathbf{A}\,[\mathbf{x} - \mathbf{x}_a] \tag{1.2}$$

The *a priori* prof le for each MLS observation is available from the `L2GP-DGG` f les. These f les (one f le per day, as for the product f les) contain swaths named according to the product, with the suff x '`-APriori`' (note the hyphen). Examples are '`Temperature-APriori`' and '`O3-APriori`'.

Note that in the case of water vapor where (as described below) a logarithmic interpolation is used for the prof le, the calculations in equation 1.2 should be performed in log space, i.e., with $\mathbf{x}$ and $\mathbf{x}_a$ containing logarithm of the given H_2O mixing ratio (leaving the $\mathbf{A}$ matrix as supplied).

The full MLS averaging kernels are complicated entities, ref ecting the two dimensional 'tomographic' nature of the MLS retrievals (see section 2.2). We anticipate that few, if any, users will need to apply these full two dimensional kernels, whose interpretation is complex (please contact the MLS team for further information on these). The full kernels can be 'collapsed' in the horizontal, to provide a single vertical averaging kernel for each product (as is done for many nadir sounding instruments). Such kernels are shown for each product (along with 'horizontal' averaging kernels) in chapter 3. The MLS averaging kernels typically change little with latitude / season / atmospheric state. Accordingly, two representative kernels are shown for each product, one for the tropics and one for polar winter conditions. These representative kernels are available to users as described below. If variability in the averaging kernels is a concern, comparison of $\hat{\mathbf{x}}$ prof les obtained using the two kernels (likely to represent two extreme cases) can provide a quantitative estimate of the magnitude of differences introduced by kernel variations.

The two averaging kernels for each product are distributed as text f les, named according to

```
MLS-Aura_L2AK-<product>-<case>_v03-30_0000d000.txt
```

where `<case>` is `Eq` or `70N` for the equator and 70°N, respectively (or `Day` and `Night` for OH, see section 3.18). These files are available from the MLS web site at

`http://mls.jpl.nasa.gov/data/ak/`

These files contain comment lines (prefixed with a semicolon) describing their format. The first non-comment line gives the name of the product and the number of levels in the vertical profile. A list of the pressure levels in the profile (matching those in the L2GP files) is then given, followed by all the values of the averaging kernel matrix, with the row index (the level in the retrieved profile) varying most rapidly.

Typically, of course, the MLS profile pressures are not those of the observation or model dataset to which the comparison is being made. In many cases, particularly where the resolution of the other dataset is comparable to that of the MLS profiles, a simple linear interpolation is the most practical manner in which to transform the other dataset into the **x** profile space. However, we note that more formal approaches have been described [Rodgers and Connor, 2003] for the case where the comparison dataset is also remotely sounded and has an averaging kernel. In cases where the comparison dataset has high vertical resolution (e.g., sonde or Lidar observations), an additional consideration is described in the following section.

1.9 Considerations for comparisons with high vertical resolution datasets

The MLS Level 2 data describe a piecewise linear representation of vertical profiles of mixing ratio (or temperature) as a function of pressure, with the tie points given in the `L2GP` files (in the case of water vapor, the representation is piecewise linear in log mixing ratio). This contrasts with some other instruments, which report profiles in the form of discrete layer means. This interpretation has important implications that may need to be considered when comparing profiles from MLS to those from other instruments or models, particularly those with higher vertical resolution.

It is clearly not ideal to compare MLS retrieved profiles with finer resolution data by simply 'sampling' the finer profile at the MLS retrieval surfaces. One might expect that instead one should do some linear interpolation or layer averaging to convert the other dataset to the MLS grid. However, in the MLS case where the state vector describes a profile at infinite resolution obtained by linearly interpolating from the fixed surfaces, it can be shown that the appropriate thing to do is to compare to a least squares fit of the non-MLS profile to the lower resolution MLS retrieval grid.

Consider a high resolution profile described by the vector $\mathbf{z}_h$, and a lower resolution MLS retrieved profile described by the vector $\mathbf{x}_l$. We can construct a linear interpolation in log pressure that interpolates the low resolution information in $\mathbf{x}_l$ to the high resolution grid of $\mathbf{z}_h$. We describe that operation by the (typically highly sparse) $n_h \times n_l$ matrix $\mathbf{H}$ such that

$$\mathbf{x}_h = \mathbf{H}\mathbf{x}_l \tag{1.3}$$

where $\mathbf{x}_h$ is the high resolution interpolation of the low resolution $\mathbf{x}_l$. It can be shown that the best estimate profile that an idealized MLS instrument could obtain, were the true atmosphere in the state described by $\mathbf{z}_h$, is given by

$$\mathbf{z}_l = \mathbf{W}\mathbf{z}_h \tag{1.4}$$

where

$$\mathbf{W} = \left[\mathbf{H}^{\mathrm{T}}\mathbf{H}\right]^{-1}\mathbf{H}^{\mathrm{T}} \tag{1.5}$$

In other words, $\mathbf{z}_l$ represents a least squares linear fit to $\mathbf{z}_h$. This operation is illustrated by an example in Figure 1.9.1. Precision uncertainty on high resolution measurements may be similarly converted to the MLS grid by applying

$$\mathbf{S}_l = \mathbf{W}\mathbf{S}_h\mathbf{W}^{\mathrm{T}} \tag{1.6}$$

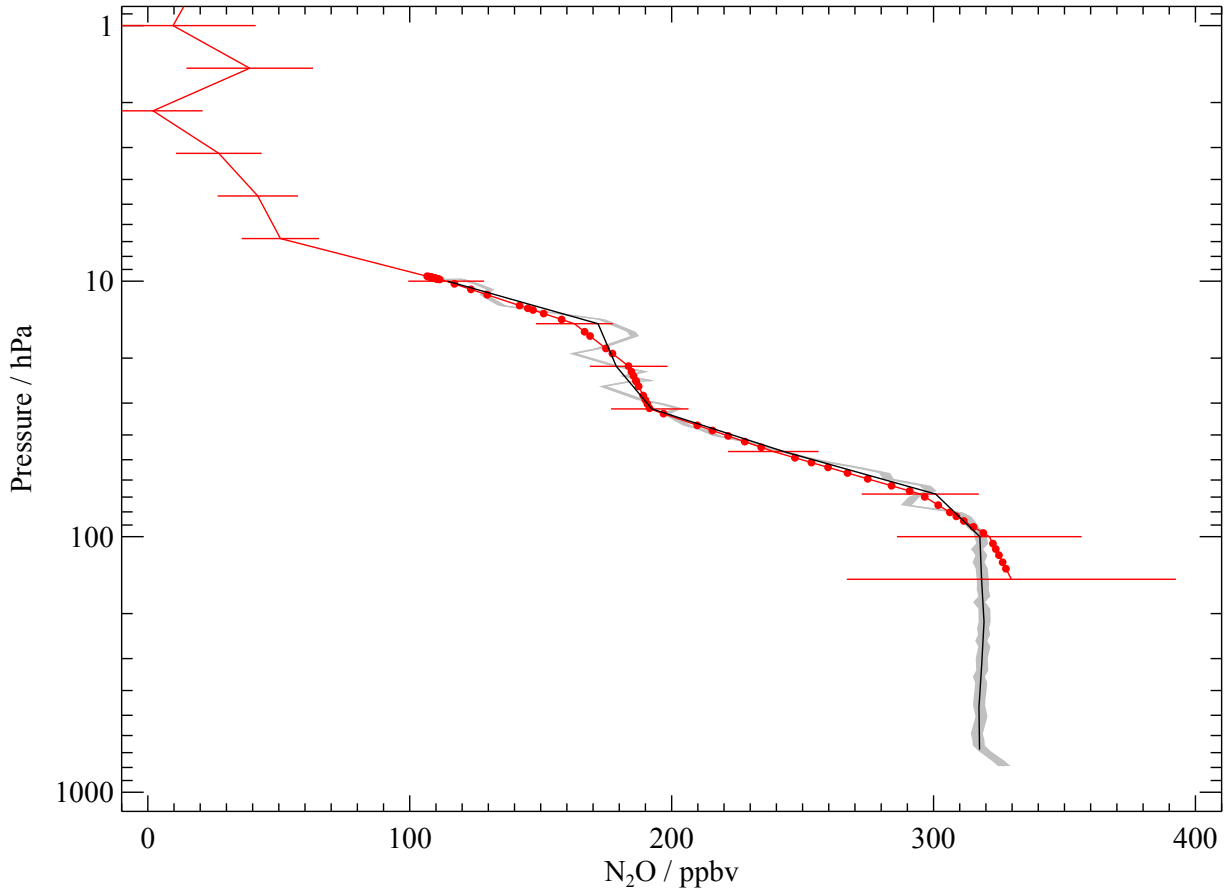

Figure 1.9.1: Comparisons of MLS (v1.5) N_2O observations with in-situ balloon data (courtesy of J. Elkins). The raw balloon data ($\mathbf{z}_h$) are shown as the grey shaded region (shading indicates precision). A coincident MLS profile ($\mathbf{x}_l$) is shown in red with the red error bars indicating precision. The red dots show the MLS data linearly interpolated to the balloon pressures using the $\mathbf{H}$ matrix (i.e., $\mathbf{x}_h$ from equation 1.3). The black line shows the 'least squares' interpolation of the balloon data onto the MLS grid using the $\mathbf{W}$ matrix as described in the text (i.e., $\mathbf{z}_l$ from equation 1.4). The black line therefore represents the closest possible match at this resolution to the original grey line, and is the appropriate quantity to compare to the red MLS profile, and to be multiplied by the averaging kernels for formal comparison.

where $\mathbf{S}_h$ is the covariance of the original high resolution data (typically diagonal) and $\mathbf{S}_l$ is its low resolution representation on the MLS pressure grid. Following this transfer of the high-resolution prof le onto the state vector vertical grid, the prof le can be multiplied by the averaging kernels, as described above, according to equation 1.2.

In some cases, the application of this least-squares 'smoothing' is as important, if not more important, than the application of the averaging kernels described above. This is particularly true when the averaging kernels are close to delta functions, indicating that the vertical resolution is comparable to the retrieved prof le level spacing.

In the case of water vapor, where a logarithmic vertical basis is used, the $\mathbf{x}$ and $\mathbf{z}$ vectors should describe the logarithm of the mixing ratio.

1.10 A note on the HCl measurements in v3.3

Starting in February 2006, the primary MLS band for measuring HCl (specifically the HCl^{35} isotopologue) (`R4:640.B13F:HCl` or 'band 13') began to exhibit symptoms of aging and was deactivated to conserve life. This is likely to be due to a radiation susceptibility issue for a batch of transistors identified shortly before launch. Useful observations of HCl are still made with the adjacent band (`R4:640.B14F:O3` or 'band 14') which, as can be seen from Figures 2.1.1 and 2.1.2 also observe the HCl^{35} line (and a smaller line for the HCl^{37} isotopologue).

In order to avoid undesirable discontinuities in the v3.3 HCl dataset, the band 13 radiances are not considered in the retrieval of the standard HCl product, even on days for which it was active (as with the earlier v2.2 algorithms). For days prior to the 16 February 2006 deactivation of band 13, and the few subsequent days when band 13 has been (or will be) reactivated, the v3.3 algorithms also produce a second HCl product (in the `HCl-640-B13` swath in the `L2GP-DGG`) file which includes the band 13 radiances, giving a product with improved precision and resolution in the upper stratosphere and mesosphere. See the section 3.9 for more information, including a list of the band 13 reactivation days to date.

As discussed in section 3.9, while the band 14 and band 13 data show very good agreement in the lower stratosphere, they disagree on the magnitude of the declining trend in upper stratospheric HCl (reflecting cuts in emissions of ozone depleting substances). At these high altitudes the HCl line is significantly narrower than the single channel in band 14 in which it resides, whereas the band 13 channels (by design as this band was targeted to HCl) resolve the line shape. Accordingly, the band 13 trend is judged to be the more accurate one.

1.11 A note on OH measurements in v3.3

The MLS OH measurements derive from observations in the 2.5-THz region of the spectrum. The local oscillator signal driving the MLS 2.5-THz radiometers is provided by a methanol laser (pumped by a CO_2 laser). In December 2009, following more than five years of operation, this laser began to show signs of aging and was temporarily deactivated (prior to the 2004 Aura launch, the expected lifetime of this laser was only two years).

Upper stratospheric and mesospheric OH are strongly affected by solar activity, which has been low during the Aura mission to date. We are conserving remaining life for the MLS OH measurements, pending the increased solar activity expected as we approach solar maximum.

Chapter 2
Background reading for users of MLS version 3.3 data

2.1 EOS MLS radiance observations

Figures 2.1.1 and 2.1.2 show the spectral coverage of the MLS instrument. The instrument consists of seven radiometers observing emission in the 118 GHz (R1A and R1B), 190 GHz (R2), 240 GHz (R3), 640 GHz (R4) and 2.5 THz (R5H and R5V) regions. With the exception of the two 118 GHz devices, these are "double sideband" radiometers. This means that the observations from both above and below the local oscillator frequencies are combined to form an "intermediate frequency" signal. In the case of the 118-GHz radiometers, the signals from the upper sideband (those frequencies above the ~126 GHz local oscillator) are suppressed. These intermediate frequency signals are then split into separate "bands". The radiance levels within these bands are quantified by various spectrometers.

In operation, the instrument performs a continuous vertical scan of both the GHz (for R1A–R4) and THz (R5H, R5V) antennæ from the surface to about 90 km in a period of about 20 s. This is followed by about 5 s of antenna retrace and calibration activity. This ~25 s cycle is known as a *Major Frame* (MAF). During the ~20 s continuous scan, radiances are reported at 1/6 s intervals known as *Minor Frames* (MIFs).

2.2 Brief review of theoretical basis

The Level 2 algorithms implement a standard *Optimal Estimation* retrieval approach [Rodgers, 1976, 2000] that seeks the "best" value for the state vector (the profiles of temperature and abundances) based on an optimal combination of the fit to the MLS radiance observations, *a priori* estimates of the state vector (from climatological fields), and constraints on the smoothness of the result. This fit must often be arrived at in an iterative manner because of the non-linear nature of the EOS MLS measurement system.

An innovative aspect of the retrieval algorithms for EOS MLS arises from taking advantage of the fact that the MLS instrument looks in the forward direction from the spacecraft. Figure 2.2.1 reviews the EOS MLS measurement geometry and shows that each radiance observation is influenced by the state of the atmosphere for several consecutive profiles. In the v3.3 Level 2 algorithms, the state vector consists of "chunks" of several profiles of atmospheric temperature and composition, which are then simultaneously retrieved from radiances measured in a similar number of MLS scans. Results from these "chunks" are then joined together to produce the products at a granularity of one day (the chunks overlap in order to avoid "edge effects").

The retrieval state vector consists of vertical profiles of temperature and composition on fixed pressure surfaces. Between these fixed surfaces, the forward models assume that species abundances and temperature vary from surface to surface in a piecewise-linear fashion (except for the abundance of H_2O, which is assumed to vary linearly in the logarithm of the mixing ratio). This has important implications for the interpretation of the data as was described in section 1.9. In addition to these profiles, the pressure at the tangent point for the mid-point of each minor frame is retrieved, based on both radiance observations and knowledge of tangent point height from the MLS antenna position encoder and the Aura spacecraft ephemeris and attitude determination.

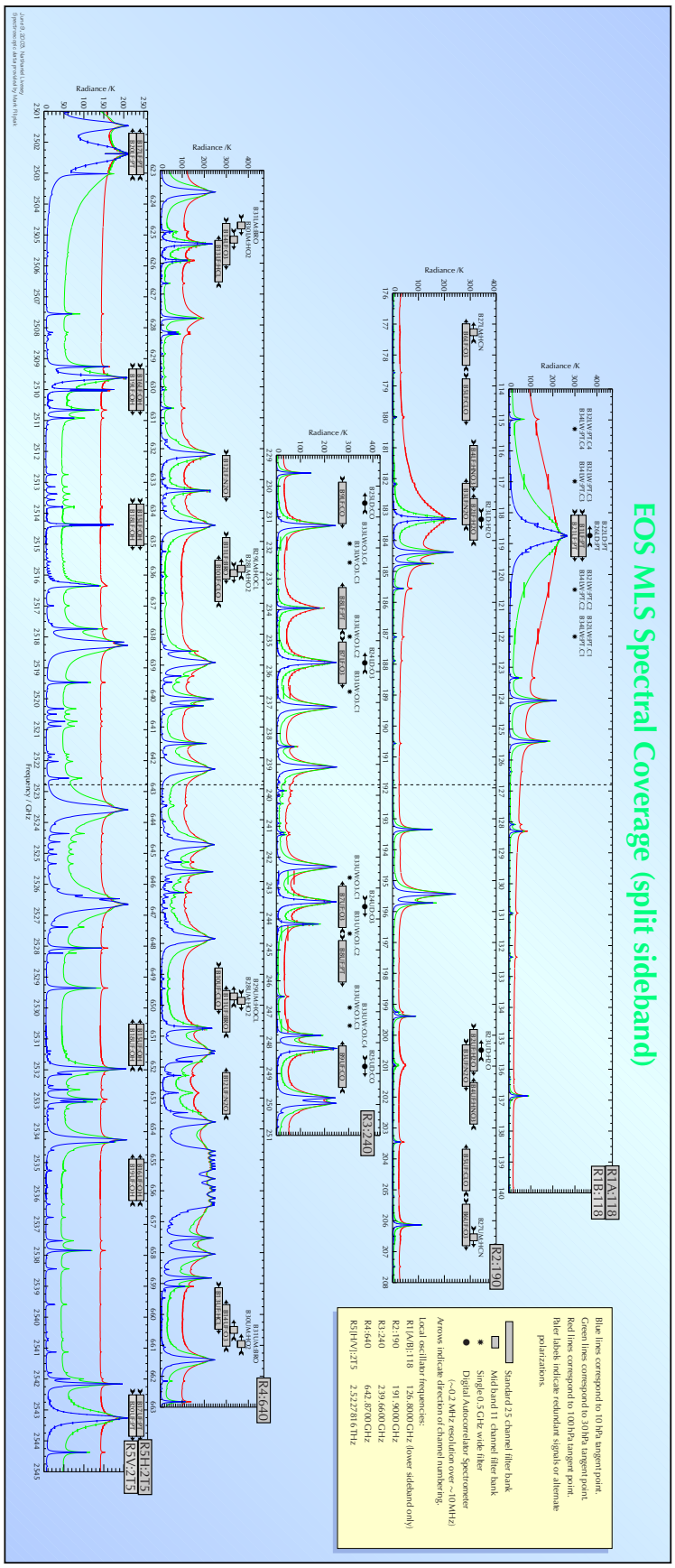

Figure 2.1.1: The five panels show the spectral regions covered by the MLS radiometers. The grey boxes and other symbols denote the position of the various "bands" observed within the spectral regions covered by each radiometer.

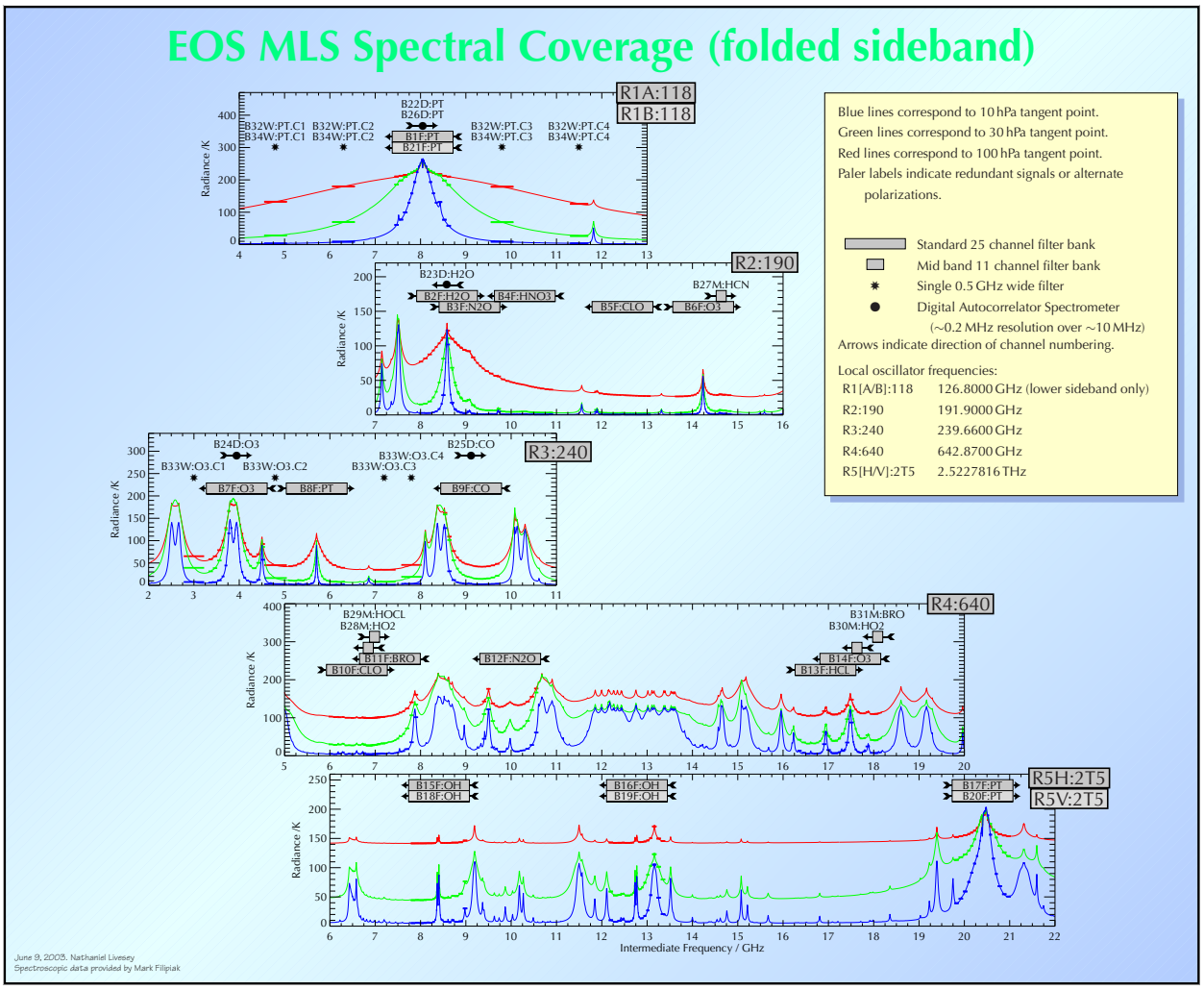

Figure 2.1.2: This is similar to figure 2.1.1, except that x-axes represent "intermediate frequency". The signal at each intermediate frequency represents a sum of the signals observed at that frequency both above and below the local oscillator (below only in the case of the 118 GHz receivers.

Most of the MLS data products are deduced from observations of spectral contrast, that is, variations in radiance as a function of frequency for a given limb pointing. Many of the systematic errors in the MLS measurement system manifest themselves as a spectrally flat error in radiance. This is true of both instrumental effects such as variations in instrument gain and offset during the limb scan, and "forward model" effects such as knowledge of continuum emission and the impact of some approximations made in the forward model in order to increase its speed. In order to account for such effects, the v3.3 algorithms also retrieve spectrally flat (or slowly spectrally varying) corrections to the MLS radiances, either in terms of an additive radiance offset or an additive atmospheric extinction.

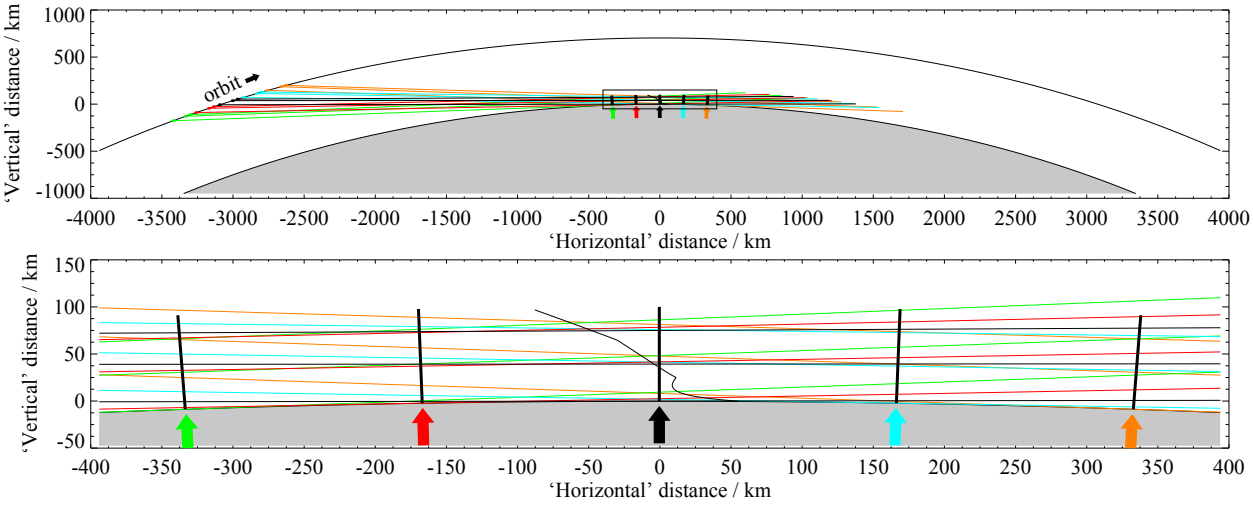

Figure 2.2.1: The top diagram shows a section of one orbit. Three of the 120 limb ray paths per scan are indicated by the "horizontal" lines. The lower diagram shows an expansion of the boxed region above. The straight radial lines denote the location of the retrieved atmospheric profiles. The limb ray scan closest to each profile is that whose color is the same as that of the arrow underneath. The thin black line under the central profile indicates the locus of the limb tangent point for this scan, including the effects of refraction.

2.3 The Core, Core+Rn approach

2.3.1 The need for separate "phases"

Many aspects of the MLS measurement system are linear in nature. In other words, there is a linear relationship between changes in aspects of the atmospheric state and consequent changes in the MLS radiance observations. However, there are some components of the state vector whose impact on the radiances is non-linear. The most non-linear of these is the estimate of the tangent pressure for each MIF of observation. The impact of water vapor in the upper troposphere on the MLS radiance observations is also highly non-linear. Solving for these aspects of the state vector therefore requires several iterations.

The computational effort involved in retrieval and forward models scales very rapidly (arguably as high as cubically) as a function of the size of the measurement system (i.e., the number of elements in the state and measurement vectors). Thus it is desirable to simplify retrievals involving strongly non-linear variables to a small subset of the complete system, in order to cut down on the effort involved in retrievals that require many iterations.

For this and other reasons, most retrieval algorithms are split into *phases*. In the case of the MLS v3.3 retrievals, there are many such phases. The first group of phases (collectively known as "Core") use the 118 GHz and 240 GHz observations of O_2 and $O^{18}O$, respectively, to establish estimates for temperature and tangent pressure. Upper tropospheric 190 GHz radiances are used in these early phases to establish a first order estimate of upper tropospheric humidity. The "Core" phases also include "cloud screening" computations (based on differences between observed and estimated clear-sky radiances). These identify minor frames where radiances in a given radiometer have been subject to significant (and currently poorly modeled) cloud scattering. Such minor frames are ignored in v3.3 processing in certain radiometers. Including information in such cloud-contaminated conditions is a goal for future MLS data processing versions.

The "Core", phases are followed by phases such as "Core+R3" and "Core+R5", where composition profiles are retrieved from a given radiometer. Sometimes (e.g., for "Core+R3") these later phases continue to retrieve temperature and pressure, continuing using information from the 118 GHz radiometers, as in

"Core". In other phases (e.g., the "Core+R2" and "Core+R4" families of phases), the 118 GHz information is neglected and temperature and pressure are constrained to the results of "Core". This choice is made based on extensive testing aimed at maximizing the information yield from MLS while minimizing the impact of inevitable systematic disagreements among the different radiometers, introduced by uncertain spectroscopy and/or calibration knowledge.

Table 2.3.1 describes the phases in more detail. Many products (e.g., ozone) are produced in more than one phase. All the separate measurements of these species are produced as diagnostic quantities, and labeled according to the spectral region from which they originated. For example, the ozone obtained from the "Core+R2" retrieval is known in the v3.3 dataset as `O3-190`. In v3.3 in order to reduce confusion for users of MLS data, the algorithms also output "standard" products, which is typically a copy of one of the products from the 'Core+Rn' phases. For example, the "standard" ozone product is a copy of the `O3-240` product. In the case of v3.3 nitric acid, the standard product represents a hybrid of the results from two phases. Details of which standard product is obtained from which phase are given in table 2.3.2.

2.4 Forward models used in v3.3

The retrieval algorithms in v3.3 make use of a variety of different forward models. The most accurate is the so-called "full" forward model described in Read et al. [2004] and Schwartz et al. [2004]. This is a hybrid line-by-line and channel averaged model that computes radiances on appropriate grids of frequency and tangent pressure that are then convolved with the MLS frequency and angular responses.

This model is generally very time consuming, although for some comparatively "clean" spectral regions the computational burden is small enough that the full forward model can be used in the operational retrievals. In the v3.3 retrieval algorithms, its use is restricted mainly to radiance channels whose focus is the upper troposphere and lower stratosphere, as these radiances generally have a non-linear relationship to the state vector.

For many of the MLS channels, a simpler "Linearized" forward model can be used. This model invokes a simple first-order Taylor series to estimate radiances as a function of the deviation of the state from one of several pre-selected representative states. The inputs to this model are pre-computed radiances and derivatives corresponding to the pre-selected states, generated by "off-line" runs of the full forward model.

This model is by its nature approximate. Many of the biases and unexpected scatter seen in the v3.3 simulation studies can be attributed to inaccuracies in this model. The model accuracy is a function of the proximity of the retrieved state to the pre-selected state used. The pre-selected states are taken from climatological fields for fixed latitudes and calendar months. In regions where the atmosphere departs dramatically from the climatological values (e.g., in the winter polar vortices), the model will generally be poorer than in other locations, giving rise to stronger biases.

In addition, a "cloud" forward model can be invoked to model the effects of scattering from cloud particles in the troposphere and lower stratosphere [Wu and Jiang, 2004]. This model was used in the simulation of radiances based on known model atmospheres for the v3.3 testing, but is not invoked in the v3.3 retrieval algorithms (the handling of clouds is described in more detail in section 2.5).

2.5 The handling of clouds in v3.3

Thin clouds and atmospheric aerosols do not affect MLS atmospheric composition measurements as the typical particle sizes are much smaller than the wavelengths of the radiation being observed. The MLS v3.3 algorithms can reliably retrieve composition in moderately cloudy cases (having small limb radiance perturbations) and in the case of the Core+R3 retrieval this is handled by retrieving RHi, acting as a frequency squared dependent extinction (including background atmospheric absorption from N_2, H_2O and unknown

Table 2.3.1: The phases that form the v3.3 retrieval algorithms.

Phase	Target species[1]	Measurements	Comment
Init-pTan	T, pTan (GHz), GPH	R1A & R1B (118 GHz)	Initial estimate of P/T, lower limit 261 hPa
Init-R2	H_2O, N_2O, CH_3CN, HCN, ClO, HNO_3, O_3, SO_2	R2 (190 GHz)	Initial trace gas estimator, lower limit 100 hPa
Update-pTan	T, pTan (GHz), GPH	R1A & R1B (118 GHz)	Better P/T estimate, lower limit 261 hPa
Init-Ext	240 GHz extinction	R3 (240 GHz), single channel	Initial R3 extinction estimate, lower limit 464 hPa
Final-Ext	240 GHz extinction, O_3	R3 (240 GHz)	Better R3 extinction and P/T estimate, lower limit 261 hPa. Also used for cloud flagging later P/T retrievals
Final-pTan	T, pTan (GHz), GPH	R1A & R1B (118 GHz), R3 (240 GHz)	Best P/T retrieval, lower limit 261 hPa
Init-RHi	UT RHi	R2 (190 GHz)	Retrieve RHi in a ∼6 km-layer centered 400 – 600 hPa. Uses only saturated radiances
Init-UTH	Upper tropospheric H_2O	R2 (190 GHz)	Low vertical resolution (6/decade)
R3Init-RHi	UT RHi[2]	R3 (240 GHz)	Retrieve RHi in a ∼6 km-layer centered 400 – 600 hPa. An initial estimate of RHi profile from an R3 window channel
Core	—	—	Product collation, and cloud flagging
Core+R3	T, pTan (GHz), GPH, O_3[3], CO, HNO_3, SO_2, RHi[b]	R1A & R1B (118 GHz), R3 (240 GHz)	Retrievals down to 316 hPa
Core+R2	H_2O, N_2O, HNO_3, ClO, O_3, HCN, CH_3CN, SO_2	R1A & R1B (118 GHz), R2 (190 GHz)	H_2O retrieved down to 316 hPa, other species 100 hPa (note no T, pTan, GPH retrieval)
High-Cloud	Cloud induced radiance, IWC, IWP	—	Used for flagging clouds in Core+R3 and later phases and forms basis for cloud ice products.
Core+R4A (B14)	ClO, BrO, HO_2, HOCl, HCl, O_3, HNO_3, CH_3CN, SO_2, CH_3Cl	R4 (640 GHz)	Retrievals down to 147 hPa
Core+R4A (B13)	HCl, O_3, SO_2	R4 (640 GHz)	Retrievals down to 147 hPa. This phase only performed when MLS band 13 is operating
Core+R4B	N_2O, SO_2	R4 (640 GHz)	Retrievals down to 147 hPa
Core+R5	T, pTan (GHz, THz), GPH, OH, O_3	R1A & R1B (118 GHz), R5H and R5V (2.5 THz)	Retrievals down to 68 hPa (147 hPa for Temperature)

[1] Tangent pressure and Geopotential height have been abbreviated to pTan (GHz/THz) and GPH respectively. Minor state vector components such as 'baseline' and/or 'extinction' have been omitted unless they are the specific focus of the phase. Temperature, IWC, H_2O, RHi are 'high resolution' (12 surfaces per decade change in pressure from 1000 hPa to 1 hPa) unless otherwise stated. O_3 is low resolution except for the Core+R3 phase.

[2] RHi from the R3 phases serves as an extinction/baseline quantity, but expressed in percent RHi units.

[3] On high vertical resolution grid

Table 2.3.2: The origin of each of the 'standard products' from v3.3.

Product	**Origin**	**Spectral region**
BrO	Core+R4A (B14)	640 GHz
CH_3Cl	Core+R4A (B14)	640 GHz
CH_3CN	Core+R4A (B14)	640 GHz
ClO	Core+R4A (B14)	640 GHz
CO	Core+R3	240 GHz
H_2O	Core+R2	190 GHz
HCl	Core+R4A (B14)	640 GHz
HCN	Core+R2	190 GHz
HNO_3	Core+R2 (15 hPa and less) Core+R3 (larger than 15 hPa)	190 GHz 240 GHz
HO_2	Core+R4A (B14)	640 GHz
HOCl	Core+R4A (B14)	640 GHz
IWC	High-Cloud	240 GHz
IWP	High-Cloud	240 GHz
N_2O	Core+R4B	640 GHz
O_3	Core+R3	240 GHz
OH	Core+R5	2.5 THz
RHi	Computed from Temperature and H_2O	190 GHz
Temperature	Final-pTan	118 & 240 GHz

Table 2.5.1: MLS frequency channels and thresholds for cloud flag

Radiometer	Cloud channel	USB/LSB frequency / GHz	Low threshold	High threshold
R1[A/B]:118	B[32/34]W:PT.C4	115.3 (LSB only)	$T_{cir} < -4$ K	none
R2:190	B5F:ClO.C1	178.8 / 204.9	$T_{cir} < -20$ K	$T_{cir} > 10$ K
R3:240	B8F:PT	233.4–234.5 / 244.8–245.9	none	$\chi^2 > 30$
R4:640	B11F:BrO.C23	635.9 / 649.8	$T_{cir} < -10$ K	none

emitters). In the other retrieval phases, by contrast, a spectrally-flat baseline is used. However, optically thick clouds can affect the MLS radiances beyond the modeling capability of this approach, mainly through scattering processes. Such situations need to be identified and the affected radiances excluded from the retrievals, or their influence down-weighted.

The first aspect of handling clouds in v3.3 is therefore the flagging of radiances that are believed to be significantly contaminated by cloud effects. To determine if a cloud is present in each MLS radiance measurement, we estimate the so-called cloud-induced radiance (T_{cir}). This is defined as the difference between the measured radiance and the radiance from a forward model calculation assuming clear-sky conditions. Specific window channels (those that see deepest into the atmosphere) in each radiometer are chosen to set these flags.

In the case of the 240 GHz radiometer (`R3:240`), instead of computing a T_{cir} parameter, the fit achieved in an early retrieval phase to the `B8F:PT` band (that measures the 233.9-GHz $O^{18}O$ line), as quantified by a χ^2-metric is used as an indicator of potential significant cloud-contamination. In computing T_{cir} for the other radiometers, the forward model calculation takes the best retrieved atmospheric state, with relative humidity capped at 110%.

Where the T_{cir} (or χ^2 for `R3:240`) values are sufficiently large (see Table 2.5.1), the radiances are flagged as being possibly contaminated. The estimated T_{cir} or χ^2 are improved as the retrieval progresses through the various phases, and finalized in the `HighCloud` phase, where T_{cir} statistics are computed and output to a diagnostic file for a wide range of channels including the window channels.

The retrievals of gas phase species abundances may choose to reject the cloud contaminated radiances, or (in the case of some less impacted channels) to inflate their estimated radiance precisions.

The other aspect of cloud handling in v3.3 is the estimation of cloud ice water content (IWC) and ice water path (IWP) products from the final T_{cir} computed by the retrieval in the `HighCloud` phase. More information on these products and their derivation is given in section 3.14.

2.6 The quantification of systematic uncertainty in MLS Level 2 data

A major component of the validation of MLS data is the quantification of the various sources of systematic uncertainty. These can arise from instrumental issues (e.g., radiometric calibration, field of view characterization), spectroscopic uncertainty, and through approximations in the retrieval formulation and implementation. A comprehensive quantification of these uncertainties was undertaken for the earlier v2.2 MLS data and the results for each product reported in the relevant validation papers (see the individual sections of Chapter 3 for references). In many cases these accuracy estimates are expected to apply for v3.3 also. Chapter 3 reports the expected accuracy for each product, taken and/or modified from the v2.2 estimates as appropriate.

For each identified source of systematic uncertainty, its impact on MLS measurements of radiance (or pointing where appropriate) has been quantified and modeled. These modeled impacts correspond to either

2-σ estimates of uncertainties in the relevant parameter(s), or an estimate of their maximum reasonable error(s) based on instrument knowledge and/or design requirements.

For most of the uncertainty sources, the impact on MLS standard products has been quantified by running perturbed radiances through the MLS data processing algorithms. Other (typically smaller) uncertainty sources have been quantified by simple perturbation calculations.

Although the term 'systematic uncertainty' is often associated with consistent biases and/or scaling errors, many sources of 'systematic' error in the MLS measurement system give rise to additional scatter. For example, an error in the O_3 spectroscopy, while being a bias on the fundamental parameter, will have an impact on the retrievals of species with weaker signals (e.g., CO) that is dependent on the amount and morphology of atmospheric ozone. The extent to which such terms can be expected to average down is estimated to first order by these 'full up studies' through their separate consideration of the bias and scatter each uncertainty source introduces.

The results of these studies are summarized as "accuracy" (and in some cases additional contributions to "precision") on a product by product basis in the next chapter. More details on the quantification for each product are given in the MLS validation papers. In addition Appendix A of Read et al. [2007] gives more specific details of the perturbations used in the study.

2.7 A brief note on the 'Quality' field

As described in section 1.6, the `Quality` field in the `L2GP` files gives a measure of the fit achieved between the observed MLS radiances and those computed by the forward model given the retrieved MLS profiles. `Quality` is computed from a χ^2 statistic for all the radiances considered to have significantly affected the retrieved species (i.e., those close to the relevant spectral lines), normalized by dividing by the number of radiances. `Quality` is simply the reciprocal of this statistic (i.e., low values indicate large χ^2, i.e., poor fits).

Ideally, the typical values of these normalized χ^2 statistics will be around one, indicating that radiances are typically fitted to around their noise levels. `Quality` will therefore also ideally have a typical value of one. For some species, however, because of uncertain knowledge of spectroscopy and/or instrument calibration, the v3.3 algorithms are known to be consistently unable to fit some observed radiances to within their predicted noise. In many of these cases, the noise reported on the radiances has been 'inflated' to allow the retrieval more leeway in fitting to radiances known to be challenging. As the noise level is the denominator in the χ^2 statistic, these species will have typical χ^2 statistics that are less than one and thus typical values of `Quality` higher than one. Accordingly, differences in `Quality` from one species to another do not reflect the species' relative validity.

Chapter 3
Results for 'standard' MLS data products

3.1 Overview of species-specific discussion

This section describes each MLS v3.3 'standard product' in more detail. An overview is given of the expected resolution, precision and accuracy of the data. The resolution is characterized by the averaging kernels described below. Precision is quantified through a combination of the precision estimated by the MLS v3.3 algorithms, through reference to the systematic uncertainty budget described in section 2.6, and through study of the actual MLS data (e.g., consideration of the observed scatter in regions where little natural variability is anticipated).

The systematic uncertainty reported is generally based on the study described in section 2.6. However, in some cases larger disagreements are seen between MLS and correlative observations than these quantifications would imply. In such cases (e.g., MLS 215 hPa CO) the uncertainty quoted reflects these disagreements.

A note on the averaging kernel plots

The averaging kernels shown in this section describe both the horizontal (along track) and vertical (pressure) resolution of the MLS v3.3 data. While the averaging kernels vary somewhat from profile to profile, their variation is sufficiently small that these samples can be considered representative for all profiles. The averaging kernel plots are accompanied by estimates of the horizontal and vertical resolution of the product defined by the full width at half maximum of the kernels. Each kernel plot also shows the integrated areas under the kernels.

3.2 Bromine monoxide

Swath name: `BrO`

Useful range: 10 – 3.2 hPa (day/night differences needed)

Contact: Nathaniel Livesey, **Email:** <Nathaniel.J.Livesey@jpl.nasa.gov>

Introduction

The standard product for BrO is taken from the 640-GHz (Core + R4A) retrievals. The spectral signature of BrO in the MLS radiances is very small, leading to a very poor signal-to-noise ratio on individual MLS observations. Signif cant averaging (e.g., monthly zonal means) is required to obtain scientif cally useful results. Large biases of between 5 to 30 pptv (typical BrO abundances range from 5 to 15 pptv) are seen in the data. These biases can be minimized by taking day/night differences. For pressures of 4.6 hPa and greater, nighttime BrO is negligible; however, for lower pressures, nighttime BrO needs to be taken into account. Table 3.2.1 summarizes the precision, accuracy, and resolution of the MLS v3.3 BrO product. The accuracy assessment is based on v2.2 data, as described in the validation paper [Kovalenko et al., 2007].

Note, the v3.3 'standard' BrO product (as with earlier versions) contain systematic biases and horizontal oscillations that present a larger challenge than for other species. Those interested in using MLS BrO in scientif c studies are strongly advise to contact the MLS team before embarking on their research. Different algorithms for BrO are under development by the MLS team, aimed at ameliorating some of these artifacts.

Vertical Resolution

Figure 3.2.2 shows that the vertical resolution for the v3.3 MLS BrO is about 5.5 km in the 10 to 4.6 hPa pressure region, degrading to 6 km at 3.2 hPa.

Precision

The expected precision in a retrieved prof le is calculated from radiance noise and reported for each retrieved data point. The value of the expected precision is f agged negative if it is worse than 50% of the value of the a priori precision. Figure 3.2.2 compares the expected precision (thick line) on an individual MLS BrO measurement with that deduced from observations of scatter in night-time observations (expected to be zero). Also shown are the expected precisions for daily, monthly, and yearly 10° zonal means. For the minimal averaging recommended, a monthly 10° zonal mean, which corresponds to about 3,000 measurements, the precision is about ±4 ppt. See Table 3.2.1 for more details.

Accuracy

The accuracy of the MLS BrO product is summarized in Table 3.2.1. The effect of each identif ed source of systematic error on MLS measurements of radiance has been quantif ed and modeled [see Read et al., 2007]. These quantif ed effects correspond to either 2σ estimates of uncertainties in each MLS product, or an estimate of the maximum reasonable uncertainty based on instrument knowledge and/or design requirements. More discussion is given in Kovalenko et al. [2007]. While that paper described v2.2 BrO, f ndings are expected to be applicable also to v3.3. The potential additive bias in MLS BrO measurements can be as high as about ±30 ppt (∼400%) at 10 hPa, decreasing to about ±6 pptv (50%) at 3.2 hPa. The potential scaling uncertainty over the pressure range of 10 to 3.2 hPa is about ±20%. The additive bias is dramatically reduced by subtracting the nighttime signal from the daytime signal. Taking day/night differences does not

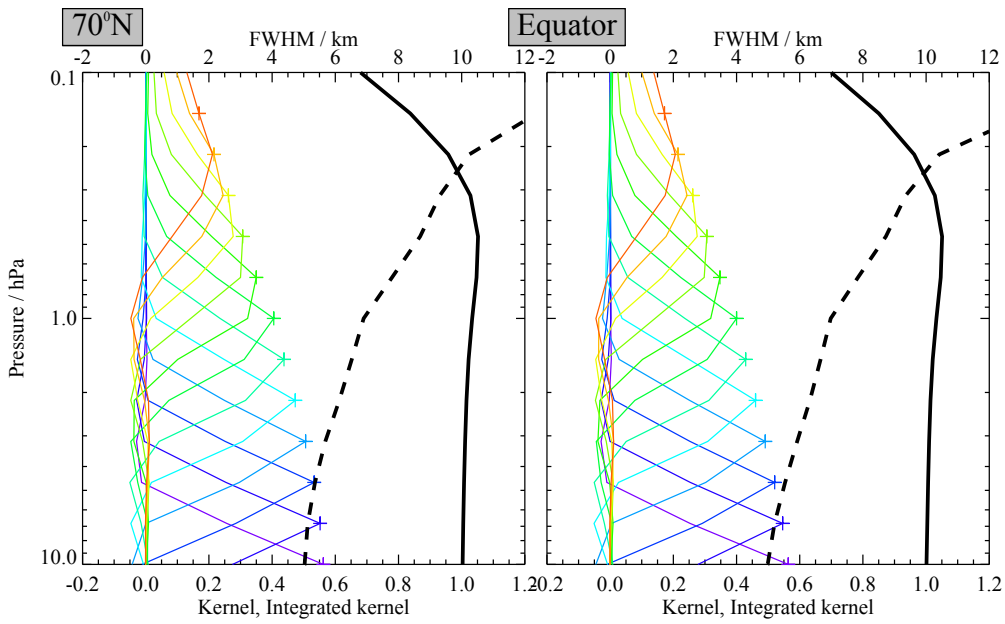

Figure 3.2.1: Typical vertical averaging kernels for the MLS v3.3 BrO data at 70°N (left) and the equator (right); variation in the averaging kernels is sufficiently small that these are representative of typical profiles. Colored lines show the averaging kernels as a function of MLS retrieval level, indicating the region of the atmosphere from which information is contributing to the measurements on the individual retrieval surfaces, which are denoted by plus signs in corresponding colors. The dashed black line indicates the vertical resolution, determined from the full width at half maximum (FWHM) of the averaging kernels, approximately scaled into kilometers (top axes). The solid black line shows the integrated area under each kernel; values near unity imply that the majority of information for that MLS data point has come from the measurements, whereas lower values imply substantial contributions from a priori information. The low signal to noise for this product necessitates the use of significant averaging (e.g., monthly zonal mean), making horizontal averaging kernels largely irrelevant.

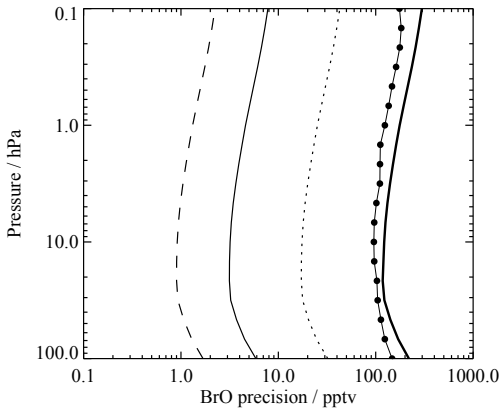

Figure 3.2.2: Comparison of the MLS v3.3 BrO precision as estimated from scatter in the retrieved data (circles) with that expected from the retrieval (thick line), for a single profile. Also shown is the expected precision for the day/night difference of 10° zonal mean profiles averaged over a day (dotted line), a month (thin line) and a year (dashed line).

affect the scaling uncertainty, which remains at about ±20%. If the MLS BrO data is used at 3.2 hP, the day/night difference value will need to be adjusted to compensate for the non-negligible nighttime BrO. We note that this method of taking day/night differences is not applicable for polar summer and winter, where there is no diurnal variation in BrO.

Data screening

Pressure range: 10 – 3.2 hPa

Values outside this range are not recommended for scientif c use.

Averaging required: Significant averaging (such as monthly zonal means) is required if useful scientific data are sought.

Diurnal differences: For use in any scientific study, day / night or ascending / descending differences should be used to alleviate biases.

Note that, for 3.2 hPa, the non-zero nighttime expected abundances BrO needs to be taken into account.

Estimated precision: Only use values for which the estimated precision is a positive number.

Values where the *a priori* information has a strong inf uence are f agged with negative precision, and should not be used in scientif c analyses (see Section 1.5).

Status flag: Only use profiles for which the 'Status' field is an even number.

Odd values of `Status` indicate that the prof le should not be used in scientif c studies. See Section 1.6 for more information on the interpretation of the `Status` f eld.

Clouds: Profiles identified as being affected by clouds can be used with no restriction.

Quality: Only profiles whose 'Quality' field is greater than 1.3 should be used.

Convergence: Only profiles whose 'Convergence' field is less than 1.05 should be used.

Artifacts

Signif cant additive biases are seen in the BrO data, as discussed above. Day / night (or ascending / descending) differences must be used to reduce these. For 3.2 hPa, nighttime BrO needs to be taken into account [Kovalenko et al., 2007].

A systematic horizontal (i.e., prof le-to-prof le) oscillation has been discovered in MLS v3.3 (and earlier) standard BrO product. This presents a signif cant challenge to the interpretation of the BrO observations. Users are strongly advised to contact the MLS team before embarking on research involving the MLS standard BrO product. Improved versions of the BrO product are under development at the time of writing.

Review of comparisons with other data sets

We have calculated total bromine, Br_y, from MLS measurements of BrO using a photochemical model, and compared this with Br_y similarly inferred from balloon-borne measurements of BrO obtained by the instruments DOAS, SAOZ, and SLS. When plotted in tracer space (e.g., as a function of N_2O), which accounts for differences in age of air, good agreement is seen [Kovalenko et al., 2007].

Table 3.2.1: Summary of the Aura MLS v3.3 BrO product.

Pressure range	Vertical res. / km	Precision[a] / pptv	Bias uncertainty[b] / pptv	Scaling uncertainty[c] / %	Comments
2.2 hPa and less	–	–	–	–	Unsuitable for scientif c use
3.2 hPa	6	±5	±6	±20	Need to account for non-negligible night time BrO
4.6	5.5	±4	±9	±20	
6.8	5.5	±4	±20	±20	
10	5.5	±4	±30	±20	
150 – 15 hPa	–	–	–	–	Unsuitable for scientif c use
1000 – 215 hPa	–	–	–	–	Not retrieved

[a]The precision quoted is for a 10° monthly zonal mean

[b]Because of large biases in the data, the daytime and nighttime BrO data are unsuitable for scientif c use, so day/night differences must be used. Note that day/night differences are not useful for polar winter and summer, where BrO does not undergo a diurnal variation.

[c]Based on modeled impacts of systematic errors

Desired improvements for future data version(s)

- Improvements will be sought in the stability of the BrO biases
- Future versions will also seek to improve the quality of the BrO observations in the mid- and lower stratosphere
- Improvements will also be sought in the polar regions, especially during summer / winter, when day / night differences are not possible

3.3 Methyl chloride

Swath name: CH3Cl

Useful range: 147 – 4.6 hPa

Contact: Michelle Santee, **Email:** <Michelle.L.Santee@jpl.nasa.gov>

Introduction

The v2.2 MLS ClO measurements were characterized by a substantial (∼0.1 – 0.4 ppbv) negative bias at retrieval levels below (i.e., pressures larger than) 22 hPa. Santee et al. [2008] suggested that contamination from an interfering species such as CH_3Cl, which has lines in two wing channels of the 640-GHz band used to measure ClO, could have given rise to the bias; they showed results from early v3 algorithms in which CH_3Cl was also retrieved that demonstrated signif cant reduction in the bias in lower stratospheric ClO. Further ref nements in the v3.3 algorithms yielded not only an improved ClO product, but also a reliable retrieval of CH_3Cl.

As for ClO, the standard CH_3Cl product is derived from radiances measured by the radiometer centered near 640 GHz. The MLS v3.3 CH_3Cl data are scientif cally useful over the range 147 to 4.6 hPa. A summary of the precision and resolution (vertical and horizontal) of the v3.3 CH_3Cl measurements as a function of altitude is given in Table 3.3.1. More details on the quality of the MLS v3.3 CH_3Cl measurements are given below.

Resolution

The resolution of the retrieved data can be described using "averaging kernels" [e.g., Rodgers, 2000]; the two-dimensional nature of the MLS data processing system means that the kernels describe both vertical and horizontal resolution. Smoothing, imposed on the retrieval system in both the vertical and horizontal directions to enhance retrieval stability and precision, degrades the inherent resolution of the measurements. Consequently, the vertical resolution of the v3.3 CH_3Cl data, as determined from the full width at half maximum of the rows of the averaging kernel matrix shown in Figure 3.3.1, is ∼4 – 6 km in most of the lower stratosphere, degrading to 8 – 10 km at and above 14 hPa. Note that there is overlap in the averaging kernels for the 100 and 147 hPa retrieval surfaces, indicating that the 147 hPa retrieval does not provide as much independent information as is given by retrievals at higher altitudes. Figure 3.3.1 also shows horizontal averaging kernels, from which the along-track horizontal resolution is determined to be ∼450 – 600 km for pressures greater than 10 hPa and ∼700 – 850 km for pressures less than or equal to 10 hPa. The cross-track resolution, set by the width of the f eld of view of the 640-GHz radiometer, is ∼3 km. The along-track separation between adjacent retrieved prof les is 1.5° great circle angle (∼165 km), whereas the longitudinal separation of MLS measurements, set by the Aura orbit, is 10° – 20° over low and middle latitudes, with much f ner sampling in the polar regions.

Precision

The precision of the MLS CH_3Cl data is estimated empirically by computing the standard deviation of the differences between matched measurement points at the intersections of the ascending (day) and descending (night) sides of the orbit. That the mean differences between paired prof les are mostly small (Figure 3.3.2) indicates the absence of signif cant systematic ascending / descending biases. Observed scatter, representing the statistical repeatability of the measurements, is 100 pptv or less throughout the vertical domain. This estimate ref ects the precision of a single prof le; in most cases precision can be improved by averaging, with

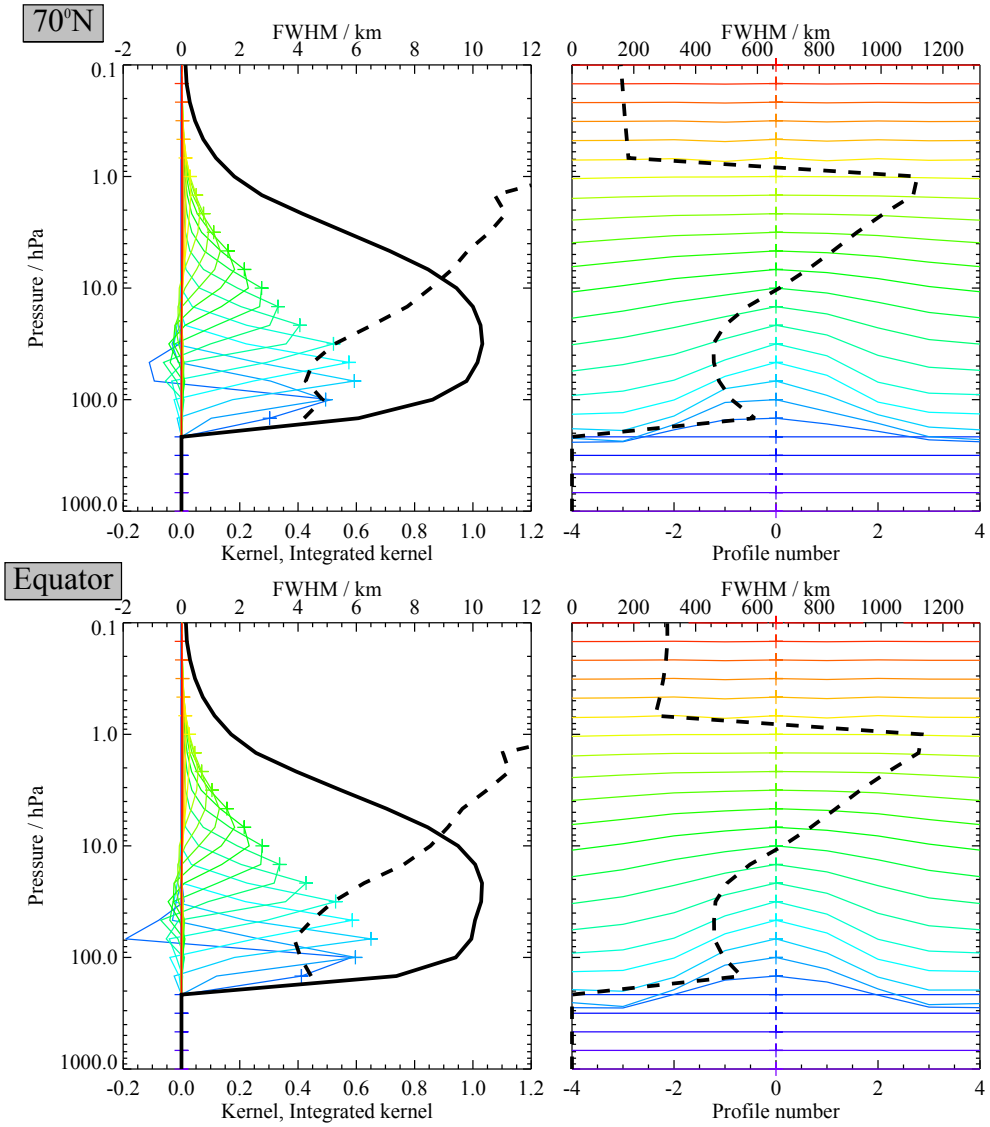

Figure 3.3.1: Typical two-dimensional (vertical and horizontal along-track) averaging kernels for the MLS v3.3 CH_3Cl data at 70°N (upper) and the equator (lower); variation in the averaging kernels is sufficiently small that these are representative of typical profiles. Colored lines show the averaging kernels as a function of MLS retrieval level, indicating the region of the atmosphere from which information is contributing to the measurements on the individual retrieval surfaces, which are denoted by plus signs in corresponding colors. The dashed black line indicates the resolution, determined from the full width at half maximum (FWHM) of the averaging kernels, approximately scaled into kilometers (top axes). (Left) Vertical averaging kernels (integrated in the horizontal dimension for five along-track profiles) and resolution. The solid black line shows the integrated area under each kernel (horizontally and vertically); values near unity imply that the majority of information for that MLS data point has come from the measurements, whereas lower values imply substantial contributions from a priori information. (Right) Horizontal averaging kernels (integrated in the vertical dimension) and resolution. The horizontal averaging kernels are shown scaled such that a unit averaging kernel amplitude is equivalent to a factor of 10 change in pressure.

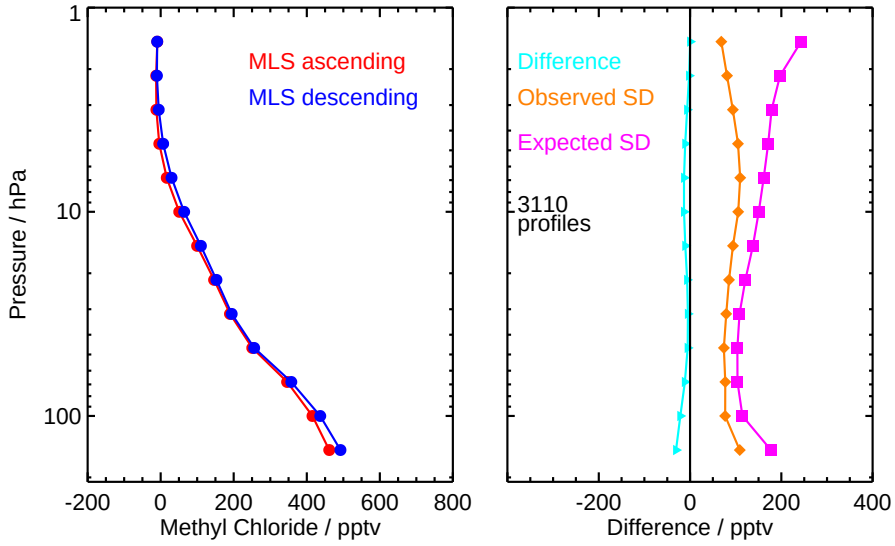

Figure 3.3.2: (left) Ensemble mean profiles for ascending (red) and descending (blue) orbit matching pairs of MLS v3.3 CH_3Cl in the latitude range 50°S–50°N averaged over 30 days in April 2008. (right) Mean difference profiles between ascending and descending orbits (cyan), the standard deviation about the mean difference (orange), and the root sum square of the precisions calculated by the retrieval algorithm (magenta). SD values are scaled by $1/\sqrt{2}$; thus the observed SD represents the statistical repeatability of the MLS measurements, and the expected SD represents the theoretical 1-σ precision for a single profile. See Lambert et al. [2007] for details.

the precision of an average of N profiles being $1/\sqrt{N}$ times the precision of an individual profile (note that this is not the case for averages of successive along-track profiles, which are not completely independent because of horizontal smearing). The theoretical precision reported by the Level 2 data processing system exceeds the observationally-determined precision throughout the vertical range, indicating that the smoothing applied to stabilize the retrieval and improve the precision has a nonnegligible influence. Because the theoretical precisions take into account occasional variations in instrument performance, the best estimate of the precision of an individual data point is the value quoted for that point in the L2GP files, but it should be borne in mind that this approach slightly overestimates the actual measurement noise.

Range

Although CH_3Cl is retrieved (and reported in the L2GP files) over the range 147 to 0.001 hPa, on the basis of the drop off in precision and resolution, the lack of independent information contributed by the measurements, and the results of simulations using synthetic data as input radiances to test the closure of the retrieval system, the data are not deemed reliable at retrieval levels above (i.e., pressures lower than) 4.6 hPa. Despite the overlap in the averaging kernels for the 147 and 100 hPa surfaces (Figure 3.3.1), maps at 147 hPa display substantial features not seen at 100 hPa (not shown) that are believed to represent real atmospheric variations. Thus we recommend that the v3.3 CH_3Cl data may be used for scientific studies between 147 and 4.6 hPa.

Accuracy

The impact of various sources of systematic uncertainty has not yet been quantified for CH_3Cl as it has for most other MLS products. This work is planned as part of a dedicated validation exercise for the v3.3 CH_3Cl data.

Review of comparisons with other datasets

Detailed comparisons with correlative data sets have not yet been undertaken. This work is planned as part of a dedicated validation exercise for the v3.3 CH_3Cl data.

Data screening

Pressure range: 147 – 4.6 hPa

Values outside this range are not recommended for scientific use.

Estimated precision: Only use values for which the estimated precision is a positive number.

Values where the *a priori* information has a strong influence are flagged with negative precision, and should not be used in scientific analyses (see Section 1.5).

Status flag: Only use profiles for which the 'Status' field is an even number.

Odd values of `Status` indicate that the profile should not be used in scientific studies. See Section 1.6 for more information on the interpretation of the `Status` field.

Clouds: Profiles identified as being affected by clouds can be used with no restriction.

Nonzero but even values of `Status` indicate that the profile has been marked as questionable, usually because the measurements may have been affected by the presence of thick clouds. Globally fewer than $\sim$1 – 2% of CH_3Cl profiles are typically identified in this manner (though this value rises to $\sim$3 – 5% in the tropics on a typical day), and clouds generally have little influence on the stratospheric CH_3Cl data. Thus profiles with even values of `Status` may be used without restriction.

Quality: Only profiles whose 'Quality' field is greater than 1.3 should be used.

This threshold for `Quality` (see section 1.6) typically excludes less than 1% of CH_3Cl profiles on a daily basis; note that it potentially discards some "good" data points while not necessarily identifying all "bad" ones.

Convergence: Only profiles whose 'Convergence' field is less than 1.05 should be used.

On a typical day this threshold for `Convergence` (see Section 1.6) discards very few (0.3% or less) of the CH_3Cl profiles, many (but not all) of which are filtered out by the other quality control measures.

Artifacts

- To be determined.

Desired improvements for future data version(s)

- To be determined.

Table 3.3.1: Summary of Aura MLS v3.3 CH_3Cl Characteristics

Pressure / hPa	Resolution V × H[a] / km	Precision[b] / pptv	Bias uncertainty / pptv	Scaling uncertainty / %	Known Artifacts or Other Comments
3.2 – 0.001	—	—	—	—	Unsuitable for scientif c use
15 – 4.6	8 – 10 × 550 – 850	±100	TBD	TBD	
100 – 22	4 – 6 × 450 – 500	±100	TBD	TBD	
147	4.5 × 600	±100	TBD	TBD	
1000 – 215	—	—	—	—	Not retrieved

[a] Vertical and Horizontal resolution in along-track direction.
[b] Precision on individual prof les.

3.4 Methyl cyanide

Swath name: CH3CN

Useful range: 46 – 1.0 hPa

Contact: Michelle Santee, **Email:** <Michelle.L.Santee@jpl.nasa.gov>

Introduction

The v2.2 standard CH_3CN data, which were derived from radiances measured by the radiometer centered near 190 GHz, were not recommended for use in scientif c studies. In v3.3, the standard CH_3CN product is taken from radiances measured by the radiometer centered near 640 GHz. In addition, the quality and reliability of the 640-GHz CH_3CN retrievals themselves have been improved in v3.3, largely because of changes in the way that the continuum is being handled for this radiometer in the v3 algorithms. The MLS CH_3CN data are now deemed scientif cally useful over the range 46 to 1 hPa, except in the winter polar vortex regions, where they may exhibit large biases below 10 hPa. In addition, the data at lower retrieval levels (i.e., higher pressures) may be used with caution in certain circumstances. A summary of the precision and resolution (vertical and horizontal) of the v3.3 CH_3CN measurements as a function of altitude is given in Table 3.4.1. More details on the quality of the MLS v3.3 CH_3CN measurements are given below.

Resolution

The resolution of the retrieved data can be described using "averaging kernels" [e.g., Rodgers, 2000]; the two-dimensional nature of the MLS data processing system means that the kernels describe both vertical and horizontal resolution. Smoothing, imposed on the retrieval system in both the vertical and horizontal directions to enhance retrieval stability and precision, degrades the inherent resolution of the measurements. Consequently, the vertical resolution of the v3.3 CH_3CN data, as determined from the full width at half maximum of the rows of the averaging kernel matrix shown in Figure 3.4.1, is $\sim$5 – 6 km in the lower stratosphere, degrading to $\sim$7 – 8 km in the upper stratosphere. Note that there is overlap in the averaging kernels for the 100 and 147 hPa retrieval surfaces, indicating that the 147 hPa retrieval does not provide as much independent information as is given by retrievals at higher altitudes. Figure 3.4.1 also shows horizontal averaging kernels, from which the along-track horizontal resolution is determined to be $\sim$400 – 700 km over most of the vertical range. The cross-track resolution, set by the width of the f eld of view of the 640-GHz radiometer, is $\sim$3 km. The along-track separation between adjacent retrieved prof les is 1.5° great circle angle ($\sim$165 km), whereas the longitudinal separation of MLS measurements, set by the Aura orbit, is 10° – 20° over low and middle latitudes, with much f ner sampling in the polar regions.

Precision

The precision of the MLS CH_3CN data is estimated empirically by computing the standard deviation of the differences between matched measurement points at the intersections of the ascending (day) and descending (night) sides of the orbit. That the mean differences between paired prof les are minimal (Figure 3.4.2) indicates the absence of systematic ascending / descending biases. Observed scatter, representing the statistical repeatability of the measurements, is 50 – 100 pptv throughout the vertical domain. This estimate ref ects the precision of a single prof le; in most cases precision can be improved by averaging, with the precision of an average of N prof les being $1/\sqrt{N}$ times the precision of an individual prof le (note that this is not the case for averages of successive along-track prof les, which are not completely independent because of horizontal

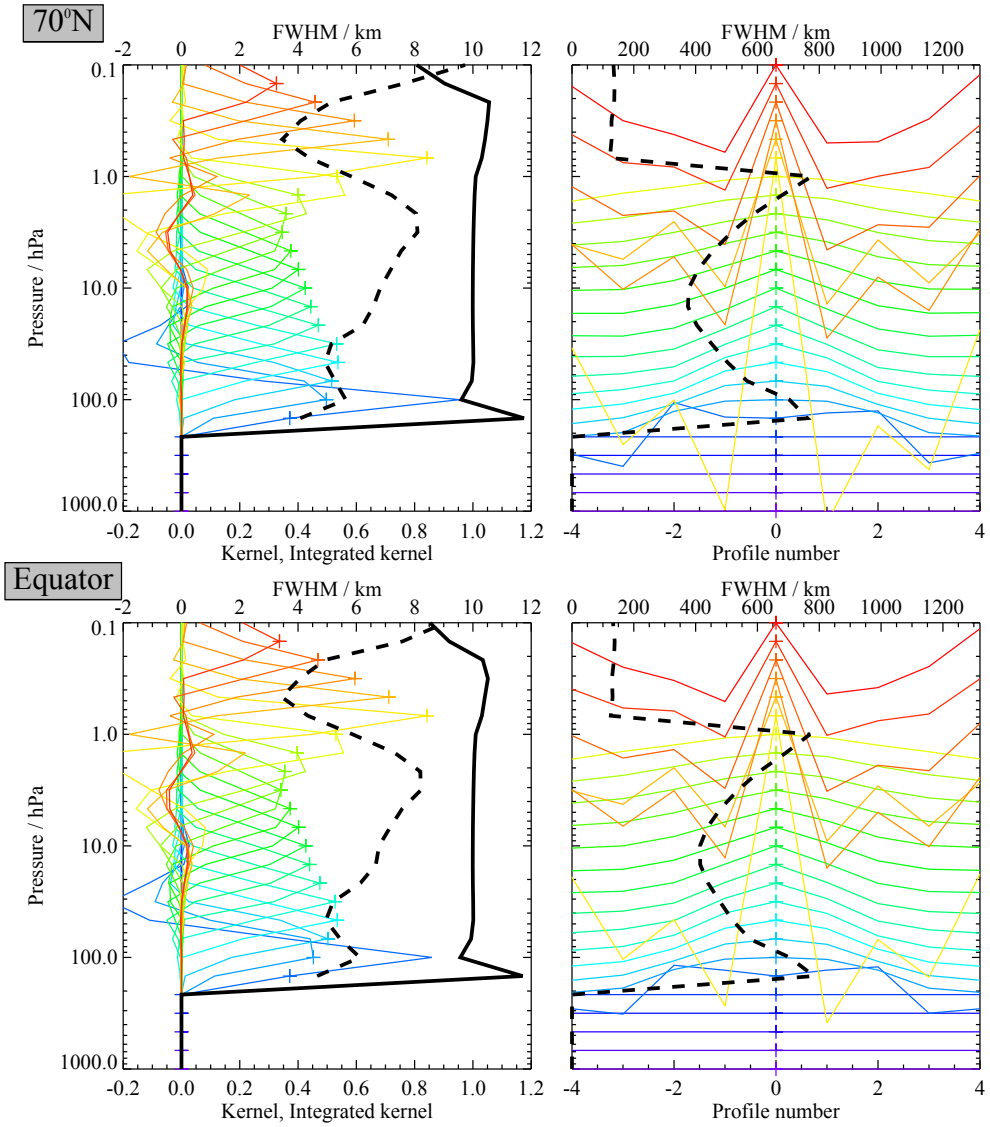

Figure 3.4.1: Typical two-dimensional (vertical and horizontal along-track) averaging kernels for the MLS v3.3 CH_3CN data at 70°N (upper) and the equator (lower); variation in the averaging kernels is sufficiently small that these are representative of typical profiles. Colored lines show the averaging kernels as a function of MLS retrieval level, indicating the region of the atmosphere from which information is contributing to the measurements on the individual retrieval surfaces, which are denoted by plus signs in corresponding colors. The dashed black line indicates the resolution, determined from the full width at half maximum (FWHM) of the averaging kernels, approximately scaled into kilometers (top axes). (Left) Vertical averaging kernels (integrated in the horizontal dimension for five along-track profiles) and resolution. The solid black line shows the integrated area under each kernel (horizontally and vertically); values near unity imply that the majority of information for that MLS data point has come from the measurements, whereas lower values imply substantial contributions from a priori information. (Right) Horizontal averaging kernels (integrated in the vertical dimension) and resolution. The horizontal averaging kernels are shown scaled such that a unit averaging kernel amplitude is equivalent to a factor of 10 change in pressure.

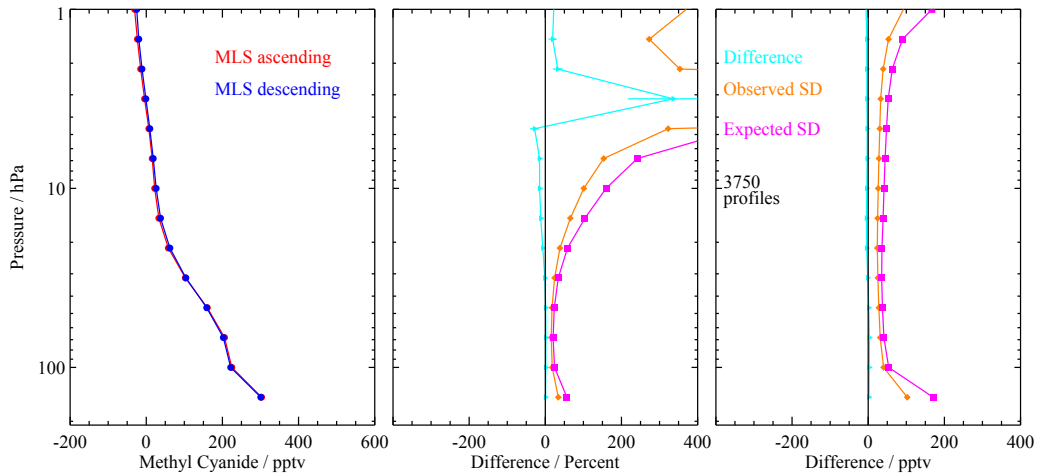

Figure 3.4.2: (left) Ensemble mean profiles for ascending (red) and descending (blue) orbit matching pairs of MLS v3.3 CH_3CN in the latitude range 50°S – 50°N averaged over 30 days in April 2008. (center) Mean percent difference profiles between ascending and descending orbits (cyan), the standard deviation about the mean difference (orange), and the root sum square of the precisions calculated by the retrieval algorithm (magenta). (right) Same, for absolute differences (pptv). SD values are scaled by $1/\sqrt{2}$; thus the observed SD represents the statistical repeatability of the MLS measurements, and the expected SD represents the theoretical 1-σ precision for a single profile. See Lambert et al. [2007] for details.

smearing). The theoretical precision reported by the Level 2 data processing system slightly exceeds the observationally-determined precision throughout the vertical range, indicating that the smoothing applied to stabilize the retrieval and improve the precision has a nonnegligible inf uence. Because the theoretical precisions take into account occasional variations in instrument performance, the best estimate of the precision of an individual data point is the value quoted for that point in the L2GP f les, but it should be borne in mind that this approach slightly overestimates the actual measurement noise.

Range

Although CH_3CN is retrieved (and reported in the L2GP f les) over the range 147 to 0.001 hPa, on the basis of the drop off in precision and resolution, the lack of independent information contributed by the measurements, and the results of simulations using synthetic data as input radiances to test the closure of the retrieval system, the data are not deemed reliable at the extremes of the retrieval range. Thus we recommend that v3.3 CH_3CN be used for scientif c studies only at the levels between 46 and 1 hPa. However, although the 147, 100, and 68 hPa retrievals are not generally recommended, they may be scientif cally useful in some circumstances. For example, the data display unphysical sharp latitudinal gradients at $\pm 30^\circ$ at 100 and 68 hPa, yet the large-scale longitudinal variations within the tropics are probably robust. Similarly, conf ned regions of signif cant enhancement at 147 hPa unaccompanied by comparably enhanced values at 100 hPa may ref ect real atmospheric features. The v3.3 CH_3CN data at these levels (147 – 68 hPa) should only be used in consultation with the MLS science team.

Accuracy

The impact of various sources of systematic uncertainty has not yet been quantif ed for CH_3CN as it has for most other MLS products. This work is planned as part of a dedicated validation exercise for the v3.3

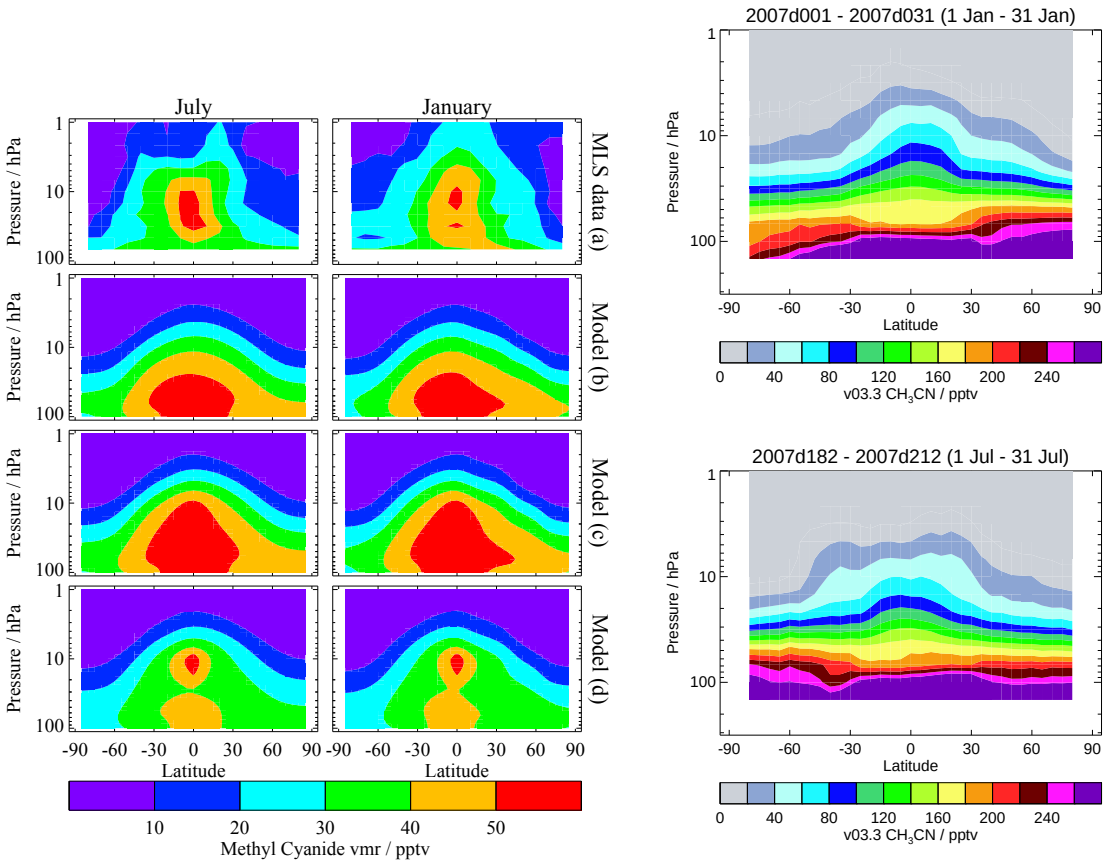

Figure 3.4.3: (left plot) Top row shows UARS MLS mean CH_3CN fields for June / July 1993 (left) and December 1992 / January 1993 (right). The other rows show results from various chemistry transport model runs. See Livesey et al. [2001] for details. (right plot) v3.3 Aura MLS CH_3CN monthly zonal means for January (top) and July (bottom) 2007.

CH_3CN data. However, preliminary comparisons with results from a two-dimensional chemistry transport model and CH_3CN retrievals from the MLS instrument on the Upper Atmosphere Research Satellite (UARS) [Livesey et al., 2001] indicate that the v3.3 Aura MLS CH_3CN mixing ratios are biased substantially high in the lower stratosphere (147 – 68 hPa, see Figure 3.4.3). Furthermore, the zonal-mean morphology of the Aura MLS CH_3CN at the lowest levels does not agree well with that either observed by UARS MLS or predicted by the model.

Review of comparisons with other datasets

Detailed comparisons with correlative data sets have not yet been undertaken. This work is planned as part of a dedicated validation exercise for the v3.3 CH_3CN data.

Data screening

Pressure range: 46 – 1.0 hPa

Values outside this range are not recommended for scientific use. The CH_3CN data at 147 – 68 hPa may be useful under certain circumstances but should not be analyzed in scientific studies without significant discussion with the MLS science team.

Estimated precision: Only use values for which the estimated precision is a positive number.

Values where the *a priori* information has a strong influence are flagged with negative precision, and should not be used in scientific analyses (see Section 1.5).

Status flag: Only use profiles for which the 'Status' field is an even number.

Odd values of `Status` indicate that the profile should not be used in scientific studies. See Section 1.6 for more information on the interpretation of the `Status` field.

Clouds: Profiles identified as being affected by clouds can be used with no restriction.

Nonzero but even values of `Status` indicate that the profile has been marked as questionable, usually because the measurements may have been affected by the presence of thick clouds. Globally fewer than ∼1 – 2% of CH_3CN profiles are typically identified in this manner (though this value rises to ∼3 – 5% in the tropics on a typical day), and clouds generally have little influence on the stratospheric CH_3CN data. Thus profiles with even values of `Status` may be used without restriction.

Quality: Only profiles whose 'Quality' field is greater than 1.4 should be used.

This threshold for `Quality` (see section 1.6) typically excludes less than 1% of CH_3CN profiles on a daily basis; note that it potentially discards some "good" data points while not necessarily identifying all "bad" ones.

Convergence: Only profiles whose 'Convergence' field is less than 1.05 should be used.

On a typical day this threshold for `Convergence` (see section 1.6) discards very few (0.3% or less) of the CH_3CN profiles, many (but not all) of which are filtered out by the other quality control measures.

Artifacts

- The retrievals at 100 and 68 hPa are characterized by unphysical sharp latitudinal gradients at $\pm 30^\circ$.
- Substantial biases may be present in the mixing ratios in the winter polar vortex regions for retrieval levels in the range 100 – 15 hPa.

Desired improvements for future data version(s)

- Improve the CH_3CN retrievals at 147 – 68 hPa.

Table 3.4.1: Summary of Aura MLS v3.3 CH_3CN Characteristics

Pressure / hPa	Resolution V × H[a] / km	Precision[b] / pptv	Bias uncertainty / pptv	Scaling uncertainty / %	Known Artifacts or Other Comments
0.68 – 0.001	—	—	—	—	Unsuitable for scientif c use
1.0	6 × 800	±100	TBD	TBD	
46 – 1.5	5 – 8 × 400 – 700	±50	TBD	TBD	
100 – 68	5 – 6 × 600 – 700	±50	TBD	TBD	Consult with MLS science team
147	4 × 800	±100	TBD	TBD	Consult with MLS science team
1000 – 215	—	—	—	—	Not retrieved

[a] Vertical and Horizontal resolution in along-track direction.
[b] Precision on individual prof les.

3.5 Chlorine Monoxide

Swath name: `ClO`

Useful range: 147 – 1.0 hPa

Contact: Michelle Santee, **Email:** <Michelle.L.Santee@jpl.nasa.gov>

Introduction

The quality and reliability of the version 2 (v2.2) Aura MLS ClO measurements were assessed in detail by Santee et al. [2008]. The ClO product has been signif cantly improved in v3.3; in particular, the substantial (∼0.1–0.4 ppbv) negative bias present in the v2.2 ClO values at retrieval levels below (i.e., pressures larger than) 22 hPa has been largely mitigated, primarily through retrieval of CH_3Cl (a new MLS product in v3.3).

As in v2.2, in v3.3 the standard ClO product is derived from radiances measured by the radiometer centered near 640 GHz. (ClO is also retrieved using radiances from the 190-GHz radiometer, but these data have poorer precision.) The MLS v3.3 ClO data are scientif cally useful over the range 147 to 1 hPa. A summary of the precision and resolution (vertical and horizontal) of the v3.3 ClO measurements as a function of altitude is given in Table 3.5.1. The impact of various sources of systematic uncertainty on the ClO retrievals was quantif ed in detail for v2.2 data [Santee et al., 2008]; Table 3.5.1 also includes estimates of the potential biases and scaling errors in the measurements compiled from that analysis under the assumption that most of the sources of uncertainty affect v3.3 retrievals in a similar manner. The overall uncertainty for an individual data point is determined by taking the root sum square (RSS) of the precision, bias, and scaling error terms (for averages, the single-prof le precision value is divided by the square root of the number of prof les contributing to the average). More details on the precision, resolution, and accuracy of the MLS v3.3 ClO measurements are given below.

Resolution

The resolution of the retrieved data can be described using "averaging kernels" [e.g., Rodgers, 2000]; the two-dimensional nature of the MLS data processing system means that the kernels describe both vertical and horizontal resolution. Smoothing, imposed on the retrieval system in both the vertical and horizontal directions to enhance retrieval stability and precision, degrades the inherent resolution of the measurements. Consequently, the vertical resolution of the v3.3 ClO data, as determined from the full width at half maximum of the rows of the averaging kernel matrix shown in Figure 3.5.1, is ∼3–4.5 km (with a mean of 3.5 km). Unlike in v2.2, which was characterized by considerable overlap in the averaging kernels for the 100 and 147 hPa retrieval surfaces, in v3.3 the averaging kernels are sharply peaked at all levels, including 147 hPa. Thus, although some degree of overlap is still present, the 147 hPa surface does provide independent information in v3. Figure 3.5.1 also shows horizontal averaging kernels, from which the along-track horizontal resolution is determined to be ∼250–500 km over most of the vertical range. The cross-track resolution, set by the width of the f eld of view of the 640-GHz radiometer, is ∼3 km. The along-track separation between adjacent retrieved prof les is 1.5° great circle angle (∼165 km), whereas the longitudinal separation of MLS measurements, set by the Aura orbit, is 10°–20° over low and middle latitudes, with much f ner sampling in the polar regions.

Precision

The precision of the MLS ClO measurements is estimated empirically by computing the standard deviation of the descending (i.e., nighttime) prof les in the 20°-wide latitude band centered around the equator. For

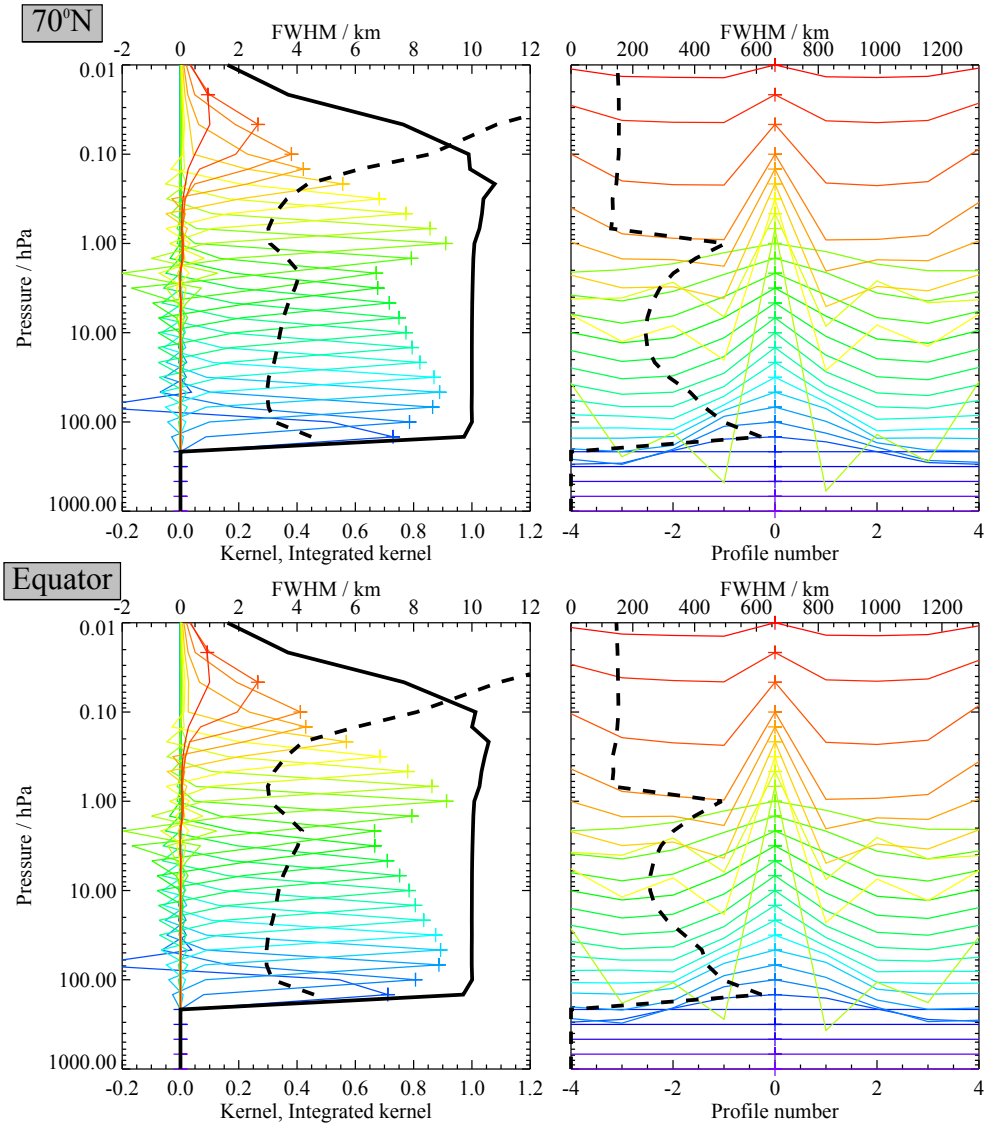

Figure 3.5.1: Typical two-dimensional (vertical and horizontal along-track) averaging kernels for the MLS v3.3 ClO data at 70°N (upper) and the equator (lower); variation in the averaging kernels is sufficiently small that these are representative of typical profiles. Colored lines show the averaging kernels as a function of MLS retrieval level, indicating the region of the atmosphere from which information is contributing to the measurements on the individual retrieval surfaces, which are denoted by plus signs in corresponding colors. The dashed black line indicates the resolution, determined from the full width at half maximum (FWHM) of the averaging kernels, approximately scaled into kilometers (top axes). (Left) Vertical averaging kernels (integrated in the horizontal dimension for five along-track profiles) and resolution. The solid black line shows the integrated area under each kernel (horizontally and vertically); values near unity imply that the majority of information for that MLS data point has come from the measurements, whereas lower values imply substantial contributions from a priori information. (Right) Horizontal averaging kernels (integrated in the vertical dimension) and resolution. The horizontal averaging kernels are shown scaled such that a unit averaging kernel amplitude is equivalent to a factor of 10 change in pressure.

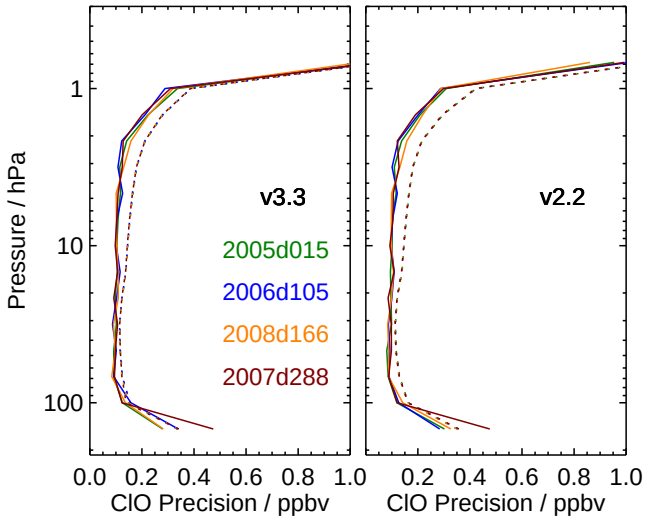

Figure 3.5.2: Precision of the (left) v3.3 and (right) v2.2 MLS ClO measurements for four representative days in different seasons (see legend). Solid lines depict the observed scatter in nighttime-only measurements obtained in a narrow equatorial band (see text); dotted lines depict the theoretical precision estimated by the retrieval algorithm.

this region and time of day, natural atmospheric variability should be negligible relative to the measurement noise. As shown in Figure 3.5.2, the observed scatter in the data is essentially unchanged in v3.3, rising from ∼0.1 ppbv over the interval 100 – 3 hPa to ∼0.3 ppbv at 1 hPa (and also 147 hPa). The smoothing of the retrieval is turned off above 1 hPa, and as a consequence the precision rises steeply above this level. The scatter in the data is essentially invariant with time, as seen by comparing the results for the different days shown in Figure 3.5.2.

The single-profile precision estimates cited here are, to first order, independent of latitude and season, but of course the scientific utility of individual MLS profiles (i.e., signal to noise) varies with ClO abundance. Outside of the lower stratospheric winter polar vortices, within which ClO is often strongly enhanced, the single-profile precision exceeds typical ClO mixing ratios, necessitating the use of averages for scientific studies. In most cases, precision can be improved by averaging, with the precision of an average of N profiles being $1/\sqrt{N}$ times the precision of an individual profile (note that this is not the case for averages of successive along-track profiles, which are not completely independent because of horizontal smearing).

The observational determination of the precision is compared in Figure 3.5.2 to the theoretical precision values reported by the Level 2 data processing algorithms. The predicted precision exceeds the observed scatter, particularly above 15 hPa, indicating that the vertical smoothing applied to stabilize the retrieval and improve the precision has a nonnegligible influence on the results at these levels. Because the theoretical precisions take into account occasional variations in instrument performance, the best estimate of the precision of an individual data point is the value quoted for that point in the L2GP files, but it should be borne in mind that this approach slightly overestimates the actual measurement noise.

Accuracy

The effects of various sources of systematic uncertainty (e.g., instrumental issues, spectroscopic uncertainty, and approximations in the retrieval formulation and implementation) on the MLS v2.2 ClO measurements were quantified through a comprehensive set of retrieval simulations; see Santee et al. [2008] for details of how the analysis was conducted and the magnitude of the expected biases, additional scatter, and possible

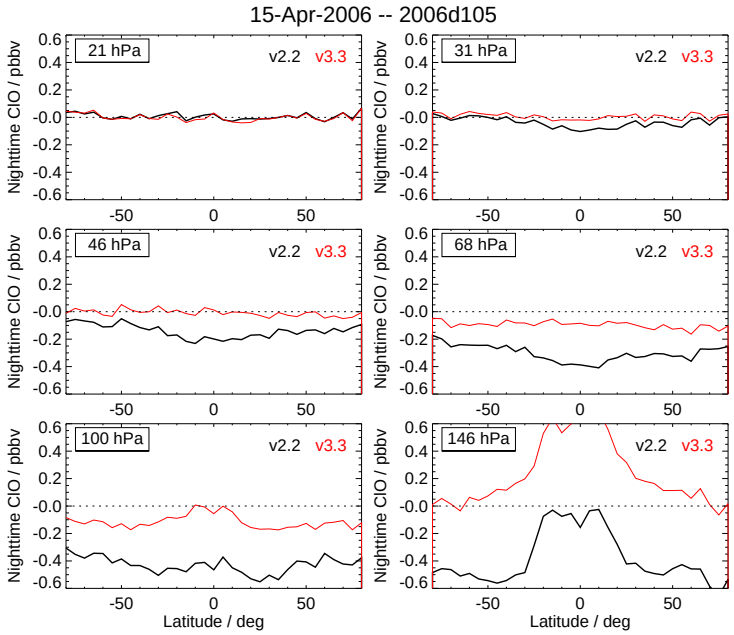

Figure 3.5.3: Nighttime v3.3 (red) and v2.2 (black) MLS ClO data as a function of latitude for the six lowest retrieval pressure surfaces (21–147 hPa). The date shown is representative of a typical northern hemisphere late spring / southern hemisphere early autumn day for which ClO is not enhanced in the lower stratosphere in either hemisphere.

scaling errors each source of uncertainty may introduce into the data. In aggregate, systematic uncertainties were estimated to induce in the v2.2 ClO measurements biases of $\sim \pm 0.1$ ppbv from 100 to 32 hPa and less than ± 0.05 ppbv above 22 hPa and multiplicative errors of $\sim \pm 5$–20% throughout the stratosphere.

Differences between v3.3 and v2.2 ClO mixing ratios are generally less than 0.05 ppbv (often considerably so) above 32 hPa. Figure 3.5.3, which depicts results for a single representative day, shows that the substantial bias present in the v2.2 (and earlier) MLS ClO data at the lowest retrieval levels (pressures greater than 22 hPa) is greatly ameliorated in v3.3. In particular, virtually no bias remains at 32 and 46 hPa. Although a small negative bias is still evident at 68 hPa, it displays less latitudinal variation than in v2.2. The bias is also considerably smaller at 100 hPa but still varies with latitude, with a smaller correction needed in the tropics. Finally, at 147 hPa, which was not formerly a recommended level, there is a strongly latitudinally-varying bias, positive over most of the globe but slightly negative in the polar regions.

In many cases the bias can be essentially eliminated by subtracting daily gridded or zonal-mean nighttime values from the individual daytime measurements. This is not a practical approach under conditions of continuous daylight or continuous darkness in the summer or winter at high latitudes, however. Moreover, under certain circumstances inside the winter polar vortices, chlorine activation leads to nonnegligible ClO abundances even at night. In this case, taking day−night differences considerably reduces the apparent degree of chlorine activation. It is instead recommended that the estimated value of the bias be subtracted from the individual measurements at each affected retrieval level.

To investigate the magnitude of the bias in the v3.3 MLS ClO data and the temporal variations in it, we show in Figure 3.5.4 monthly zonal means of MLS nighttime ClO measurements from two years (2005 and 2006) for pressure levels 147–68 hPa. For each panel, a calendar month of data in each year is binned and averaged in 5°-wide latitude bands between $\pm 85°$. Figure 3.5.5 is a similar plot, but encompasses all of the MLS nighttime ClO data over the entire 6^+-year mission for pressure levels 147–10 hPa. To guide

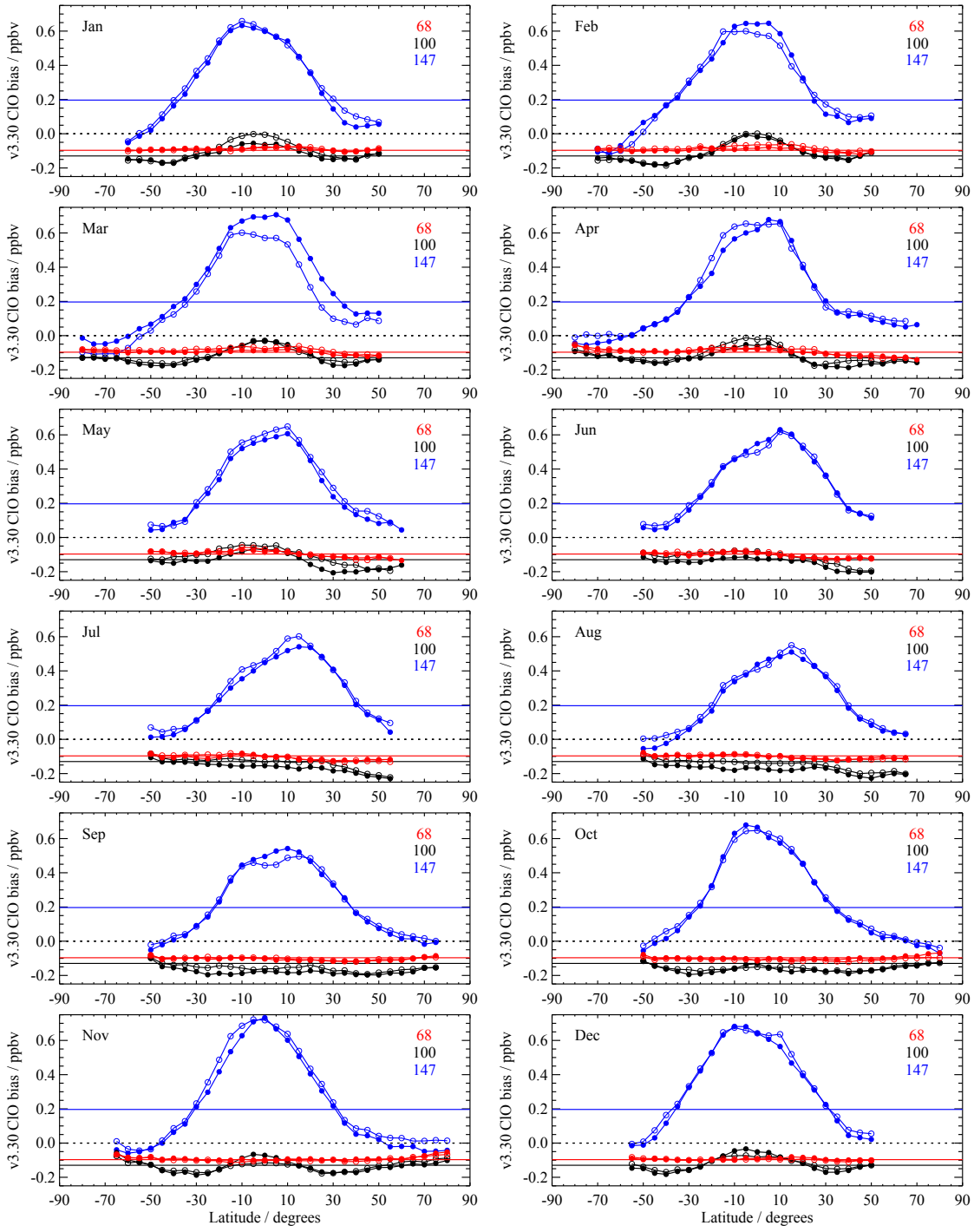

Figure 3.5.4: Estimates of the bias in MLS v3.3 ClO data in 5°-wide geographic latitude bands on the 147, 100, and 68 hPa MLS retrieval pressure surfaces (see legend). Each panel shows monthly zonal means of MLS nighttime (solar zenith angle (SZA) > 100°) ClO measurements from 2005 (filled circles) and 2006 (open circles). The dotted line marks the zero level. The colored solid lines denote the overall mission (6^+ years) global mean bias estimate at each level.

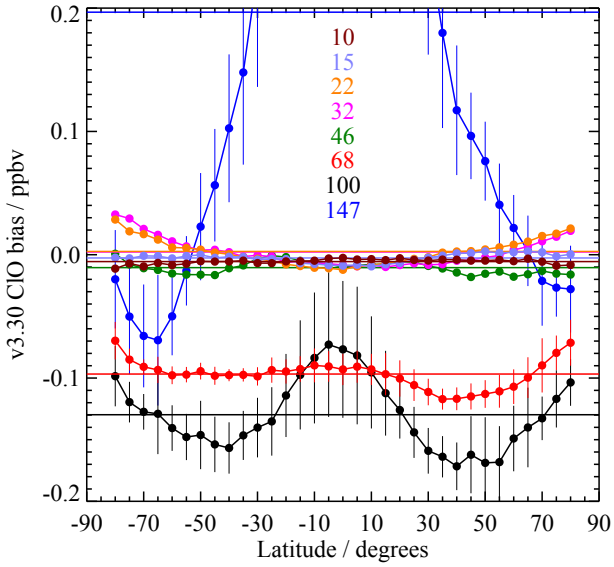

Figure 3.5.5: Estimates of the bias in MLS v3.3 ClO data in 5°-wide geographic latitude bands on MLS retrieval pressure surfaces from 147 to 10 hPa (see legend) calculated from the entire mission data set for which v3.3 data were available at the time of writing (1720 days spanning all seasons). To ensure that ClO was not enhanced, consideration was restricted to latitudes equatorward of 50°S for the days between 1 May and 1 November and to latitudes equatorward of 50°N for the days between 1 December and 1 April. Vertical error bars reflect the standard deviations in the averages in each latitude bin of the values from the 24 months (2005 and 2006) represented in Figure 3.5.4. The colored solid lines denote the overall mission global mean bias estimate at each level. Note that the large positive bias at low latitudes at 147 hPa is cut off in this figure.

the eye, the overall mission global mean value of the bias is indicated for each level (colored solid lines) in both f gures. As discussed above, the magnitude, and at 147 hPa even the sign, of the bias varies with latitude, and Figures 3.5.4 and 3.5.5 make clear that application of a constant bias correction for all latitudes is not appropriate. However, although Figure 3.5.4 reveals signif cant month-to-month and, in some cases, interannual variability, for most studies a time-invariant latitudinally-varying bias correction is adequate. An ASCII f le containing the altitude- and latitude-dependent v3.3 ClO bias correction values is available from the MLS web site. We are in the process of exploring whether the bias in the ClO data can be characterized as a function of geophysical rather than geographic variables; for example, we are investigating the eff cacy of a correction formulated in terms of quantities, such as ozone and temperature, most likely to be giving rise to the spectral features that induce the bias.

Review of comparisons with other data sets

Extensive comparisons of MLS v2.2 ClO data with a variety of different platforms (ground-based, balloon-borne, aircraft, and satellite instruments) were presented by Santee et al. [2008]. Results from a subset of these comparisons repeated with v3.3 ClO data are shown here.

As part of the Aura validation effort, measurements of ClO were obtained near Aura overpasses from the JPL Submillimeterwave Limb Sounder-2 (SLS-2) during a balloon campaign carried out from Ft. Sumner, New Mexico, in September 2005. Comparisons between the balloon measurements and coincident MLS measurements are shown in Figure 3.5.6, where the MLS prof les are within 1° of latitude, 12° of longitude, and 4 hours of the balloon measurements. Good agreement is seen in the upper stratosphere, in terms of both the altitude and the approximate magnitude of the high-altitude peak. The two data sets also agree well

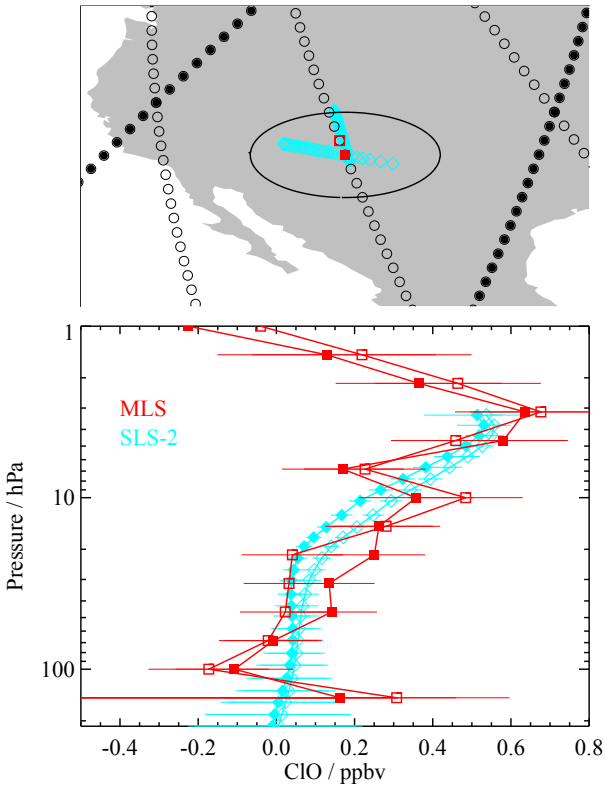

Figure 3.5.6: (Top) Path traversed by measurements from the balloon-borne SLS-2 instrument (cyan diamonds) during the flight from Ft. Sumner, NM, on 20–21 September 2005. Measurement tracks from nearby MLS ascending (daytime, open circles) and descending (nighttime, filled circles) orbit legs are also shown. The two MLS data points closest to the balloon measurements geographically and temporally are indicated by red squares, with the closer one denoted by a solid symbol; the 500-km radius around the closest MLS point is overlaid in black. (Bottom) Profiles of ClO, corresponding to the symbols in the top panel, from MLS (red squares) and SLS-2 (cyan open and solid diamonds). Error bars represent the estimated precisions of each instrument, taken from the data files.

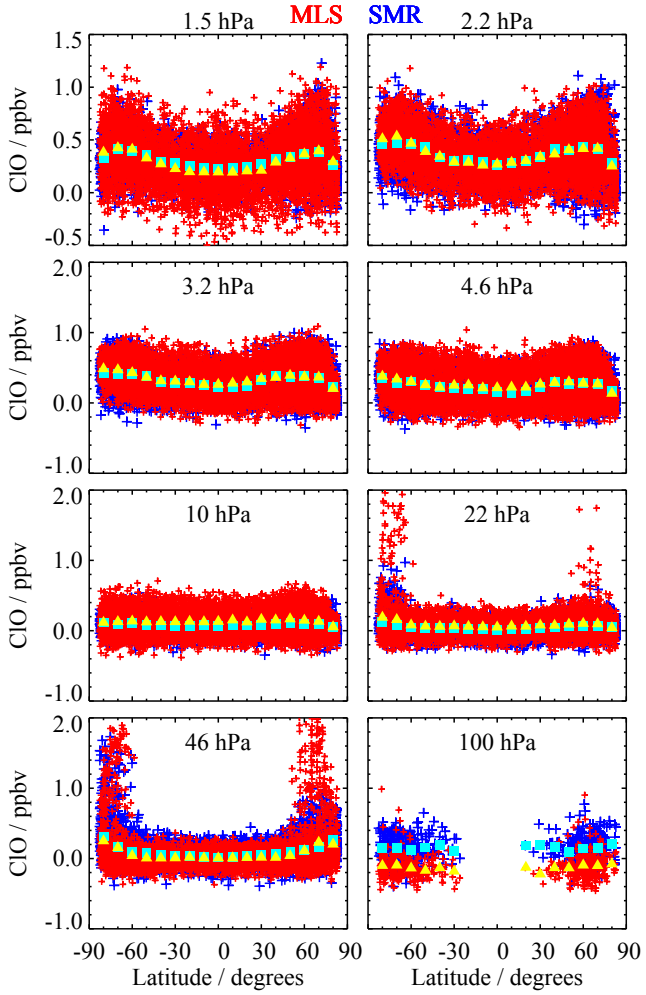

Figure 3.5.7: Scatter plot of coincident ClO profiles from MLS v3.3 data (red) and Odin/SMR Chalmers version 2.1 data (blue), as a function of latitude for eight selected retrieval surfaces. Overplotted are the zonal-mean values calculated in 10°-wide latitude bands for both the MLS (yellow triangles) and SMR (cyan squares) data.

throughout the lower stratosphere, except at 100 (147) hPa, where a signif cant negative (positive) bias in the v3.3 MLS ClO data is known to be present (see the previous subsection).

Satellite measurements provide the opportunity for more spatially and temporally extensive intercomparisons than data sets from other platforms. They are also typically well matched to the MLS horizontal and vertical resolution. Here we focus on comparisons with ClO measured by the Submillimetre Radiometer (SMR) onboard the Swedish-led Odin satellite [Murtagh et al., 2002], launched in February 2001 into a near-polar, sun-synchronous, ∼600-km altitude orbit with an 18:00 ascending node. SMR observes limb thermal emission from ClO using an auto-correlator spectrometer centered at 501.8 GHz. Operational Level 2 ClO retrievals are produced by the Chalmers University of Technology (Göteborg, Sweden). Here we use Chalmers version 2.1 data [Urban et al., 2006], which for ClO are very similar to those in version 2.0, with differences typically smaller than ∼50 pptv. The Chalmers version 2.0 ClO data have horizontal resolution of ∼300–600 km, vertical resolution of 2.5–3 km, and single-scan precision better than 0.15 ppbv over the range from 15 to 50 km [Urban et al., 2005, 2006]; similar values apply for the version 2.1 ClO data. The

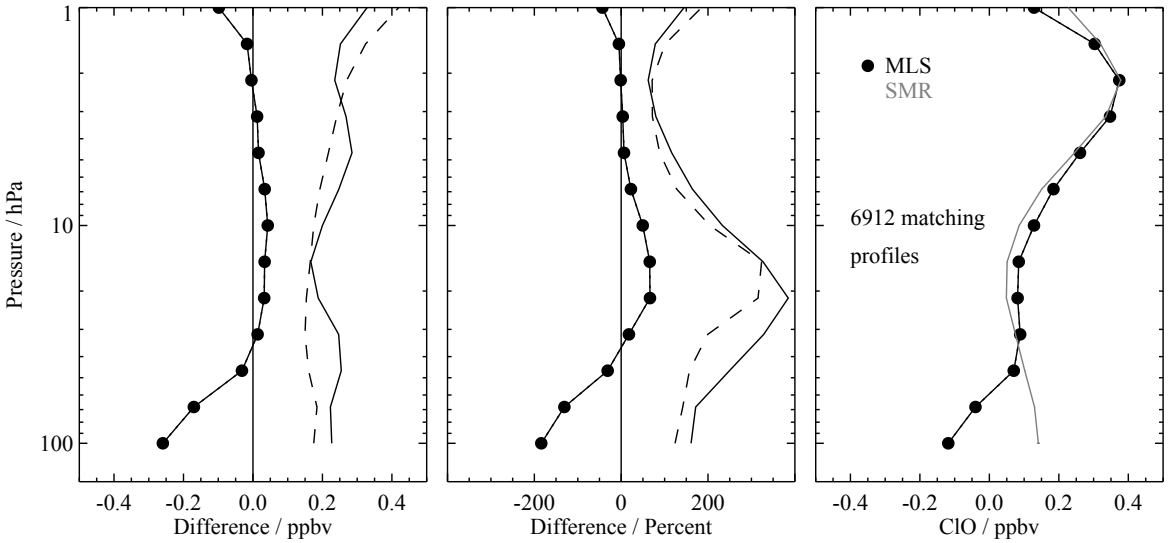

Figure 3.5.8: Comparison of coincident ClO profiles from MLS v3.3 data and Odin/SMR Chalmers version 2.1 data. (Left) Absolute differences (MLS−SMR). The black line with dots (symbols indicate MLS retrieval surfaces) shows mean differences, the solid line shows the standard deviation about the mean differences, and the dashed line shows the root sum square of the theoretical precisions of the two data sets. (Middle) Same, for percent differences, where percentages have been calculated by dividing the mean differences by the global mean SMR value at each surface. (Right) Global mean profiles for MLS (black line with dots) and SMR (grey).

estimated total systematic error is less than 0.1 ppbv throughout the vertical range [Urban et al., 2005, 2006]. Only good quality SMR data points are included in these comparisons (i.e., assigned f ag QUALITY = 0, and a measurement response for each retrieved mixing ratio larger than 0.75 to ensure that the information has been derived from the measurements, with a negligible contribution from the climatological a priori prof le [Urban et al., 2005; Barret et al., 2006]).

Figures 3.5.7 and 3.5.8 compare all coincident prof les obtained within ±1° in latitude, ±4° in longitude, and ±12 hours from all days (2004–2010) for which both SMR and v3.3 MLS data are available. All seasons are represented in this set of comparison days. Because the vertical resolution of the SMR ClO measurements is similar to that of the Aura MLS ClO measurements, for these comparisons the SMR prof les have been linearly interpolated in log-pressure to the f xed MLS retrieval pressure surfaces. The scatter plots of Figure 3.5.7 indicate excellent agreement in the general morphology of the ClO distribution, although the MLS data indicate slightly stronger enhancements in the polar regions, particularly in the north; this apparent disparity is most likely related to solar zenith angle and local solar time differences between the matched prof les. The small negative bias in the MLS retrievals is evident in the comparisons at the lowest levels, with the average difference between MLS and SMR ClO reaching ∼0.25 ppbv at 100 hPa (Figure 3.5.8). A possible high bias of 0.1–0.2 ppbv in the SMR lower stratospheric measurements obtained outside the vortex during nighttime, when ClO abundances fall below the detection limit of the instrument [Berthet et al., 2005], may also contribute to the observed offset between the two data sets. Differences are typically within ∼0.05 ppbv at and above 46 hPa, with MLS values larger throughout most of this region. The amplitude and the altitude of the secondary peak in ClO in the upper stratosphere are matched well.

The analysis presented in Figures 3.5.7 and 3.5.8 takes no account of the differences in solar zenith angle (SZA) in the two ClO data sets. Barret et al. [2006] estimated that a 2° increase in SZA roughly corresponds to a 0.1 ppbv decrease in ClO, on the order of the estimated single-scan precision of the mea-

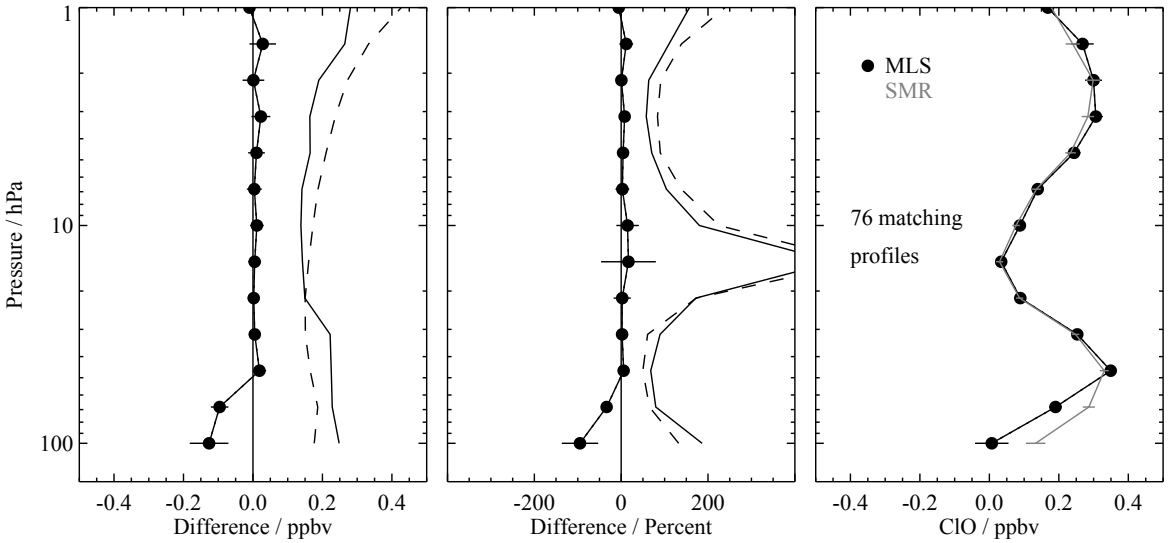

Figure 3.5.9: As in Figure 3.5.8, with additional SZA and LST coincidence criteria imposed (see text).

surements; they concluded that a SZA coincidence criterion of $\pm 2^\circ$ is appropriate for an intercomparison of the ClO measurements from MLS and SMR. Because of differences in the observational patterns of the two instruments (both in sun-synchronous orbits), measurement points satisfying this SZA filter occur only at the highest latitudes, poleward of 70° in both hemispheres. In Figure 3.5.9 we summarize the comparison results obtained by imposing the additional SZA criterion and tightening the local solar time criterion to ± 2 hours. Such stringent coincidence criteria greatly reduce the number of matched points but significantly improve the agreement between the two data sets, with differences less than 0.03 ppbv (corresponding to $\sim$15% or less) everywhere except at the bottom two levels, where biases are known to be present.

Data screening

Pressure range: 147 – 1.0 hPa

Values outside this range are not recommended for scientific use.

Estimated precision: Only use values for which the estimated precision is a positive number.

Values where the *a priori* information has a strong influence are flagged with negative precision, and should not be used in scientific analyses (see Section 1.5).

Status flag: Only use profiles for which the 'Status' field is an even number.

Odd values of `Status` indicate that the profile should not be used in scientific studies. See Section 1.6 for more information on the interpretation of the `Status` field.

Clouds: Profiles identified as being affected by clouds can be used with no restriction.

Nonzero but even values of `Status` indicate that the profile has been marked as questionable, usually because the measurements may have been affected by the presence of thick clouds. Globally fewer than $\sim$1–2% of ClO profiles are typically identified in this manner (though this value rises to $\sim$3–5% in the tropics on a typical day), and clouds generally have little influence on the stratospheric ClO data. Thus profiles with even values of `Status` may be used without restriction.

Quality: Only profiles whose 'Quality' field is greater than 1.3 should be used.

This threshold for `Quality` typically excludes less than 1% of ClO profiles on a daily basis; note that it potentially discards some "good" data points while not necessarily identifying all "bad" ones.

Convergence: Only profiles whose 'Convergence' field is less than 1.05 should be used.

On a typical day this threshold for `Convergence` discards very few (0.3% or less) of the ClO profiles, many (but not all) of which are filtered out by the other quality control measures.

Artifacts

- Significant biases are present in both daytime and nighttime v3.3 ClO mixing ratios at and below (i.e., pressures larger than) 68 hPa. The bias should be corrected by subtracting from the individual measurements at each affected retrieval level the altitude- and latitude-dependent bias estimates given in the ASCII file available from the MLS web site.

Desired improvements for future data version(s)

- Reduce the biases present at the lowest retrieval levels (147–68 hPa).

Table 3.5.1: Summary of Aura MLS v3.3 ClO Characteristics

Pressure / hPa	Resolution V × H[a] / km	Precision[b] / ppbv	Bias uncertainty[c] / ppbv	Scaling uncertainty[c] / %	Known Artifacts or Other Comments
0.68–0.001	—	—	—	—	Unsuitable for scientific use
1.0	3 × 500	±0.3	±0.05	±15%	
15–1.5	3.5–4.5 × 250–400	±0.1	±0.05	±5–15%	
46–22	3 × 300–400	±0.1	±0.1	±20%	
68	3 × 450	±0.1	±0.1	±20%	Latitude-dependent bias[d]
100	3 × 500	±0.1	±0.1	±20%	Latitude-dependent bias[d]
147	4.5 × 600	±0.3	±0.2	±40%	Latitude-dependent bias[d]
1000–215	—	—	—	—	Not retrieved

[a] Vertical and Horizontal resolution in along-track direction.

[b] Precision on individual profiles, determined from observed scatter in nighttime (descending) data in a region of minimal atmospheric variability.

[c] Values should be interpreted as 2-σ estimates of the probable magnitude and, at the higher pressures, are the uncertainties after subtraction of the known bias.

[d] Correct for the bias by subtracting from the individual measurements at this level the latitude-dependent bias estimates given in the ASCII file available from the MLS web site.

3.6 Carbon monoxide

Swath name: CO

Useful range: 215 – 0.0046 hPa

Contact: Hugh C. Pumphrey (stratosphere/mesosphere), **Email:** <H.C.Pumphrey@ed.ac.uk>
Michael Schwartz (troposphere), **Email:** <Michael.J.Schwartz@jpl.nasa.gov>

Introduction

Carbon monoxide is retrieved from radiance measurements of two bands in the MLS 240 GHz radiometer: R3:240:B9F:CO and R3:240.B25D:CO. Full details are given in Pumphrey et al. [2007] and Livesey et al. [2008].

Differences between v3.3 and v2.2

In the stratosphere, the main change has been that the smoothing used in the retrieval has been tightened up somewhat. The resulting f eld is rather less noisy at the cost of slightly degraded vertical resolution (typically 3.5 – 5 km where v2.2 had 2.7 – 4.0 km). In the troposphere, the 50% positive bias at 215 hPa has been more-or-less eliminated. However, the ability of the retrieval to separate clouds and CO is considerably worse than in v2.2. Users need to screen tropospheric data, as described below, in order to avoid cloud-contaminated prof les.

At certain times of the year, the CO data are contaminated by a signal from the core of the galaxy, as described by Pumphrey et al. [2009]. In v2.2 the affected prof les were not f agged as bad and the user had to eliminate them based on time and latitude. In v3.3 the prof les affected are f agged as having too few radiances and will be rejected by the usual procedure of rejecting any prof le for which Status is odd.

Resolution

Figure 3.6.1 shows the horizontal and vertical averaging kernels for v3.3 MLS CO. The vertical resolution is in the range 3.5 – 5 km from the upper troposphere to the lower mesosphere, degrading to 6 – 7 km in the upper mesosphere. Down to the 215 hPa level, the vertical averaging kernels are sharply peaked at the level being retrieved, but while the 316-hPa measurement contains contribution from 316 hPa, it has a larger contribution from 215 hPa and a negative contribution around 100 hPa of similar magnitude to that at 316 hPa. The retrieved value at 316 hPa is thus more an extrapolation of the prof le higher in the UTLS than it is an independent measurement at 316 hPa, and it is not recommended for scientif c use. The horizontal resolution is about 200 km in the mesosphere, degrading slowly to 300 km with decreasing height in the stratosphere and more rapidly to about 700 km in the UT/LS region.

Precision

The MLS data are supplied with an estimated precision (the f eld L2gpPrecision) which is the a postiori precision as returned by the optimal estimation. This precision is usually a smaller number in v3.3 than in v2.2. In both versions the precision is greater than the scatter observed in the data in regions of low natural variability. Where the estimated precision is greater than 50% of the a priori precision the data will be inf uenced by the a priori to an undesirably large extent. In such cases, L2gpPrecision is set to be negative to indicate that the data should not be used. Figure 3.6.2 shows both the scatter and estimated precision for CO, with typical prof les for comparison. Note that the random errors are larger than 100% of the mixing

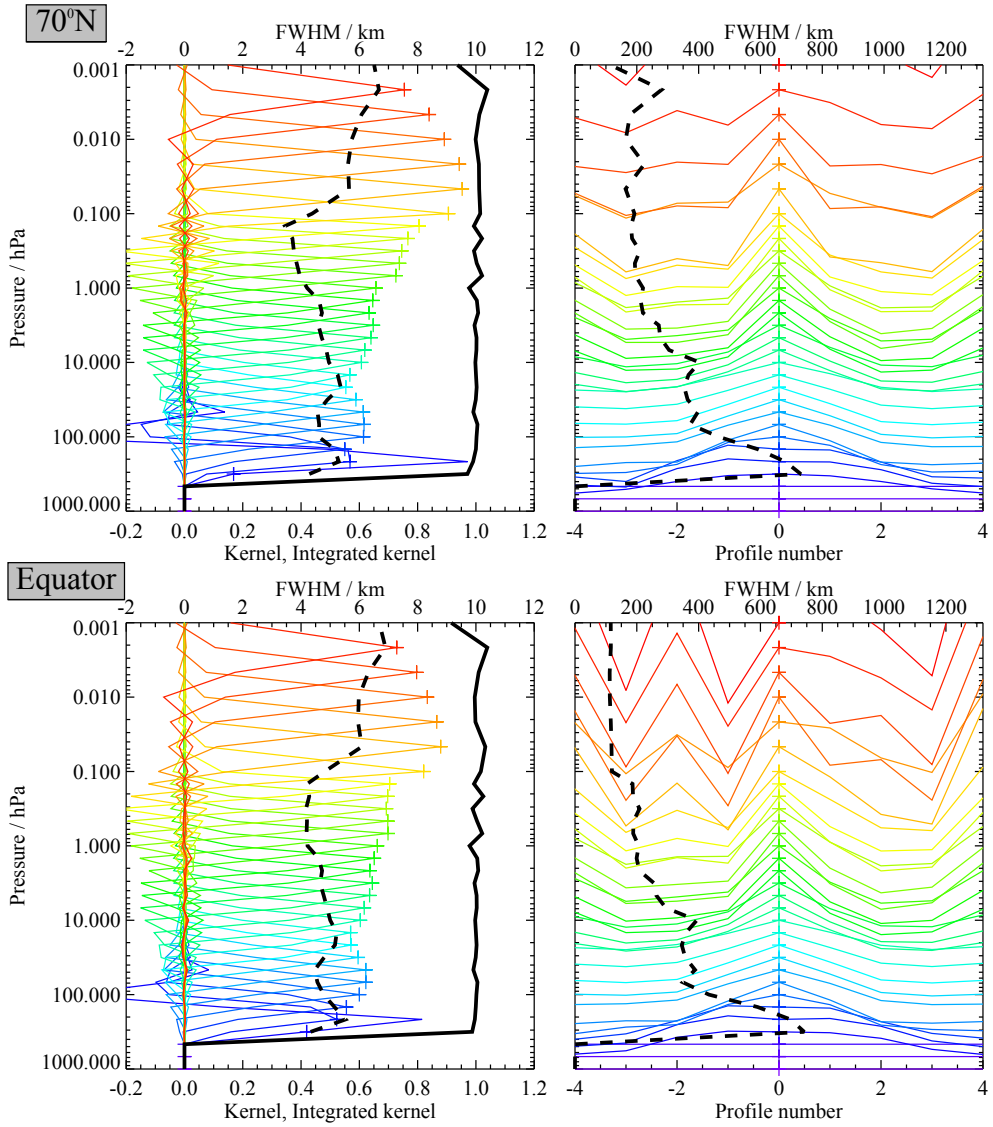

Figure 3.6.1: Typical two-dimensional (vertical and horizontal along-track) averaging kernels for the MLS v3.3 CO data at 70°N (upper) and the equator (lower); variation in the averaging kernels is sufficiently small that these are representative of typical profiles. Colored lines show the averaging kernels as a function of MLS retrieval level, indicating the region of the atmosphere from which information is contributing to the measurements on the individual retrieval surfaces, which are denoted by plus signs in corresponding colors. The dashed black line indicates the resolution, determined from the full width at half maximum (FWHM) of the averaging kernels, approximately scaled into kilometers (top axes). (Left) Vertical averaging kernels (integrated in the horizontal dimension for five along-track profiles) and resolution. The solid black line shows the integrated area under each kernel (horizontally and vertically); values near unity imply that the majority of information for that MLS data point has come from the measurements, whereas lower values imply substantial contributions from a priori information. (Right) Horizontal averaging kernels (integrated in the vertical dimension) and resolution. The horizontal averaging kernels are shown scaled such that a unit averaging kernel amplitude is equivalent to a factor of 10 change in pressure.

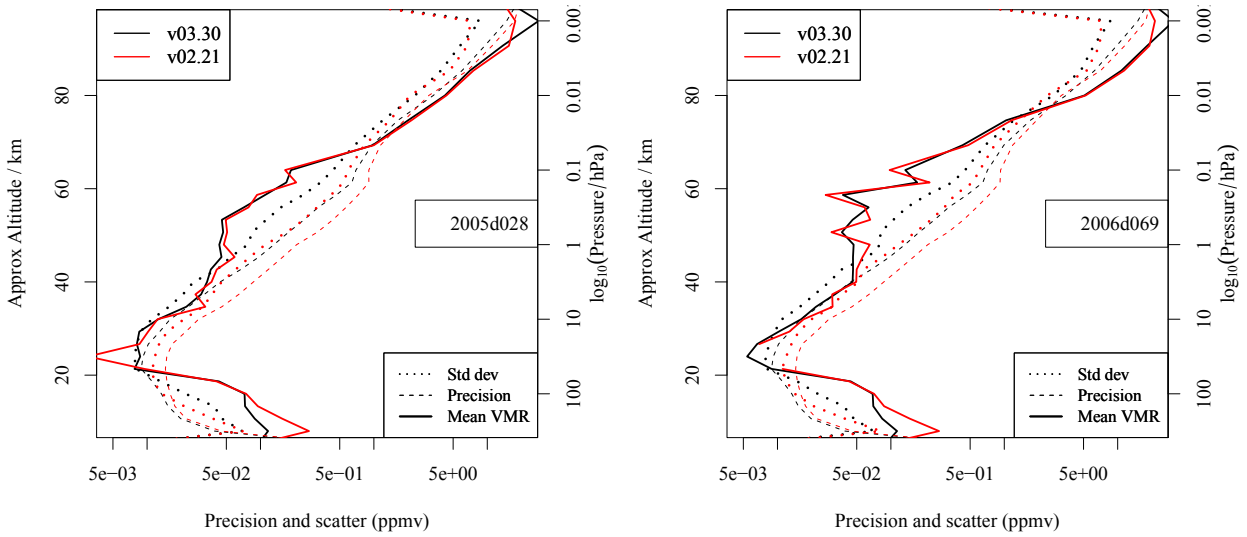

Figure 3.6.2: Scatter (standard deviation) and (estimated) precision for MLS v3.3 (black) and v2.2 (red) CO. The statistics shown are generated from all profiles within 20° of the equator on 28 January 2005 and 10 March 2006. Profiles of the mean volume mixing ratio (VMR) are shown for comparison. The vertical co-ordinate is $16(3 - \log_{10}(\text{Pressure}/\text{hPa}))$ so that 16 km on the axis is exactly 100 hPa.

ratio for much of the vertical range, meaning that signif cant averaging (e.g., daily zonal mean or weekly map) is needed to make use of the data.

Accuracy

The estimated accuracy is summarized in Table 3.6.1. In the middle atmosphere the accuracies are estimated by comparisons with the ACE-FTS instrument; see Pumphrey et al. [2007] for further details. Close inspection of the data suggests that the accuracy in this region is best represented as a purely multiplicative error. The MLS v2.2 CO data at 215 hPa showed high (factor of ∼2) biases compared to other observations. The morphology, however, is generally realistic [Livesey et al., 2008]. In v3.3 this bias has been essentially eliminated through a change in the approach to modeling the background radiance upon which the CO spectral line sits, and a small reduction in the number of MLS spectral channels considered in the retrieval.

Data screening

Pressure range: 215 – 0.0046 hPa.

Values outside this range are not recommended for scientif c use.

Estimated precision: Only use values for which the estimated precision is a positive number.

Values where the *a priori* information has a strong inf uence are f agged with negative precision, and should not be used in scientif c analyses (see Section 1.5).

Status flag: Only use profiles for which the 'Status' field is an even number.

Odd values of `Status` indicate that the prof le should not be used in scientif c studies. See Section 1.6 for more information on the interpretation of the `Status` f eld.

Clouds: Clouds have no impact for pressures of 31 hPa or less. More complex screening rules are needed in the upper troposphere and lower stratosphere, as described below.

Scattering from thick clouds leads to unrealistic values for MLS v3.3 CO in the UTLS, mostly in low latitudes. The application of the `Quality` and `Convergence` screening approaches described below capture many of these. For studies of the upper stratosphere and mesosphere, (at pressures of 31 hPa or smaller) it is not necessary to screen the data for clouds. The low-cloud 'warning' bit set in `Status` identifies most of the profiles that are obviously impacted by clouds, but most of the profiles flagged (11% of profiles globally and 30% in the tropics) are not obviously 'bad,' either geophysically or from the standpoint of retrieval performance.

A more discriminating cloud flagging may be accomplished using the MLS Ice Water Content (IWC) product. Rejection of profiles for which the 147-hPa IWC value is greater than 0.008 g/m^3 discards only 0.8% of global profiles and 3% below 20 degrees latitude and, when used in conjunction with recommended `Quality` <1.1 and `Convergence` >1.4 flagging, does a reasonable job of rejecting cloud impacts while discarding 4.5% of profiles globally and 14% in the tropics.

Quality: Only use profiles with quality greater than 0.2 for pressures of 100 hPa or smaller, and profiles with quality greater than 1.1 at larger pressures

In the stratosphere and mesosphere ($p \leq 100$ hPa) only profiles with a value of the `Quality` field (see Section 1.6) *greater* than 0.2 should be used in scientific study. In the UT/LS ($p > 100$ hPa) a stricter cutoff of 1.1 should be used. This stricter value removes about 4% of the data globally, 9% between 30°S and 30°N.

Convergence: Only profiles whose 'Convergence' field is less than 1.4 should be used.

This test rejects about 1% of profiles; these are typically contiguous blocks of profiles for which the retrieval has failed to converge, so that the retrieved profiles are similar to the a priori.

Artifacts

- Positive systematic error of 20 – 50% throughout the mesosphere.
- Negative systematic error of 50 – 70% near 30 hPa.
- Retrieved profiles are rather jagged, especially between 1 hPa (48 km) and 0.1 hPa (64 km). The greater smoothing applied in v3.3 has reduced this problem considerably but has not eliminated it entirely.
- There is a tendency for negative values to occur at the level below a large positive value. The most striking examples occur in the polar vortex, where air with high CO mixing ratios descends to the mid-stratosphere. This problem is slightly worse in v3.3 – this was considered an acceptable trade-off for the less jagged profiles obtained over most of the middle atmosphere.
- As discussed above, the v3.3 CO retrievals are sensitive to the presence of thick clouds, and the screening procedure described above should be applied before any scientific application of the MLS CO data at pressures greater than 100 hPa.

Review of comparisons with other datasets

In the upper troposphere, comparisons with various in situ CO observations (NASA DC-8, WB-57 and the MOZAIC dataset) indicate that the MLS v2.2 215 hPa CO product is biased high by a factor of ∼2. Initial comparisons show this bias to be largely eliminated in v3.3. Further validation of the v3.3 CO UT/LS retrival levels are underway at the time of this writing.

Table 3.6.1: Data quality summary for MLS version 3.3 CO.

Pressure / hPa	Resolution / km Vert × Horiz.	Precision / ppbv	Systematic Uncertainty	Comment
< 0.001	—	—	—	Not retrieved
0.0022-0.001	—	—	—	Unsuitable for scientif c use
0.0046	7 × 200	11000	+20% to +50%	
0.01	6 × 200	4000	+20% to +50%	
0.046	6 × 200	1200	+20% to +50%	
0.14	3.5 × 200	700	+20% to +50%	
1	4 × 220	150	+20% to +50%	
10	5 × 400	15	±10%	
31	5 × 350	14	−70% to −50%	
100	4.5 × 450	14	±20 ppbv and ±30%	
147	5 × 600	15	±30 ppbv and ±30%	
215	5.5 × 700	19	±30 ppbv and ±30%	
316	—	—	—	Unsuitable for scientif c use
>316	—	—	—	Not retrieved

In the mesosphere, comparisons of v2.2 MLS CO with ODIN-SMR and ACE-FTS suggest a positive bias: 30% – 50% against ACE-FTS, 50% – 100% against SMR. Near 31 hPa, the MLS values are lower than SMR and ACE-FTS by at least 70%. The MLS values have not changed much between v2.2 and v3.3 in the middle atmosphere, so these comparisons may mostly be considered valid for V3.3. What change there is consists of a slight lowering of the MLS values, bringing them slightly towards the ACE-FTS data; 20% is now a better estimate than 30% of the MLS-ACE bias in much of the middle atmosphere.

Desired improvements for future data version(s)

The main goal for future versions is to improve the quality of the CO product in the upper troposphere in the presence of clouds.

CO

3.7 Geopotential Height

Swath name: GPH

Useful range: 261 – 0.001 hPa

Contact: Michael J. Schwartz, **Email:** <Michael.J.Schwartz@jpl.nasa.gov>

Introduction

The MLS v2.2 geopotential height (GPH) product is described in Schwartz et al. [2008]. The v3.3 product is very similar. GPH is retrieved, along with temperature and the related assignment of tangent pressures to limb views, primarily from bands near O_2 spectral lines at 118-GHz and 234 GHz. GPH and Temperature are coupled through hydrostatic balance and the gas law; the change of pressure between levels is the weight of the column between the levels. The GPH difference between a given pressure level and the 100 hPa reference level is the integrated temperature with respect to log-pressure between the levels, scaled by $R/M/g_0$, where R is the gas constant, M is the molar mass of air, and g_0 is mean sea-level gravity. Only one element of GPH (chosen to be the value at 100 hPa in the MLS Level 2 processing) is independent of the temperature prof le. Table 3.7 summarizes the measurement precision, modeled accuracy and observed biases. The following sections provide details.

Differences between v3.3 and v2.2

The v3.3 GPH product is very similar to the v2.2 product, with typical mean differences ranging from 0 – 20 m from 261 hPa to 0.01 hPa and with typical scatter about the mean difference of 25 – 50 m up to 0.05 hPa. At 0.001 hPa, v3.3 has a 50 – 150 m high bias with respect to v2.2, and the scatter between the two versions rises to 100 – 200 m at 0.01 – 0.001 hPa, with the largest differences near the equator. Seasonal and latitudinal variations in the difference between v2.2 and v3.3 GPH are on the order of ±40 m peak-to-peak from 261 –1 hPa increasing to greater 200 m at 0.001 hPa. As with temperature, the 316-hPa level of v3.3 GPH is not recommended for scientif c use. The standard v3.3 GPH product is reported on the same 55-level grid as is the v3.3 temperature rather than the 47-level grid of v2.2, adding eight more levels in the upper stratosphere.

Vertical resolution

The GPH prof le is vertically-integrated temperature, so its vertical resolution is not well-def ned. The vertical resolution of the underlying temperature given in Section 3.21 is repeated in Table 3.7.

Precision

MLS v3.3 GPH precision is summarized in Table 3.7. Precision is the random component of measurements that will average-down if a measurement is repeated. The retrieval software returns an estimate of GPH precision only for the 100 hPa reference level, as this is the only element included in the MLS "state vector." GPH precision at other standard-product prof le levels (summarized in column 2 of Table 3.7) is calculated from the GPH precision at the reference level and the prof le of temperature precisions. Calculated precision values are ∼35 m from 261 hPa to 100 hPa, ∼45 m at 1 hPa, ∼110 m at 0.001 hPa. Off-diagonal elements of the temperature/GPH error covariance matrix are neglected in this GPH-precision-prof le calculation, but resulting errors are believed to be small (∼5 m near 100 hPa.)

Accuracy

The accuracy of the v2.2 GPH was modeled based upon consideration of a variety of sources of systematic error, as discussed in [Schwartz et al., 2008]. V3.3 accuracy is believed to be substantially similar and the results of the v2.2 calculations are given in column four of Table 3.7. Of the error sources considered, modeled amplifier non-linearity had the largest impact, just as is the case with the calculation for temperature. Simulations suggest that gain compression introduces a positive biases in MLS GPH of ∼150 m at 100 hPa that increase to 200 m at 10 hPa and to 700 m at 0.001 hPa. These values are the first terms in column four of Table 3.7. The second terms in column four are model-based estimates of the bias magnitude from other sources including uncertainty in pointing/field-of-view, uncertainty in spectroscopic parameters, and retrieval numerics. The combined bias magnitudes due to these sources is 100 – 150 m.

"Observed bias uncertainty" in Table 3.7 is an estimate of bias based upon comparisons with analyses and with other previously-validated satellite-based measurements. These comparisons were made using MLS v2.2, but as the biases between v2.2 and v3.3 GPH are generally less than 20 m from 261 –0.1 hPa, these results hold for v3.3 as well. The primary sources of correlative data were the Goddard Earth Observing System, Version 5.0.1 data assimilation system (GEOS-5) [Reinecker et al., 2007], used in the troposphere and lower stratosphere, and the Sounding of the Atmosphere using Broadband Radiometry (SABER) [Mlynczak and Russell, 1995], used in the upper stratosphere through the mesosphere. MLS has a 150 m high bias relative to analyses (GEOS-5) at 100-hPa that drops to 100 m at 1 hPa. Biases with respect to SABER are small at 0.1 hPa but increasingly negative at higher levels, reaching -600 m at 0.001 hPa, but with significant latitudinal and seasonal variability.

Data screening

GPH should be screened in the same way as is temperature:

Pressure range: 261 – 0.001 hPa.

Values outside this range are not recommended for scientific use.

Estimated precision: Only use values for which the estimated precision is a positive number.

Values where the *a priori* information has a strong influence are flagged with negative precision, and should not be used in scientific analyses (see Section 1.5).GPH precision is set negative at and beyond any level in the integration of temperature away from the 100-hPa reference level where temperature has negative precision.

Status flag: Only use profiles for which the 'Status' field is an even number.

Odd values of `Status` indicate that the profile should not be used in scientific studies. See Section 1.6 for more information on the interpretation of the `Status` field.

Clouds: Clouds can impact GPH measurements in the upper troposphere (261 – 100 hPa). Screening rules are given below.

GPH `Status` Clouds impact MLS v3.3 GPH only in the troposphere, predominantly in the tropics and to a lesser extent in mid-latitudes. Recommended screening in the troposphere is the same as for temperature. If the low-cloud bit (the fifth least significant bit) is set in either of the two profiles following a given profile, then that profile should be considered to be potentially impacted by cloud. The misalignment of cloud information by 1 – 2 profiles along track is discussed in Wu et al. [2008]. The method flags 16% of tropical and 5% of global profiles as cloudy. The last two profiles of a day cannot be screened this way, and should not be used in the troposphere.

Region	Resolution Vert. × Horiz. / km	Precision[a] / meters	Modeled bias uncertainty / m	Observed bias uncertainty / m	Comments
<0.001 hPa	—	—	—	—	Unsuitable for scientif c use
0.001 hPa	10–13 × 220	±110	700±150	−450	
0.01 hPa	8–12 × 185	±85	600±100	−100	
0.1 hPa	6 × 165	±60	500±150	0	
1 hPa	7 × 165	±45	300±100	100	
10 hPa	4.3 × 165	±35	200±100	100	
100 hPa	5.2 × 165	±30	150±100	150	
261 hPa	5.3 × 170	±35	100±150	150	
1000 – 316 hPa	—	—	—	—	Unsuitable for scientif c use

[a]Precision on individual prof les

Quality: Only profiles whose 'Quality' field is greater than 0.65 should be used.

This threshold typically excludes 1% of prof les.

Convergence: Only profiles whose 'Convergence' field is less than 1.2 should be used.

Use of this threshold typically discards 0.1% of prof les.

Review of comparisons with other data sets

The 100 hPa reference GPH is typically 100 – 250 m higher than GEOS-5 in the northern high latitudes and 50 – 200 m higher than GEOS-5 in the Southern high latitudes. As GPH prof les are calculated relative to the reference level, biases at 100 hPa move entire prof les up and down. At low latitudes, the GPH observations taken on the ascending branch of the orbit are typically 0 – 120 m higher than GEOS-5. while those from descending branch are 100 – 200 m higher. A seasonal cycle in the daily mean ascending/descending differences of ∼100 m peak-to-peak is evident in the high-southern latitudes (peaking in January) and in the ascending branch of the equatorial mean differences (peaking in July) There has been a general downward trend in the MLS minus GEOS-5 bias of 40 – 50 m/year over the life of the mission. Like v2.2 GPH, v3.3 GPH has a bias of ∼100 m at 10 hPa with respect to GEOS-5 and SABER, and the bias with respect to SABER becomes increasingly negative at lower pressures: ∼ −100 m at 0.01 hPa and ∼ −500 m at 0.001 hPa. These negative biases ref ect the general low temperature bias of MLS with respect to SABER.

Desired improvements for future data version(s)

Reduction of biases in the GPH product likely requires improvement of our ability to model atmospheric radiative transfer and/or the measurement system to improve the f t between the forward model and observed radiances near the O_2 spectral lines from which temperature and pointing information are extracted. The simple model of "gain compression" proposed during v2.2 validation proved inadequate during v3.3 development, but research in this area is ongoing. Some seasonally and latitudinally-repeating systematic errors in GPH may be the result of error in the absolute pointing reference that is taken from the spacecraft attitude and ephemeris data stream. Reduction of these systematic errors is an area of ongoing research.

GPH

3.8 Water Vapor

Swath name: H2O

Useful range: 316 – 0.002 hPa

Contact: Alyn Lambert (stratosphere/mesosphere), **Email:** <Alyn.Lambert@jpl.nasa.gov>
William Read (troposphere), **Email:** <William.G.Read@jpl.nasa.gov>

Introduction

The standard water vapor product is taken from the 190 GHz (CorePlusR2A) retrieval. The vertical grid for H_2O is: 1000 – 1 hPa, 12 levels per decade change in pressure (lpd), 6 lpd for 1.0 – 0.1 hPa, and 3 lpd for $0.1 - 10^{-5}$ hPa. The horizontal grid is every 1.5° along the orbit track. It is unusual among MLS products in that it is assumed that the logarithm of the mixing ratio, and not mixing ratio itself, varies linearly with log pressure.

The MLS v3.3 H_2O between 1000 and 383 hPa is taken from a retrieval of relative humidity with respect to ice (RHi) product converted to specif c humidity using the Goff-Gratch vapor pressure over ice equation. This RHi is not a vertically resolved measurement and all levels between 1000 and 383 hPa have the same RHi. See section 3.19 for more information. Validation of MLS v2.2 water vapor is presented in Read et al. [2007] and Lambert et al. [2007]. This section reiterates the key information from those studies, and updates them for v3.3. Table 3.8.1 gives a summary of MLS v3.3 H_2O precision, resolution, and accuracy.

Summary of changes from v2.2

The H_2O line width was narrowed by 4% based on cavity absorption measurements by A. Meshkov [Ph. D. Thesis, 2006]. The f ne grid (12 lpd) representation basis was extended upwards from 22 hPa to 1 hPa. These changes successfully removed the H_2O kink artifact present in v2.2 at 32/26 hPa. Vertical smoothing was relaxed near 1.0 hPa to improve the vertical resolution of H_2O in the mesosphere.

Figure 3.8.1 compares MLS v3.3 to v2.2. At most levels, the average difference is small – less than 10%. The zig-zag artifact in v2.2 between 31 and 26 hPa has been removed in v3.3. At higher latitudes, where the 215 hPa surface is mostly in the stratosphere, v3.3 is now ∼20% wetter. The moistening of the 215 hPa surface is a good development but as can be seen in Figure 3.8.1, it is likely that MLS is still too dry at latitudes $>60°$, at this pressure.

Humidity data at pressures greater than 316 hPa are derived from a broad layer relative humidity retrieval (using low limb viewing MLS wing channel radiances) similar to that obtained from NOAA operational humidity sounders such as TOVS. As noted in [Read et al., 2007], the v2.2 retrieval at these pressures was likely to be ∼30% too high based on comparisons with AIRS. The accuracy of this retrieval is highly sensitive to the transmission eff ciency of the MLS optics system. In v3.3 this was adjusted empirically (within the uncertainty range established from MLS calibration) to give better agreement with AIRS in the tropics. This retrieval is used as an a priori and prof le constraint for the humidity prof le at pressures greater than 316 hPa which are not retrieved in the standard H_2O product retrieval. As explained in Read et al. [2007], the empirical adjustment to the antenna transmission has essentially no direct affect on the H_2O retrievals at smaller pressures. A bigger indirect impact is that the 316 hPa level becomes moister to compensate for the drier sub 316 hPa levels.

The third panel in Figure 3.8.1 shows the mean estimated single prof le precision and the measured variability (which includes instrument noise and atmospheric variability). The precisions for the two versions are nearly identical except for pressures less than 21 hPa where the higher grid resolution in v3.3 leads to poorer precision. The v3.3 H_2O is ∼0.2 – 0.3 ppmv wetter than v2.2 in the pressure range 83 – 0.1 hPa

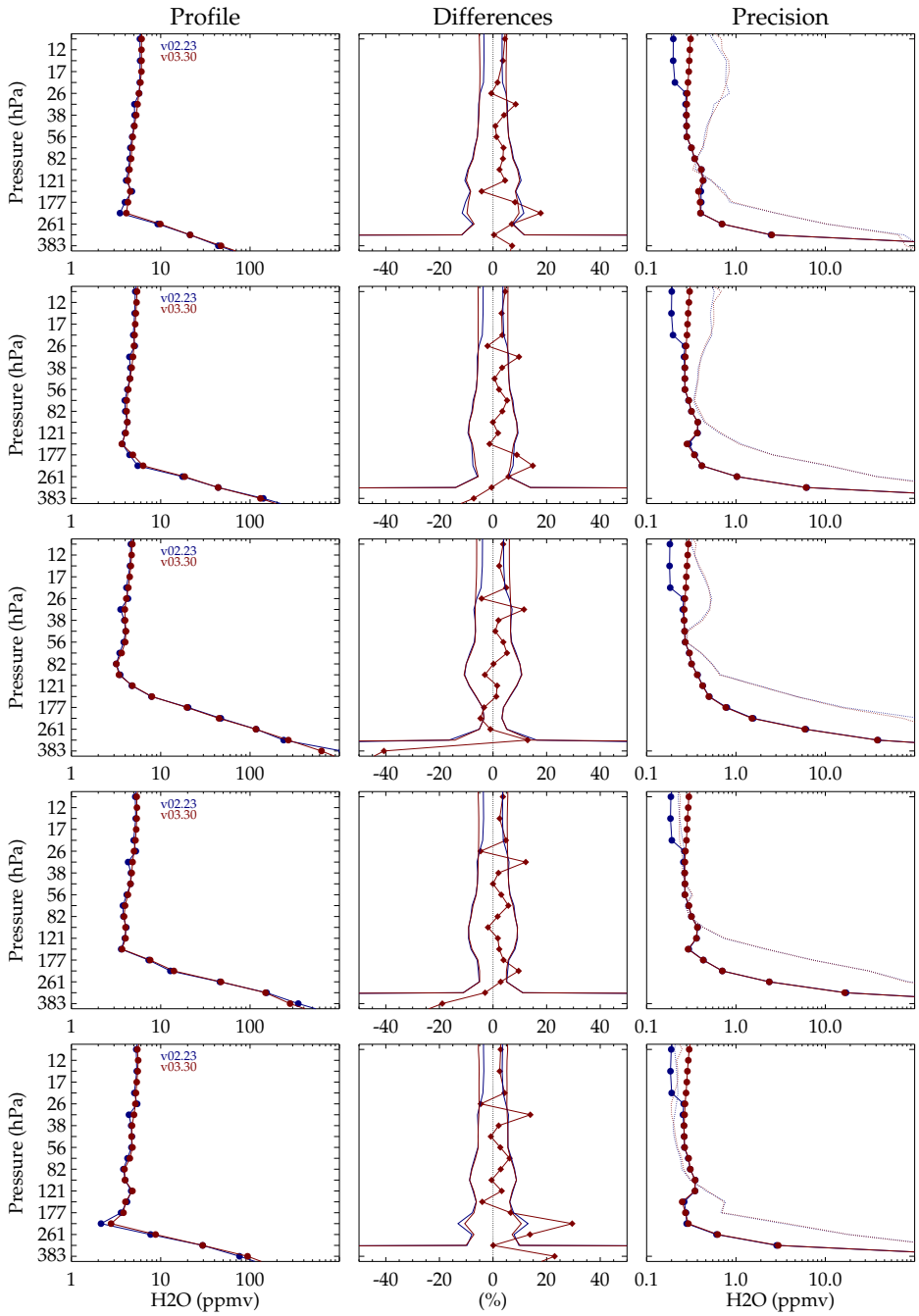

Figure 3.8.1: A comparison of v2.2 (blue) to v3.3 (red) water vapor for Jan-Feb-Mar 2005 in 5 lattiude bands. Other time periods are similar. The left panel compares mean profiles, the center shows the mean difference (red diamonds) surrounded by each versions' estimated precision, and the right panel shows the estimated retrieval precision (solid and bullets) and measured variability (dotted) which includes atmospheric variability about the mean profile.

Resolution

The spatial resolution is obtained from examination of the averaging kernel matrices shown in Figure 3.8.2. The vertical resolution for H_2O is in the range 2.0 – 3.7 km from 316-0.22 hPa and degrades to 6 – 11 km for pressures lower than 0.22 hPa. The along track horizontal resolution is ∼210 – 360 km for pressures greater than 4.6 hPa, and degrades to 400 – 740 km at lower pressures. The horizontal cross-track resolution is the 7 km full width half maximum of the MLS 190-GHz field-of-view for all pressures. The longitudinal separation of the MLS measurements is 10° – 20° over middle and lower latitudes, with much finer sampling in polar regions.

Precision

Table 3.8.1 summarizes the estimated precision of the MLS v3.3 H_2O data. For pressures ≥83 hPa, the precisions given are the 1-σ scatter about the mean of coincident comparison differences, which are larger than the formal retrieval precisions [Read et al., 2007]. For pressures ≤68 hPa, a summary of the formal retrieval precisions calculated by the Level 2 algorithms are given. These are generally comparable to the scatter of coincident ascending/descending MLS profile differences, but become larger in the mesosphere [Lambert et al., 2007]. The individual Level 2 precisions are set to negative values in situations when the retrieved precision is larger than 50% of the a priori precision – an indication that the data are biased toward the a priori value.

Accuracy

The values for accuracy are based primarily on two sources: comparisons with validated instruments and a systematic error analysis performed on the MLS measurement system [Read et al., 2007] and [Lambert et al., 2007] (performed for v2.2, but expected to be equally applicable to v3.3). For pressures between 316 – 178 hPa, Comparisons between AIRS v5 and MLS v3.3 have larger biases than were present between AIRS v4 and MLS v2.2. For MLS retrieved values between 10 and 100 ppmv, AIRS v5 is on average ∼20% wetter than MLS. At the low humidity extreme (10 ppmv), MLS measures about half that of AIRS. For MLS measurements greater than 100 ppmv – only affecting pressures between 215 – 316 hPa, the agreement is much better, near 5%.

The values in the table for these pressures are AIRS validated accuracies which are better than those theoretically expected for the MLS measurement system. For the pressure range 178 – 83 hPa, the quoted values come directly from the systematic error analysis performed on the MLS measurement system. Few comparisons with reliable instrumentation exist for pressures between 178 – 147 hPa. These comparisons which include in situ sensors on the WB57 and frostpoint hygrometers flown on balloons indicate better performance than indicated in the table. An estimate of the accuracy between 121 – 83 hPa is also from the systematic error analysis performed on the MLS measurement system. Comparisons among in situ sensors on the WB57 high altitude aircraft and frostpoint hygrometers flown on balloons show 30% disagreements – well in excess of the estimate accuracy of each instrument including MLS – near the tropopause and lower stratosphere. The balloon based frost point hygrometer shows agreement better than indicated in the table. The validation paper describes in detail why a 30% spread is inconsistent with the MLS measurements [Read et al., 2007]. For pressures less than 83 hPa, the accuracy is based on the systematic error analysis.

Data screening

Pressure range: 316 – 0.002 hPa.

Values outside this range are not recommended for scientific use.

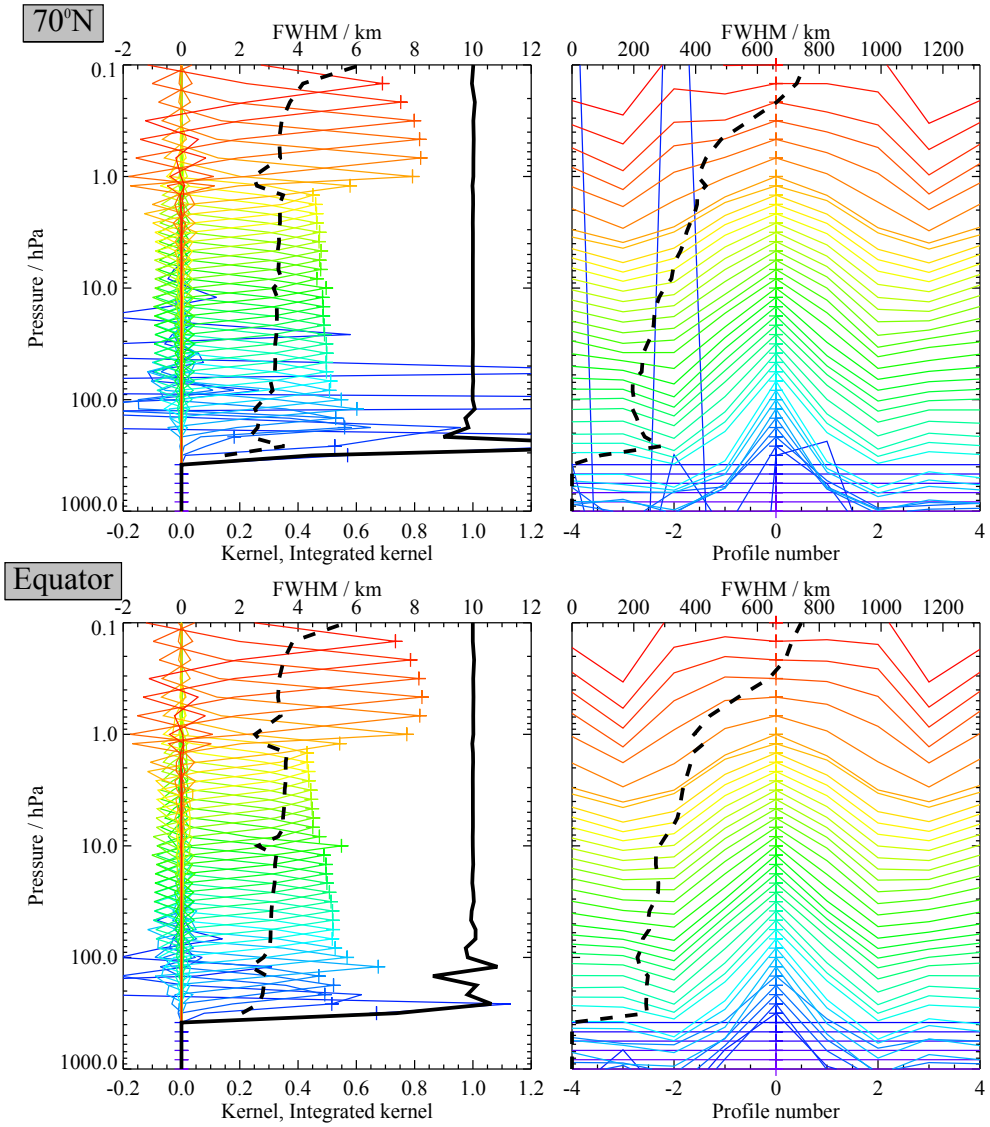

Figure 3.8.2: Typical two-dimensional (vertical and horizontal along-track) averaging kernels for the MLS v3.3 H_2O data at 70°N (upper) and the equator (lower); variation in the averaging kernels is sufficiently small that these are representative of typical profiles. Colored lines show the averaging kernels as a function of MLS retrieval level, indicating the region of the atmosphere from which information is contributing to the measurements on the individual retrieval surfaces, which are denoted by plus signs in corresponding colors. The dashed black line indicates the resolution, determined from the full width at half maximum (FWHM) of the averaging kernels, approximately scaled into kilometers (top axes). (Left) Vertical averaging kernels (integrated in the horizontal dimension for five along-track profiles) and resolution. The solid black line shows the integrated area under each kernel (horizontally and vertically); values near unity imply that the majority of information for that MLS data point has come from the measurements, whereas lower values imply substantial contributions from a priori information. (Right) Horizontal averaging kernels (integrated in the vertical dimension) and resolution. The horizontal averaging kernels are shown scaled such that a unit averaging kernel amplitude is equivalent to a factor of 10 change in pressure.

Estimated precision: Only use values for which the estimated precision is a positive number.

Values where the *a priori* information has a strong influence are flagged with negative precision, and should not be used in scientific analyses (see Section 1.5).

Status flag: Only use profiles for which the 'Status' field is an even number.

Odd values of `Status` indicate that the profile should not be used in scientific studies. See Section 1.6 for more information on the interpretation of the `Status` field.

Clouds: The cloud status flag bits (16 or 32) can be ignored for pressures less than 100 hPa. For pressures $\geq$ 100 hPa, profiles having the high or low cloud status flag bits set should be ignored in scientific studies. See artifacts for more details.

Quality: Only profiles whose 'Quality' field is greater than 1.3 should be used.

This eliminates ∼5% of the profiles on a typical day.

Convergence: Only profiles whose 'Convergence' field is less than 2.0 should be used.

Artifacts

There is a minimum concentration where MLS H_2O measurements become unreliable. This is given in Table 3.8.1 under the "Min. H_2O" column. The lowest allowable H_2O is 0.1 ppmv. Differences between middle tropospheric H_2O constraint used in the retrieval and the real atmospheric state can cause errors at 316 and 261 hPa. The error manifests as dry ($<$1 ppmv) and moist spikes in an orbital time series. Such data are often accompanied with good quality and status.

Clouds in the field of view degrade the data in unpredictable ways. Most instances of quality $<$1.3 occur in the presence of clouds; and therefore when clouds adversely affect the incoming MLS signal are successfully screened. However, not all MLS signals are obviously affected. Coincident comparisons of MLS cloud flagged H_2O (`status` bit 16 or 32 set between 316 – 215 hPa) with good quality AIRS show a small mean bias of 10% but exhibit a 50% increase in variability for the individual differences. Therefore users should be aware that, although the overall biases for measurements inside clouds are similar to that for clear sky, individual profiles will exhibit greater variability about the actual atmospheric humidity.

Review of comparisons with other datasets

Figure 3.8.3 shows a latitude-value zonal mean comparison among several satellite data sets. The satellite datasets include MLS v3.3, AIRS v5, ACE-FTS v2, MIPAS IMK v4, HALOE v19, Odin SMR continuum H_2O, and Odin SMR line resolved H_2O. Agreement with ACE-FTS is much better than is suggested in figure 3.8.3 if only coincidently measured profiles are compared [Lambert et al., 2007]. The ACE-FTS comparison shown here is degraded by the very different sampling between the thermal emission and occultation techniques. With few exceptions, MLS shows very good agreement with MIPAS at most pressures and latitudes and with AIRS. One likely issue in MLS is its tendency to underestimate H_2O at 215 and 261 hPa at high latitude where these pressure levels are near the tropopause. This behavior is also present in the MLS v2.2 product. Other satellite techniques such as MIPAS and ACE-FTS show significantly wetter values. AIRS also shows wetter values but they are probably mostly a priori because the AIRS technique is not accurate for such low values.

Apart from the differences noted above, the MLS v3.3 H_2O is similar to the MLS v2.2 product described and validated in Read et al. [2007] and Lambert et al. [2007]. A revised validation paper for H_2O is not planned in the near future and users are encouraged to read Read et al. [2007] and Lambert et al. [2007] for more information.

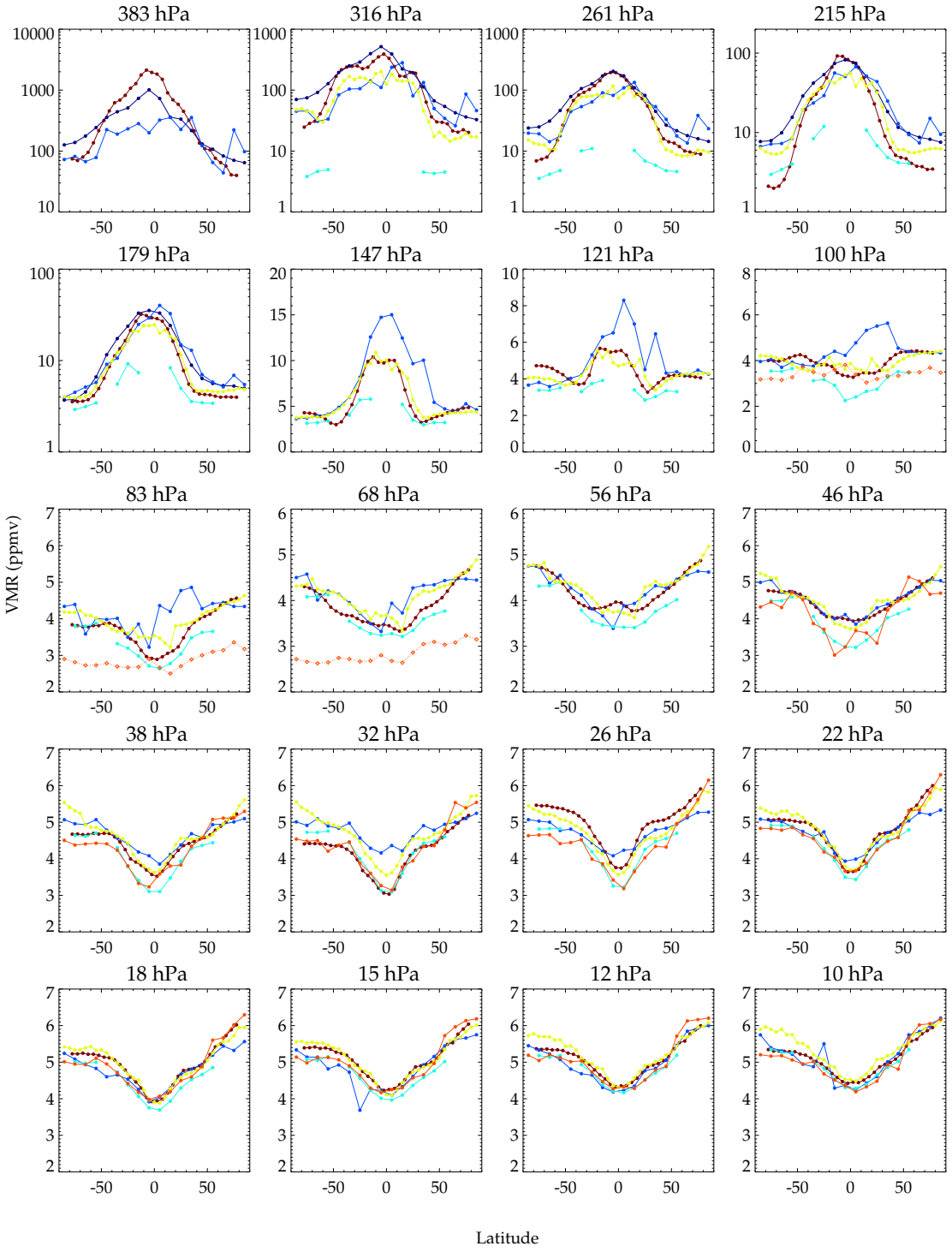

Figure 3.8.3: A comparison of MLS v3.3 (red) water vapor for Jan-Feb-Mar 2005 with other satellite observations shown as latitude-value zonal means. Each panel represents a pressure surface. The satellites are: AIRS v5 (dark blue), ACE-FTS v2 (light blue), MIPAS IMK v4 (yellow-green), HALOE v19 (cyan), Odin SMR 544 GHz continuum product (orange open diamonds), and Odin SMR line resolved product (orange solid bullets).

Table 3.8.1: Summary of MLS v3.3 H_2O product.

Pressure / hPa	Resolution V×H / km	Precision[a] / %	Accuracy / %	Min. / ppmv[b]	Comments
<0.002	—	—	—	—	Unsuitable for scientif c use
0.002	11 × 410	190	34	0.1	
0.004	12 × 560	86	16	0.1	
0.010	10 × 680	54	11	0.1	
0.022	10 × 740	42	9	0.1	
0.046	8 × 540	30	8	0.1	
0.10	6 × 490	20	8	0.1	
0.22	3.7 × 680	18	7	0.1	
0.46	3.4 × 510	13	6	0.1	
1.00	2.5 × 410	7	4	0.1	
2.15	3.5 × 400	6	5	0.1	
4.64	3.4 × 360	6	7	0.1	
10	3.2 × 300	6	9	0.1	
22	3.3 × 270	6	7	0.1	
46	3.2 × 240	6	4	0.1	
68	3.1 × 220	8	6	0.1	
83	3.1 × 220	10	7	0.1	
100	2.8 × 210	15	8	0.1	
121	2.5 × 210	20	12	0.1	
147	2.7 × 230	20	15	0.1	
178	2.6 × 230	25	20	3	
215	2.7 × 240	40	25	3	Large low bias for latitudes > 60°
261	2.5 × 240	35	20	4	Large low bias for latitudes > 60°
316	2.0 × 240	65	15	7	Occasionally erroneous low value < 1 ppmv and high value f iers are retrieved in the tropics, usually in clouds.
>316	—	—	—	—	Unsuitable for scientif c use

[a] Precision for a single MLS prof le

[b] Minimum H_2O is an estimate of the minimum H_2O concentration measurable by v3.3 MLS.

Desired improvements for future data version(s)

We want to improve performance in clouds by incorporating a cloud radiation scattering forward model and reduce the dry bias at high lattiudes for pressures near the tropopause (261 and 215 hPa).

3.9 Hydrogen Chloride

Swath name: HCl

Useful range: 100 – 0.32 hPa

Contact: Lucien Froidevaux, **Email:** <Lucien.Froidevaux@jpl.nasa.gov>

Introduction

As in the previous MLS HCl data version, v2.2, the MLS v3.3 retrievals of the HCl standard product (from the 640 GHz radiometer) use channels from band 14, as a result of the deterioration observed since early 2006 in nearby band 13, originally targeted (with narrower channels than band 14) at the main HCl emission line center. Full measurement days with band 13 on from February 15, 2006, to the time of writing (December 2010) are as follows: March 15, 2006 (2006d074), April 14, 2006 (2006d104), January 6 through 8, 2009 (2009d006 – 2009d008), and January 24 through 27, 2010 (2010d024 – 2010d027). For days prior to February 16, 2006 and for the few days (as listed above) when band 13 is turned on thereafter, the MLS Level 2 software also produces a separate HCl-640-B13 product (stored in the L2GP-DGG file), using the band 13 radiances. This product has slightly better precision and vertical resolution in the upper stratosphere than the standard HCl product. The MLS team plans to turn band 13 on for a few days about once every year or two (or maybe even less frequently) in order to preserve its lifetime, estimated at a few days to a few weeks, based on the channel counts and channel noise characteristics observed during the 3-day turn-on period in late January, 2010. It is possible/likely that this band will not be turned on again until early 2012. Band 13 should provide better trend information for upper stratospheric data, given its narrower channels. Upper stratospheric trends from the (uninterrupted 2004 to present) band 14 retrievals are too small, compared to band 13 data and expectations (as well as versus ACE-FTS HCl data).

See Figure 3.9.1 for an illlustration of the trend differences between these two MLS band measurements of upper stratospheric HCl. In the lower stratosphere, however, variations in the two HCl products are closer together, and seasonal/geographical variability are more pronounced. We believe that the band 14 daily global retrievals are completely suitable for use in studies of seasonal and geographical variations (e.g., during polar winter/spring).

Table 3.9.1 summarizes the MLS HCl resolution, precision, and accuracy estimates as a function of pressure. More discussion and data screening recommendations for the MLS HCl v3.3 data are provided below. Analyses describing detailed validation of the MLS (v2.2) product and comparisons with other data sets are described in Froidevaux et al. [2008b]. Based on the fairly small overall changes in v3.3 HCl data (versus v2.2), the conclusions of the latter reference should remain essentially unchanged. Any minor updates will result from new comparisons between MLS (v3.3) HCl and ACE-FTS HCl, which is also being updated to a newer version (version 3). We do not expect the systematic uncertainty estimates in Table 3.9.1 to change significantly; however, an MLS team review of those estimates is anticipated.

Changes from v2.2

While there were no large v3.3 algorithmic changes relating to HCl, one difference in the retrievals for HCl and other products derived from the 640-GHz MLS retrievals is that temperature information is now obtained from the first retrieval phase ('Core'), as opposed to the 640-GHz phases themselves; this led to overall improved efficiency, convergence, and stability for the v3.3 640-GHz products. A Level 1 change, resulting from a small error in the spectral calibration files, which led to all filter channel responses being shifted by a small fraction (1%) of the nominal channel widths, also had an impact on the HCl results.

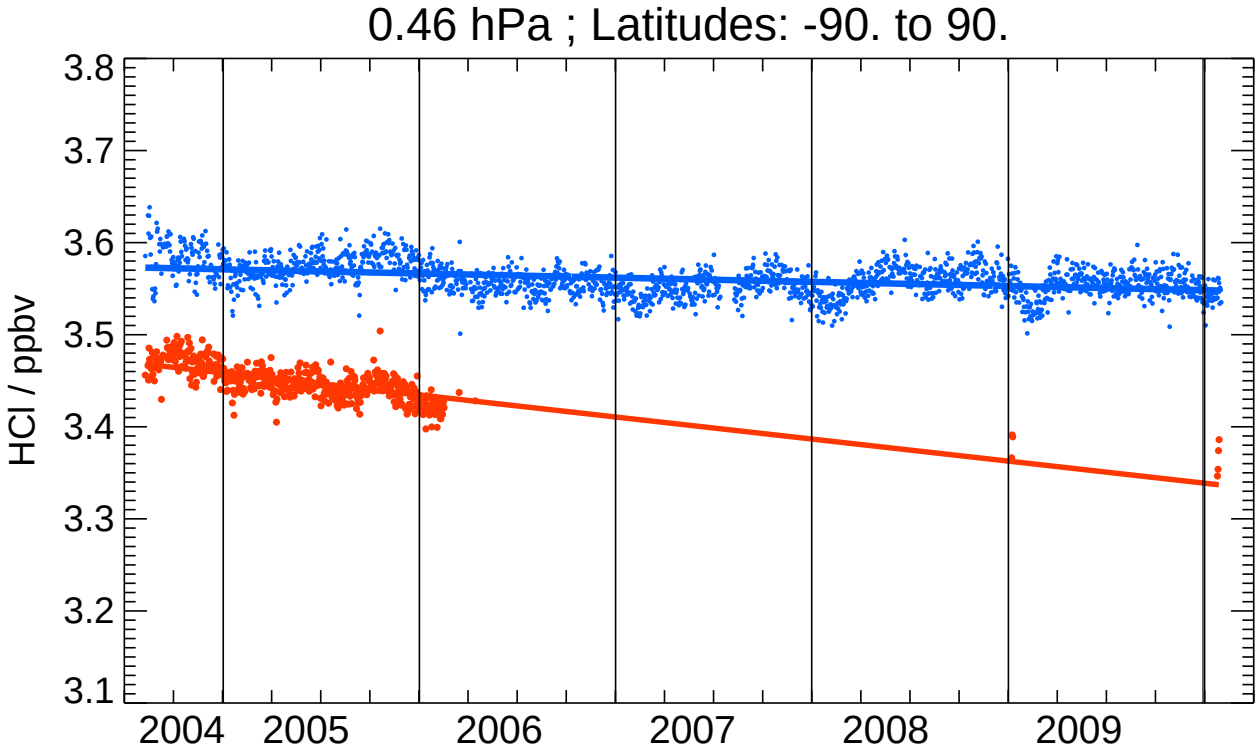

Figure 3.9.1: Daily zonal averages for MLS HCl at 0.46 hPa, from mid-August, 2004, through January, 2010, for the originally-targeted band 13 measurements (red points), now available only on occasion (to preserve lifetime), and the band 14 data (blue points). The lines are simple linear fits through the daily data points; trend differences are apparent in this region of the atmosphere, where the information obtained from band 14 HCl data is not reliable enough.

Mainly because of this change, v3.3 MLS HCl abundances near and just above the stratopause are a few percent less than the v2.2 abundances, and exhibit a steeper slope near very the top of the recommended pressure range. The slight oscillating behavior in HCl near 0.15 to 0.1 hPa has led us to change the top boundary for recommended HCl profiles to the MLS retrieval level at 0.32 hPa. This issue does not seem to affect the band 13 MLS measurement of HCl, which can in principle be used (on available measurement days) up to the 0.15 hPa level.

Other changes relating to the treatment of forward model radiance continuum had an impact on species in the 640-GHz retrievals (mainly in the lower stratosphere). The background observed in the 640 GHz radiances includes emissions from N_2, O_2, and H_2O. There are laboratory-based and ground-based models for the continuum absorptions that are the basis for the MLS absorption model [*Pardo, 2001*, and references therein]. These models were tested against MLS extinction measurements from the wing channels in the 640 GHz radiometer; the latitude dependence of this extinction was found to agree better with the expected most plus dry continuum extinction values if the dry and moist continuum functions were scaled by factors close to 20%. The incorporation of this change improved the lower stratospheric retrievals of most of the 640-GHz species (generally in terms of average negative biases and their latitude dependence).

A comparison plot showing zonal average HCl contours and differences between the two data versions for a typical month (April, 2006) is provided in Figure 3.9.2. For pressures larger than or equal to 0.22 hPa, the average differences between the two data versions are typically within 0.1 ppbv (a few percent). The average changes (globally within a few percent in most of this pressure range for typical months) are within the estimated accuracy values (see Table 3.9.1), which we have now changed (increased) to a value of 10% (or about 0.3 ppbv) for pressures less than 10 hPa, given the trend issue for upper stratospheric HCl mentioned above. The largest percentage changes in HCl occur for very small mixing ratio values; v3.3 values can be larger than the v2.2 values by 20 to 50% (or more) under low HCl conditions in the lower stratosphere at low latitudes or during winter at polar latitudes, even if these percentages typically only reflect an increase of 0.1 ppbv (or less). On occasion, however, v2.2 zonal averages at 100 hPa (mainly) or during southern hemisphere polar winter conditions at low altitude were slightly negative; this is no longer the case for v3.3 data. Whether the larger v3.3 values at 100 hPa (with averages now slightly above 0.1 ppbv at low latitudes) are more realistic than v2.2 data remains to be seen, but this is a fairly minor change. The precision estimated in the Level 2 files is essentially unchanged from v2.2.

Resolution

Typical (rounded off) values for resolution are provided in Table 3.9.1. Based on the width of the averaging kernels shown in Figure 3.9.3, the vertical resolution for the standard HCl stratospheric product is ~3 km (2.7 km at best in the lower stratosphere), or about double the 640 GHz radiometer vertical field of view width at half-maximum; the vertical resolution degrades to 4–6 km in the lower mesosphere. The along-track resolution is ~200 to 350 km for pressures of 2 hPa or more, and ~500 km in the lower mesosphere. The cross-track resolution is set by the 3 km width of the MLS 640 GHz field of view. The longitudinal separation of MLS measurements, set by the Aura orbit, is $10^\circ - 20^\circ$ over middle and lower latitudes, with much finer sampling in polar regions.

Precision

The estimated single-profile precision reported by the Level 2 software varies from ~0.2 to 0.6 ppbv in the stratosphere (see Table 3.9.1), with poorer precision obtained in the lower mesosphere. These precision values have not changed significantly for v3.3 data. The Level 2 precision values are often only slightly lower than the observed scatter in the data, as evaluated from a narrow latitude band centered around the equator where atmospheric variability is often smaller than elsewhere, or as obtained from a comparison

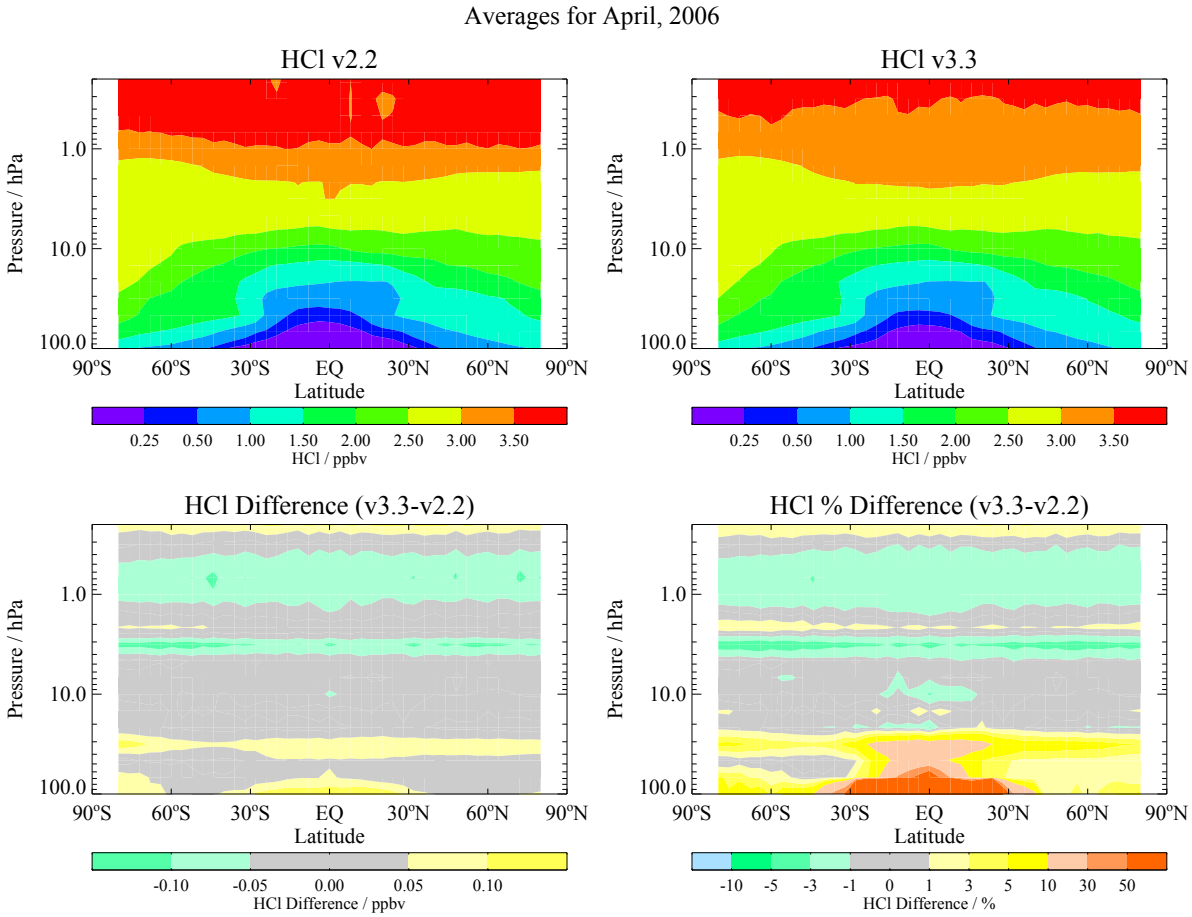

Figure 3.9.2: Zonal averages for MLS HCl profiles during April, 2006, showing the MLS v2.2 HCl mixing ratio contours (top left panel), the v3.3 contours (top right panel), and their differences in ppbv (v3.3 minus v2.2, bottom left panel) and percent (v3.3 minus v2.2 versus v2.2, bottom right panel).

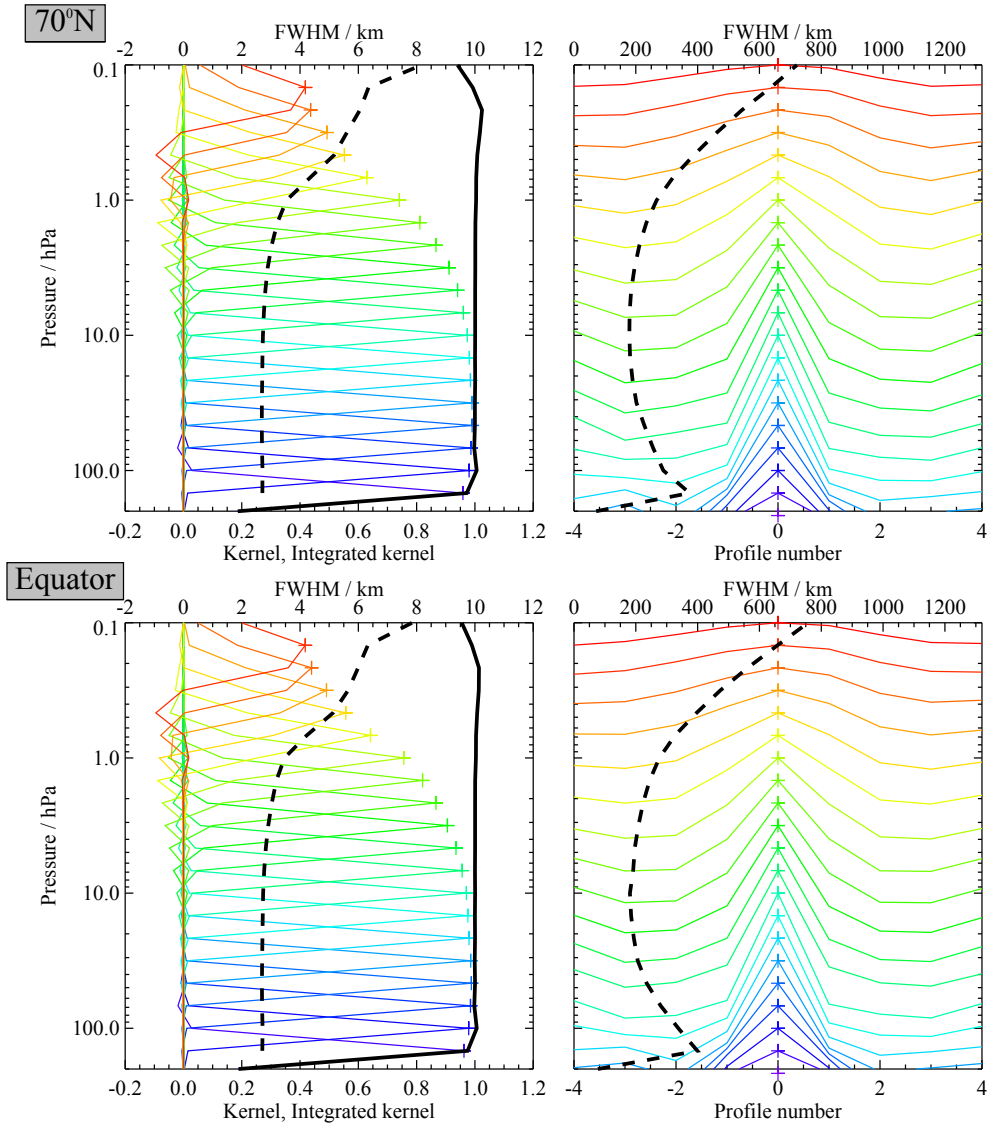

Figure 3.9.3: Typical two-dimensional (vertical and horizontal along-track) averaging kernels for the MLS v3.3 HCl data at 70°N (upper) and the equator (lower); variation in the averaging kernels is sufficiently small that these are representative of typical profiles. Colored lines show the averaging kernels as a function of MLS retrieval level, indicating the region of the atmosphere from which information is contributing to the measurements on the individual retrieval surfaces, which are denoted by plus signs in corresponding colors. The dashed black line indicates the resolution, determined from the full width at half maximum (FWHM) of the averaging kernels, approximately scaled into kilometers (top axes). (Left) Vertical averaging kernels (integrated in the horizontal dimension for five along-track profiles) and resolution. The solid black line shows the integrated area under each kernel (horizontally and vertically); values near unity imply that the majority of information for that MLS data point has come from the measurements, whereas lower values imply substantial contributions from a priori information. (Right) Horizontal averaging kernels (integrated in the vertical dimension) and resolution. The horizontal averaging kernels are shown scaled such that a unit averaging kernel amplitude is equivalent to a factor of 10 change in pressure.

between ascending and descending coincident MLS profiles. The scatter in MLS data and in simulated MLS retrievals (using noise-free radiances) becomes smaller than the theoretical precision (given in the Level 2 files) in the upper stratosphere and mesosphere, where there is a larger impact of a priori and smoothing constraints. The HCl precision values increase rapidly at pressures less than 0.2 hPa, and are generally flagged negative at pressures less than 0.1 hPa; this indicates an increasing influence from the *a priori* (with poorer measurement sensitivity and reliability).

Accuracy

The accuracy estimates in the Table for v2.2 data came from a quantification of the combined effects of possible systematic errors in MLS calibration, spectroscopy, etc. on the HCl retrievals. These values are intended to represent 2 sigma estimates of accuracy. For more details, see the MLS validation paper by Froidevaux et al. [2008b]. For v3.3, however, given the trend issues affecting the (band 14) standard HCl product in the upper stratosphere and lower mesosphere, we now need to recommend a more conservative accuracy estimate of 10% in this region (or about 0.3 ppbv), rather than the smaller numbers from the original (formal) estimates, which should still apply to the (now very occasional) band 13 retrievals. Given the better agreement between the two bands' retrievals in the lower stratosphere, we maintain the formal accuracy estimates in this region (see Table 3.9.1). Data users should be able to reliably study seasonal and geographical changes in lower stratospheric HCl (e.g., at high latitudes in winter or spring) with the current (band 14) standard HCl product.

Data screening

Pressure range: 100 – 0.32 hPa

Values outside this range are not recommended for scientific use. We note that the MLS values at 147 hPa are are biased high, at least at low to mid-latitudes, and slightly more in the v3.3 data than in the v2.2 data – and these values are not recommended (particularly at low latitudes). Also, although the vertical range at the top end is recommended up to 0.32 hPa, users should note the significant issues relating to HCl trend estimates in the upper stratosphere and lower mesosphere; average profiles in this region can be used for studies not involving trends (or accuracy requirements not as tight as 10%). The use of the band 13 (intermittent) HCl data can/will continue to be carefully evaluated for trend-related issues.

Estimated precision: Only use values for which the estimated precision is a positive number.

Values where the *a priori* information has a strong influence are flagged with negative precision, and should not be used in scientific analyses (see Section 1.5).

Status flag: Only use profiles for which the 'Status' field is an even number.

Odd values of `Status` indicate that the profile should not be used in scientific studies. See Section 1.6 for more information on the interpretation of the `Status` field.

Clouds: Profiles identified as being affected by clouds can be used with no restriction.

Quality: Only profiles whose 'Quality' field is greater than 1.2 should be used.

This criterion removes profiles with the poorest radiance fits, typically significantly less than 1% of the daily profiles. Results in this respect have improved, in comparison to v2.2 data. For HCl (and for other 640 GHz MLS products), this screening correlates well with the poorly converged sets of profiles (see below); we recommend the use of both the `Quality` and `Convergence` fields for data

screening. The use of this screening criterion sometimes (but rarely) removes up to a few percent of global daily data (for example, during the first half of September, 2006, when some high latitude convergence and quality issues arose).

Convergence: Only profiles whose 'Convergence' field is less than 1.05 should be used.

For the vast majority of profiles (99% or more for most days), this field is less than 1.05. Results in this respect have improved, in comparison to v2.2 data. Nevertheless, on occasion, sets of profiles (typically one or more groups of ten profiles, retrieved as a 'chunk') have this `Convergence` field set to larger values. These profiles are usually almost noise-free and close to the *a priori* profile, and need to be discarded as non-converged. The `Quality` field (see above) most often yields poorer quality values for these non-converged profiles. The use of this screening criterion sometimes (but rarely) removes up to a few percent of global daily data (for example, during the first half of September, 2006, when some high latitude convergence and quality issues arose).

Review of comparisons with other datasets

Froidevaux et al. [2008b] provided results of generally good comparisons between MLS HCl and other satellite, balloon, and aircraft measurements. Both MLS and ACE-FTS HCl values are generally larger (by about 10 to 15%) than the HCl values from HALOE, especially at upper stratospheric altitudes; this feature has not changed, overall, with the new data version(s) from both MLS and ACE-FTS. MLS HCl at 147 hPa is biased high versus WB-57 aircraft in-situ (CIMS) measurements (low to mid-latitudes); while this is still true for v3.3 data, MLS data on this pressure level may be useful and accurate enough at high latitudes.

Artifacts

- We do not recommend the use of the MLS HCl standard product (from band 14) in the upper stratosphere and lower mesosphere, in terms of detailed trend studies, for reasons mentioned above. The MLS HCl global results from band 13, although very infrequent (after early 2006), are observed (and expected) to be more reliable in this respect.
- The HCl values at 147 hPa are biased high and generally not usable (except possibly at high latitudes). Please consult the MLS team for further information.
- Users should screen out the non-converged and poorest quality HCl profiles, as such profiles (typically a very small number per day) tend to behave unlike the majority of the other MLS retrievals. See the criteria listed above.

Table 3.9.1: Summary for MLS hydrogen chloride

Pressure	Precision[a]		Resolution V × H	Accuracy[b]		Comments
hPa	ppbv	%	km	ppbv	%	
0.2	—	—	—	—	—	Unsuitable for scientif c use
0.5	0.7	20	5 × 400	0.3	10	Unsuitable for trend studies
1	0.5	15	4 × 300	0.3	10	Unsuitable for trend studies
2	0.4	15	3 × 250	0.3	10	Unsuitable for trend studies
5	0.3	10	3 × 200	0.3	10	Unsuitable for trend studies
10	0.2	10	3 × 200	0.2	10	
20	0.2	15	3 × 200	0.1	10	
46	0.2	10 to > 40	3 × 250	0.2	10 to > 40	
68	0.2	15 to > 80	3 × 300	0.2	10 to > 80	
100	0.3	30 to > 100	3 × 350	0.15	10 to > 100	
147	0.4	50 to > 100	3 × 400	0.3	50 to > 100	High bias at low lats. (use with caution elsewhere)

[a]Precision (1 sigma) for individual prof les; note that % values tend to vary strongly with latitude in the lower stratosphere.

[b]2 sigma estimate from systematic uncertainty characterization tests (but see text for estimates at pressures lower than 10 hPa); note that percent values tend to vary strongly with latitude and season in the lower stratosphere, due to the variability in HCl.

3.10 Hydrogen Cyanide

Swath name: HCN

Useful range: 10 – 0.1 hPa

Contact: Hugh C. Pumphrey, **Email:** <H.C.Pumphrey@ed.ac.uk>

Introduction

HCN is retrieved from bands encompassing, in the lower sideband, the 177.26 GHz spectral line of HCN. Although the target line is in an uncluttered part of the spectrum, the upper sideband contains many interfering lines of O_3 and HNO_3. As a result, the v3.3 HCN product is not recommended for general use in the lower stratosphere. In the recommended range it is usable, but has rather poor precision and resolution.

It is possible to retrieve weekly zonal means of HCN over a greater vertical range by first averaging the radiances. Results of this process and further information on the HCN measurement may be found in Pumphrey et al. [2006].

Differences between v2.2 and v3.3

No changes specific to the HCN retrieval were made between v2.2 and v3.3. Any differences in the retrieved values are caused by changes made to the retrieval other quantities, with temperature and pointing being the most important. Figure 3.10.2 shows that the precisions are essentially unchanged. The retrieved mixing ratios change very little in the region where use is recommended but are considerably different in the lower stratosphere where the data are not recommended for general use.

Vertical resolution

The HCN signal is rather small, so a rather strong smoothing constraint has to be applied to ensure that the retrieval is at all useful. As Figure 3.10.1 shows, the vertical resolution is about 8 km at 10 hPa, degrading to 12 km at 0.1 hPa. The horizontal resolution along the measurement track is between 2 and 4 profile spacings.

Precision

Figure 3.10.2 shows the estimated precision (values of the field `L2gpPrecision`), together with the observed standard deviation in an equatorial latitude band where the natural variability of the atmosphere is small. The observed scatter is smaller than the estimated precision due to the effects of retrieval smoothing.

Accuracy

The accuracy of the HCN product has not been assessed in detail because a cursory inspection reveals that the product has extremely large systematic errors in the lower stratosphere. For this reason the data are not considered to be useful at pressures greater than 10 hPa (altitudes below ∼32 km). In the upper stratosphere the values are in line with current understanding of the chemistry of HCN. Comparison to historical values suggests an accuracy of no worse than 50%. The precision, resolution and accuracy of the HCN data are summarized in table 3.10.1.

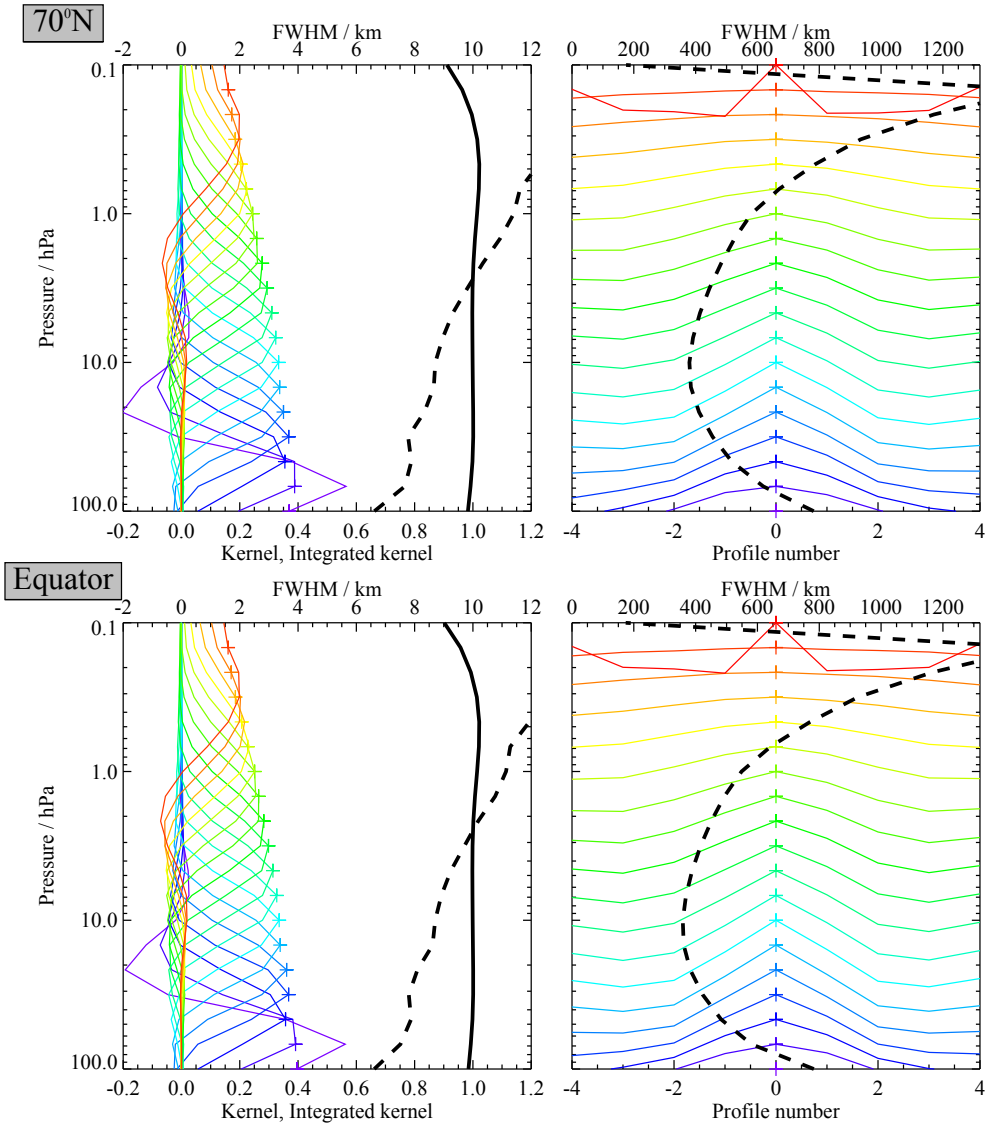

Figure 3.10.1: Typical two-dimensional (vertical and horizontal along-track) averaging kernels for the MLS v3.3 HCN data at 70°N (upper) and the equator (lower); variation in the averaging kernels is sufficiently small that these are representative of typical profiles. Colored lines show the averaging kernels as a function of MLS retrieval level, indicating the region of the atmosphere from which information is contributing to the measurements on the individual retrieval surfaces, which are denoted by plus signs in corresponding colors. The dashed black line indicates the resolution, determined from the full width at half maximum (FWHM) of the averaging kernels, approximately scaled into kilometers (top axes). (Left) Vertical averaging kernels (integrated in the horizontal dimension for five along-track profiles) and resolution. The solid black line shows the integrated area under each kernel (horizontally and vertically); values near unity imply that the majority of information for that MLS data point has come from the measurements, whereas lower values imply substantial contributions from a priori information. (Right) Horizontal averaging kernels (integrated in the vertical dimension) and resolution. The horizontal averaging kernels are shown scaled such that a unit averaging kernel amplitude is equivalent to a factor of 10 change in pressure.

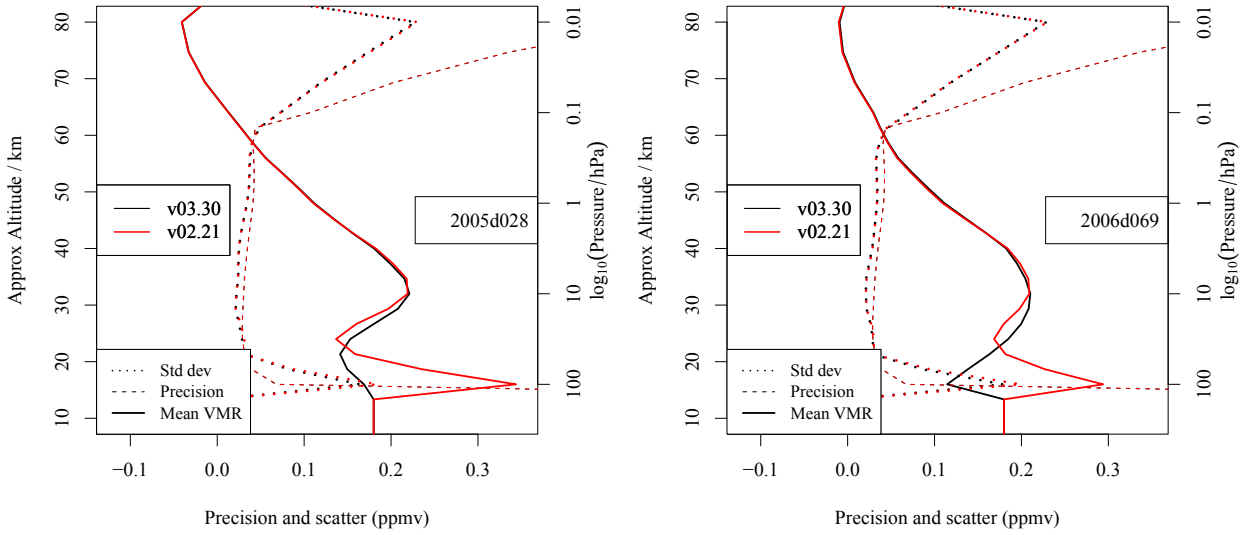

Figure 3.10.2: Estimated precision `L2gpPrecision` and observed standard deviation for MLS v3.3 (black) and v3.3 (red) HCN. The data shown are all profiles within 20° of the equator for 28 January, 2005 and 10 March 2006. Mean mixing ratio (VMR) profiles are shown for comparison. Note that these are essentially the same in v2.2 and v3.3 for the region recommended for use (10 hPa - 0.1 hPa).

HCN

Table 3.10.1: Resolution and precision of MLS V3.3 HCN. The precision shown is the estimated precision (`L2gpPrecision`); the observed scatter is about 80% of this value.

Pressure	Resolution V × H / km	Precision / pptv	Accuracy / %	Comments
< 0.1 hPa	—	—	—	Unsuitable for scientif c use
1 – 0.1 hPa	500 × 12	50	50	
10 – 1 hPa	300 × 10	30	50	
100 – 10 hPa	300 × 10	50	Very poor	Unsuitable for scientif c use
> 100 hPa				Not Retrieved

Data screening

Pressure range: 10 – 0.1 hPa

Values outside this range are not recommended for scientific use.

Estimated precision: Only use values for which the estimated precision is a positive number.

Values where the *a priori* information has a strong influence are flagged with negative precision, and should not be used in scientific analyses (see Section 1.5).

Status flag: Only use profiles for which the 'Status' field is an even number.

Odd values of `Status` indicate that the profile should not be used in scientific studies. See Section 1.6 for more information on the interpretation of the `Status` field.

Clouds: Clouds have no impact, profiles with non-zero even values of `Status` are suitable for use.

As HCN is only useable in the upper stratosphere, profiles which have either, both or neither of the cloud flags set may be used.

Quality: Only profiles whose 'Quality' field is greater than 0.2 should be used.

Values of `Quality` are usually near 1.5; occasional lower values do not seem correlated with unusual profiles, but we suggest as a precaution that only profiles with `Quality` > 0.2 be used. Typically this will eliminate only 1-2% of profiles.

Convergence: Only profiles whose 'Convergence' field is less than 2.0 should be used.

This should eliminate any chunks which have obviously failed to converge – typically this is only 1-2% of the total.

Artifacts

There are no obvious artefacts within the recommended altitude range

Desired improvements for future data version(s)

Hopefully it will prove possible to retrieve HCN in the lower stratosphere.

3.11 Nitric Acid

Swath name: HNO3

Useful range: 215 – 1.5 hPa (1.0 hPa under enhanced conditions)

Contact: Gloria Manney, **Email:** <Gloria.L.Manney@jpl.nasa.gov>

Introduction

The quality and reliability of the Aura MLS v2.2 HNO_3 measurements were assessed in detail by Santee et al. [2007]. The HNO_3 in v3.3 has been greatly improved over that in version v2.2; in particular, a low bias through much of the stratosphere (especially evident at levels with pressure greater than or equal to 100 hPa) has been largely eliminated. Figure 3.11.1 shows an example of typical differences between v2.2 and v3.3 HNO_3. Improvement in HNO_3 resulted from indirect effects of adding interline interference terms to the O_3 line shape model, an updated CO line width parameter, using a different 240 GHz channel conf guration for retrieving HNO_3, and a change the manner in which continuum signals are accounted for (see 1.4); these changes contribute approximately equally to the HNO_3 improvement. However, an unfortunate side effect of the change to continuum handling is that it is more adversely affected by clouds, causing spikes in the retrieval of 240-GHZz products including HNO_3. In addition, it also appears that the new continuum treatment has led to a noisier HNO_3 product in the UTLS than that in v2.2. Lower v3.3 values in Figure 3.11.1 in the tropics at the lowest levels result largely from these effects.

The MLS v3.3 HNO_3 data are scientif cally useful over the range 215 to 1.5 hPa; values at 1 hPa are also expected to be scientif cally useful under conditions of enhanced HNO_3 in the upper stratosphere, but should be used with caution and in consultation with the MLS team. HNO_3 values in the upper stratosphere, at 3.2 through 1.0 hPa, are frequently very low and may require averaging (this will usually be the case at 1.5 and 1 hPa, where the values are also noisier than at lower levels), but during periods of enhancement in the upper stratosphere, coherently evolving atmospheric signals with realistic morphology are seen in individual daily maps. The standard HNO_3 product is derived from the 240-GHz retrievals at pressures equal to or greater than 22 hPa and from the 190-GHz retrievals for lesser pressures. The `Quality` and `Convergence` information included in the standard HNO_3 f les are from the 240-GHz retrievals, and *apply only to pressures 22 hPa or greater* (see the data screening discussion below).

A summary of the precision and resolution (vertical and horizontal) of the v3.3 HNO_3 measurements as a function of altitude is given in Table 3.11.1. The impact of various sources of systematic uncertainty was quantif ed for v2.2, and it is expected that these estimates will be similar for v3.3. Table 3.11.1 also includes estimates of the potential biases and scaling errors in the measurements compiled from the v2.2 uncertainty analysis (to be updated for v3.3 at a later date). The overall uncertainty for an individual data point is determined by taking the root sum square (RSS) of the precision, bias, and scaling error terms (for averages, the single-prof le precision value is divided by the square root of the number of prof les contributing to the average). More details on the precision, resolution, and accuracy of the MLS v3.3 HNO_3 measurements are given below.

Resolution

The resolution of the retrieved data can be described using ‘averaging kernels’ [e.g., Rodgers, 2000]; the two-dimensional nature of the MLS data processing system means that the kernels describe both vertical and horizontal resolution. Smoothing, imposed on the retrieval system in both the vertical and horizontal directions to enhance retrieval stability and precision, reduces the inherent resolution of the measurements.

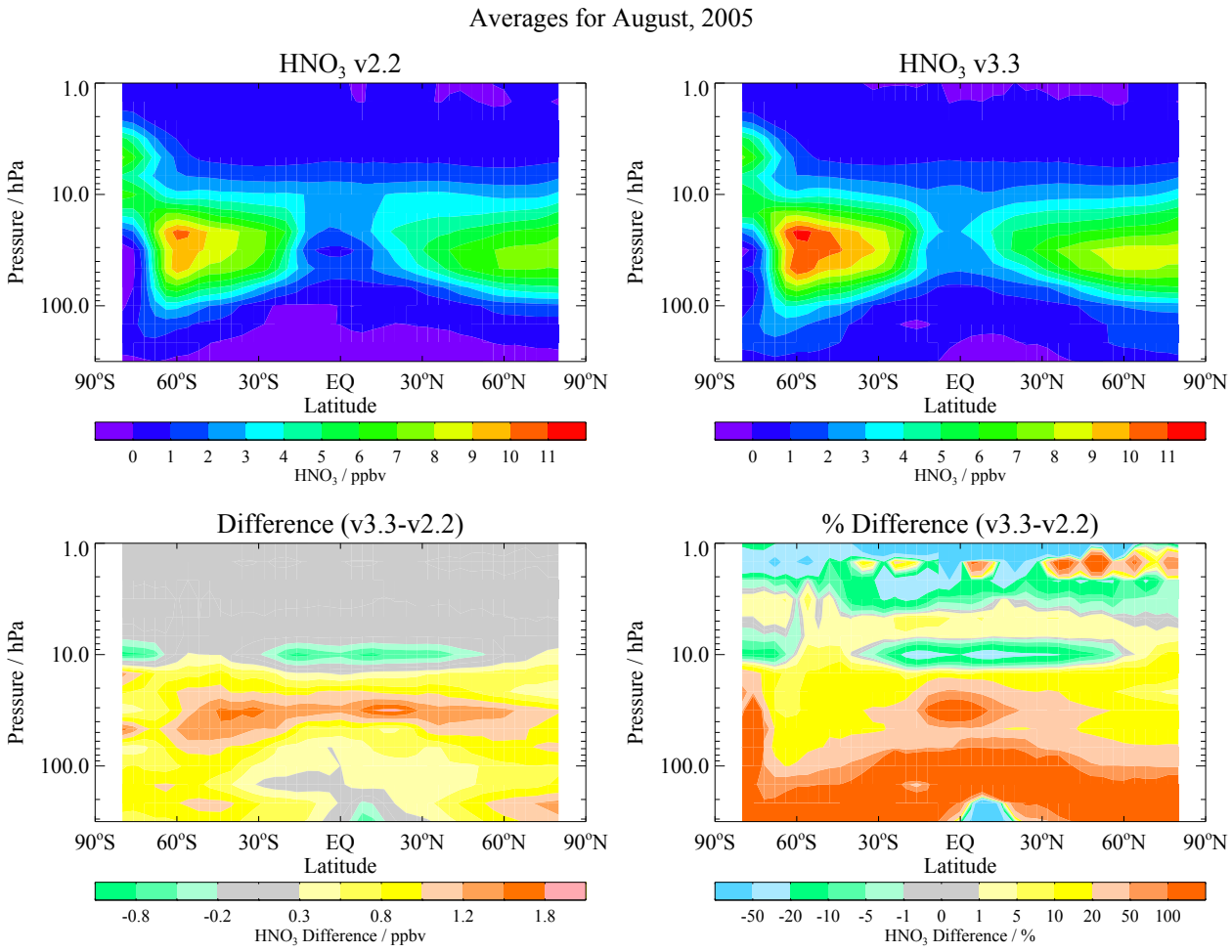

Figure 3.11.1: V2.2 (top left) and v3.3 (top right) zonal mean HNO_3 for August 2005, and differences (v3.3 – v2.2) expressed in ppbv (bottom left) and percent (bottom right).

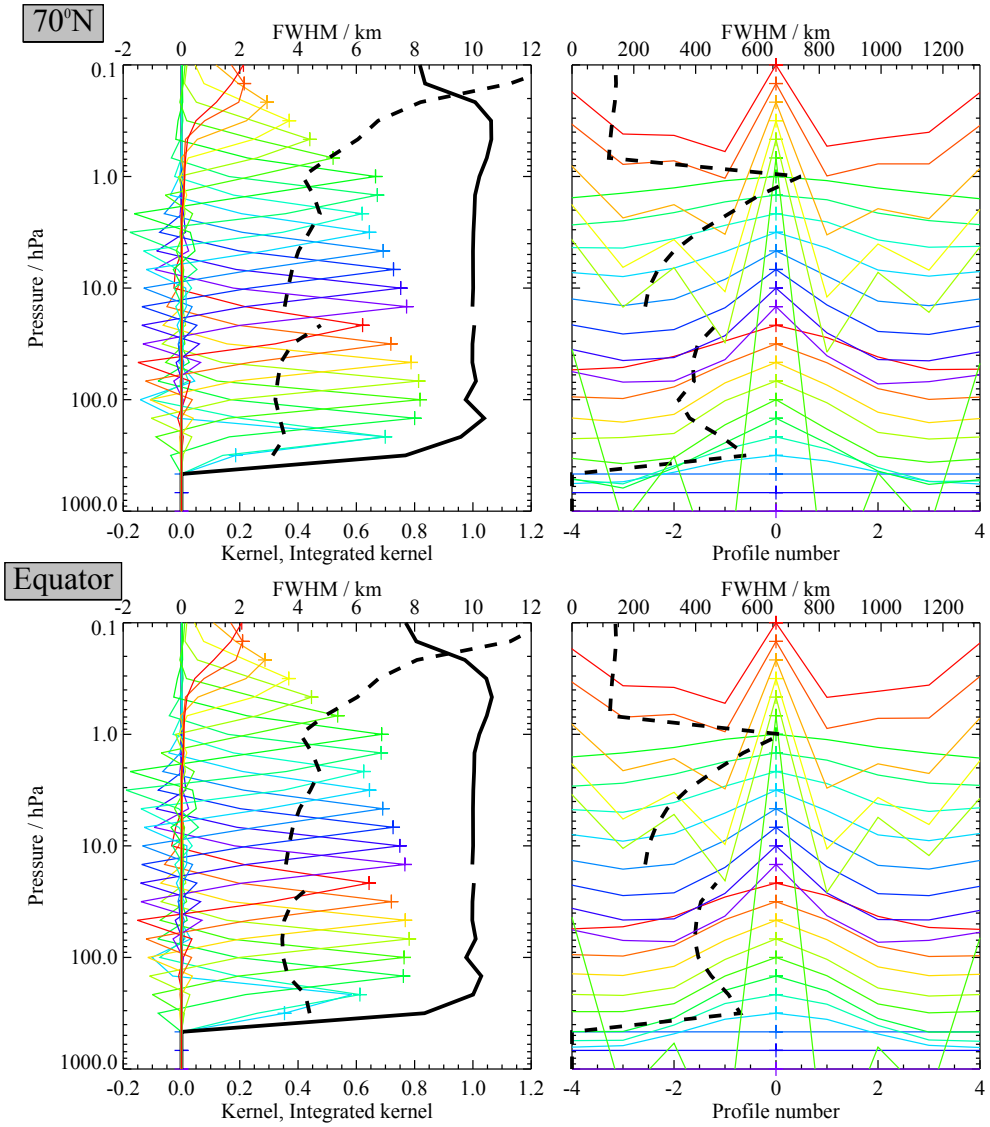

Figure 3.11.2: Typical two-dimensional (vertical and horizontal along-track) averaging kernels for the MLS v3.3 HNO_3 data at 70°N (upper) and the equator (lower); variation in the averaging kernels is sufficiently small that these are representative of typical profiles. Colored lines show the averaging kernels as a function of MLS retrieval level, indicating the region of the atmosphere from which information is contributing to the measurements on the individual retrieval surfaces, which are denoted by plus signs in corresponding colors. The dashed black line indicates the resolution, determined from the full width at half maximum (FWHM) of the averaging kernels, approximately scaled into kilometers (top axes). (Left) Vertical averaging kernels (integrated in the horizontal dimension for five along-track profiles) and resolution. The solid black line shows the integrated area under each kernel (horizontally and vertically); values near unity imply that the majority of information for that MLS data point has come from the measurements, whereas lower values imply substantial contributions from a priori information. (Right) Horizontal averaging kernels (integrated in the vertical dimension) and resolution. The horizontal averaging kernels are shown scaled such that a unit averaging kernel amplitude is equivalent to a factor of 10 change in pressure.

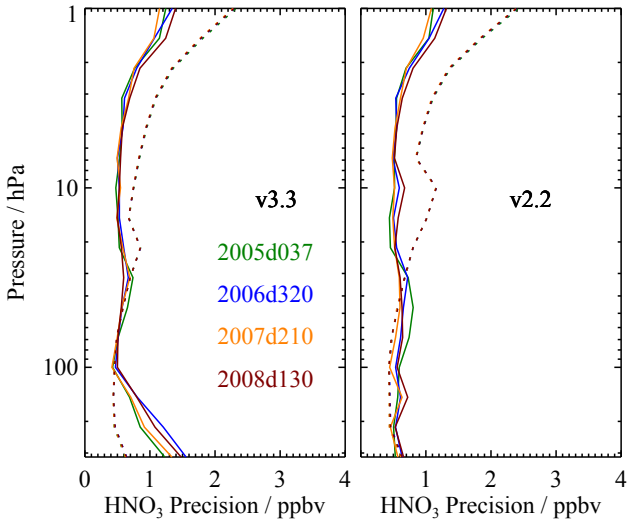

Figure 3.11.3: Precision of the (left) v3.3 and (right) v2.2 MLS HNO_3 measurements for four representative days (see legend). Solid lines depict the observed scatter in a narrow equatorial band (see text); dotted lines depict the theoretical precision estimated by the retrieval algorithm.

Consequently, the vertical resolution of the v3.3 HNO_3 data, as determined from the full width at half maximum of the rows of the averaging kernel matrix shown in Figure 3.11.2, is 3 – 4 km through most of the useful range, degrading to ∼5 km at 22 hPa and some levels in the upper stratosphere (see Table 3.11.1). Note that the averaging kernels for the 215 and 316 hPa retrieval surfaces overlap over most of their depth, indicating that the 316 hPa retrieval provides little independent information. Figure 3.11.2 also shows horizontal averaging kernels, from which the along-track horizontal resolution is determined to be 450 – 500 km over most of the vertical range, improving to 250 – 300 km between 15 and 4.6 hPa, and degrading to 600 – 750 km at 1.5 and 1 hPa. The cross-track resolution, set by the widths of the fields of view of the 190-GHz and 240-GHz radiometers, is ∼10 km. The along-track separation between adjacent retrieved profiles is 1.5° great circle angle (∼165 km), whereas the longitudinal separation of MLS measurements, set by the Aura orbit, is 10° – 20° over low and middle latitudes, with much finer sampling in the polar regions.

Precision

The precision of the MLS HNO_3 measurements is estimated empirically by computing the standard deviation of the profiles in the 20°-wide latitude band centered around the equator, where natural atmospheric variability should be small relative to the measurement noise. Because meteorological variation is never completely negligible, however, this procedure produces a upper limit on the precision-related variability. As shown in Figure 3.11.3, the observed scatter in the v3.3 data is ∼0.6 – 0.7 ppbv throughout the range from 100 to 3.2 hPa, below and above which it increases sharply. The scatter is essentially invariant with time, as seen by comparing the results for the different days shown in Figure 3.11.3.

The single-profile precision estimates cited here are, to first order, independent of latitude and season, but it should be borne in mind that the large geographic variations in HNO_3 abundances gives rise to wide range'signal to noise' ratios. At some latitudes and altitudes and in some seasons, HNO_3 abundances are smaller than the single-profile precision, necessitating the use of averages for scientific studies. In most cases, precision can be improved by averaging, with the precision of an average of N profiles being $1/\sqrt{N}$ times the precision of an individual profile (note that this is not the case for averages of successive along-track profiles, which are not completely independent because of horizontal smearing).

The observational determination of the precision is compared in Figure 3.11.3 to the theoretical precision values reported by the Level 2 data processing algorithms. Although the two estimates compare very well between 100 and 32 hPa, above 22 hPa the predicted precision substantially exceeds the observed scatter. This indicates that the a priori information and the vertical smoothing applied to stabilize the retrieval are influencing the results at the higher retrieval levels. Because the theoretical precisions take into account occasional variations in instrument performance, the best estimate of the precision of an individual data point is the value quoted for that point in the L2GP files, but it should be borne in mind that this approach overestimates the actual measurement noise at pressures less than 22 hPa. Conversely, the observed scatter at pressures higher than 100 hPa is considerably larger than the theoretical precision. This is related to the spikes and increased noise in the UTLS in v3.3 versus v2.2 HNO_3 mentioned above. Procedures for screening outliers in this region are discussed below.

Accuracy

The effects of various sources of systematic uncertainty (e.g., instrumental issues, spectroscopic uncertainty, and approximations in the retrieval formulation and implementation) on the MLS v2.2 HNO_3 measurements were quantified through a comprehensive set of retrieval simulations; results for v3.3, to be completed at a later date, are expected to be similar. The results of the v2.2 uncertainty analysis are summarized in Table 3.11.1; see Santee et al. [2007] for further details of how the analysis was conducted and the magnitude of the expected biases, additional scatter, and possible scaling errors each source of uncertainty may introduce into the data. In aggregate, systematic uncertainties are estimated to induce in the HNO_3 measurements biases that vary with altitude between ± 0.5 and ± 2 ppbv and multiplicative errors of $\pm 5-15\%$ through most of the stratosphere, rising to $\sim \pm 30\%$ at 215 hPa and $\sim 50\%$ at and above 2.2 hPa. These uncertainty estimates are generally consistent with the results of comparisons with correlative datasets, as discussed briefly below.

Data screening – all data

Pressure range: 215 – 1.5 hPa

Values outside this range are not recommended for scientific use.

Estimated precision: Only use values for which the estimated precision is a positive number.

Values where the *a priori* information has a strong influence are flagged with negative precision, and should not be used in scientific analyses (see Section 1.5).

Status flag: Only use profiles for which the 'Status' field is an even number.

Odd values of `Status` indicate that the profile should not be used in scientific studies. See Section 1.6 for more information on the interpretation of the `Status` field.

Data screening – upper troposphere, lower stratosphere (pressures of 22 hPa or greater)

The `Quality` and `Convergence` fields included in the standard HNO_3 files are appropriate for use in screening at levels at and below (that is, pressures greater than) 22 hPa. For those levels:

Quality: Only profiles whose 'Quality' field is greater than 0.5 should be used.

This threshold for `Quality` typically excludes $\sim 2-4\%$ of HNO_3 profiles on a daily basis; it is a conservative value that potentially discards a significant fraction of "good" data points while not necessarily identifying all "bad" ones.

Convergence: Only profiles whose 'Convergence' field is less than 1.4 should be used.

On a typical day this threshold for `Convergence` discards a very small fraction of the data, but on occasion it leads to the elimination of $\sim 0.5-1\%$ of the HNO_3 profiles.

Clouds: Clouds impact HNO_3 data in the UTLS, see discussion below and the discussion on 'outliers' that follows.

Nonzero but even values of `Status` indicate that the profile has been marked as questionable, typically because the measurements may have been affected by the presence of thick clouds. Globally $\sim 10-15\%$ of profiles are identified in this manner, with the fraction of profiles possibly impacted by clouds rising to $\sim 25-35\%$ on average in the tropics. Clouds generally have little influence on the stratospheric HNO_3 data. In the lowermost stratosphere and upper troposphere, however, thick clouds can lead to spikes in the HNO_3 mixing ratios in the equatorial regions. Therefore, it is recommended that at and below 100 hPa all profiles with nonzero values of `Status` be used with caution (i.e., in conjunction with the 'outlier screening' described below) or discarded because of the potential for cloud contamination. This has the unfortunate consequence of rejecting many profiles that are probably not significantly impacted by cloud effects; the outlier screening procedures discussed below may eliminate many of the profiles affected by clouds while discarding a smaller fraction of useful data.

Outliers: Alternative screening approaches in the UTLS remove outliers while reducing 'false positives'

Outliers in v3.3 HNO_3 at levels between 316 and 100 (sometimes to 68) hPa frequently appear as highly negative mixing ratios at the lowest several retrieval levels, often as part of oscillatory profiles with unrealistically high values at higher altitudes. A simple procedure is recommended to screen such profiles based on eliminating all profiles with large negative mixing ratios at pressure levels between 316 and 68 hPa. Through extensive examination of data screened in this way, flagging profiles that have either HNO_3 vmr less than -2.0 ppbv at 316 hPa or less than -1.6 ppbv at any level between 215 and 68 hPa eliminates most of the troublesome outliers, including those with positive vmr spikes overlying the negative ones that are directly flagged by these criteria. This screening procedure is recommended for any studies focusing on the UTLS, and retains a larger fraction of useful data than rejecting all profiles with non-zero values of `Status`. That it effectively removes most of the suspect profiles was evaluated as described in the following paragraphs:

We compared the outlier screening method described above with a procedure based on using MLS cloud information: If the MLS ice water content (IWC) at 147 hPa is greater than 0.003 g/m^3 (indicating the presence of some cloud) for a profile, that profile, and the immediately adjacent ones along the orbit track are flagged (adjacent profiles are flagged assuming that the 1-D nature of the IWC retrieval versus the 2-D nature of the HNO_3 retrieval results in some uncertainty in the relative location of the cloud signal with respect to the trace gas profile). Figure 3.11.4 shows the fraction of points eliminated by this procedure and the simpler recommended procedure based on direct identification of unphysical mixing ratios; the simpler procedure that is recommended compares very favorably with the more rigorous procedure based on cloud information: Each procedure eliminates a similar fraction of profiles ($\sim$4% globally, $\sim$15% in the tropics, considerably fewer than requiring `Status` to be zero), and is effective for removing most of the outliers. Screening using MLS IWC as described here could be used (or compared with the recommended procedure) in analyses that are expected to be especially sensitive to the exact values in the tropical UTLS, but is not needed to obtain a high-quality HNO_3 dataset in most cases.

Figure 3.11.5 shows an example of the results of screening profiles by each of the `Quality`, `Convergence` and the recommended outlier flagging on a typical 'bad' day (i.e., one with a relatively large

number of outliers). The Quality screening removes many of the profiles that are strongly negative at the bottom, and most or all of the remainder of these are flagged by the outlier screening; many of these profiles are oscillatory, so this screening also removes most or all of the strong positive outliers (typically at 147 hPa). Most of the profiles flagged by any of the criteria are in the tropics, as expected; the figure indicates that, at southern hemisphere high latitudes, low values of HNO_3 associated with the denitrified polar vortex are not triggering the outlier flagging. As is often (but not always) the case, it is not clear in this example that the profiles flagged only by Convergence are unphysical or extreme.

Data screening – upper stratosphere (pressures of 15 hPa or less)

The above screening criteria *should not be used* for 15 hPa and higher altitudes, as they result in filtering profiles for which all quality indicators are good when the Quality and Convergence values are properly taken from the 190-GHz HNO_3 information, and not filtering ones with indications of poor quality. For any studies focusing on the upper stratosphere, it is highly recommended that the user read from the L2GP-DGG files to obtain the appropriate Quality and Convergence values for the 190-GHz HNO_3 (from the HNO3-190 swath), and use them to apply the following screening criteria:

Clouds: Profiles where the Status field for HNO3-190 has a non-zero even number can be used without restriction.

Clouds generally have little influence on the stratospheric HNO_3 data at these altitudes.

Quality: Only profiles with a value of the Quality field for HNO3-190 (see section 1.6) *greater* than 1.0 should be used in scientific study.

This threshold for Quality typically excludes $\sim 1-3\%$ of HNO_3 profiles on a daily basis; it is a conservative value that potentially discards a significant fraction of "good" data points while not necessarily identifying all "bad" ones.

Convergence: Only profiles with a value of the Convergence field (see section 1.6) for the HNO3-190 product *less* than 1.6 should be used in investigations.

On a typical day this threshold for Convergence discards $\sim 0.5-1.5\%$ of the HNO_3 profiles.

Outliers: For levels at and above (pressures less than) 4.6 hPa, especially at 2.2 hPa and above, some profiles show vertically oscillatory behavior in conditions where HNO_3 is very low. The Quality and Convergence criteria defined above, when used together, eliminate many of these profiles; screening using both of these thresholds is thus particularly important.

Review of comparisons with other datasets

Comparisons of v3.3 HNO_3 with correlative datasets from a variety of different platforms are in progress. A consistent picture is emerging of much closer agreement in v3.3 than v2.2 with HNO_3 measurements from ground-based, balloon-borne, and satellite instruments, especially in the upper troposphere through the mid-stratosphere where MLS v2.2 HNO_3 mixing ratios were uniformly low by $10-30\%$. Example comparisons with balloon-borne measurements (Figures 3.11.6 and 3.11.7) and Atmospheric Chemistry Experiment-Fourier Transform Spectrometer satellite measurements (Figure 3.11.8) are shown. The GBMS balloon measurements (Figure 3.11.7) highlight the change from v2.2 to v3.3; in all years, MLS HNO_3 values increased from v2.2 to v3.3 over most/all of the altitude range, and in 2004 – 2005 and 2006 – 2007 show much closer agreement with GBMS measurements; in all years, MLS HNO_3 agrees with GBMS

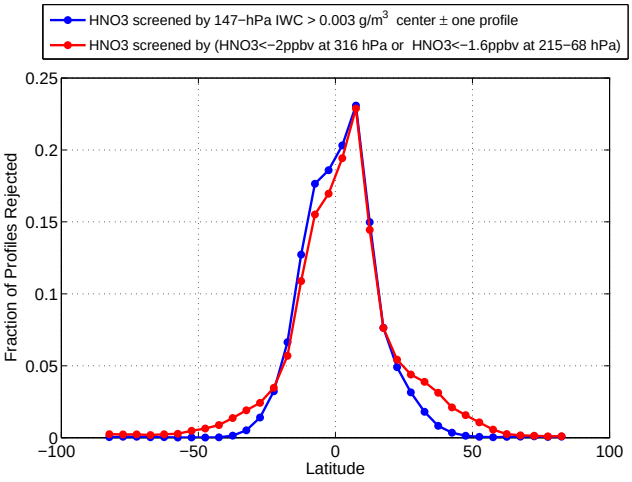

Figure 3.11.4: Fraction of profiles flagged by two suggested outlier screening procedures for the UTLS as a function of latitude for all currently available v3.3 data during 2006.

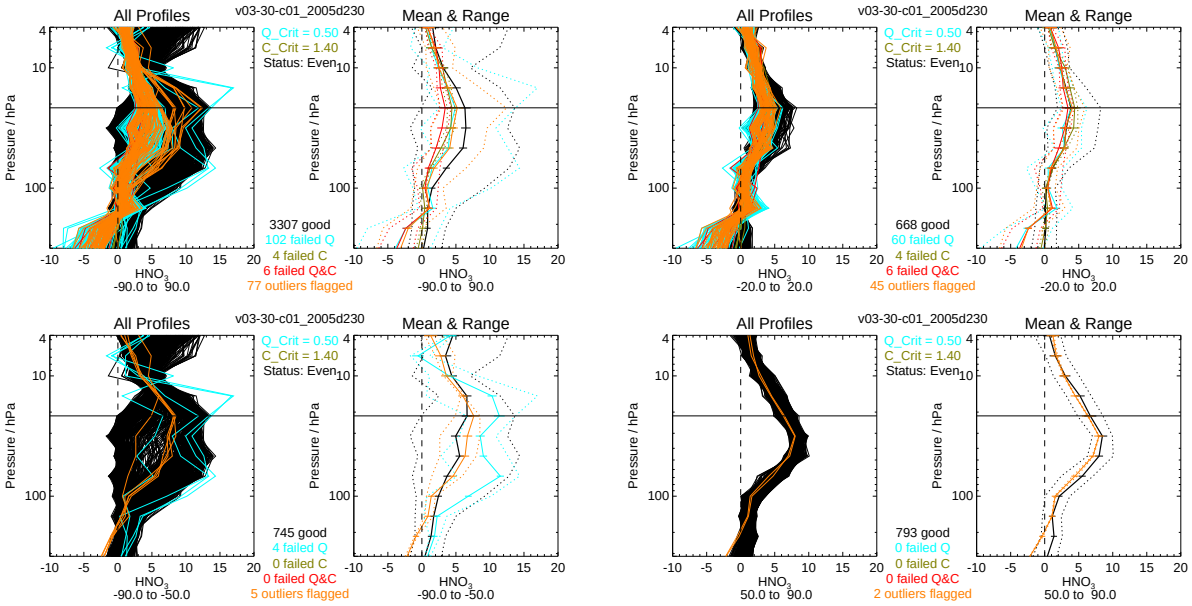

Figure 3.11.5: HNO_3 profiles on 18 Aug 2005 color-coded by screening. Cyan profiles have `Quality` less than 0.5, olive-green `Convergence` greater than 1.4, and red both `Quality` less than 0.5 and `Convergence` greater than 1.4. Orange profiles are those flagged by the simple screening procedure described above (using large negative mixing ratios at high pressures) after the profiles that failed `Quality` and/or `Convergence` tests were removed. Black profiles are all those remaining (the 'good' profiles) after the screening. The left panels show all individual profiles in the day; the right panels show the means in each category, with the standard deviation shown as bars and the range as dotted lines. The horizontal line is at 22 hPa, above which HNO_3 is from the 190-GHz radiometer and thus not appropriately screened by these criteria. The four pairs of panels show all profiles (top left), profiles between −20 and 20° latitude (top right), profiles between −90 and −50° latitude (bottom left) and profiles between 50 and 90° latitude.

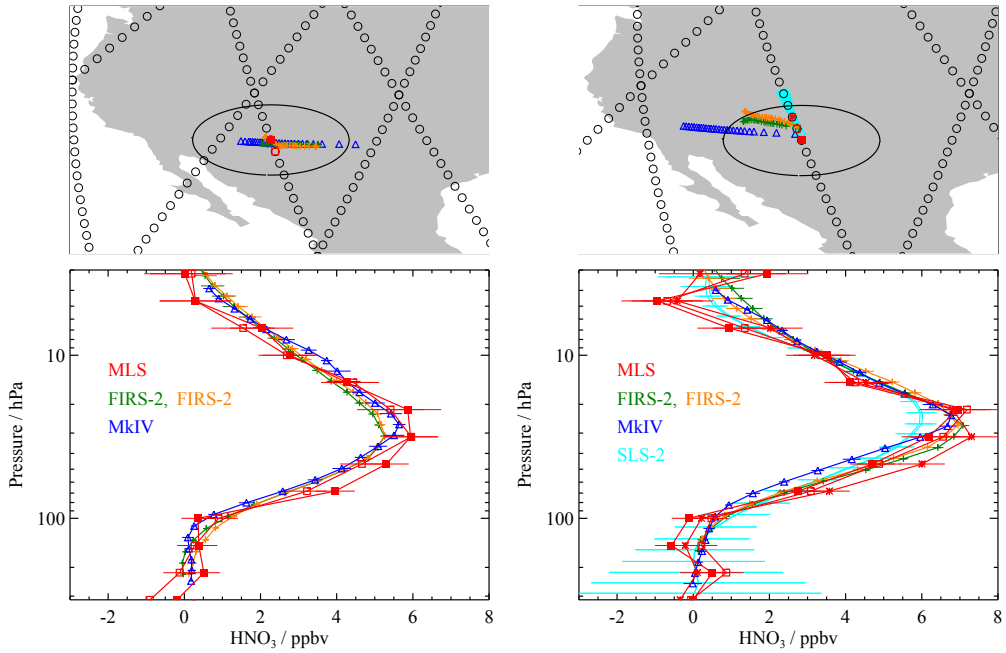

Figure 3.11.6: Comparisons with balloon-borne measurments at Ft. Sumner in 2004 (left) and 2005 (right). (Top panels) Path traversed by measurements from the balloon-borne MkIV (blue triangles) and FIRS-2 (green and orange crosses represent two separate profiles) instruments during the flights from Ft. Sumner, NM, on 23 – 24 September 2004 (left) and 20 – 21 September 2005 (right). Measurement tracks from nearby MLS orbits are also shown (open circles). The two MLS data points closest to the balloon measurements in time and space are indicated by red squares, with the closer one denoted by a filled symbol; the 500-km radius around the closest MLS point is overlaid in black. (Bottom) Profiles of HNO_3 from MLS (red squares), MkIV (blue triangles), and FIRS-2 (green and orange crosses), corresponding to the symbols in the top panel. Error bars represent the estimated precisions of each instrument, taken from the data files.

within the error bars. The 2005 – 2006 winter was characterized by extremely strong dynamical activity, which may contribute to the different relationship between MLS and GBMS measurements in that year; detailed GBMS/MLS comparisons are described by Fiorucci et al. [in preparation].

The Ft. Sumner balloon comparisons also show much improved agreement between HNO_3 measured by several instruments with v3.3 MLS data (compare Figure 3.11.6 with Figures 11 and 12 of Santee et al. [2007]). ACE-FTS comparisons also show improvements, with the low bias in MLS virtually eliminated over the entire altitude range shown in the top panel comparing with ACE-FTS v2.2 data in May 2008 (other months show similar results) – this can be contrasted with Figure 25 of Santee et al. [2007], which showed a low bias in MLS v2.2 data with respect to ACE v2.2 throughout the useful altitude range.

ACE-FTS data are being reprocessed with v3.0, and HNO_3, though not yet validated, is expected to be improved in the UTLS, and to be useful up to ∼60 km. The bottom panels of Figure 3.11.8 show a comparison of ACE-FTS v3.0 data with MLS v3.3 data during Jan 2005, indicating good agreement throughout the altitude range. Further correlative comparisons are underway, and will include comparisons with the Odin/SMR and the MIPAS satellite instruments; retrievals from the latter that extend to ∼60 km should help validate v3.3 HNO_3 in the upper stratosphere.

Preliminary comparisons also indicate closer agreement for version 3 HNO_3 with aircraft measurements in the UTLS than for version 2.

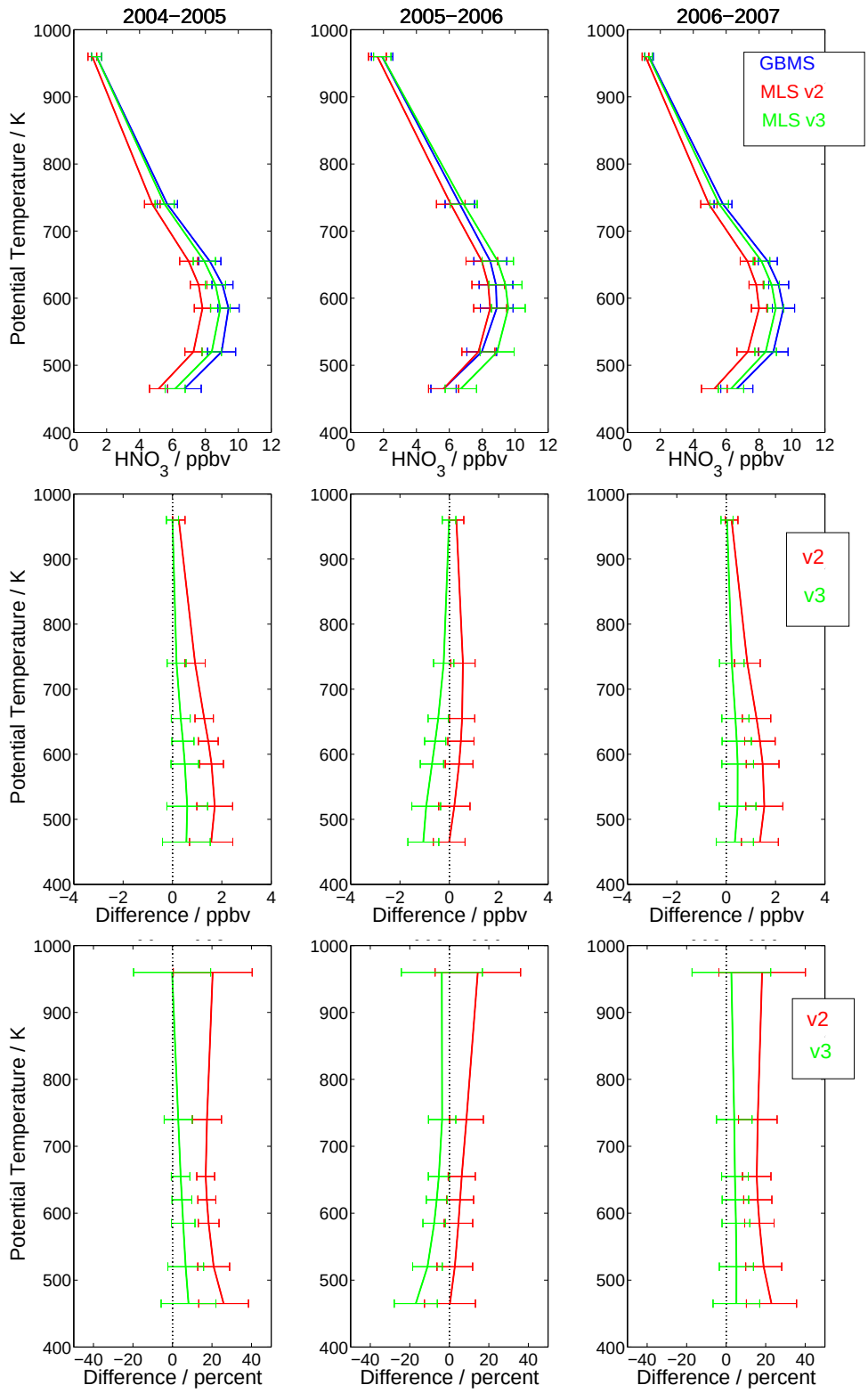

Figure 3.11.7: Comparisons with GBMS balloon measurements. (Top) Averages of all GBMS (blue) profiles and closest MLS (v2.2 in red, v3.3 in green) coincidences at Testa Grigia (45.9°N, 7.7°E) during the 2004–2005, 2005–2006, and 2006–2007 winters; bars are standard deviation of the mean. (Center) Differences between mean profiles shown in top panels (GBMS - MLS) in ppbv; (bottom) same differences, expressed as percentages.

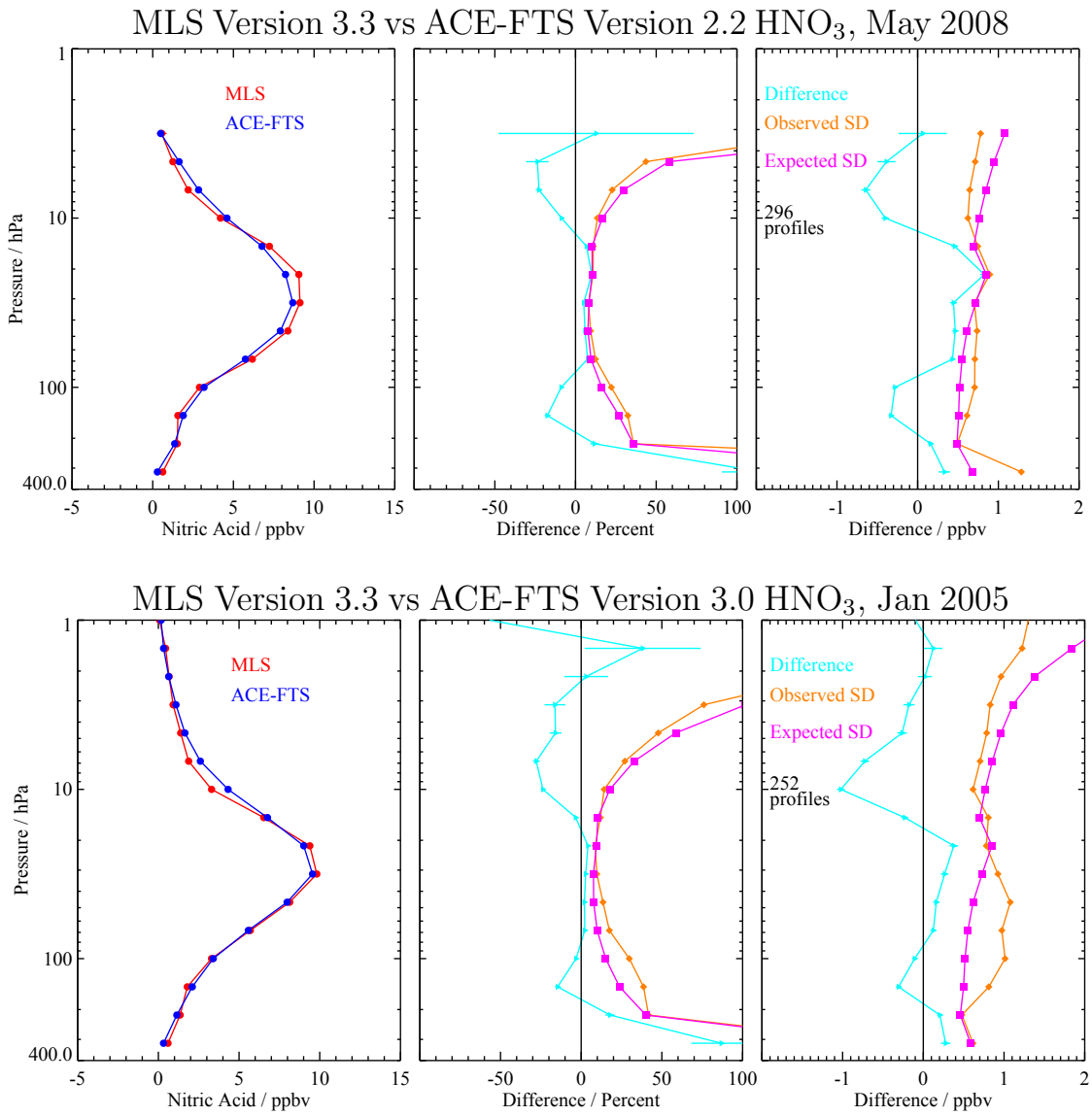

Figure 3.11.8: Comparisons with ACE-FTS v2.2 measurements during May 2008 (top) and ACE-FTS v3.3 measurements during Jan 2005 (bottom). (left) Global ensemble mean profiles of the collocated matches for both instruments (MLS, red; ACE-FTS, blue). (middle) Mean percentage difference profiles between the two measurements (MLS - ACE-FTS) (cyan); standard deviation about the mean differences (Observed SD; orange) and the percentage root sum square of the precisions on both instrument measurements (Expected SD; magenta). (right) As in Figure 13 (middle) except plotted in mixing ratio.

Table 3.11.1: Summary of Aura MLS v3.3 HNO_3 Characteristics

Pressure / hPa	Resolution V × H[a] / km	Precision[b] / ppbv	Bias uncertainty[c] / ppbv	Scaling uncertainty[c] / %	Comments
0.68 – 0.001	—	—	—	—	Unsuitable for scientif c use
1.0	4 × 650 – 750	±1.2	±0.5	±50%	Caution, averaging recommended
1.5	4.5 × 550 – 600	±1.0	±0.5	±50%	Averaging recommended
2.1	5 × 500	±0.9	±1.0	±50%	
3.2	4.5 × 400	±0.7	±0.5	±10 – 15%	
15 – 6.8	3 – 4 × 250 – 300	±0.7	±1 – 2	±10%	
22	5 × 450	±0.7	±1 – 2	±10%	
100 – 32	3 – 4 × 350 – 400	±0.7	±0.5 – 1	±5 – 10%	
147	3.5 × 400 – 450	±0.8	±0.5	±15%	
215	3.5 – 4 × 500	±1.2	±1	∼ ±30%	
316	—	—	—	—	Unsuitable for scientif c use
1000 – 464	—	—	—	—	Not retrieved

[a] Horizontal resolution in along-track direction.
[b] Precision on individual prof les, determined from observed scatter in the data in a region of minimal atmospheric variability.
[c] Values should be interpreted as 2-σ estimates of the probable magnitude.

Desired improvements for future data version(s)

- Reduce noise/spikes in UTLS and in upper stratosphere.
- Minimize the impact of thick clouds on the retrievals to further improve the HNO_3 measurements in the upper troposphere and lowermost stratosphere.

3.12 Peroxy Radical

Swath name: HO2

Useful range: 22 – 0.046 hPa

Contact: Shuhui Wang, **Email:** <Shuhui.Wang@jpl.nasa.gov>

Introduction

A description of HO_2 data quality, precision, systematic errors, and validation for an earlier version, v2.2, is given in Pickett et al. [2008]. An early validation using v1.5 software is also described in Pickett et al. [2006a]. While there are signif cant improvements from v1.5 to v2.2, the HO_2 data quality in v3.3 is generally similar to v2.2 except that v3.3 has fewer non-convergent retrievals and therefore better zonal mean precisions in a given latitude bin. The estimated uncertainties, precisions, and resolution for v3.3 HO_2 are summarized below in Table 3.12.1. Note that the systematic uncertainties are from v2.2 and are not expected to change signif cantly in v3.3.

Resolution

Figure 3.12.1 shows the HO_2 averaging kernel for daytime at 70°N and the Equator. The latitudinal variation in the averaging kernel is very small. The vertical resolution for pressures greater than 0.1 hPa is generally about 5 km.

Precision

A typical HO_2 prof le and the associated precisions (for both v2.2 and v3.3) are shown in Figure 3.12.2. The prof le is shown in both volume mixing ratio (vmr) and density units. All MLS data are reported in vmr for consistency with the other retrieved molecules. However, use of density units (10^6 cm^{-3}) reduces the apparent steep gradient of HO_2 vertical prof le, allowing one to see the prof le with more detail. The night HO_2 prof le is expected to exhibit a narrow layer near the altitudes of the nighttime OH layer at ∼82 km [Pickett et al., 2006b], which is not shown in Figure 3.12.2 since MLS HO_2 data is not recommended for altitudes above 0.046 hPa (∼70 km). Precisions are such that an HO_2 zonal average within a 10° latitude bin can be determined with better than 10% relative precision with 20 days of data (∼2000 samples) for most pressure levels over 22 – 0.046 hPa.

Accuracy

Table 3.12.1 summarizes the accuracy expected for HO_2. The scaling uncertainty is the part of the systematic uncertainty that scales with HO_2 concentration, e.g. spectroscopic line strength. Bias uncertainty is the part of the uncertainty that is independent of concentration. For both bias and scaling uncertainty, quantif cation of the combined effect in MLS calibration, spectroscopy etc., on the data product was determined by calculating the effects of each source of uncertainty. These accuracy calculations are for v2.2 products. While no signif cant change is expected from v2.2 to v3.3, a comprehensive error analysis for v3.3 will be conducted. Bias uncertainty can be eliminated by taking day-night differences over the entire recommended pressure range. The accuracy of the HO_2 measurement due to systematic errors is a product of scaling uncertainty and the observed HO_2 concentration. The overall uncertainty is the square root of the sum of squares of the precision and accuracy.

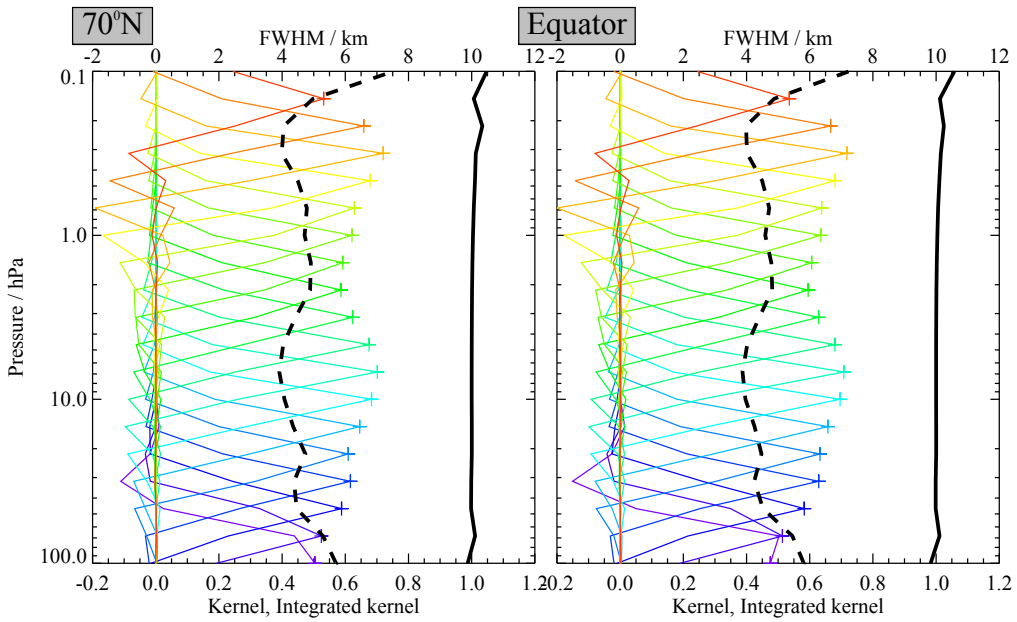

Figure 3.12.1: Typical vertical averaging kernels for the MLS v3.3 HO_2 data at 70°N (left) and the equator (right); variation in the averaging kernels is sufficiently small that these are representative of typical profiles. Colored lines show the averaging kernels as a function of MLS retrieval level, indicating the region of the atmosphere from which information is contributing to the measurements on the individual retrieval surfaces, which are denoted by plus signs in corresponding colors. The dashed black line indicates the vertical resolution, determined from the full width at half maximum (FWHM) of the averaging kernels, approximately scaled into kilometers (top axes). The solid black line shows the integrated area under each kernel; values near unity imply that the majority of information for that MLS data point has come from the measurements, whereas lower values imply substantial contributions from a priori information. The low signal to noise for this product necessitates the use of significant averaging (e.g., monthly zonal mean), making horizontal averaging kernels largely irrelevant.

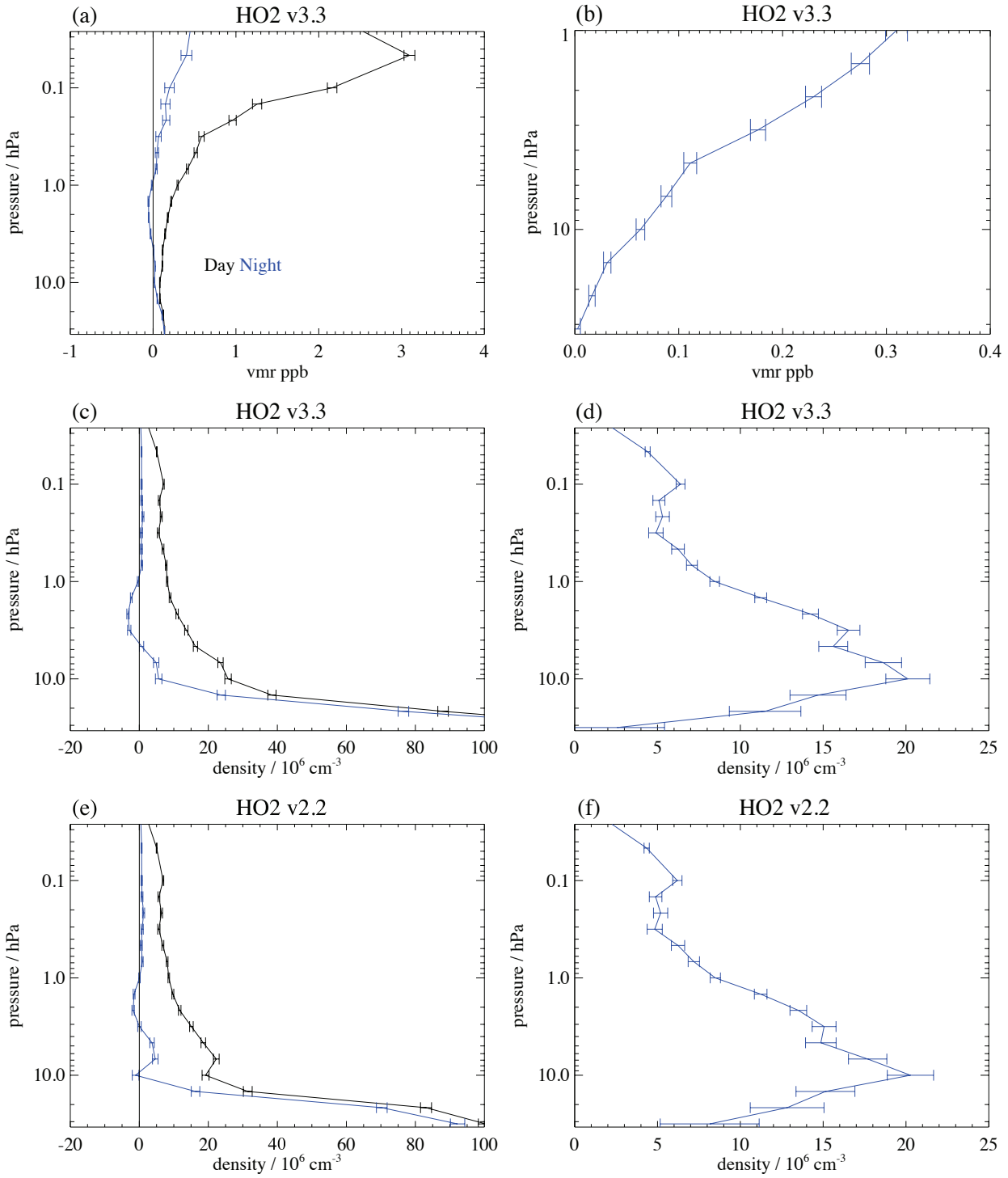

Figure 3.12.2: Monthly zonal mean of retrieved HO_2 and its estimated precision (horizontal error bars) for September, 2005 averaged over 29°N to 39°N. Panel (a) shows v3.3 HO_2 vmr vs. pressure for day (black) and night (blue). Panel (b) shows the same data plotted for the stratosphere as a day-night difference (note that a day-night difference is required for HO_2 for all pressure levels). Panel (c) shows the same data in (a) converted into density units. Panel (d) shows the day-night differences for the data in panel (c). Panels (e) and (f) are equivalent to (c) and (d) but using v2.2 data. The average in panels (a) – (d) using v3.3 data includes 3052 profiles, while the average in panels (e) – (f) using v2.2 data includes 2695 profiles.

Table 3.12.1: Summary of precisions, resolution, and uncertainties for the MLS v3.3 HO_2 product

Pressure / hPa	Vertical resolution km	Precision[a] / 10^6 cm^{-3}	Bias uncertainty / 10^6 cm^{-3}	Scaling uncertainty / %	Comments
< 0.03 hPa	—	—	—	—	Unsuitable for scientif c use
0.046 hPa	10	6	0.39	22	Use day–night difference
0.10 hPa	7	10	0.46	16	Use day–night difference
1.0 hPa	5	11	1.1	6	Use day–night difference
10 hPa	4	50	37	20	Use day–night difference
> 22 hPa	—	—	—	—	Unsuitable for scientif c use

[a]Precision for a single prof le

Data screening

It is recommended that HO_2 data values be used in scientif c investigations if all the following tests are successful:

Pressure range: 22 – 0.046 hPa

Values outside this range are not recommended for scientif c use.

Estimated precision: Only use values for which the estimated precision is a positive number.

Values where the *a priori* information has a strong inf uence are f agged with negative precision, and should not be used in scientif c analyses (see Section 1.5).

Status flag: Only use profiles for which the 'Status' field is an even number.

Odd values of `Status` indicate that the prof le should not be used in scientif c studies. See Section 1.6 for more information on the interpretation of the `Status` f eld.

Quality: MLS v3.3 HO_2 data can be used irrespective of the value of the `Quality` field.

Convergence: Only profiles whose 'Convergence' field is less than 1.1 should be used.

In version v2.2 this test often fails for 100 out of 3500 prof les in a day. In the current version, v3.3, there are often zero or very few non-convergence prof les.

Artifacts

Currently there are no known artifacts in the HO_2 product. The primary limitation is the precision and the altitude range.

Review of comparisons with other datasets

HO_2 data from MLS v2.2 software have been validated with two balloon-borne remote-sensing instruments. Details of the comparison are given in Pickett et al. [2008]. The comparison between v2.2 and v3.3 show no signif cant differences.

3.13 Hypochlorous Acid

Swath name: HOCl

Useful range: 10 – 2.2 hPa

Contact: Lucien Froidevaux, **Email:** <Lucien.Froidevaux@jpl.nasa.gov>

Introduction

The HOCl retrieval is quite noisy for individual profiles and HOCl data require some averaging (e.g., in 10° zonal means for one or more weeks) to get useful precision of better than 10 pptv, in comparison to typical upper stratospheric HOCl abundances of 100 – 150 pptv. Table 3.13.1 summarizes the MLS HOCl resolution, precision, and accuracy estimates for the upper stratosphere. More discussion and a brief validation summary are given in the following sections, along with data screening recommendations, which should be of particular interest to MLS data users.

Changes from v2.2

While there were no large v3.3 algorithmic changes relating to HOCl, one difference in the retrievals for HOCl and other products derived from the 640-GHz MLS retrieval phase is that temperature information is now obtained from the first retrieval phase ('Core'), as opposed to the 640-GHz phase itself; this led to overall improved efficiency, convergence, and stability for the v3.3 640-GHz products.

Other changes relating to the treatment of forward model radiance continuum had an impact on species in the 640-GHz retrieval phase (mainly in the lower stratosphere). The background observed in the 640-GHz radiances includes emissions from N_2, O_2, and H_2O. There are laboratory-based and ground-based models for the continuum absorptions that are the basis for the MLS absorption model [Pardo et al., 2001, and references therein]. These models were tested against MLS extinction measurements from the wing channels in the 640-GHz radiometer; the latitude dependence of this extinction was found to agree better with the expected moist plus dry continuum extinction values if the dry and moist continuum functions were scaled by factors close to 20%. The incorporation of this change improved the lower stratospheric retrievals of most of the 640-GHz species (generally in terms of average biases and their latitude dependence).

A comparison plot showing zonal average upper stratospheric HOCl contours (from 10 to 2 hPa) and differences between the two data versions for a typical month (September, 2006) is provided in Figure 3.13.1. The v3.3 HOCl abundances are slightly larger than the v2.2 retrievals, typically by ∼20 pptv (or ∼20%). The estimated precision values are essentially unchanged from v2.2.

Resolution

Based on the width of the averaging kernels shown in Figure 3.13.2, the vertical resolution for upper stratospheric HOCl is ∼6 km (significantly worse than the 640 GHz radiometer vertical field of view width of 1.4 km). This reflects the choice of smoothing constraints for HOCl which favor precision over vertical resolution.

Precision

The estimated single-profile precision reported by the Level 2 software is about 300 to 400 pptv in the upper stratosphere. A more useful number of 10 pptv is quoted in Table 3.13.1 for the typical precision of a 10° weekly zonal mean for this product.

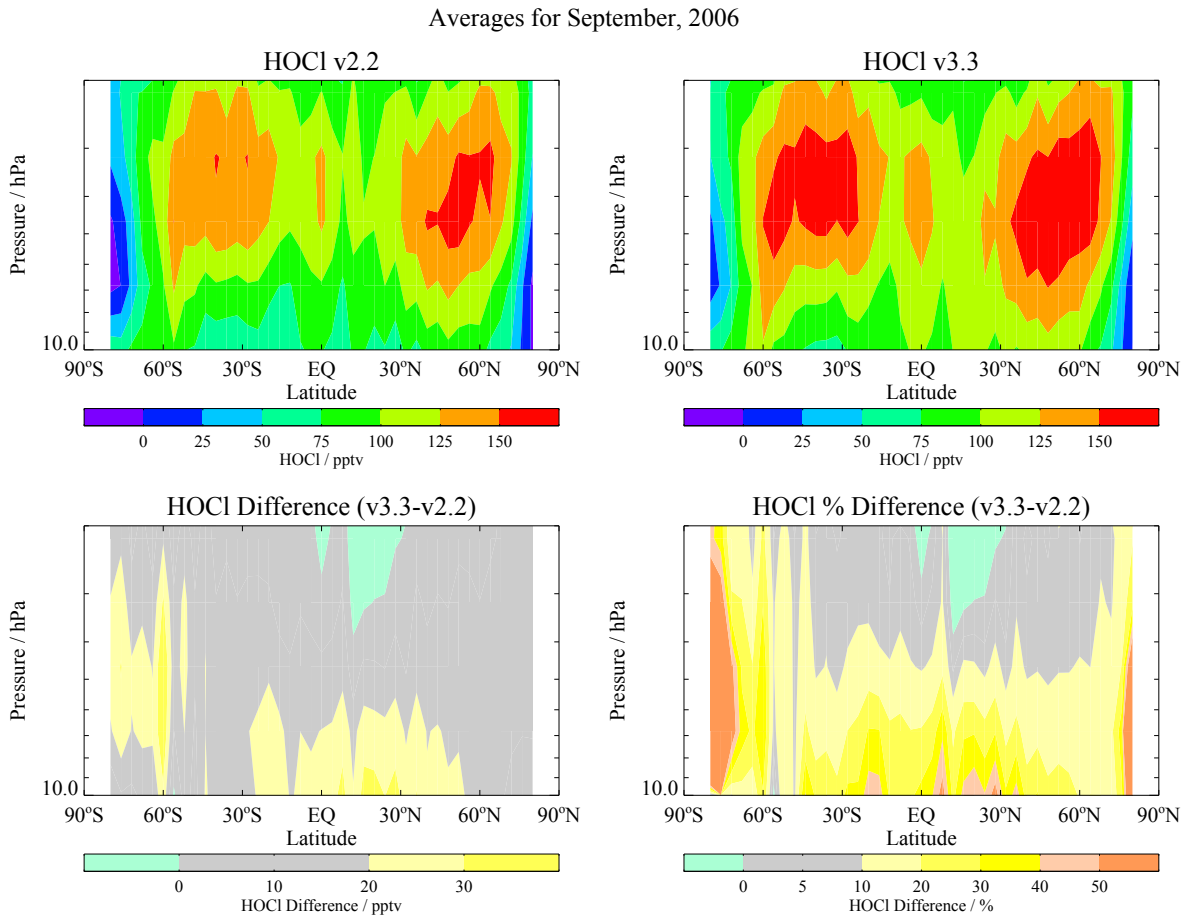

Figure 3.13.1: Zonal averages for upper stratospheric MLS HOCl profiles during September, 2006, showing the MLS v2.2 HOCl mixing ratio contours (top left panel), the v3.3 contours (top right panel), and their differences in pptv (v3.3 minus v2.2, bottom left panel) and percent (v3.3 minus v2.2 versus v2.2, bottom right panel).

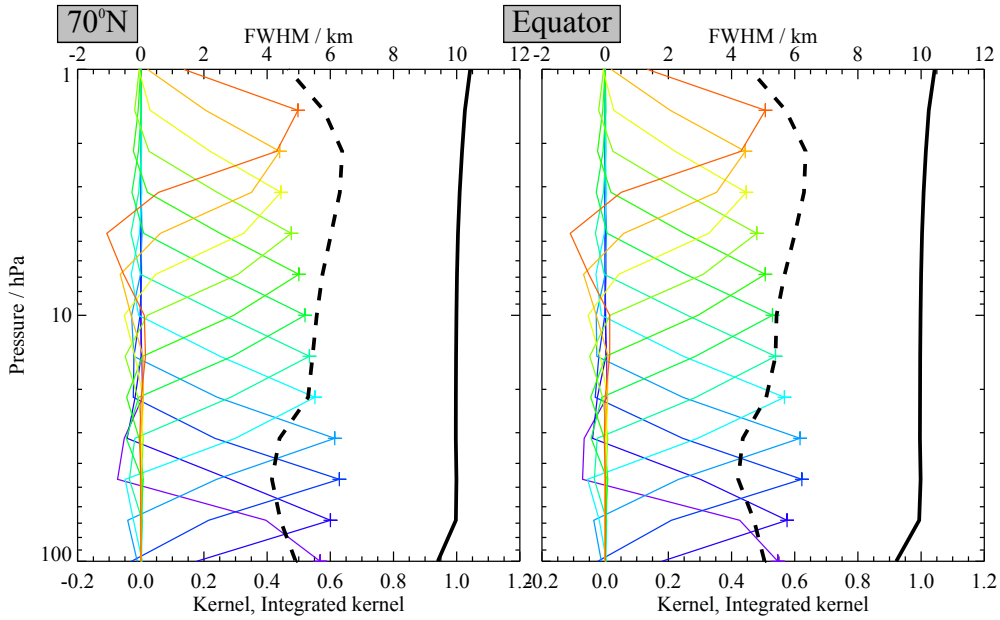

Figure 3.13.2: Typical vertical averaging kernels for the MLS v3.3 HOCl data at 70°N (left) and the equator (right); variation in the averaging kernels is sufficiently small that these are representative of typical profiles. Colored lines show the averaging kernels as a function of MLS retrieval level, indicating the region of the atmosphere from which information is contributing to the measurements on the individual retrieval surfaces, which are denoted by plus signs in corresponding colors. The dashed black line indicates the vertical resolution, determined from the full width at half maximum (FWHM) of the averaging kernels, approximately scaled into kilometers (top axes). The solid black line shows the integrated area under each kernel; values near unity imply that the majority of information for that MLS data point has come from the measurements, whereas lower values imply substantial contributions from a priori information. The low signal to noise for this product necessitates the use of significant averaging (e.g., monthly zonal mean), making horizontal averaging kernels largely irrelevant.

Accuracy

The accuracy estimates shown in the Table come from a formal quantification of the combined effects of possible systematic errors in MLS calibration, spectroscopy, etc. on the HOCl retrievals [Read et al., 2007]. These values are intended to represent 2 sigma estimates of accuracy. The largest contributors to possible errors for HOCl are contaminant species, gain compression, and sideband ratio uncertainties. The Table gives a range of error estimates (for low and high pressures). The average changes for upper stratospheric HOCl between v2.2 and v3.3 are well within the quoted accuracy estimates (which may be somewhat conservative).

Data screening

Pressure range: 10 – 2.2 hPa

Values outside this range are not recommended for scientific use. Artifacts (negative averages) for pressures larger than about 10 hPa currently make this product unsuitable for use in the lower stratosphere, although the negative biases observed in v2.2 for this region have been reduced and positive averages are retrieved in v3.3 down to 32 hPa. However, we cannot recommend these values for scientific investigations until more checks and validation are performed; we intend to provide updates on this topic in the not too distant future. Regarding the topmost altitude range, the sensitivity to *a priori* increases rapidly at pressures of 1 hPa or less; we continue to recommend the use of (average) HOCl values only up to 2.2 hPa.

Estimated precision: Only use values for which the estimated precision is a positive number.

Values where the *a priori* information has a strong influence are flagged with negative precision, and should not be used in scientific analyses (see Section 1.5).

Status flag: Only use profiles for which the 'Status' field is an even number.

Odd values of `Status` indicate that the profile should not be used in scientific studies. See Section 1.6 for more information on the interpretation of the `Status` field.

Quality: Only profiles whose 'Quality' field is greater than 1.2 should be used.

This criterion removes profiles with the poorest radiance fits, typically significantly less than 1% of the daily profiles. Results in this respect have improved, in comparison to v2.2 data. For HOCl (and for other 640 GHz MLS products), this screening correlates well with the poorly converged sets of profiles (see below); we recommend the use of both the `Quality` and `Convergence` fields for data screening. The use of this screening criterion sometimes (but rarely) removes up to a few percent of global daily data (for example, during the first half of September, 2006, when some high latitude convergence and quality issues arose).

Convergence: Only profiles whose 'Convergence' field is less than 1.05 should be used.

For the vast majority of profiles (99% or more for most days), this field is less than 1.05. Results in this respect have improved, in comparison to v2.2 data. Nevertheless, on occasion, sets of profiles (typically one or more groups of ten profiles, retrieved as a 'chunk') have this `Convergence` field set to larger values. These profiles are usually almost noise-free and close to the *a priori* profile, and need to be discarded as non-converged. The `Quality` field (see above) most often yields poorer quality values for these non-converged profiles. The use of this screening criterion sometimes (but rarely) removes up to a few percent of global daily data (for example, during the first half of September, 2006, when some high latitude convergence and quality issues arose).

Table 3.13.1: Summary for MLS hypochlorous acid

Pressure	Precision[a]		Vertical Resolution	Accuracy[b]		Comments
hPa	pptv	%	km km	pptv	%	
1.5 or less	—	—	—	—	—	Unsuitable for scientif c use
2.2 to 10	10	10	6	30 – 80	∼30 – 100	
15 or more	—	—	—	—	—	Unsuitable for scientif c use

[a]Precision (1 sigma) for 1 week/10 degrees zonal means or 2 weeks/5 degrees zonal means
[b]2 sigma estimate from systematic uncertainty characterization tests

Clouds: Profiles identified as being affected by clouds can be used with no restriction.

Review of comparisons with other datasets

The MLS HOCl retrievals exhibit the expected morphology in monthly mean latitude / pressure contour plots; for example, such plots for September months from MLS compare favorably, to f rst-order, with results produced by the Michelson Interferometer for Passive Atmospheric Sounding (MIPAS) for September, 2002 [von Clarmann et al., 2006]. MLS HOCl averages at midlatitudes are close to the results from balloon-borne infrared measurements. The slight increase in MLS v3.3 values (versus v2.2) should actually improve the overall agreement in these comparisons. As mentioned above, more work is needed to review these issues, especially for any altitudes below the 10 hPa level.

Artifacts

- The 640 GHz radiometer bands 10 (for ClO) and 29 (for HOCl) were turned off for a few time periods in 2006 to investigate degradation issues that might affect these channels in the future. These bands were off on April 8,9, and 10, 2006, and also for April 17, 2006 (after 19:52 UT) through May 17, 2006. There are essentially no useful HOCl (or ClO) data for these time periods. The v3.3 software correctly f ags these incidents with poor (odd) `Status` values (which should be screened out); we note that the v2.2 software did not f ag these days with odd `Status`.
- There are still signif cant artifacts in the mean values (large negative values) for HOCl in the lower stratosphere, where the use of this product is not recommended, despite the fact that some seasonal-type changes in both hemispheres appear to be consistent with expectations of realistic atmospheric enhancements in this region.
- Users should screen out the non-converged and poorest quality HOCl prof les, as such prof les (typically a very small number per day) tend to behave unlike the majority of the other MLS retrievals. See the criteria listed above.

3.14 Cloud Ice Water Content

Swath name: IWC

Units: g/m^3

Useful range: 215 – 83 hPa

Contact: Alyn Lambert, **Email:** <Alyn.Lambert@jpl.nasa.gov>

Introduction

The MLS IWC is retrieved from cloud-induced radiances (T_{cir}) of the 240-GHz window channel in a separate processing step after the atmospheric state (Temperature and tangent pressure) and important gaseous species (H_2O, O_3, HNO_3) have been finalized in the retrieval processing. The derived T_{cir} are binned onto the standard horizontal (1.5° along track) and vertical (12 surfaces per decade change in pressure) grids, and converted to IWC using the modeled T_{cir} – IWC relations [Wu et al., 2006]. The standard IWC profile has a useful vertical range between 215 – 83 hPa although the validation has been conducted for a subset of the range of IWC values. IWC measurements beyond the value ranges specified in Table 3.14.1 are to be regarded currently as giving only qualitative information on cloud ice. They require further validation for quantitative interpretation.

Resolution

In the IWC ranges specified in Table 3.14.1, each MLS measurement can be quantitatively interpreted as the average IWC for the volume sampled. This volume has a vertical extent of ∼3 km, with ∼300 km and 7 km along and cross track respectively.

Precision

The precision values quoted in the IWC files do not represent the true precision of the data. The precision for a particular measurement must be evaluated on a daily basis using the method described in the screening section below. The precision listed in Table 3.14.1 reflects typical values obtained from the method described below.

Accuracy

The IWC accuracy values listed in Table 3.14.1 are estimates from comparisons of the earlier v2.2 MLS data product with CloudSat and detailed analyses on the v2.2 error budget can be found in Wu et al. [2008].

Data screening

Pressure range (215 – 83 hPa): Values outside this range are not recommended for scientific use. The maximum detectable IWC is ∼100 mg/m^3.

Status flag: The user is recommended to screen the IWC data using the status field in the collocated temperature profile to exclude bad retrievals [Schwartz et al., 2008]. In other words, only IWC profiles for which temperature Status is an even number should be used.

Other screening: The IWC product derives from differences between measured radiances and those predicted assuming cloud free conditions. Spectroscopic and calibration uncertainties give rise to temporally and geographically varying biases in this difference, and hence the IWC product. These biases must be iteratively identified and removed, using a '$2\sigma - 3\sigma$' screening method, as described below.

1. MLS IWC signals derive from differences between observed radiances and those predicted assuming clear sky. Uncertainties in spectroscopy and atmospheric composition are manifested as residual biases in the IWC fields which should be identified and removed as follows. IWC data should be averaged in a 10° latitude bins and outliers rejected iteratively by excluding measurements greater than 2σ standard deviation about the mean (μ) of the bin. Repeat the σ and μ calculations after every new set of rejections. Convergence is usually reached within $5-10$ iterations, and the final σ is the estimated precision for the IWC measurements.
2. Interpolate the final σ and μ to the latitude of each measurement, and subtract μ from IWC for each measurement.
3. Finally, apply the 3σ threshold to determine if an IWC measurement is statistically significant. In other words, it must have IWC $> \mu + 3\sigma$ in order to be considered as a significant cloud hit. The 3σ threshold is needed for cloud detection since a small percentage of clear-sky residual noise can result in a large percentage of 'false alarms' in cloud detection.

Artifacts

At wintertime mid-to-high latitudes, strong stratospheric gravity waves may induce large fluctuations in the retrieved tangent pressure, and cause false cloud detection with the $2\sigma - 3\sigma$ screening method. The false cloud detection seems to affect the 100 hPa pressure level most, as expected for such impact coming from the lower stratosphere.

Comparisons with other datasets

Compared to v2.2 IWC the v3.3 IWC values are systematically smaller by $5-20\%$ over the pressure range $215-100$ hPa and generally the random noise in v3.3 IWC is larger than in v2.2 (see Figure 3.14.1 and Table 3.14.1). Apart from the differences noted above, the MLS v3.3 IWC is similar to the MLS v2.2 product described and validated in Wu et al. [2008]. A revised validation paper for IWC is not planned in the near future and users are encouraged to read Wu et al. [2008] for more information.

Comparisons between v2.2 MLS and CloudSat IWC showed good agreement with PDF differences $<50\%$ for the IWC ranges specified in Table 3.14.1. Comparisons with AIRS, OMI and MODIS suggest that MLS cloud tops are slightly higher by $\sim$1 km than the correlative data in general.

Desired improvements for future data version(s)

The IWC retrieval in v3.3 and the earlier versions is a simple first-order conversion, applied independently to each T_{cir} measurement. A 2-D cloudy-sky radiative transfer model is under development for version 4 processing which will allow IWC profiles to be retrieved jointly with the T_{cir} measurements from adjacent scans.

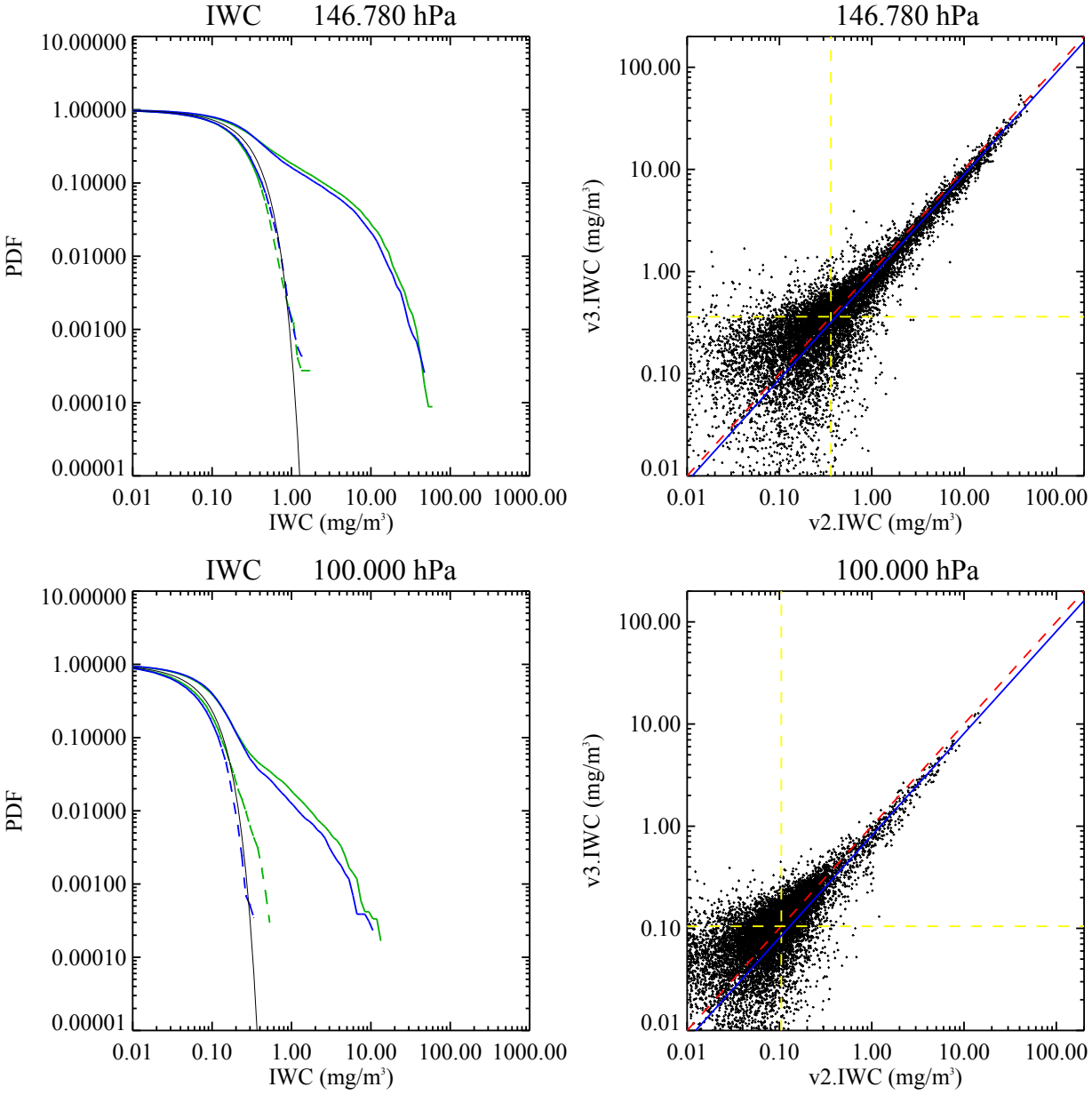

Figure 3.14.1: MLS v3 and v2 IWC comparisons for a 42 day period in May-June 2008 at 146 hPa and 100 hPa. (a) Left: Probability density functions (PDF) (v3 (blue) and v2 (green)) with dashed lines showing the corresponding noise levels (obtained by folding the negative IWC values about the origin) and the thin black lines representing the gaussian error function. (b) Right: Scatter plots of IWC v3 vs v2 (black points) with dashed red lines indicating the 1:1 line, dashed yellow lines the 1-sigma uncertainties and the blue lines are linear fits to the data.

Table 3.14.1: Summary of MLS v3.3 IWC precision, accuracy, and resolution.

Pressure / hPa	Resolution[a] / km	Typical precision[b] / mg/m^3	Accuracy[c] / mg/m^3		Valid IWC range[d] / mg/m^3
			<10 mg/m^3	>10 mg/m^3	
$p<70$		Unsuitable for scientif c use			
83	200×7×5	0.07	100%	—	0.02 – 50
100	200×7×5	0.10	100%	150%	0.02 – 50
121	250×7×4	0.15	100%	100%	0.04 – 50
147	300×7×4	0.25 – 0.35	100%	100%	0.1 – 50
177	300×7×4	0.5 – 1.0	150%	100%	0.3 – 50
215	300×7×4	1.2 – 2.1	300%	100%	0.6 – 50
$p>260$		Unsuitable for scientif c use			

[a]The along-track, cross-track and vertical extent, respectively of the atmospheric volume sampled by an individual MLS measurement.

[b]These are typical 1σ precisions where the better values are for the extratropics and the poorer values for the tropics. The precision for a particular measurement must be evaluated on a daily basis using the method described in the text.

[c]Estimated from comparisons with CloudSat.

[d]This is the range where the stated precision, accuracy and resolution are applied. In this range MLS measurements can be quantitatively interpreted as the average IWC for the volume sampled. IWC values above this range, currently giving qualitative information on cloud ice, require further validation for quantitative interpretation.

3.15 Cloud Ice Water Path

Swath name: IWP (stored as an additional swath in the L2GP-IWC file).

Units: g/m^2

Useful range: MLS IWP is the ice water column above ~6 km

Contact: Alyn Lambert, **Email:** <Alyn.Lambert@jpl.nasa.gov>

Introduction

MLS standard IWP is retrieved from cloud-induced radiances (T_{cir}) of the 240-GHz window channel at 650 hPa tangent pressure (see Figure 3.15.1). It represents a partial column above ~6 km, and is stored in the v3.3 L2GP IWC file as a separate swath. For the IWP retrieval, T_{cir} is first converted to a near horizontal slant path (with a ~3° elevation angle) IWP 'hIWP', using the modeled T_{cir} – hIWP relation. The hIWP is then converted to the nadir IWP at the tangent point location, and interpolated to the MLS standard horizontal grid.

Resolution

In the IWP ranges specified in the summary at the end of this section, each MLS measurement can be quantitatively interpreted as the average IWP for the volume sampled. The MLS IWP volume is a vertical column above ~6 km, with 60 km and 7 km along and cross track extent respectively.

Precision

The precision values quoted in the IWP swaths do not represent the true precision of the data. The precision for a particular measurement must be evaluated on a daily basis using the method described in the screening section below. The 3 g/m^2 precision given the summary at the end of this section reflects *typical values* for MLS IWP measurements.

Accuracy

The IWP accuracy is ~50%, as estimated from comparisons of the earlier v2.2 MLS data product with CloudSat and detailed analyses on the v2.2 error budget can be found in Wu et al. [2009].

Data screening

The standard IWP product has a useful sensitivity up to 200 g/m^2 where MLS measurements can be quantitatively interpreted as the average IWP for the volume sampled. The user is recommended to screen the IWP data using the status field in the collocated temperature profile to exclude bad retrievals [Schwartz et al., 2008]. Only IWP values for which temperature Status is an even number should be used. In addition to the status screening, the user is also recommended to screen the IWP data for significant cloud hits on a daily basis using the '$2\sigma - 3\sigma$' method described in the IWC section (3.14). The 3σ threshold is needed for cloud detection since a small percentage of clear-sky residual noise can result in a large percentage of false alarm in cloud detection.

Artifacts

High-latitude high-land surface can be mistakenly detected as a cloud when the atmosphere is very dry, allowing MLS 240-GHz radiances to penetrate down to the surface. Surface emission/scattering can then reduce brightness temperature. Surface effects (e.g., over the highland over Antarctica) may introduce artif cial IWP values as large as 10 g/m^2. In addition, the geographical location of MLS IWP is currently registered at the tangent point, which is $\sim$2 prof les away from the actual location of the IWP column as shown in Figure 3.15.1. The user needs to correct this offset by replacing the IWP location with the one at 2 prof les earlier.

Comparisons with other datasets

Compared to v2.2 IWP the v3.3 IWP values are systematically larger by $\sim$2 % and the random noise is slightly smaller than in v2.2 (see Figure 3.15.2). Apart from the differences noted above, the MLS v3.3 IWP is similar to the MLS v2.2 product described and validated in Wu et al. [2009]. A revised validation paper for IWP is not planned in the near future and users are advised to read Wu et al. [2009] for more information.

Comparisons between v2.2 MLS and CloudSat IWP showed good agreement with PDF differences $<$50% for the IWP range specif ed in the summary at the end of this section.

Desired improvements for future data version(s)

The IWP retrieval in v3.3 is a simple f rst-order conversion, applied independently to each T_{cir} measurement. Plans for future versions include development of 2-D cloudy-sky radiative transfer model. This will allow IWP to be retrieved jointly with the T_{cir} measurements from adjacent scans.

Summary for IWP

IWP Column Bottom: 6 km (estimated from MLS radiative transfer model calculations).

The calculation of the bottom height of the IWP column depends on the tropospheric water vapor loading and on the IWP itself and is discussed in Wu et al. [2009].

Typical precision: 3 g/m^2 is the typical 1σ precision.

The precision for a particular measurement must be evaluated on a daily basis using the method described in the text.

Accuracy: 50% (estimated from comparisons with CloudSat)

Resolution: 60 km along track, 7 km across track (the volume of air sampled by MLS)

Valid IWP range: $\leq$200 g/m^2

This is the range where the stated precision, accuracy and resolution are applied. In this range MLS measurements can be quantitatively interpreted as the average IWP for the volume sampled. IWP values above this range, currently giving qualitative information on cloud ice, require further validation for quantitative interpretation.

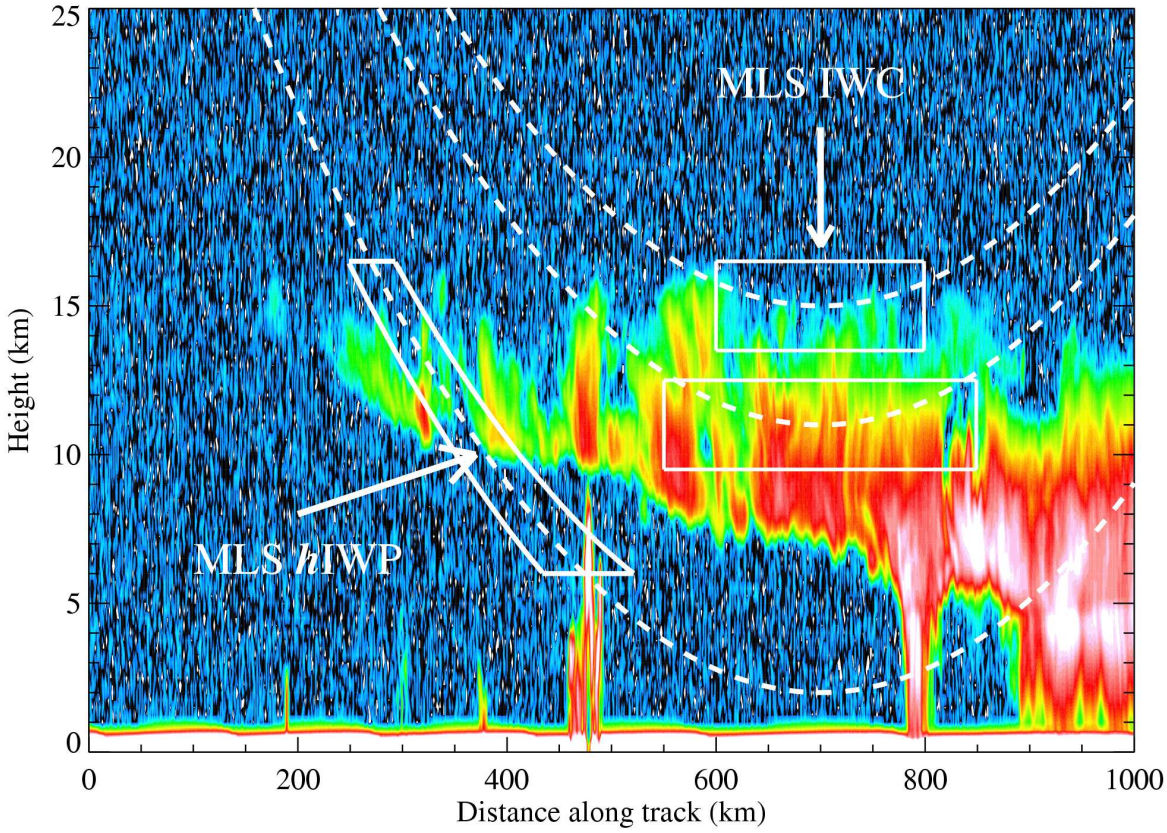

Figure 3.15.1: Diagram to illustrate the MLS IWC and IWP measurement. The dashed lines are the MLS tangential beams. At high tangent heights, the beams penetrate through the limb and become sensitive to a volume-averaged IWC, whereas at low tangent heights the MLS beams cannot penetrate through the limb due to strong gaseous absorption and become only sensitive to a partial slant column of IWP, with a shallow (∼3°) angle, 'hIWP'. Note that the actual volume of the air represented by hIWP is centered ∼300 km away from the tangent point, or ∼2 profiles from the location of the nominal profile.

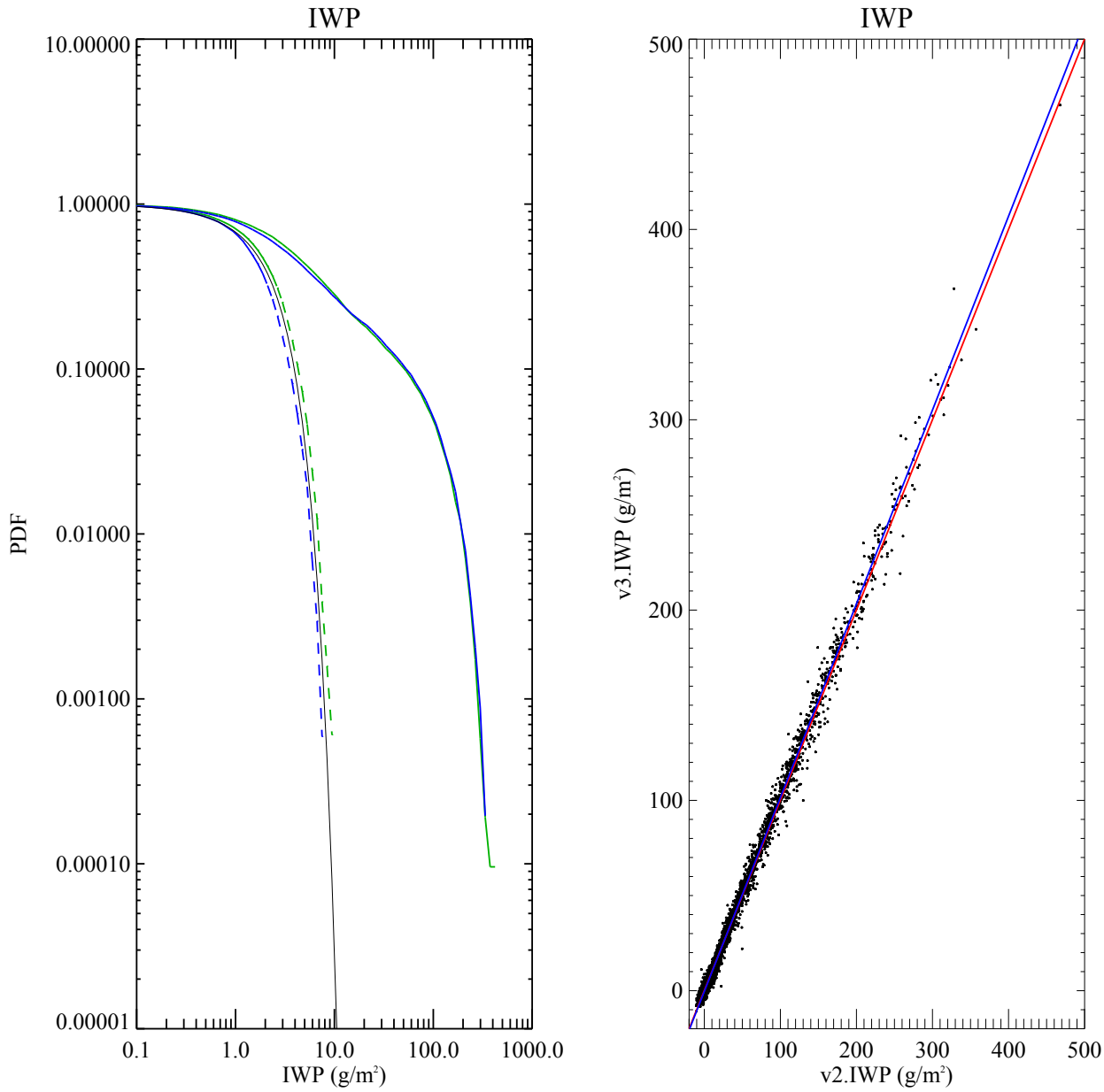

Figure 3.15.2: MLS v3 and v2 IWP comparisons for a 42 day period in May-June 2008. Left: Probability density functions (PDF) (v3 (blue) and v2 (green)) with dashed lines showing the corresponding noise levels (obtained by folding the negative IWP values about the origin) and the thin black lines representing the gaussian error function. Right: Scatter plot of IWP v3 vs v2 (black points) with a dashed red lined indicating the 1:1 line and a linear fit to the data shown as a blue line.

3.16 Nitrous Oxide

Swath name: N2O

Useful range: 100 – 0.46 hPa

Contact: Alyn Lambert, **Email:** <Alyn.Lambert@jpl.nasa.gov>

Introduction

The standard product for v3.3 N_2O is taken from the 640 GHz ('Core+R4B') retrieval and details of the retrieval method and validation results are presented in [Lambert et al., 2007]. All of the v3.3 640-GHz retrieval phases use the temperature and tangent pressure information from and earlier retrieval phase, instead of including a joint temperature/pTan retrieval as was done for v2.2. This change has signif cantly reduced the number of 'non convergent' 640-GHz retrievals in v3.3 compared to v2.2.

Resolution

The spatial resolution reported by the averaging kernel matrices shown in Figure 3.16.1. The vertical resolution is 4 – 6 km and the horizontal along-track resolution is 300 – 600 km over most of the useful range of the retrievals. The horizontal cross-track resolution is set by the 3 km width of the MLS 640-GHz f eld-of-view for all pressures. The longitudinal separation of the MLS measurements is 10° – 20° over middle and lower latitudes, with much f ner sampling in polar regions.

Precision

Precision as def ned here is the 1-σ uncertainty in the retrieved value calculated by the Level 2 algorithms and has been validated against the scatter about the mean of coincident ascending/descending MLS prof le differences. The estimated precision on a single retrieved prof le given in Table 3.16.1 varies with height from ∼12 – 24 ppbv. The N_2O values at the 147 hPa pressure level have a large a priori inf uence and practically all precisions are f agged negative at this level.

Accuracy

The 'accuracy' values given in Table 3.16.1 are taken from the detailed analysis presented of MLS v2.2 data in Lambert et al. [2007] to quantify the systematic uncertainties associated with the MLS instrument calibration, spectroscopic uncertainty and approximations in the retrieval formulation and implementation. Accuracy of v3.3 N_2O data are expected to be little different from that established for v2.2.

Data screening

Pressure range: 100 – 0.46 hPa

Values outside this range are not recommended for scientif c use. In the upper stratosphere and lower mesosphere v3.3 N_2O requires signif cant averaging for useful signals, but see the note under 'Artifacts' for issues above 0.1 hPa.

Estimated precision: Only use values for which the estimated precision is a positive number.

Values where the *a priori* information has a strong inf uence are f agged with negative precision, and should not be used in scientif c analyses (see Section 1.5).

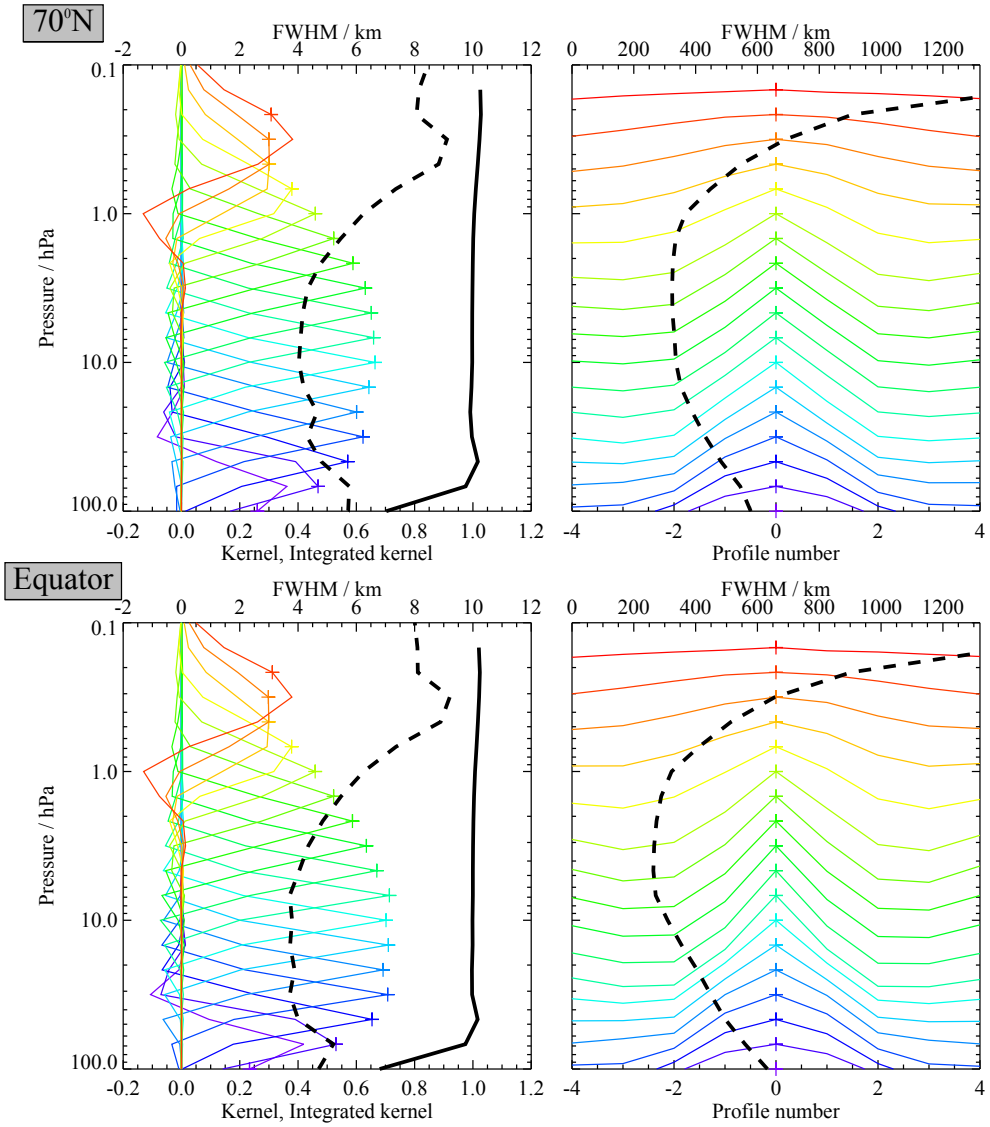

N_2O

Figure 3.16.1: Typical two-dimensional (vertical and horizontal along-track) averaging kernels for the MLS v3.3 N_2O data at 70°N (upper) and the equator (lower); variation in the averaging kernels is sufficiently small that these are representative of typical profiles. Colored lines show the averaging kernels as a function of MLS retrieval level, indicating the region of the atmosphere from which information is contributing to the measurements on the individual retrieval surfaces, which are denoted by plus signs in corresponding colors. The dashed black line indicates the resolution, determined from the full width at half maximum (FWHM) of the averaging kernels, approximately scaled into kilometers (top axes). (Left) Vertical averaging kernels (integrated in the horizontal dimension for five along-track profiles) and resolution. The solid black line shows the integrated area under each kernel (horizontally and vertically); values near unity imply that the majority of information for that MLS data point has come from the measurements, whereas lower values imply substantial contributions from a priori information. (Right) Horizontal averaging kernels (integrated in the vertical dimension) and resolution. The horizontal averaging kernels are shown scaled such that a unit averaging kernel amplitude is equivalent to a factor of 10 change in pressure.

Status flag: Only use profiles for which the 'Status' field is an even number.

Odd values of `Status` indicate that the profile should not be used in scientific studies. See Section 1.6 for more information on the interpretation of the `Status` field.

Quality: Only profiles whose 'Quality' field is greater than 1.4 should be used.

A small fraction of N_2O profiles (typically less than 0.5%) will be discarded via this screening.

Convergence: Only profiles whose 'Convergence' field is less than 1.01 should be used.

A fraction of the N_2O data (typically less than 2%) at this level will be discarded via this screening.

Clouds: Clouds can impact the N_2O product at the lowest altitudes. See below for details.

Very thick clouds in the tropics produce a low rate of artifacts in the N_2O product, consisting of abnormally high (and, more rarely, low) values at 100 hPa (and 147 hPa, not recommended for scientific use). Such cases are not always detected by the `Quality` and `Convergence` flags, and the cloud bits of the `Status` field are too blunt a tool to identify these cases, needlessly discarding reasonable data. We recommend checking for the occurrence of N_2O values greater than 350 ppbv on the 68 hPa MLS retrieval level in order to remove significant outliers from the 100 – 46 hPa data.

Artifacts

The v3.3 N_2O retrievals are improved at 100 – 68 hPa, where the v2.2 retrievals often showed signs of poor convergence resulting in sets of consecutive 'smooth' profiles. There are occasional nonphysical values of N_2O in the v3.3 data, and screening using the convergence and quality fields (see above) is recommended to remove the majority of these data points.

The retrieval restricts N_2O values to be greater than -40 ppbv (approximately three times the retrieval noise level in the recommended pressure range) in order to prevent problems in the minimization search process. The low bound is applied at all levels, but it is only evident in the data for pressures less than 0.1 hPa, where the vertical smoothing is relaxed and the retrieval noise becomes comparable to the magnitude of the low bound value. Accordingly, statistical averaging of the data (zonal means or longer time periods) cannot be applied successfully for pressures at and less than 0.1 hPa as the -40 ppbv hard limit introduces a positive bias in any average.

Review of comparisons with other datasets

Average values for v3.3 N_2O are 20% larger than in v2.2 for the 100 hPa pressure level, up to 10% smaller at the 46 – 32 hPa levels, and within 5% for pressures greater than 22 hPa (see Figure 3.16.2).

Apart from the differences noted above, the MLS v3.3 N_2O is similar to the MLS v2.2 product described and validated in Lambert et al. [2007]. Comparisons of v2.2 N_2O with coincident measuremements by ACE-FTS, Odin/SMR, and Envisat/MIPAS and balloon borne observations are shown in Lambert et al. [2007]. A revised validation paper for N_2O is not planned in the near future and users are encouraged to read Lambert et al. [2007] for more information.

Desired improvements for future data version(s)

Retrievals of N_2O to pressures greater than 147 hPa *may* be possible in later versions, however, these data would be taken from the 190-GHz observations rather than the 640-GHz which currently form the standard product.

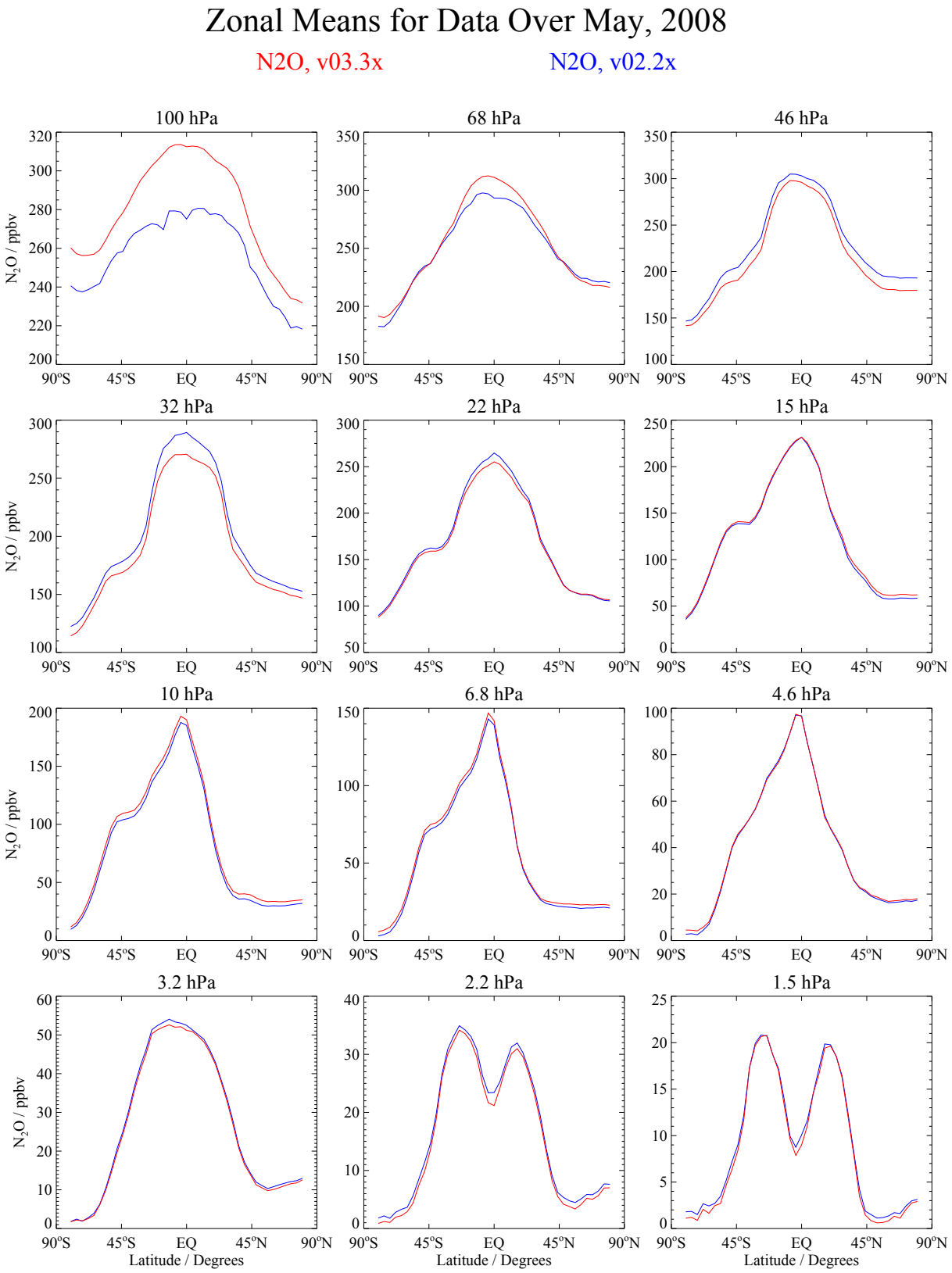

Figure 3.16.2: MLS v3.3 N_2O compared to MLS v2.2 for May 2008

Table 3.16.1: Summary of MLS v3.3 N_2O product.

Region	Resolution	Precision[a]		Accuracy		Comments
	Vert. × Horiz.					
hPa	km	ppbv	%	ppbv	%	
≤0.33	—	—	—	—	—	Unsuitable for scientif c use
0.46	8.8 × 530	12	>100%	0.5	16	
0.68	7.3 × 430	13	>100%	0.6	15	
1.00	6.3 × 340	14	>100%	0.6	12	
2.15	4.8 × 300	15	>100%	1.2	9	
4.64	4.2 × 280	14	41	3	9	
10.0	4.0 × 320	13	12	7	9	
21.5	4.7 × 400	13	9	19	13	
46.4	4.8 × 490	16	8	32	14	
68.1	5.8 × 550	20	8	32	13	
100	5.7 × 610	24	9	70	25	
147	—	—	—	—	—	Unsuitable for scientif c use
≥215	—	—	—	—	—	Not retrieved

[a]Precision on individual prof les

3.17 Ozone

Swath name: O3

Useful range: 261 – 0.02 hPa

Contact: Lucien Froidevaux (stratosphere/mesosphere), **Email:** <Lucien.Froidevaux@jpl.nasa.gov>
Michael Schwartz (upper troposphere), **Email:** <Michael.J.Schwartz@jpl.nasa.gov>

Introduction

The v3.3 standard O_3 product is taken from the 240-GHz retrieval, which provides the highest sensitivity down into the upper troposphere, as well as in the mesosphere. Table 3.17.1 summarizes the typical resolution, precision, and systematic uncertainty estimates as a function of pressure. Papers describing detailed validation of the MLS v2.2 product and comparisons with other data sets were published in a special Aura validation issue of the *Journal of Geophysical Research*, see [Froidevaux et al., 2008a; Jiang et al., 2007; Livesey et al., 2008]. In the stratosphere and above, v3.3 ozone profiles are very similar to the v2.2 profiles, so the stratospheric results from the above references will generally hold for the v3.3 product. Initial documentation of changes, improvements, and issues with v3.3 data are discussed here, including data screening criteria (which are now somewhat more complex than in v2.2 data). The morphology of the (zonal mean) v3.3 ozone data appears to be more reliable (realistic) for the largest pressure values where ozone is retrieved in the upper troposphere, notably at 316 hPa and also at 261 hPa (a new level for v3.3). The 316 hPa ozone retrievals will, however, require further validation before we can recommend this pressure surface for scientific use.

There are 2 separate stratospheric ozone columns (typically in very good agreement) in the L2GP-O3 files, with swath names '`O3␣column-MLS`' and '`O3␣column-GEOS5`', corresponding to the use of tropopause pressures (WMO definition) determined from MLS or GEOS-5 temperatures, respectively. Data users can also provide their own calculations of column ozone values (with better screening), based on the MLS ozone profiles, given that poorly defined tropopause values can lead to relatively large scatter at certain places (and times) for ozone column results.

Comparison of v3.3 with v2.2

Between 316 hPa and 1 hPa, v3.3 ozone profiles are retrieved on 12 surfaces per decade, a grid twice as fine as the 6-level-per-decade grid used in v2.2. This finer grid makes possible some improvement in vertical resolution in the UTLS, with retrieved precisions similar to (or slightly larger than) the v2.2 values, but at the cost of poorer horizontal resolution (see Table3.17.1.) For pressures less than 1 hPa, the retrieval grid has not changed from the v2.2 grid; it becomes coarser, with 6 surfaces per decade change in pressure between 1 and 0.1 hPa, and 3 surfaces per decade change in pressure from 0.1 hPa to 0.01 hPa. Other changes in the retrievals for the 240-GHz phase (affecting CO and HNO_3 as well as ozone) include the manner in which the spectral baseline is modeled. The v3.3 retrieval fits a relative-humidity-like, frequency squared extinction baseline at the lowest retrieval levels, rather than a spectrally flat extinction profile, as used in v2.2. This modification reduces ozone biases in the upper troposphere in moist clear air (or thin cloud) conditions, but gives a poorer fit to the impacts of thick clouds (scattering from ice particles in convective cores). Cloud effects lead to more scatter and vertically-oscillating profiles in v3.3, for the most part in the tropics, and methods to screen out cloud-impacted profiles are discussed below. Also, there have been relatively minor spectroscopic changes for these v3.3 ozone retrievals: the line mixing parameters are now taken from the recent (unpublished) work of *DeLucia et al.*.

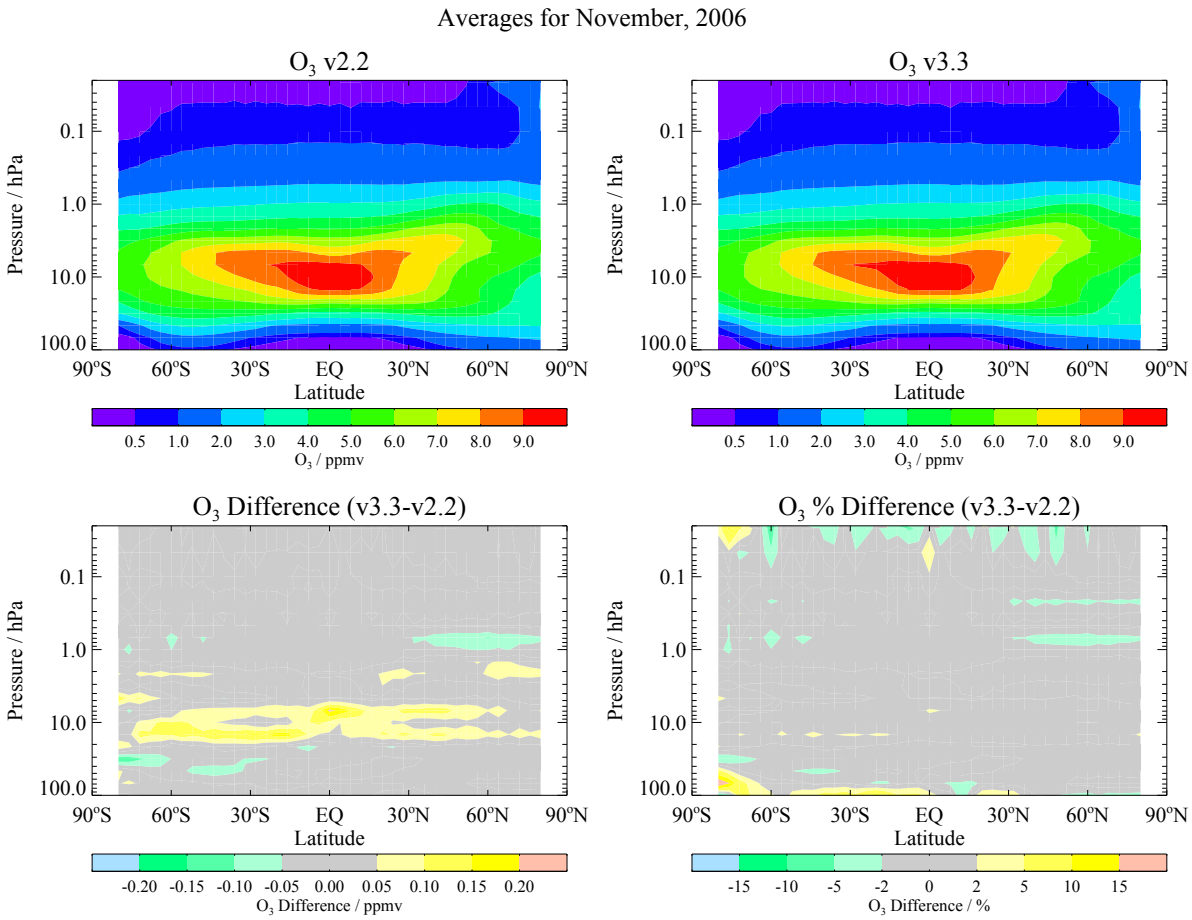

Figure 3.17.1: Zonal averages for stratospheric and mesospheric MLS ozone profiles during November, 2006, showing the MLS v2.2 ozone mixing ratio contours (top left panel), the v3.3 contours (top right panel), and their differences in ppmv (v3.3 minus v2.2, bottom left panel) and percent (v3.3 minus v2.2 versus v2.2, bottom right panel).

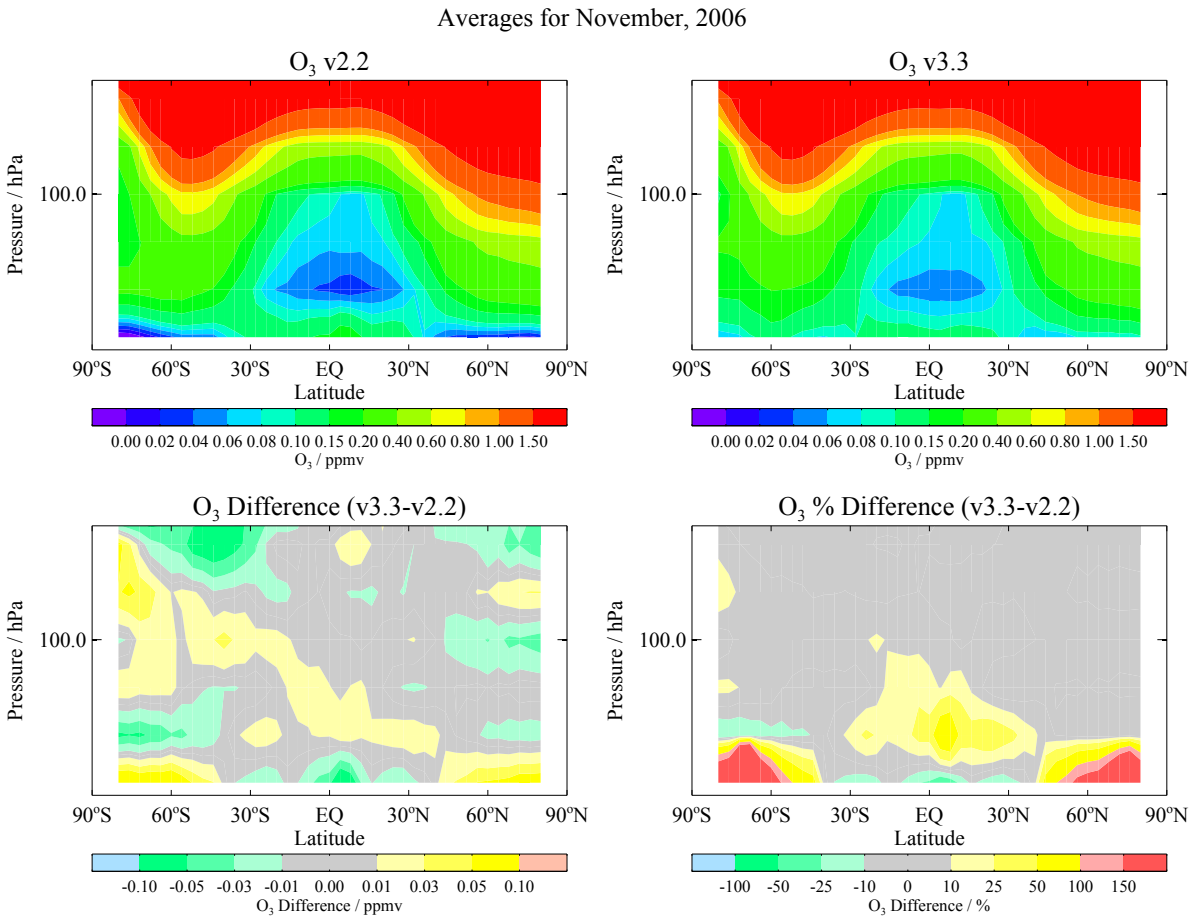

Figure 3.17.2: Zonal averages for UTLS MLS ozone profiles during November, 2006, showing the MLS v2.2 ozone mixing ratio contours (top left panel), the v3.3 contours (top right panel), and their differences in ppmv (v3.3 minus v2.2, bottom left panel) and percent (v3.3 minus v2.2 versus v2.2, bottom right panel).

Figures 3.17.1 and 3.17.2 show zonally averaged fields for the (full) month of November, 2006, with only the properly screened profiles from v2.2 and v3.3 being used; mean differences (ppmv and percent) are also shown. The averages for stratospheric (and lower mesospheric) ozone have typically not changed (typically) by more than 0.1 ppmv,or 1 to 2%; see Figure 3.17.1. At low latitudes, zonal-mean v3.3 tends to be ∼10 ppbv larger than v2.2 from 215 hPa to 100 hPa, while at higher latitudes, the v2.2/v3.3 relationship tends to switch signs, with v3.3 higher than v2.2 at 316 hPa and 147 hPa, and lower at 215 hPa and 100 hPa (see Figure 3.17.2). Also, we note that the version 3.3 mean tropical profiles in the UTLS can exhibit significant systematic vertical oscillations, mostly apparent during certain months (see the 'Artifacts' section below).

Ozone Columns: Changes in the MLS stratospheric ozone columns (or in columns down to pressures between 100 and 316 hPa) for v3.3 are quite small; typical daily zonal averages are within one percent, and often within one DU. There is no significant systematic offset (offsets can change slightly between pressure levels and versus latitude, including changes in sign). The most significant difference is the change in scatter, as observed for example in standard deviations about zonal averages (with v3.3 scatter often lower than in v2.2 by several DU); this is largely a result of (and at the expense of) changes in the horizontal smoothing, and poorer horizontal resolution for v3.3 data (see below).

Resolution

Vertical and horizontal smoothing constraints were changed for v3.3 data in an attempt to capitalize upon the higher vertical resolution offered by the finer grid, while minimizing the vertical oscillations invited by the additional vertical degrees of freedom. Based on the width of the averaging kernels shown in Figures 3.17.3 and 3.17.4, the vertical resolution for the standard O_3 product is ∼2.5 km in the uppermost troposphere and stratosphere, but degrades to 4 to 6 km in the upper mesosphere and to ∼3 km at 316 hPa. At best, lower stratospheric resolution can be about 2.3 km, which is an improvement over v2.2 data (but not by a factor of two – the best resolution offered by the new 12-per-decade grid). The along-track resolution in the stratosphere has changed from ∼ 200 km in v2.2 to 300 to 450 km in v3.3, depending on altitude (the upper stratosphere shows poorer resolution). In the mesosphere, this along-track resolution varies between about 300 and 700 km. In the upper troposphere, the along-track resolution degrades from ∼300 km at 120 hPa to ∼450 km at 261 hPa. Typical resolution values are provided in the summary Table 3.17.1. The cross-track resolution is set by the 6 km width of the MLS 240 GHz field of view. The longitudinal separation of MLS measurements, set by the Aura orbit, is $10^\circ - 20^\circ$ over middle and lower latitudes, with much finer sampling in polar regions.

Precision

The horizontal smoothing changes in v3.3, coupled with the finer vertical retrieval grid, have led to some changes in estimated precision (keeping in mind, however, the poorer v3.3 horizontal resolution). In the upper stratosphere, the precisions are improved (smaller values) by about 30% in the v3.3 data, although there is no need to quote substantially different values than the (rounded off) values that are given in Table 3.17.1. In the UTLS, the Level 2 ozone precision (uncertainty) values have worsened slightly (by ∼20 to 30%) from v2.2 to v3.3. As found previously for v2.2 data, the Level 2 precision values are often slightly lower than the observed scatter in the data, evaluated in a narrow latitude band centered around the equator where atmospheric variability is expected to be small, or obtained from a comparison between ascending and descending coincident MLS profiles.

Negative precision values for ozone occur essentially for every data point at pressures smaller than 0.01 hPa, indicating increasing influence from the *a priori*, although some MLS information exists (e.g.,

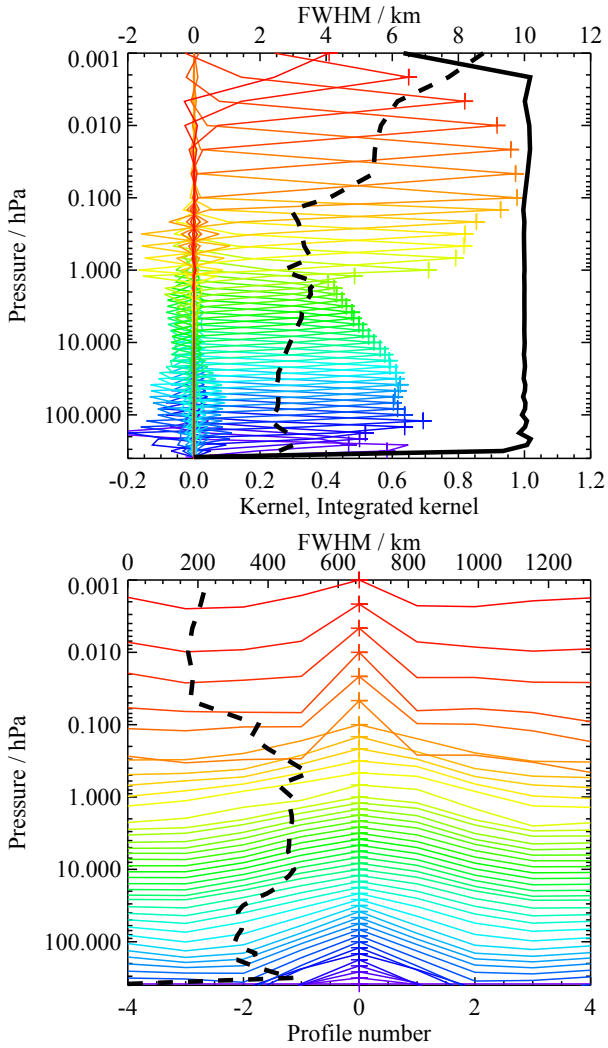

Figure 3.17.3: Typical two-dimensional (vertical and horizontal along-track) averaging kernels for the MLS v3.3 O_3 at the equator; variation in the averaging kernels is sufficiently small that these are representative of typical profiles. Colored lines show the averaging kernels as a function of MLS retrieval level, indicating the region of the atmosphere from which information is contributing to the measurements on the individual retrieval surfaces, which are denoted by plus signs in corresponding colors. The dashed black line indicates the resolution, determined from the full width at half maximum (FWHM) of the averaging kernels, approximately scaled into kilometers (top axes). (Upper) Vertical averaging kernels (integrated in the horizontal dimension for five along-track profiles) and resolution. The solid black line shows the integrated area under each kernel (horizontally and vertically); values near unity imply that the majority of information for that MLS data point has come from the measurements, whereas lower values imply substantial contributions from a priori information. (Lower) Horizontal averaging kernels (integrated in the vertical dimension) and resolution. The averaging kernels are scaled such that a unit change is equivalent to one decade in pressure.

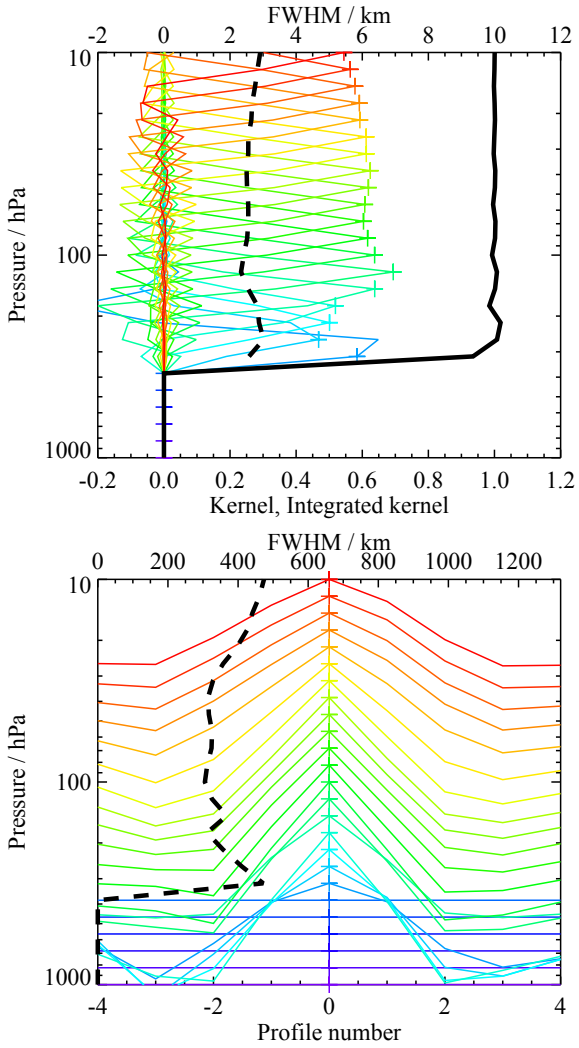

Figure 3.17.4: As for 3.17.3 but zooming in on the upper troposphere and lower stratosphere region.

regarding average day/night differences) into the uppermost mesosphere and lower thermosphere. Generally, however, we recommend that scientific studies be restricted to pressures of 0.02 hPa or larger.

Column values: As for the v2.2 retrievals, the estimated precisions for the v3.3 MLS column ozone abundances down to pressures of 100 to 215 hPa are 2% or less. The typical empirical precision in the columns based on (1-σ) variability in the tropics is 2 to 3%. However, see the comments above regarding the somewhat poorer along-track (horizontal) resolution for v3.3 data.

Accuracy

The accuracy estimates shown in Table 3.17.1 are from an analysis which propagated estimated systematic errors in MLS calibration, spectroscopy, etc., through the v2.2 measurement system. Results using the v3.3 algorithms are not expected to differ significantly. The values shown here are intended to represent 2σ estimates of accuracy. Overall, we see no evidence, based on a number of (published) comparisons with well established data sets, that significant disagreements (outside the combined accuracy estimates) or MLS-related issues exist for the MLS ozone product. For more details, see the MLS validation papers by Froidevaux et al. [2008a], Jiang et al. [2007]. and Livesey et al. [2008], as well as references therein; some more recent references relevant to MLS ozone and ozone columns are available on the MLS website under 'Publications'. Future validation studies using v3.3 data will focus on longer-term changes and on the UTLS region.

Column values: Sensitivity tests using systematic changes in various parameters that could affect the accuracy of the MLS retrievals lead to possible biases (2-σ estimates) of about 4%, as an estimated accuracy for the MLS column values (from integrated MLS ozone profiles down to 100, 147, and 215 hPa). See also the (v2.2) validation papers (and subsequent ozone-related publications, e.g., available from the MLS website) for results on column ozone comparisons versus satellite, sonde, and lidar data.

Data screening

Pressure range: 261 – 0.02 hPa.

Values outside this range are not recommended for scientific use.

Estimated precision: Only use values for which the estimated precision is a positive number.

Values where the *a priori* information has a strong influence are flagged with negative precision, and should not be used in scientific analyses (see Section 1.5).

Status flag: Only use profiles for which the 'Status' field is an even number.

Odd values of `Status` indicate that the profile should not be used in scientific studies. See Section 1.6 for more information on the interpretation of the `Status` field.

Quality: Only profiles whose 'Quality' field is greater than 0.6 should be used.

Convergence: Only profiles whose 'Convergence' field is less than 1.18 should be used.

Clouds: Scattering from thick clouds can lead to oscillatory values for O_3 in the UT/LS, see below for screening rules.

Most of the affected profiles are removed by the `Quality`, `Convergence`, and outlier screening methods, as described below, specifically for the v3.3 data.

'Outlier' Screening: The v3.3 ozone product has more tropical outliers than the v2.2 data in the lower stratosphere (mainly a few to a few tens of positive outliers at 68 hPa on a typical day) and in the upper troposphere, where both negative or positive spikes can dominate, depending on the pressure level. As for CO, these often appear to be related to thick clouds, and large values of ice water content (IWC) in the vicinity of the affected profiles.

We have found that using explicit thresholds for negative ozone spikes at pressures larger than the 46 hPa MLS pressure level can effectively screen out most of the outliers, including most of the *positive* outliers in the UTLS. The recommended screening method for v3.3 ozone should therefore also include a test for significantly negative values for the MLS pressure range from 56 to 261 hPa (inclusive). We then recommend rejection of *all values in this range* when a (negative) mixing ratio less than -0.15 ppmv is encountered (for any level in this range); in addition, any value at 316 hPa less than -0.30 ppmv should also lead one to discard the applicable UTLS values. These outlier thresholds are chosen so that large negative values outside those thresholds are generally outside the '5 sigma level', in relation to typical ozone values and MLS ozone precisions (or scatter) in the UTLS; we have also checked that these criteria do not impact the screening of high latitude ozone values in any significant way (e.g., under ozone hole conditions).

In summary, one should *reject* profiles with odd `Status` *or* even `Status` profiles with `Convergence` above the convergence threshold *or* `Quality` below the quality threshold, or with values from 316 to 56 hPa (inclusive) that get eliminated by the negative outlier criteria. Conversely, one should *keep* profile values with even status *and* good `Convergence` *and* good `Quality` *and*, UTLS values in the 316 to 56 hPa MLS pressure range that do not get discarded by the negative outlier criteria. This methodology does remove some profile values that are not in the 'outlier' category but no method will cleanly remove only the exact number of profiles that are suspicious for every day of the MLS mission. The current recommendations typically remove $\sim$4 to 6 % of global daily data, with some tropical latitudes showing much larger fractional removal (e.g., 20 to 30% in 10° bins near the equator). This screening generally maintains sufficient coverage for a near-complete daily map (for any given day), even in the UTLS.

Compared to the v2.2 UT data screening recommendations, the screening of v3.3 UTLS data generally removes slightly more ozone profiles on a typical day (although on occasion, slightly less).

Finally, we note that since there is essentially no impact from the outliers (spikes) in the UTLS (this is also largely a tropical issue) on the ozone mixing ratios at pressures less than 50 hPa, it is safe to ignore the outlier flag in the data screening if a study is only concerned with pressures smaller than or equal to the 46 hPa MLS pressure level; in this case, users can simply apply the `Quality` and `Convergence` (and `Status`) tests to obtain a satisfactory data screening method, with fewer profiles removed (typically less than about 2% per day, globally) than if the UTLS screening method were used.

Review of comparisons with other datasets

O_3 comparisons have indicated general agreement at the $5-10$ % level with stratospheric profiles from a number of comparisons using satellite, balloon, aircraft, and ground-based data. A high MLS v2.2 bias at 215 hPa has been obtained in some comparisons versus ozonesondes, but this is not observed consistently in other comparisons. We have found that latitudinal and temporal changes observed in various correlative data sets are well reproduced by the MLS ozone product. Future (and ongoing) validation studies using v3.3 data will focus more on longer-term changes and on the UTLS region, where improvements will still be sought, especially in the tropics (see below).

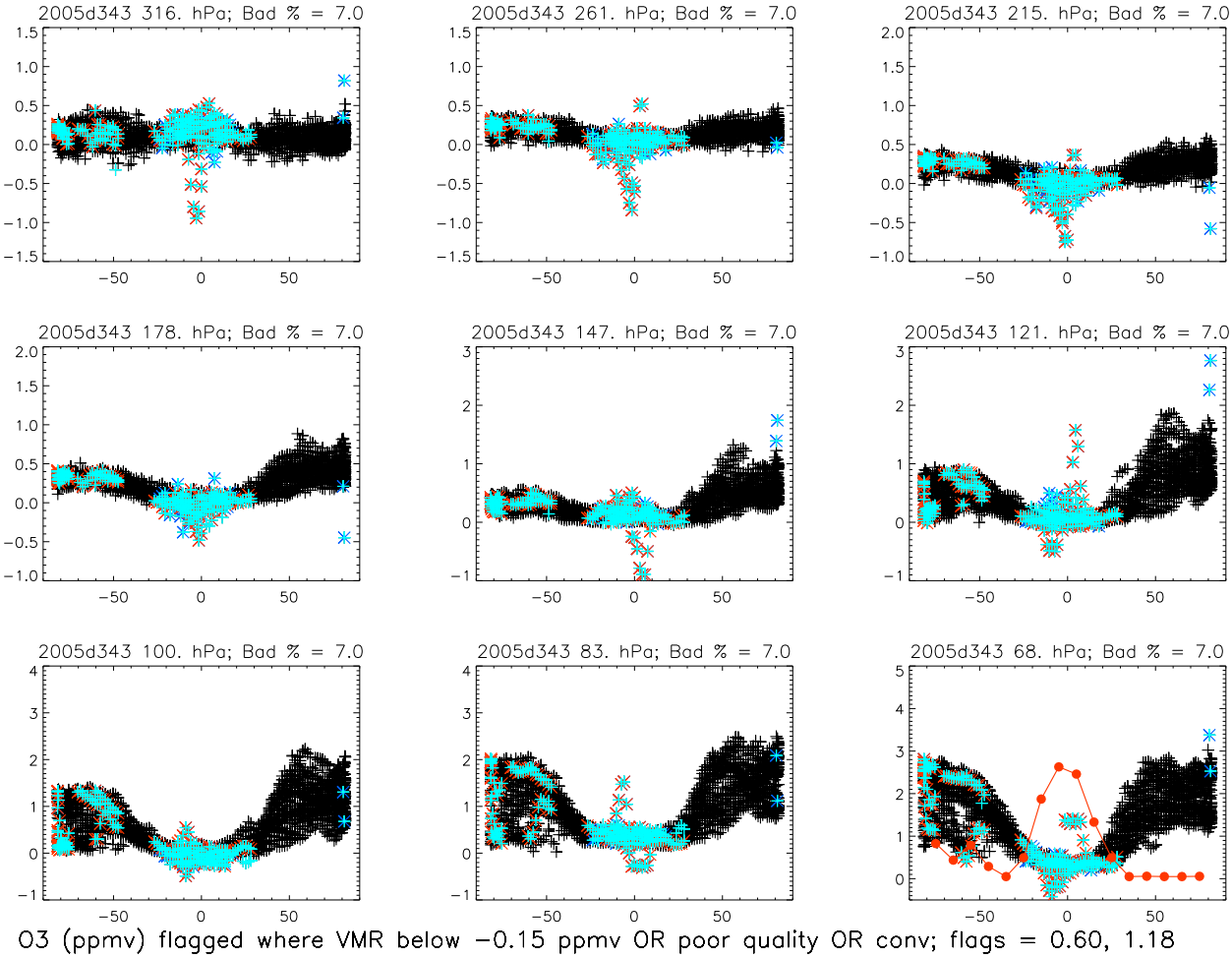

Figure 3.17.5: Example of the MLS ozone mixing ratio distribution versus latitude for one day, showing various pressure levels in the UTLS and which points are flagged by recommended quality, convergence, and outlier criteria (for 2005d343, one of the days showing the most outliers). The bottom right panel (for 68 hPa) also shows (red curve) the percentage of points getting screened out in 10° latitude bins (with the y-axis scaled by a factor of 10) – close to 30% of points can be thrown out in some bins, on this relatively poor quality day.

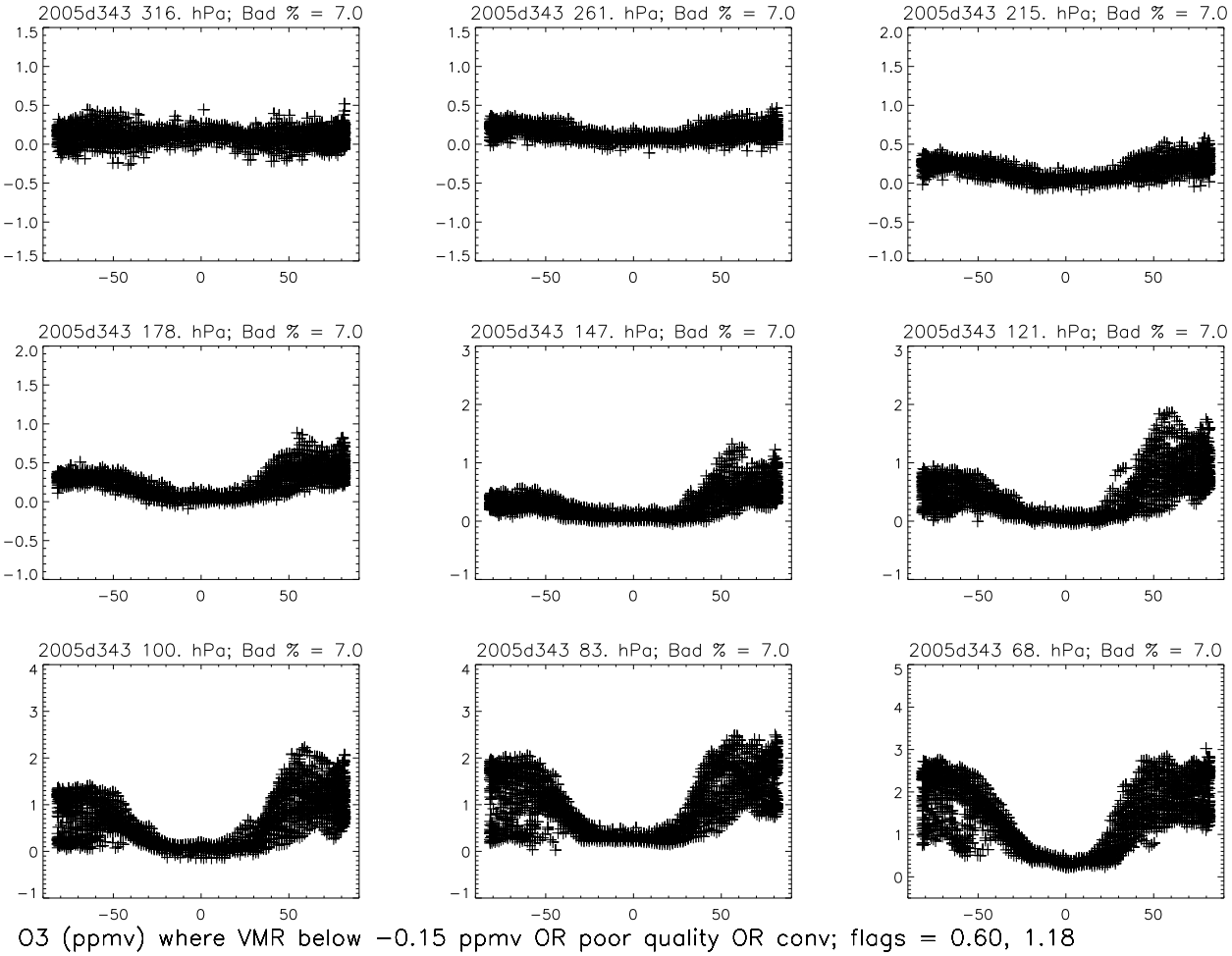

Figure 3.17.6: Example of the MLS ozone mixing ratio distribution versus latitude for one day, showing various pressure levels in the UTLS and which points remain *after* removal of the flagged (colored) points shown in the previous Figure.

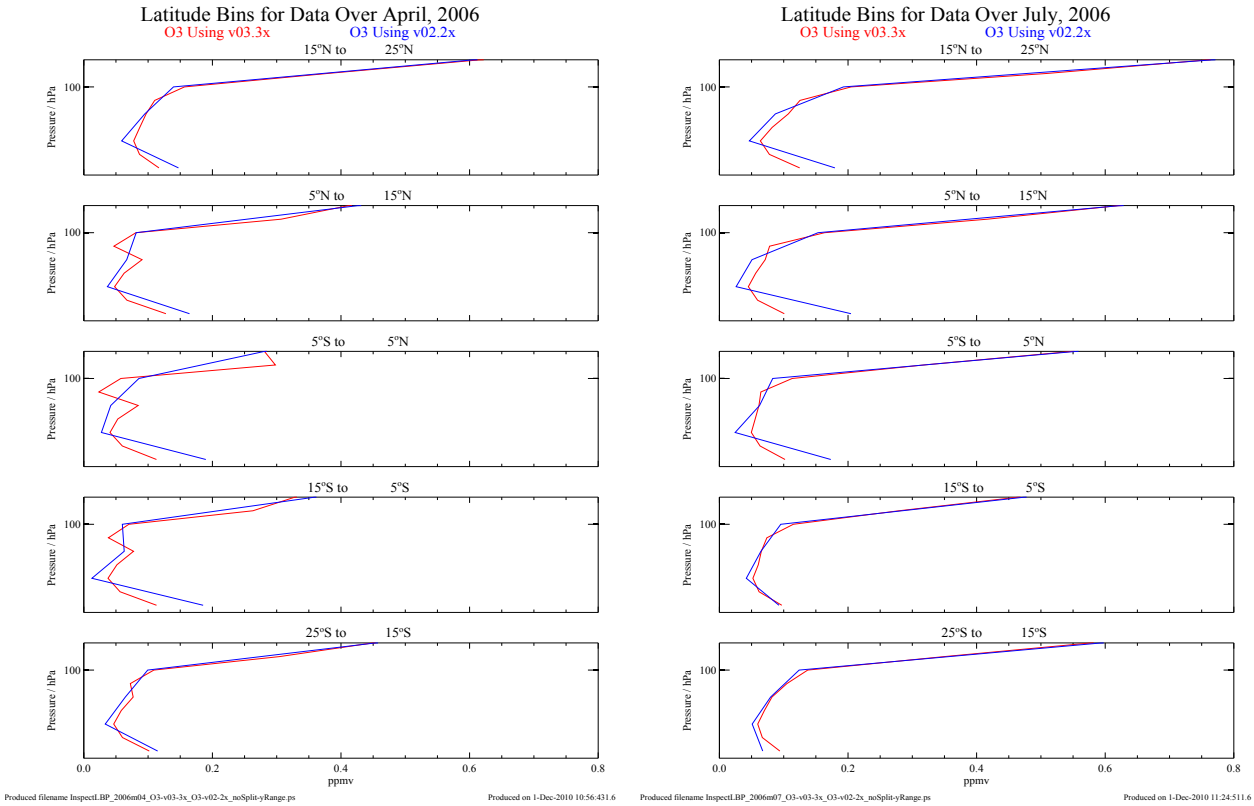

Figure 3.17.7: Monthly zonal average MLS ozone profiles in the tropical UTLS (here, from 316 to 68 hPa) for 2006 April (left panels) and July (right panels), for five 10° latitude bins (top to bottom: 15° N–25° N, 5° N–15° N, 5° S–5° N, 15° S–5° S, 25° S–15° S,). The v3.3 profiles are in red, while the v2.2 profiles are in blue.

Artifacts

Oscillations in tropical UTLS ozone: The f ner resolution and new retrieval methodology (and screening) for v3.3 allow for improved values at 261 hPa (and to some extent at 316 hPa, although not a recommended level), but some artifacts (oscillations) exist in the tropical upper tropospheric prof les. Indeed, vertical patterns exist in monthly means, as shown in Figure 3.17.7 with larger artifacts apparent in April (or May) than in July (or August), for example. Further detailed validation and characterization of the MLS tropical UT data (in particular) is warranted, in order to more fully understand the MLS data limitations for various applications.

Outliers: Even with the data screening procedures that are recommended herein, a few outliers will remain unscreened for some days at some pressure levels (with the vast majority of outliers occurring at pressures larger than the MLS 46 hPa level). Caution is advised, not to over-interpret such occasional events.

Columns: Users of column ozone data above the tropopause from the MLS Level 2 f les should be aware that the accuracy of these values depends on the tropopause pressure accuracy, and that artifacts can occur in these calculations, especially at high latitudes (under certain temperature gradient conditions). Users should therefore inspect the MLS f le values of tropopause pressure if using this product (swath) from the MLS ozone f les.

Table 3.17.1: Summary for MLS ozone

Pressure / hPa	Resolution Vert. × Horiz.	Precision[a] ppmv	Precision[a] %	Accuracy[b] ppmv	Accuracy[b] %	Comments
≤ 0.01	—	—	—	—	—	Unsuitable for scientif c use
0.02	5.5 × 200	1.4	300	0.1	35	
0.05	5.5 × 200	0.9	150	0.2	30	
0.1	4 × 400	0.5	60	0.2	20	
0.2	3 × 450	0.5	40	0.1	7	
0.5	3.5 × 550	0.3	20	0.1	5	
1	3 × 450	0.2	7	0.2	7	
2	3.5 × 450	0.15	3	0.2	5	
5	3 × 450	0.15	2	0.3	5	
10	3 × 500	0.1	2	0.3	5	
22	2.5 × 400	0.1	2	0.2	5	
46	2.5 × 350	0.06	3	0.2	8	
68	2.5 × 350	0.04	3–10	0.05	3–10	
100	2.5 × 300	0.04	20–30	[0.05 + 5%]		
150	2.5 × 400	0.03	5–100	[0.02 + 5%]		
215	3 × 400	0.02	5–100	[0.02 + 20%]		
261	3 × 450	0.03	5–100	—	—	Requires further evaluation
316	2.5 × 500	0.05	—	—	—	Not recommended (until further evaluation)
1000 – 464	—	—	—	—	—	Not retrieved

[a] Precision on individual prof les

[b] As estimated from systematic uncertainty characterization tests. Stratospheric values are expressed in ppmv with a typical *equivalent* percentage value quoted. 215 – 100 hPa errors are the sum of the ppmv *and percentage* scaling uncertainties quoted. Accuracy values, especially for pressures from 100 to 316 hPa will be re-evaluated, but the estimates for v2.2 data are currently used in this Table.

Priorities for future data version

- Reduction of oscillations in UTLS tropical prof les, and retrieval improvements in the presence of thick clouds.

3.18 Hydroxyl Radical

Swath name: OH

Useful range: 32 – 0.0032 hPa

Contact: Shuhui Wang, **Email:** <Shuhui.Wang@jpl.nasa.gov>

Introduction

The THz radiometer is dedicated to measuring OH in the 2.5 THz spectral region. A description of OH data quality, precision and systematic errors for an earlier version, v2.2, is given in Pickett et al. [2008]. The validation studies are described in Pickett et al. [2008] and Wang et al. [2008]. An early validation using v1.5 software is also described in Pickett et al. [2006a]. While there are signif cant improvements from v1.5 to v2.2, the OH data quality in v3.3 is generally similar to v2.2. One noticeable difference is the larger nighttime offset below 10 hPa in v3.3. This offset can be removed with the day-night difference, which is recommended for altitudes below 10 hPa.

The estimated uncertainties, precisions, and resolution for v3.3 OH are summarized in Table 3.18.1. Note that the systematic uncertainties are from v2.2, but are not expected to change signif cantly in v3.3.

Resolution

Figure 3.18.1 shows the OH averaging kernel for daytime and nighttime at 35°N. The reason to separate daytime and nighttime is that the largest natural variability in OH is diurnal. The vertical resolution is slightly different between day and night. The nighttime resolution is suff cient to allow the study of (for example) the "nighttime OH layer" around 82 km. The vertical width of the averaging kernel for pressures greater than 0.01 hPa is 2.5 km. The horizontal width of the averaging kernel is equivalent to a width of 1.5° (165 km distance) along the orbit. The changes in vertical resolution above 0.01 hPa are due mainly to use of a faster instrument vertical scan rate for tangent heights above 70 km. The horizontal resolution across track is 2.5 km. The averaging kernel and resolution for high and low latitudes are very similar to Figure 3.18.1 for most pressure levels. At the topmost two pressure levels, 0.0046 hPa and 0.0032 hPa, the vertical resolution is slightly better at the equator than at 70°N.

Precision

A typical OH prof le and the associated precisions (for both v2.2 and v3.3) are shown in Figure 3.18.2. The prof le is shown in both volume mixing ratio (vmr) and density units. All MLS data are reported in vmr for consistency with the other retrieved molecules. However, use of density units (10^6 cm^{-3}) reduces the apparent steep gradient of OH vertical prof le, allowing one to see the prof le with more detail, especially in the stratosphere where most atmospheric OH is present. Additionally, at THz frequencies the collisional line-width is approximately equal to the Doppler width at 1 hPa. Above 1 hPa, Doppler broadening is dominant and the peak intensity of OH spectral absorption is proportional to density, while below 1 hPa the peak intensity is proportional to vmr. The daytime OH density prof le shows two peaks at ∼45 km and ∼75 km. The night OH prof le exhibits the narrow layer at ∼82 km [Pickett et al., 2006b]. Precisions are such that an OH zonal average within a 10° latitude bin can be determined with better than 10% relative precision with one day of data (∼100 samples) over 21 – 0.01 hPa. With 4 days of data, the 10% precision limits can be extended to 32 – 0.0046 hPa.

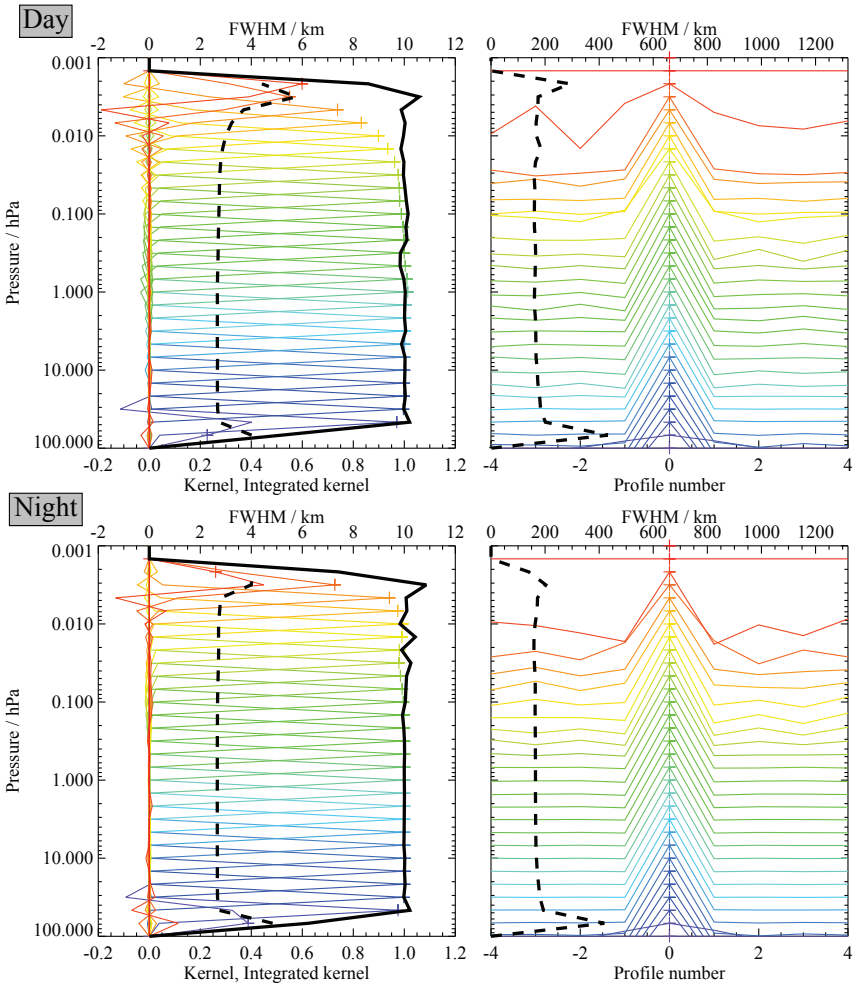

Figure 3.18.1: Typical two-dimensional (vertical and horizontal along-track) averaging kernels for the MLS v3.3 OH data at 35°N for daytime (upper) and nighttime (lower); variation in the averaging kernels is sufficiently small that these are representative of typical profiles. Colored lines show the averaging kernels as a function of MLS retrieval level, indicating the region of the atmosphere from which information is contributing to the measurements on the individual retrieval surfaces, which are denoted by plus signs in corresponding colors. The dashed black line indicates the resolution, determined from the full width at half maximum (FWHM) of the averaging kernels, approximately scaled into kilometers (top axes). (Left) Vertical averaging kernels (integrated in the horizontal dimension for five along-track profiles) and resolution. The solid black line shows the integrated area under each kernel (horizontally and vertically); values near unity imply that the majority of information for that MLS data point has come from the measurements, whereas lower values imply substantial contributions from a priori information. (Right) Horizontal averaging kernels (integrated in the vertical dimension) and resolution. The averaging kernels are scaled such that a unit change is equivalent to one decade in pressure.

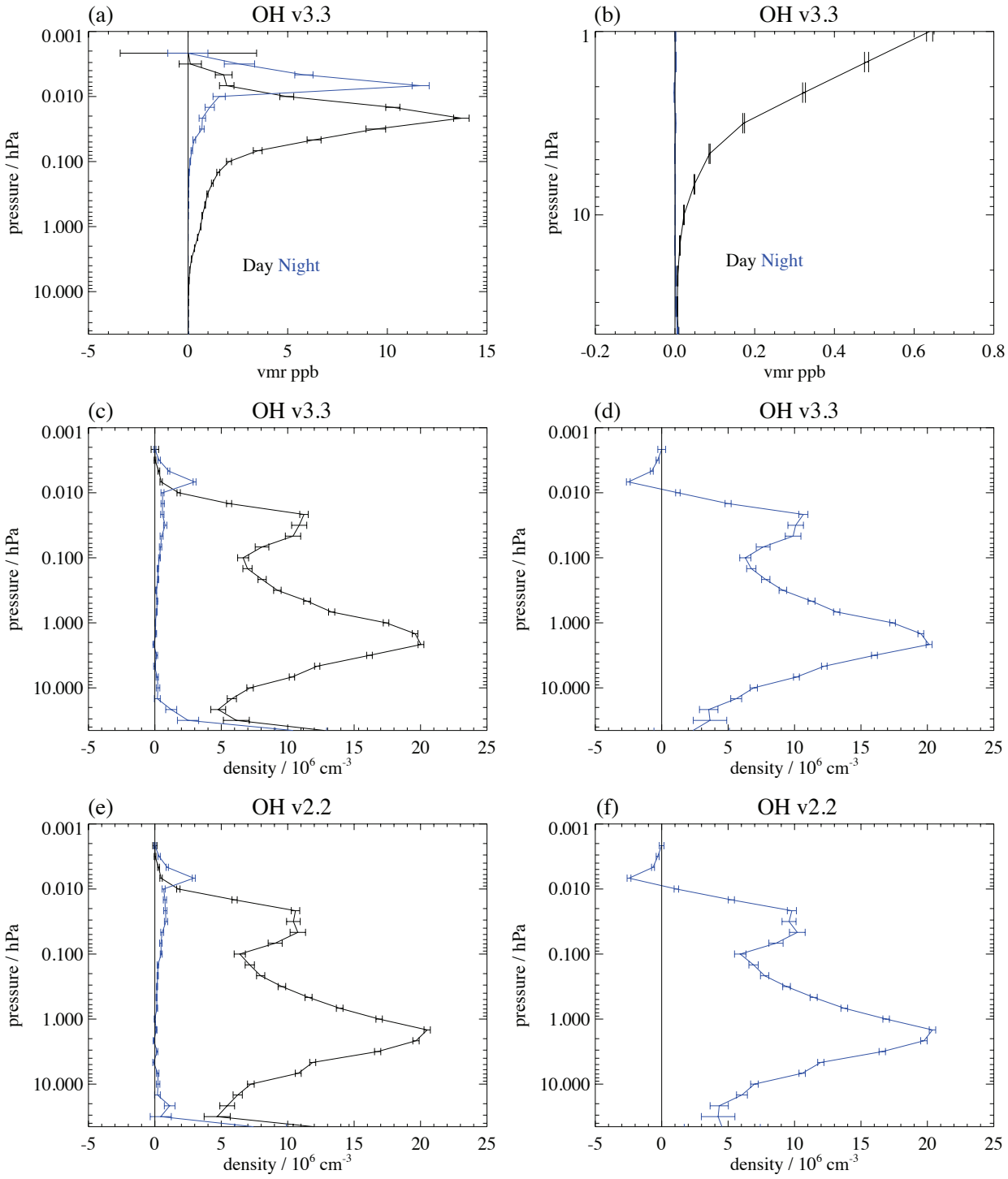

Figure 3.18.2: Zonal mean of retrieved OH and its estimated precision (horizontal error bars) for September 20, 2005 averaged over 29°N to 39°N. The average includes 98 profiles. Panel (a) shows v3.3 OH vmr vs. pressure for day (black) and night (blue). Panel (b) shows the same data plotted for the stratosphere. The retrieved night OH concentration is near zero for altitudes below 1 hPa. Panel (c) shows the same data in (a) converted into density units. Panel (d) shows the day-night differences for the data in panel (c). Note that the day-night difference is required for altitudes below 10 hPa. Panels (e) and (f) are equivalent to (c) and (d) but using v2.2 OH data.

Accuracy

Table 3.18.1 summarizes the accuracy expected for OH. The scaling uncertainty is the part of the systematic uncertainty that scales with OH concentration, e.g. spectroscopic line strength. Bias uncertainty is the part of the uncertainty that is independent of concentration. For both bias and scaling uncertainty, quantif cation of the combined effect in MLS calibration, spectroscopy etc., on the data product was determined by calculating the effects of each source of uncertainty. These accuracy calculations are for v2.2 products. While no signif cant change is expected from v2.2 to v3.3, a comprehensive error analysis for v3.3 will be conducted. Bias uncertainty can be eliminated by taking day-night differences from 32 – 14 hPa. For 10 – 0.1 hPa, the observed night OH concentration is small and day-night differencing is not ordinarily needed. The accuracy of the OH measurement due to systematic errors is a product of scaling uncertainty and the observed OH concentration. The overall uncertainty is the square root of the sum of squares of the precision and accuracy.

Data screening

It is recommended that OH data values be used in scientif c investigations if all the following tests are successful:

Pressure range: 32 – 0.0032 hPa.

Values outside this range are not recommended for scientif c use.

Estimated precision: Only use values for which the estimated precision is a positive number.

Values where the *a priori* information has a strong inf uence are f agged with negative precision, and should not be used in scientif c analyses (see Section 1.5).

Status flag: Only use profiles for which the 'Status' field is an even number.

Odd values of `Status` indicate that the prof le should not be used in scientif c studies. See Section 1.6 for more information on the interpretation of the `Status` f eld.

Quality: MLS v3.3 HO_2 data can be used irrespective of the value of the `Quality` field.

Convergence: Only profiles whose 'Convergence' field is less than 1.1 should be used.

Artifacts

For some seasons, the Gas Laser Local Oscillator (GLLO) for the THz receiver is automatically relocked as many as 5 times during a day. These relock events occur when the tuning range of the laser is less than the thermal excursion over an orbit and over a day. This thermal effect depends on the albedo of the Earth as seen by the GLLO radiator. In these cases the `Status` f ag is set to 257 and the prof le is ignored. This can present a problem when compiling maps, because the missing data may appear at the same latitude and longitude on successive days.

Review of comparisons with other datasets

Data from MLS v2.2 software have been validated with two balloon-borne remote-sensing instruments and with ground-based column measurements. Details of the comparison are given in Pickett et al. [2008] and Wang et al. [2008]. The comparison between v2.2 and v3.3 show no signif cant differences.

Table 3.18.1: Summary of precisions, resolution, and uncertainties for the MLS OH product

Pressure	Resolution V × H /km	Precision[a] (day/night) / 10^6 cm^{-3}	Bias uncertainty / 10^6 cm^{-3}	Scaling uncertainty /%	Comments
<0.003 hPa	—	—	—	—	Unsuitable for scientif c use
0.003 hPa	5.0 × 220	0.5 / 0.5	0.034	90	
0.01 hPa	2.5 × 180	1.1 /1.1	0.031	41	
0.1 hPa	2.5 × 165	3.3 / 0.6	0.12	3.1	
1.0 hPa	2.5 × 165	1.9 / 0.4	0.50	7	
10 hPa	2.5 × 165	2.3 / 1.4	0.18	1.5	
32 – 14 hPa	2.5 × 165	6 – 10 / 4 – 8	0.50	1.3	Use day–night difference
>32 hPa	—	—	—	—	Unsuitable for scientif c use

[a]Precision on an individual prof le

3.19 Relative Humidity with respect to Ice

Swath name: RHI

Useful range: UTRHI, mean layer value for pressures larger than 317 hPa. Prof le from 316 – 0.002 hPa.

Contact: William Read, **Email:** <William.G.Read@jpl.nasa.gov>

Introduction

RHi is relative humidity with respect to ice. The vertical grid for RHi is 12 levels per decade change in pressure for 1000 – 1.0 hPa thinning to 6 levels per decade for 1.0 – 0.1 hPa and f nally 3 levels per decade for $0.1 - 10^{-5}$. The RHi product is a fusion of information from two separate retrievals. From 1000 – 383 hPa, RHi is retrieved directly from optically thick radiances using measurement and retrieval principles similar to nadir sounding humidity receivers (e.g., TOVS). All grid levels between 1000 – 383 hPa are f lled with the same value and this product is referred above as an UTRHI (upper tropospheric relative humidity with respect to ice) product. This humidity is used as a lower altitude constraint and a priori for the vertically resolved humidity product that begins at 316 hPa.

The second RHi product from 316 hPa and lower pressures is computed from the standard products of water and temperature using the Goff-Gratch ice humidity saturation formula. RHi validation is presented in Read et al. [2007]. Table 3.19.1 is summary of precision, resolution, and accuracy.

Changes from v2

The H_2O line width was narrowed by 4% based on cavity absorption measurements by A. Meshkov [Ph. D. Thesis, 2006]. The f ne grid (12 lpd) representation basis was extended upwards from 22 hPa to 1 hPa. These changes successfully removed the H_2O kink artifact present in v2.2 at 32/26 hPa. Vertical smoothing was relaxed near 1.0 hPa to improve the vertical resolution of H_2O in the mesosphere.

Resolution

RHi for pressures of 316 hPa and smaller is a derived product and therefore a retrieval averaging kernel is not directly available. An estimate for the spatial resolution (vertical X along track) of this product is a convolution of the temperature and H_2O resolutions. Since temperature has lower spatial resolution than H_2O in the troposphere and lower stratosphere it is assumed that the spatial resolution of temperature shown in Figure 3.21.1 best represents the resolution of the RHi product. The cross track resolution is probably 12 km, the larger of temperature and H_2O cross track resolutions. These resolutions are only true in the limit that the mean log(H_2O) doesn't change appreciably over the broader temperature measurement volume. The longitudinal separation of the MLS measurements, set by the Aura orbit, is $10^\circ - 20^\circ$ over middle and lower latitdudes, with much f ner sampling in polar regions.

The RHi described by the values for pressures greater than 316 hPa, represents a mean value in a broad layer (4 – 6 km) whose sensitivity peaks between ∼350 hPa (in the moist tropics) and ∼650 hPa (typical for dry high latitudes).

Precision

The values for precision are the root sum square (RSS) precisions for H_2O and temperature propagated through the Goff-Gratch relationship, see sections 3.8 and 3.21 for more details. The precisions are set to negative values in situations when the retrieved precision is larger than 50% of the a priori precision for either temperature or H_2O — an indication that the data is biased toward the a priori value.

Accuracy

The values for accuracy are the RSS accuracies for H_2O and temperature scaled into %RHi units. see sections 3.8 and 3.21 for more details. These may change for the v3 RHi product. The MLS team plans to repeat the v2 exercise with the v3 software and release the results in a subsequent version of this document.

Data screening

Pressure range: Profile from 316 – 0.002 hPa. UTRHI (values for pressures larger than 317 hPa) represents mid/upper troposphere column.

Values outside this range are not recommended for scientific use.

Estimated precision: Only use values for which the estimated precision is a positive number.

Values where the *a priori* information has a strong influence are flagged with negative precision, and should not be used in scientific analyses (see Section 1.5).

Status flag: Only use profiles for which the 'Status' field is an even number.

Odd values of `Status` indicate that the profile should not be used in scientific studies. See Section 1.6 for more information on the interpretation of the `Status` field.

Clouds: Ignore the cloud flag bits for pressures less than 100 hPa. For pressures $\geq$100 hPa, reject profiles having status flag bit 16 or 32 set to 1. See artifacts for more details.

Quality: Only profiles with a value of the RHi 'Quality' greater than 1.3 and Temperature 'Quality', greater than 0.65 should be used in scientific studies.

This eliminates $\sim$5% of the profiles on a typical day.

Convergence: Only profiles with a value of the RHi 'Convergence' less than 2.0 and Temperature 'Convergence' less than 1.2 should be used in scientific studies.

Artifacts

See sections 3.8 for H_2O and 3.21 for temperature for specific issues related to these parent products. Effects of MLS temperature precision ($\sim$1 – 2 K) must be considered if one wishes to use MLS RHi to study supersaturation probability distributions. In simulation studies, systematic errors (such as tangent pressure retrieval and errors), in addition to introducing biases, also increase variability in differences with respect to a "truth" data set particularly for pressures greater than 200 hPa. This will add to the frequency of supersaturation in the tail of MLS RHi distribution functions. Therefore, MLS RHI is not recommended for studying statistics of supersaturation at pressures greater than 178 hPa. For lower pressures, one must remove the contribution from temperature noise as part of the analysis. Measurements taken in the presence of clouds significantly degrade the precision, that is increases the scatter about the mean, but the mean bias as compared to AIRS changes by less than 10%. See section 3.8 for more details.

Review of comparisons with other datasets

Figure 3.19.1 shows a comparison between MLS v2.2 and v3.3 RHi. As for H_2O, the differences are minor except near 26 hPa, where the zig-zag artifact is now removed in v3.3. Other noteworthy changes are the increase in RHi at 215 and 261 hPa at high latitudes and a decrease in RHi for pressures greater than 215 hPa in the tropics.

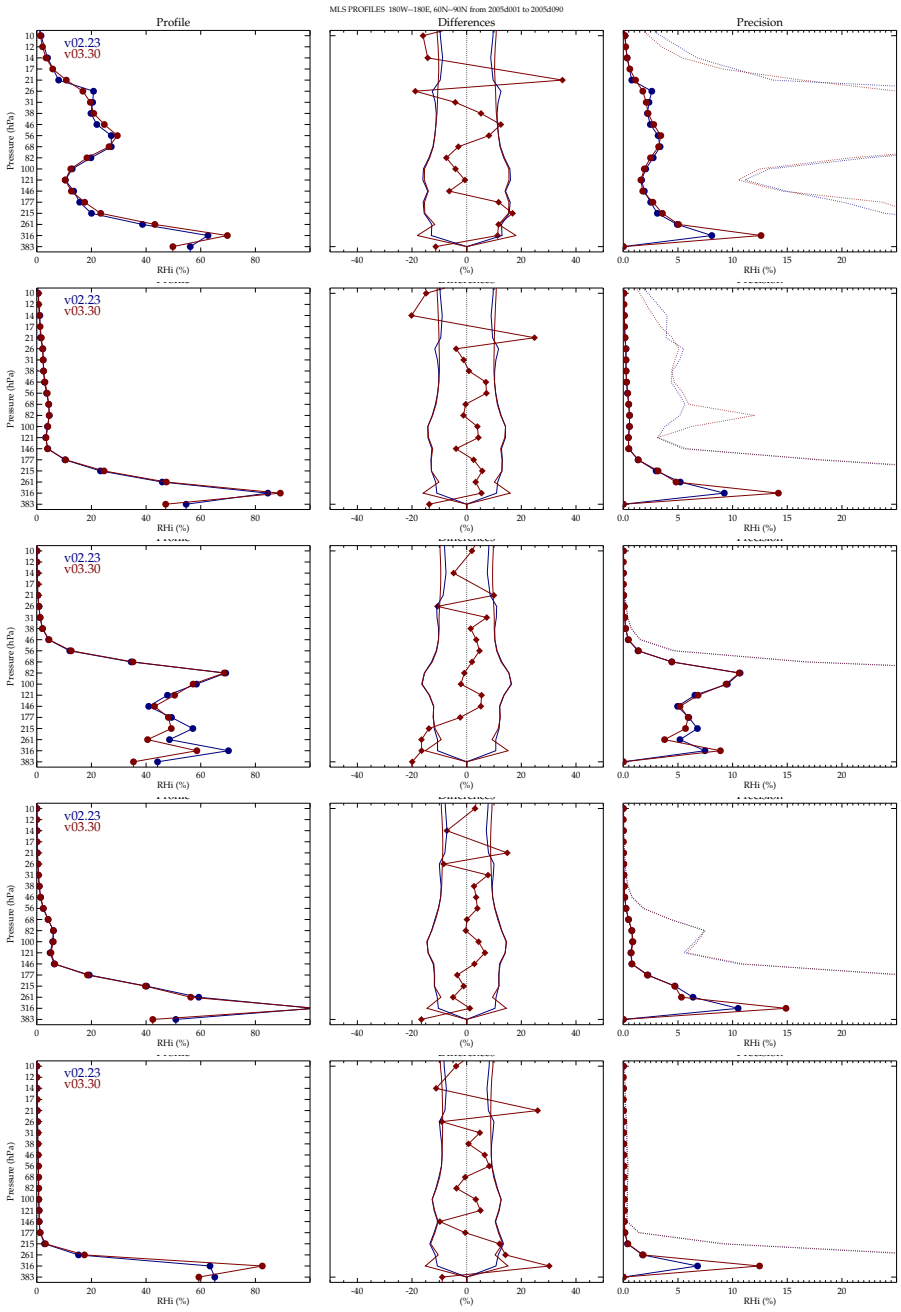

Figure 3.19.1: A comparison of v2.2 (blue) to v3.3 (red) RHi for Jan-Feb-Mar 2005 in 5 lattiude bands. Other time periods are similar. The left panel compares mean profiles, the center shows the mean difference (red diamonds) surrounded by each versions' estimated precision, and the right panel shows the estimated retrieval precision (solid and bullets) and measured variability (dotted) which includes atmospheric variability about the mean profile.

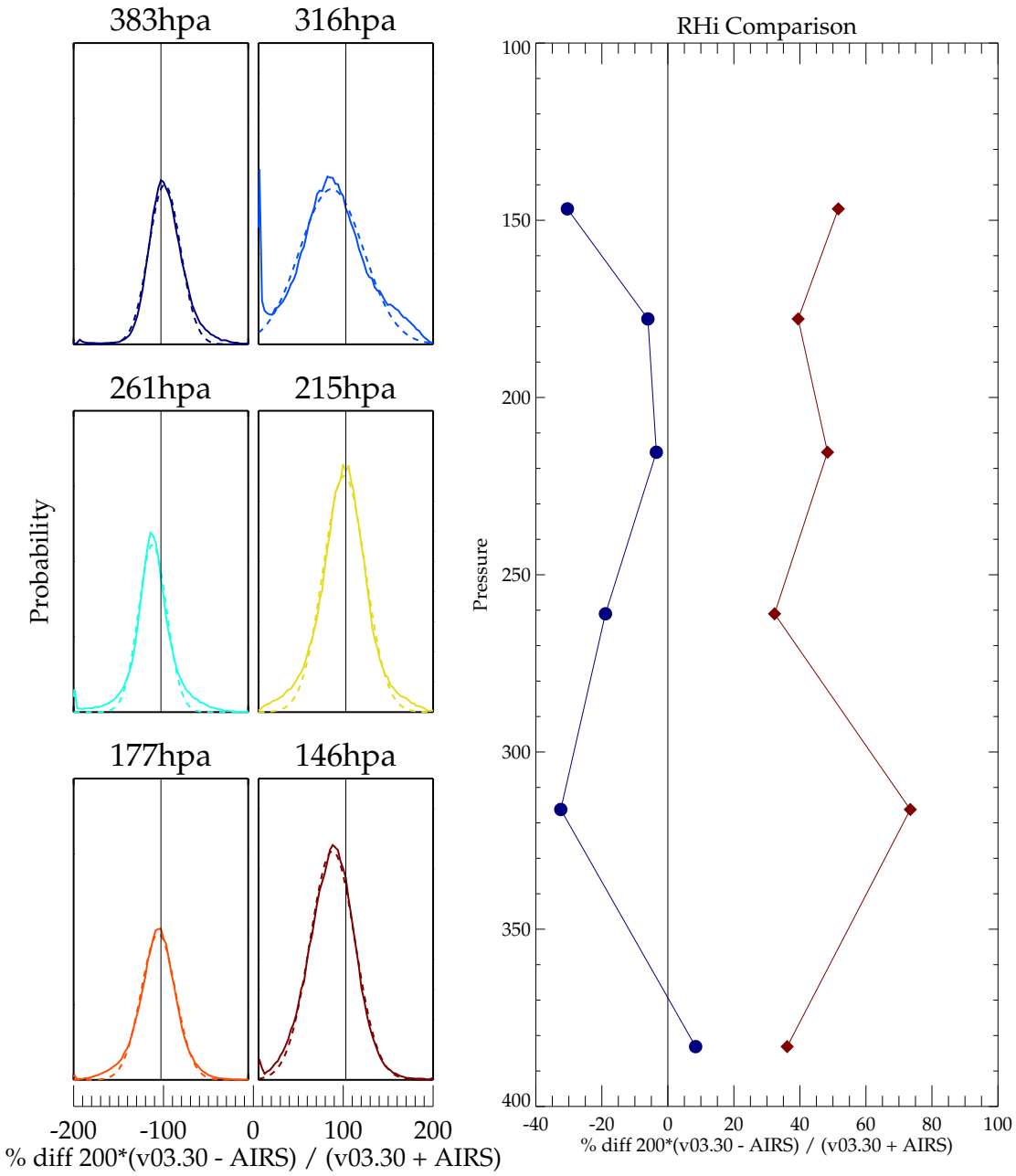

RHI

Figure 3.19.2: A comparison of MLS v3.3 and AIRS v5 RHi for selected pressures between 30°S–30°N during Jan-Feb-Mar 2005. The panels on the left show the pdf function (solid) of differences between MLS and AIRS for selected pressure levels. The dashed lines are a best fit Gaussian. The x-axis value of the peak indicates the average bias between MLS and AIRS, and the width of the function peak indicates the variability among the individual differences. The plot at right shows a vertical profile, the mean bias (blue) and standard deviation (red) of the differences between MLS and AIRS.

Figure 3.19.1 shows a comparison of coincidently measured profiles between MLS and AIRS for low latitudes. It is noteworthy that the agreement and variability of the UTRHI product (shown as 383 hPa value) agrees much better than 316 hPa. This is because the remote sounding principle of the v3 UTRHI measurement is more similar to AIRS. The 316 hPa measurement is transitional between limb saturated radiances which are proportional to logRHi and limb partially opaque radiances which are proportional to vmr but at this pressure in a non-linear fashion. Because the 316 hPa pressure level is at the retrieval extreme of the MLS H_2O retrieval scheme and most non-linear, it is also most subject to systematic errors and will not be as good as retrieval at smaller pressures or even the UTRHI product (provided that the altitude registration limitations are taken into consideration). The MLS 316 hPa RHi also has a large number of dry spikes as seen in the PDF spike at -200%.

The validation of the v2.2 RHi is discussed in Read et al. [2007].

Desired improvements

Improvements are covered under section 3.8 for H_2O and section 3.21 for temperature.

Table 3.19.1: Summary of MLS v3.3 UTLS RHi product.

Pressure / hPa	Resolution V × H km	Single profile precision [a] / %	Accuracy[b] / %	Comments
<0.002	—	—	—	Unsuitable for scientif c use
0.002	13 × 230	190	100	
0.004	13 × 260	100	100	
0.010	12 × 590	50	100	
0.022	12 × 750	40	100	
0.046	16 × 400	30	100	
0.10	14 × 420	30	100	
0.22	8 × 370	20	90	
0.46	8 × 320	15	75	
1.00	8 × 280	15	60	
2.15	8 × 250	15	35	
4.64	6 × 220	15	15	
10	4 × 210	15	15	
22	4 × 210	15	20	
46	4 × 210	15	25	
68	4 × 200	15	25	
83	4 × 200	20	25	
100	4 × 200	20	20	
121	4 × 200	25	20	
147	4 × 200	25	20	
178	4 × 200	35	30	
215	4 × 200	45	35	see Table 3.8.1
261	4 × 200	45	30	see Table 3.8.1
316	6 × 200	70	20	see Table 3.8.1
UTRHI, >316	6 × 150	40(est)	10(est)	measurement height depends on atmospheric humidity

[a] Absolute error in percent

[b] Fractional error ([error in RHi] / RHi) in percent

RHI

3.20 Sulfur Dioxide

Swath name: SO2

Useful range: 215 – 10.0 hPa

Contact: William Read, **Email:** <William.G.Read@jpl.nasa.gov>

Introduction

The standard SO_2 product is taken from the 240-GHz retrieval. MLS can only measure signif cantly enhanced concentrations above nominal background such as that from volcanic injections. SO_2 has not yet been validated.

Changes from v2

The v3 SO_2 retrieval will be impacted by the addition of interline interference terms in the O_3 line shape model, an updated CO line width parameter, and using a different set of 240 GHz channels. Another v3 change is the spectral baseline treatment that now uses a frequency-squared extinction term, conf gured as a relative humidity-like (RH) species. The RH treatment responds better to high extinction conditions when the middle troposphere is very humid. This enhancement eliminated a high bias in 316 hPa O_3 in the tropics that is present in v2. An unfortunate side effect of the RH baseline is that it is more adversely affected by clouds, causing spikes in the retrieval of R3 products including SO_2.

Resolution

Based on Figure 3.20.1, the vertical resolution for SO_2 is ∼3 km and the horizontal resolution is 170 km. The horizontal resolution perpendicular to the orbit track is 6 km for all pressures.

Precision

The estimated precision for SO_2 is ∼3 ppbv for all heights between 215 – 10 hPa. The precisions are set to negative values in situations when the retrieved precision is larger than 50% of the a priori precision – an indication that the data is biased toward the a priori value.

Accuracy

The values for accuracy are based on the v2 systematic error analysis performed on the MLS measurement system [Read et al., 2007]. The accuracy is estimated to be ∼5 ppbv for pressures less than 147 hPa increasing to ∼20 ppbv at 215 hPa. These may change for the v3 SO_2 product. The MLS team plans to repeat the v2 exercise with the v3 software and release the results in a subsequent version of this document.

Data screening

Pressure range: 215 – 10.0 hPa

Values outside this range are not recommended for scientif c use.

Estimated Precision: Values with negative precision can be used, though with caution.

Although it is generally recommended not to use values where precision is f agged negative, SO_2 is an exception and it is OK to use values with negatively f agged precision (provided that the entire prof le

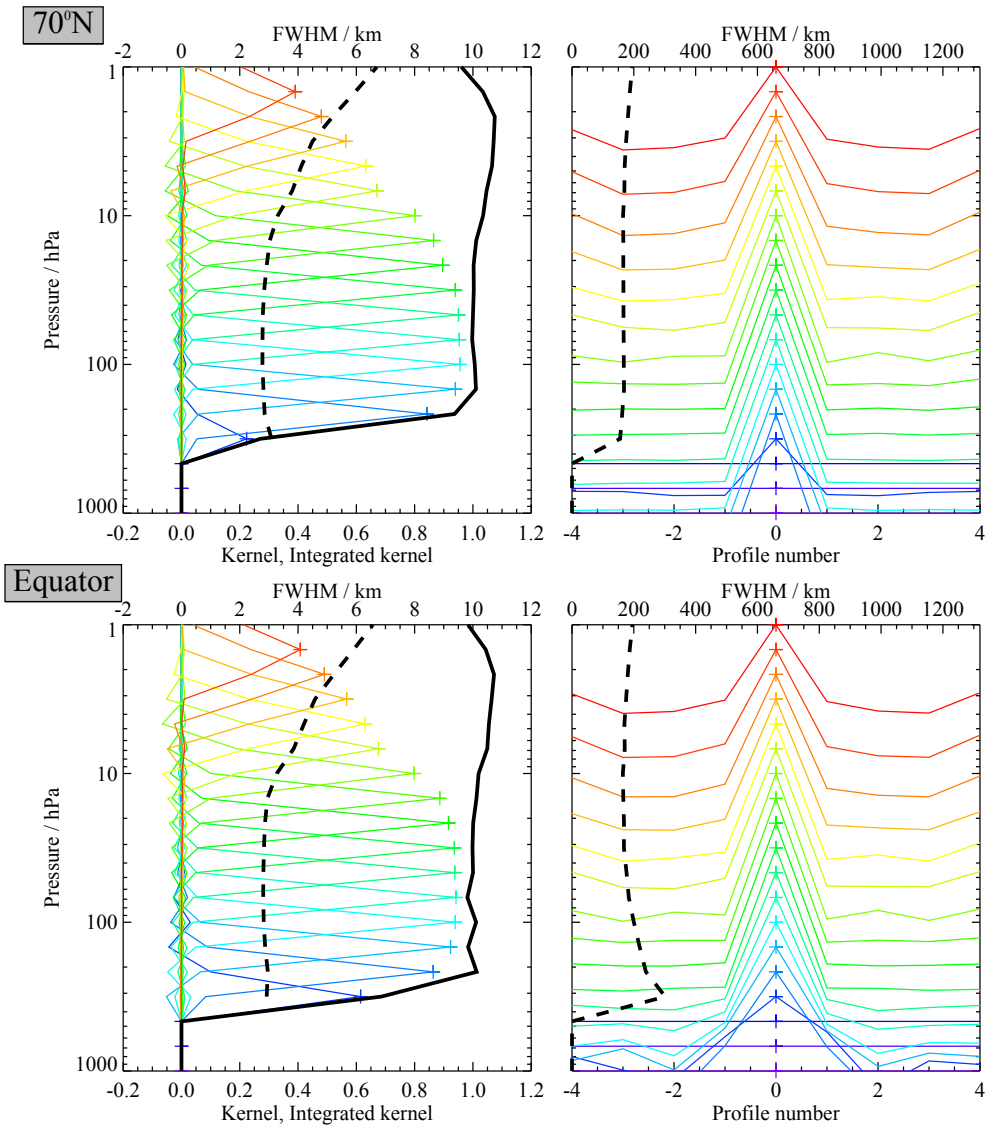

Figure 3.20.1: Typical two-dimensional (vertical and horizontal along-track) averaging kernels for the MLS v3.3 SO_2 data at 70°N (upper) and the equator (lower); variation in the averaging kernels is sufficiently small that these are representative of typical profiles. Colored lines show the averaging kernels as a function of MLS retrieval level, indicating the region of the atmosphere from which information is contributing to the measurements on the individual retrieval surfaces, which are denoted by plus signs in corresponding colors. The dashed black line indicates the resolution, determined from the full width at half maximum (FWHM) of the averaging kernels, approximately scaled into kilometers (top axes). (Left) Vertical averaging kernels (integrated in the horizontal dimension for five along-track profiles) and resolution. The solid black line shows the integrated area under each kernel (horizontally and vertically); values near unity imply that the majority of information for that MLS data point has come from the measurements, whereas lower values imply substantial contributions from a priori information. (Right) Horizontal averaging kernels (integrated in the vertical dimension) and resolution. The horizontal averaging kernels are shown scaled such that a unit averaging kernel amplitude is equivalent to a factor of 10 change in pressure.

is not so flagged). High retrieved values of SO_2 at the higher pressures (e.g. 215 and 147 hPa) will also have larger precision values which are sometimes large enough to trigger the "too much *a priori* influence" flag. While a priori influence is present and the retrieved value is probably smaller than reality because the retrieval is being pulled towards the a priori value of zero, this does not detract from the fact that greatly enhanced SO_2 is being reported, reflecting the detection of a plume.

Status flag: Only use profiles for which the 'Status' field is an even number.

Odd values of `Status` indicate that the profile should not be used in scientific studies. See Section 1.6 for more information on the interpretation of the `Status` field.

Quality: Only profiles whose 'Quality' field is greater than 0.6 should be used.

Convergence: Only profiles whose 'Convergence' field is less than 1.8 should be used.

Artifacts

The product is unvalidated. There is a tendency for the v3.3 SO_2 product, as for CO, to have spikes in the presence of clouds.

Review of comparisons with other datasets

MLS has successfully detected SO_2 from sixteen eruptions since launch. These include Manam (Papua, New Guinea – 3 events), Anatahan (Mariana Islands), Sierra Negra (Galapogos Island), Soufriere Hills (Montserrat, West Indies), Tunguraua (Ecuador), Rabaul (Papua New Guinea), Piton de la Fournaise (Reunion Island), Jebel al-Tair (Yemen), Okmok (Alaska), Kasatochi (Alaska), Dalaffilla (Ethiopia), Redoubt (Alaska), Sarychev (Kuril Islands, Russia), Pacaya (Guatamala), and Merapi (Indonesia).

Figure 3.20.2 shows an overlay comparison of column SO_2 measured by OMI and the same calculated by MLS for two days following the Kasatochi eruption. It is clear that MLS detects the main plume dispersal features. It also appears that MLS columns are much smaller than those from OMI. Interpreting the significance of this is not straightforward given that OMI has to make assumptions regarding the profile shape and can observe SO_2 down to the boundary layer. The MLS column begins at 215 hPa and integrates upward neglecting the tropospheric contributions. Another limitation is that OMI can only make measurements during the day whereas MLS can make them day and night. Since the plume is moving relatively quickly over the 12 hour measurement separation time, MLS nighttime measurements often miss and/or detect plume features differently than OMI. MLS vertically resolved measurement shows that this plume has separated into distinct layers at different altitudes.

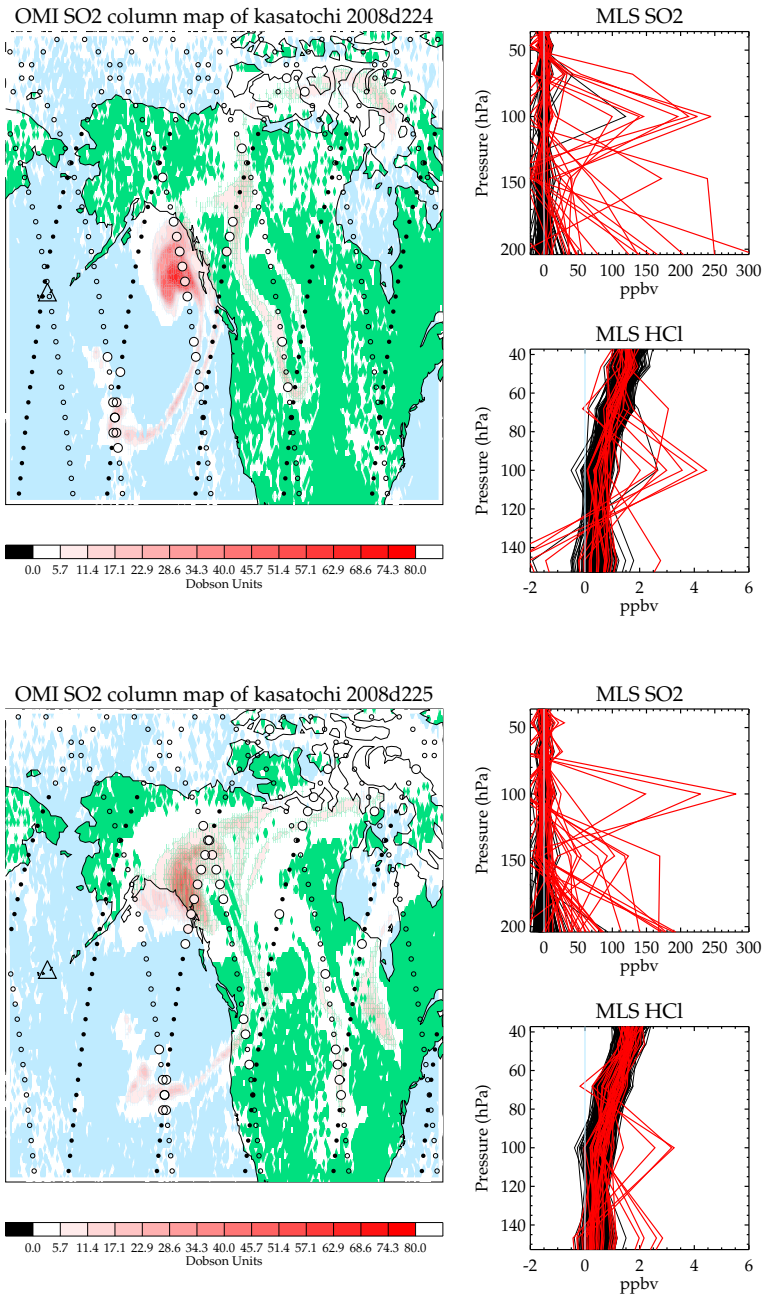

Figure 3.20.2: An overlay of MLS measurement tracks on an OMI SO_2 measurement on 11 and 12 August 2008 (separate maps) showing the dispersial of SO_2 from the Kasatochi eruption (8 Aug 2008, black triangle). The color scale indicates the SO_2 column measured by OMI. The daytime MLS tracks are small open circles and the nighttime tracks are filled black. When the calculated column from MLS exceeds 1 DU, that measurement is indicated by a larger open circle filled with the color of the column measurement as indicated by the color scale below (same as for OMI). The panels at right show all the measured profiles covering the area shown in the maps for SO_2 and HCl. Profiles where the MLS column calculation exceeds 1 DU are highlighted in red.

Table 3.20.1: Summary of MLS v3.3 SO_2 product.

Pressure / hPa	Resolution V × H km	Single profile precision [a] / ppbv	Accuracy / ppbv	Comments
< 10	—	—	—	Unsuitable for scientif c use
10	3 × 180	3.5	6	
15	3 × 180	3.5	3	
22	3 × 180	3.2	4	
32	3 × 180	3.2	5	
46	3 × 180	3.0	5	
68	3 × 180	3.0	6	
100	3 × 180	3.0	6	
147	3 × 180	3.1	10	
215	3 × 180	3.8	20	
>215	—	—	—	Unsuitable for scientif c use

[a] Absolute error in percent

3.21 Temperature

Swath name: `Temperature`

Useful range: 261 – 0.001 hPa

Contact: Michael J. Schwartz, **Email:** <Michael.J.Schwartz@jpl.nasa.gov>

Introduction

The MLS v3.3 temperature product is similar to the v2.2 product that is described in Schwartz et al. [2008]. MLS temperature is retrieved from bands near O_2 spectral lines at 118 GHz and 239 GHz that are measured with MLS radiometers R1A/B and R3, respectively. The isotopic 239-GHz line is the primary source of temperature information in the troposphere, while the 118-GHz line is the primary source of temperature in the stratosphere and above. MLS v3.3 temperature has a ~ -1 K bias with respect to correlative measurements in the troposphere and stratosphere, with 2 – 3 K peak-to-peak additional systematic vertical structure. Table 3.21.1 summarizes the measurement precision, resolution, and modeled and observed biases. The following sections provide details.

Differences between v3.3 and v2.2

The MLS v3.3 temperature retrieval algorithms are largely unchanged from those of v2.2, using the same subsets of the same radiance bands, so the resulting products are very similar. An exception is the 316-hPa level, which in v3.3 is noisier and has larger biases relative to analyses than in v2.2. The v3.3 temperature 316-hPa level is not recommended for scientif c use. Version v3.3 has eight more retrieval levels in the upper stratosphere, giving 12 levels per decade from the surface to 1 hPa. Noise and biases have been reduced at "chunk boundaries", the breaks between the 10-prof le blocks of data that are concurrently retrieved by the 2-D algorithms. The non-convergence of the retrieval over substantial sections of the polar autumn in v2.2 has been eliminated in version v3.3. Vertical smoothing has been reduced in the mesosphere and lower thermosphere, improving vertical resolution at a cost of less than a factor of two in precision, but also resulting in what, in preliminary validation, appears to be some vertically oscillating prof les in the mesopause region, particularly at the equator. The *a priori* temperature prof les used in v3.3 are consistently GEOS-5.2, while v2.2 used GEOS-5.1 before September of 2008. GEOS-5.1 has a low bias in the upper stratosphere of 0 – 15 K, particularly at high latitudes, and resulted in biases of $\sim$1 K near the stratopause.

Resolution

The vertical and horizontal resolution of the MLS temperature measurement is shown by averaging kernels in Figure 3.21.1. Vertical resolution, shown on the left panel, is $\sim$5 km from 261 hPa to 100 hPa, improves to 3.6 km at 31.6 hPa and then degrades to 4.3 km at 10 hPa, 5.5 km at 3.16 hPa and 6 km at 0.01 hPa. Along track resolution is $\sim$170 km from 261 hPa to 0.1 hPa and degrades to 220 km at 0.001 hPa. The cross-track resolution is set by the 6-km width of the MLS 240-GHz f eld of view in the troposphere and by the 12-km width of the MLS 118-GHz f eld of view in the stratosphere and above. The longitudinal separation of MLS measurements from a given day, which is determined by the Aura orbit, is $10^\circ - 20^\circ$ over middle and low latitudes and much f ner in polar regions.

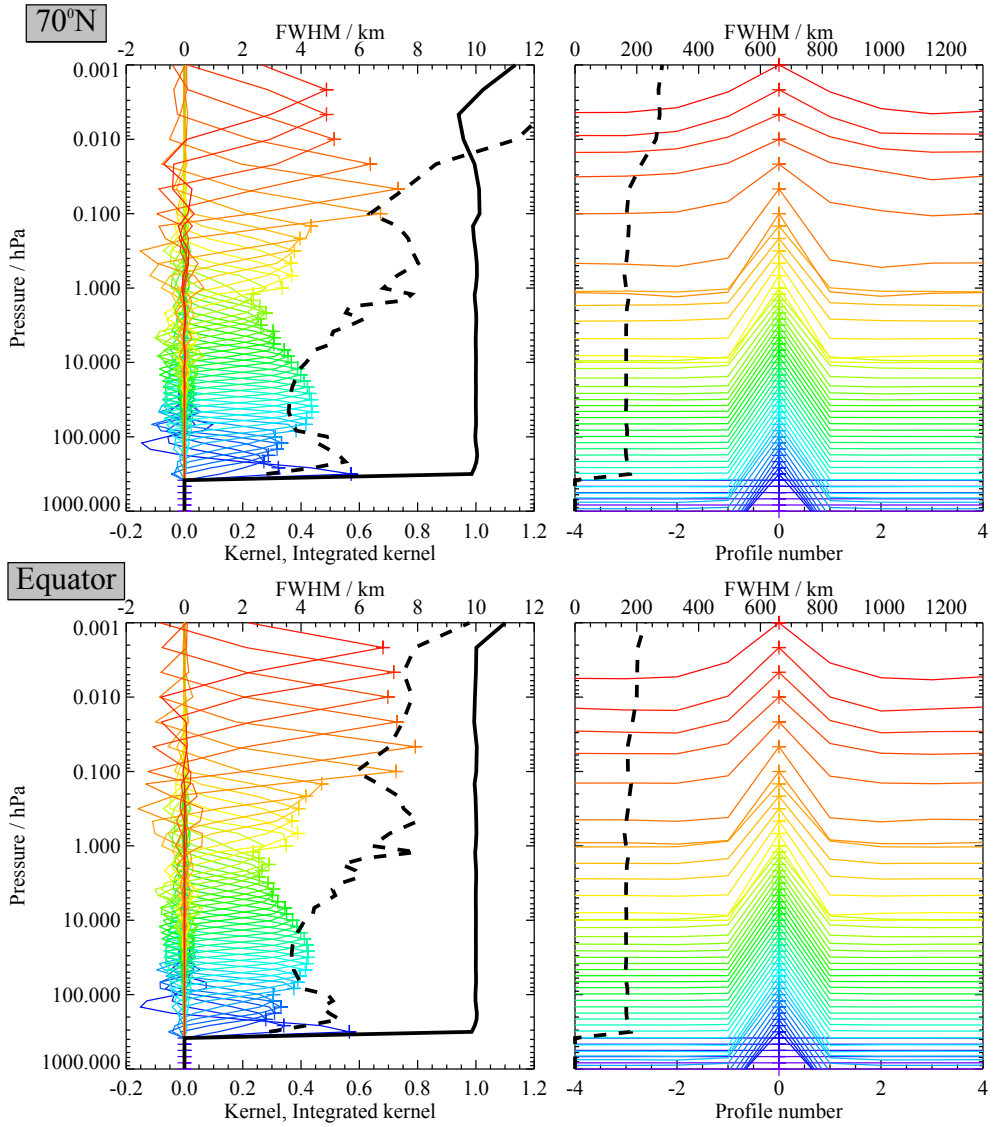

Figure 3.21.1: Typical two-dimensional (vertical and horizontal along-track) averaging kernels for the MLS v3.3 Temperature data at 70°N (upper) and the equator (lower); variation in the averaging kernels is sufficiently small that these are representative of typical profiles. Colored lines show the averaging kernels as a function of MLS retrieval level, indicating the region of the atmosphere from which information is contributing to the measurements on the individual retrieval surfaces, which are denoted by plus signs in corresponding colors. The dashed black line indicates the resolution, determined from the full width at half maximum (FWHM) of the averaging kernels, approximately scaled into kilometers (top axes). (Left) Vertical averaging kernels (integrated in the horizontal dimension for five along-track profiles) and resolution. The solid black line shows the integrated area under each kernel (horizontally and vertically); values near unity imply that the majority of information for that MLS data point has come from the measurements, whereas lower values imply substantial contributions from a priori information. (Right) Horizontal averaging kernels (integrated in the vertical dimension) and resolution. The horizontal averaging kernels are shown scaled such that a unit averaging kernel amplitude is equivalent to a factor of 10 change in pressure.

Precision

The precision of the MLS v3.3 temperature measurement is summarized in Table 3.21.1. Precision is the random component of measurements which would average down if the measurement were repeated. The retrieval software returns an estimate of precision based upon the propagation of radiometric noise and *a priori* uncertainties through the measurement system. These values, which range from 0.6 K in the lower stratosphere to 2.5 K in the mesosphere, are given, for selected levels, in column 2. Column 3 gives the rms of differences of values from successive orbits (divided by the square-root of two as we are looking at the difference of two noisy signals) for latitudes and seasons where longitudinal variability is small and/or is a function only of local solar time. The smallest values found, which are for high-latitude summer, are taken to be those least impacted by atmospheric variability, and are what is reported in column 3. These values are slightly larger than those estimated by the measurement system in the troposphere and lower stratosphere, and a factor of ∼1.4 larger from the middle stratosphere through the mesosphere.

Accuracy

A substantial study of sources of systematic error in MLS measurements was done as a part of the validation of v2.2, and as the measurement system is substantially unchanged, those results are repeated here. The accuracy of the v2.2 temperature measurements was estimated both by modeling the impact of uncertainties in measurement and retrieval parameters that could lead to systematic errors, and through comparisons with correlative data sets. Column 5 of Table 3.21.1 gives estimates from the propagation of parameter uncertainties, as discussed in Schwartz et al. [2008]. This estimate is broken into two pieces. The first term was modeled as amplifier non-linearity, referred to as "gain compression," and was believed to have a known sign, as gain is known to drop at high background signal levels. Correction of these linearity's was a goal of v3.3, but closer examination of the simple non-linearity model found that it did not close foreword model and measured radiances as expected. It had been hoped that better radiance closure would permit the use of more radiances in the middle of the 118-GHz O_2 band, giving better resolution, precision and accuracy in the upper stratosphere and better accuracy everywhere. This work is still ongoing, and it is hoped that advances will manifest in improvements in a future version.

The second term of column 5 combines 2-σ estimates of other sources of systematic uncertainty, such as spectroscopic parameters, retrieval numerics and pointing, for which the sign of resulting bias is unknown. Gain compression terms range from -1.5 K to $+4.5$ K, and predicted vertical structure is very similar to observed biases relative to correlative data in the troposphere and lower stratosphere. The terms of unknown sign are of ∼2 K magnitude over most of the retrieval range, increasing to 5 K at 261 hPa and to 3 K at 0.001 hPa.

Column 6 contains estimates of bias based upon comparisons with analyses and with other previously-validated satellite-based measurements. In the troposphere and lower stratosphere, the observed biases between MLS and most correlative data sets are consistent to within ∼1.5 K, and have vertical oscillation with an amplitude of 2 – 3 K and a vertical frequency of about 1.5 cycles per decade of pressure. A global average of correlative measurements is shown in Figure 3.21.2.

Data screening

Pressure range: 261 – 0.001 hPa

Values outside this range are not recommended for scientific use.

Estimated precision: Only use values for which the estimated precision is a positive number.

Values where the *a priori* information has a strong influence are flagged with negative precision, and should not be used in scientific analyses (see Section 1.5).

Status flag: Only use profiles for which the 'Status' field is an even number.

Odd values of `Status` indicate that the profile should not be used in scientific studies. See Section 1.6 for more information on the interpretation of the `Status` field.

Cloud consideration: Observe the higher order bits for the `Status` field for cloud issues, described below.

As an additional screen, the fifth-least-significant bit of `Status` (the "low cloud" bit) is used to flag profiles that may be significantly impacted by clouds. At pressures of 147 hPa and lower (higher in the atmosphere), the cloud bits may generally be ignored. In the troposphere an attempt has been made to screen out radiances that have been influence by clouds, but some cloud-induced negative biases in retrieved temperature of up to 10 K are still evident, particularly in the tropics. The "low-cloud" `Status` bits from the two profiles which follow a given profile have been found to provide significantly better screening of cloud-induced temperature retrieval outliers than do the profile's own `Status` bits. Temperatures in the tropopause (261 hPa – 178 hPa) should be rejected as possibly influenced by cloud if the "low-cloud" Status bit is set in either of the two profiles following the profile in question. The screening method flags 16% of tropical and 5% of global profiles as cloudy and captures 86% of the tropical 261 hPa values for which the difference between MLS T and its a priori is more than -4.5 K ($\sim 2\sigma$) below the mean of the difference.

Quality field: Only profiles whose 'Quality' field is greater than 0.65 should be used.

The `Quality` diagnostic in v3.3 is has fewer low values that did v2.2, reflecting better closure of the radiances used in the temperature retrieval. This threshold typically excludes 1% of profiles.

Convergence field: Only profiles whose 'Convergence' field is less than 1.2 should be used.

The `Convergence` diagnostic has far fewer high values in v3.3 than it had in v2.2, as there are far fewer poorly-converged "chunks" in the new version. Use of this threshold typically discards 0.1% of profiles, compared to 2% or profiles flagged in v2.2.

Artifacts

MLS temperature has persistent, vertically oscillating biases, in the troposphere and stratosphere, which are believed to be due to shortcomings in the instrument forward model and are an area of continued research. The impact of clouds is generally limited to tropospheric levels in the tropics, and to a lesser extent, mid-latitudes. The greatest impacts of clouds are ~ -10 K, at 261 hPa, while impacts are negligible at 100 hPa and smaller pressures. Flagging of clouds is discussed above. Biases of >1 K that were seen in v2.2, particularly in the troposphere, at the boundaries of the nominally-10-profile "chunks" in which the retrieval is processed have been greatly reduced in v3.3. Unusually short chunks often occur at the beginnings and ends of days and these may contain spurious values. Further discussion of artifacts may be found in Schwartz et al. [2008].

Review of comparisons with other datasets

Schwartz et al. [2008] describes detailed comparisons of MLS v2.2 temperature with products from the Goddard Earth Observing System, version 5 [Reinecker et al., 2007] (GEOS-5), the European Center for Medium-Range Weather Forecast [e.g., Simmons et al., 2005] (ECMWF), the CHAllenging Minisatellite Payload (CHAMP) [Wickert et al., 2001], the combined Atmospheric Infrared Sounder / Advanced Microwave Sounding Unit (AIRS/AMSU), the Sounding of the Atmosphere using Broadband Radiometry (SABER) [Mlynczak and Russell, 1995], the Halogen Occultation Experiment [Hervig et al., 1996]

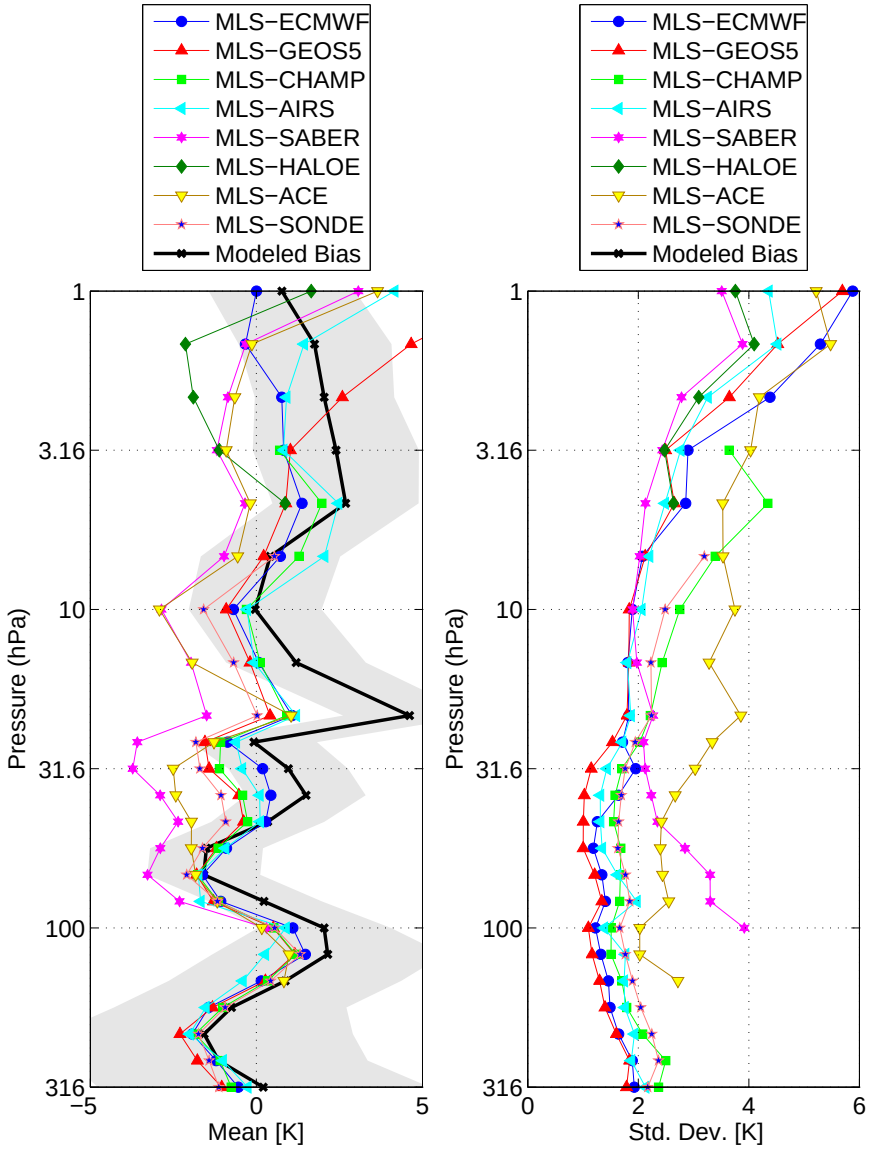

Figure 3.21.2: The left panel shows globally-averaged mean differences between MLS temperature and eight correlative data sets. Criteria for coincidences are described in detain in Schwartz et al. [2008]. The right panel shows the global standard deviations about the means.

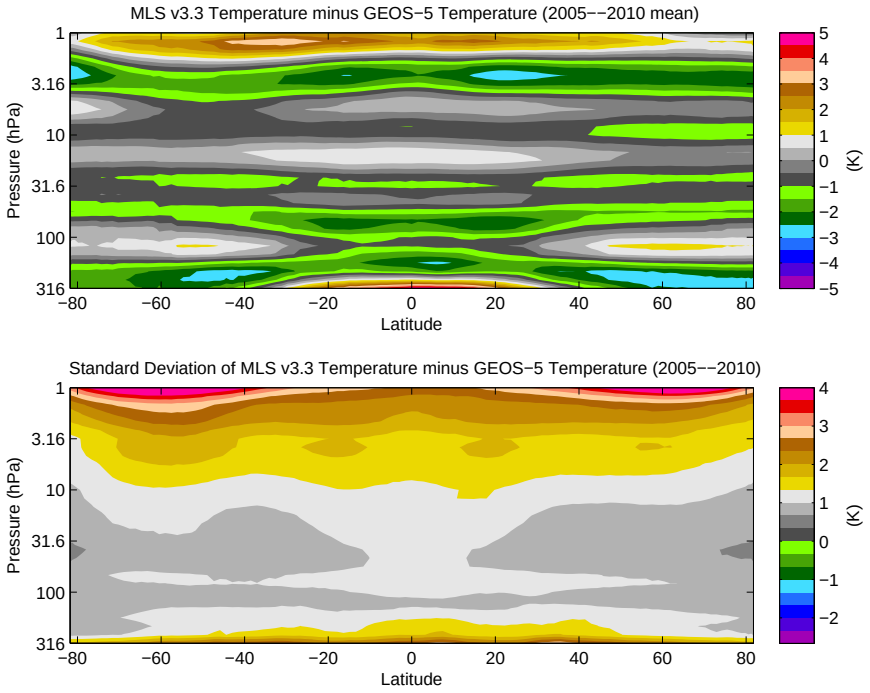

Figure 3.21.3: Zonal mean of the difference between MLS v3.3 temperature and GEOS-5.2 temperature (upper), and variability about that mean (lower), averaged for 2005–2010.

(HALOE) and the Atmospheric Chemistry Experiment [Bernath et al., 2004] (ACE), as well as to radiosondes from the global network. From 261 hPa to ∼10 hPa there is generally agreement to ∼1 K between the assimilations (ECMWF and GEOS-5) and AIRS, radiosondes and CHAMP, with SABER and ACE having generally warm biases of ∼2 K relative to this group. Figure 3.21.2 shows the global mean biases in the left panel and the 1 σ scatter about the mean in the right panel for these eight comparisons. Between 1 hPa and 0.001 hPa, MLS has biases with respect to SABER of +1 K to −5 K between 1 hPa and 0.1 hPa, of 0 K to −3 K between 0.1 K and 0.01 K and increasing in magnitude to −10 K at 0.001 hPa. Estimates of systematic error in the MLS temperature are shown in black, with 2-σ uncertainty shown with gray shading. The black line is the modeled contribution of "gain compression," which was hoped would explain much of the vertical structure of MLS biases in the upper troposphere and lower stratosphere. As discussed above, the gain-compression model used in this study does not adequately close the retrieval's radiance residuals, so further study is needed to understand the forward-model inadequacies.

Figure 3.21.3 shows zonal mean temperature and its variability averaged over 93 days processed with v2.2. Persistent vertical structure in the troposphere and lower stratosphere is evident, with the oscillations somewhat stronger at the equator and poles than at mid-latitudes. In the upper stratosphere, MLS has a general warm bias relative to GEOS-5 at mid and high latitude that increases to more than 10 K in the poles at 1 hPa. The bias at 1 hPa is much smaller in polar summer, but persists in polar winter.

Desired improvements

Improvement of the forward model, perhaps through inclusion of some combination of amplifier nonlinearity or filter shifts to better-closed radiance residuals, would permit the concurrent use of all of the 118-GHz and 239-GHz O_2 bands, and improve accuracy throughout the profile and precision and resolution in the stratosphere.

Table 3.21.1: Summary of MLS Temperature product

Pressure	Precision[a] / K	Observed Scatter[b] / K	Resolution V × H / km	Modeled Bias uncertainty / K	Observed Bias uncertainty / K	Comments
<0.001 hPa	—	—	—	—	—	Unsuitable for scientif c use
0.001 hPa	±2.5	±3.5	10–13 × 220	+2 ± 3	−9	
0.01 hPa	±2.2	±3	8–12 × 185	+2 ± 3	−2 to 0	
0.1 hPa	±2	±2.3	6 × 170	+2 ± 2	−8 to 0	
0.316 hPa	±1	±1.5	7.5 × 165	+3 ± 2	−7 to −4	
1 hPa	±1	±1.4	7.0 × 165	+1 ± 2	0 to +5	
3.16 hPa	±0.8	±1	5.5 × 165	+2 ± 2	+1	
10 hPa	±0.6	±1	4.3 × 165	0 ± 2	−1 to 0	
14.7 hPa	±0.6	±1	3.9 × 165	+4 ± 2	0 to +1	
31.6 hPa	±0.6	±1	3.6 × 165	+1 ± 2	−2 to 0	
56.2 hPa	±0.8	±0.8	3.8 × 165	−1 ± 2	−2 to 0	
100 hPa	±0.8	±0.8	5.0 × 165	+2 ± 2	0 to +1	
215 hPa	±1	±1	5.0 × 170	−1.5 ± 4	−2.5 to −1.5	
261 hPa	±1	±1	5.0 × 170	0 ± 5	−2 to 0	
1000 – 316 hPa	—	—	—	—	—	Unsuitable for scientif c use

[a]Precision on individual prof les

[b]Precision inferred from differences of individual prof les from successive orbits (v2.2 results shown)

Bibliography

B. Barret, P. Ricaud, M. L. Santee, J. L. Attié, J. Urban, E. LeFlochmoën, G. Berthet, D. Murtagh, P. Eriksson A. Jones, J. de La Noë, L. Froidevaux, N. J. Livesey, J. W. Waters, and M. J. Filipiak. Intercomparison of trace gas prof les form the Odin/SMR and Aura/MLS limb sounders. *J. Geophys. Res.*, 111:D21302, doi:10.1029/2006JD007305, 2006.

P. F. Bernath et al. Atmospheric chemistry experiment (ACE): mission overview. *Proceedings of SPIE*, 5542:146–156, 2004.

G. Berthet, P. Ricaud, F. Lefèvre, E. Le Flochmoën, J. Urban, B. Barret, N. Lautié, E. Dupuy, De La Noë, and D. Murtagh. Nighttime chlorine monoxide observations by the Odin satellite and implications for the ClO/Cl_2O_2 equillibrium. *Geophys. Res. Lett.*, 32:L11812, doi:10.1029/2005GL022649, 2005.

R. E. Cof eld and P. C. Stek. EOS Microwave Limb Sounder GHz optics design and f eld-of-view calibration. *IEEE Trans. Geosci. Remote Sens.*, 44(5):1166–1181, 2006.

C. Craig, K. Stone, D. Cuddy, S. Lewicki, P. Veefkind, P. Leonard, A. Fleig, and P. Wagner. HDF-EOS Aura f le format guidelines. Technical report, National Center For Atmospheric Research, 2003.

D. T. Cuddy, M. Echeverri, P. A. Wagner, A. Hanzel, and R. A. Fuller. EOS MLS science data processing system: A description of architecture and capabilities. *IEEE Trans. Geosci. Remote Sens.*, 44(5):1192–1198, 2006.

M. J. Filipiak, N. J. Livesey, and W. G. Read. Precision estimates for the geophysical parameters measured by EOS MLS. Technical report, University of Edinburgh, Department of Meteorology, 2004.

L. Froidevaux, Y. B. Jiang, A. Lambert, N. J. Livesey, W. G. Read, J. W. Waters, E. V. Browell, J. W. Hair, M. A. Avery, T. J. McGee, L. W. Tiwgg, G. K. Sumnicht, K. W. Jucks, J. J. Margitan, B. Sen, R. A. Stachnik, G. C. Toon, P. F. Bernath, C. D. Boone, K. A. Walker, M. J. Filipiak, R. S. Harwood, R. A. Fuller, G. L. Manney, M. J. Schwartz, W. H. Daffer, B. J. Drouin, R. E. Cof eld, D. T. Cuddy, R. F. Jarnot, B. W. Knosp, V. S. Perun, W. V. Snyder, P. C. Stek, R. P. Thurstans, and P. A. Wagner. Validation of Aura Microwave Limb Sounder stratospheric and mesospheric ozone measurements. *J. Geophys. Res.*, 113: D15S20, doi:10.1029/2007JD008771, 2008a.

L. Froidevaux, Y. B. Jiang, A. Lambert, N. J. Livesey, W. G. Read, J. W. Waters, R. A. Fuller, T. P. Marcy, P. J. Popp, R. S. Gao, D. W. Fahey, K. W. Jucks, R. A. Stachnik, G. C. Toon, L. E. Christensen, C. R. Webster, P. F. Bernath, C. D. Boone, K. A. Walker, H. C. Pumphrey, R. S. Harwood, G. L. Manney, M. J. Schwartz, W. H. Daffer, B. J. Drouin, R. E. Cof eld, D. T. Cuddy, R. F. Jarnot, B. W. Knosp, V. S. Perun, W. V. Snyder, P. C. Stek, R. P. Thurstans, and P. A. Wagner. Validation of Aura Microwave Limb Sounder HCl measurements. *J. Geophys. Res.*, 113(D15):D15S25, doi:10.1029/2007JD009025, 2008b.

M. E. Hervig, J. M. Russell III, L. L. Gordley, S. R. Drayson, K. Stone, R. E. Thompson, M. E. Gelman, I. S. McDermid, A. Hauchecorne, P. Keckhut, et al. Validation of temperature measurements from the Halogen Occultation Experiment. *J. Geophys. Res.*, 101(10):10 277–10,286, 1996.

R. F. Jarnot, V. S. Perun, and M. J. Schwartz. Radiometric and spectral performance and calibration of the GHz bands of EOS MLS. *IEEE Trans. Geosci. Remote Sens.*, 44(5):1131–1143, 2006.

Y. B. Jiang, L. Froidevaux, A. Lambert, N. J. Livesey, W. G. Read, J. W. Waters, B. Bojkov, T. Leblanc, I. S. McDermid, S. Godin-Beekmann, M. J. Filipiak, R. S. Harwood, R. A. Fuller, W. H. Daffer, B. J. Drouin, R. E. Cofeld, D. T. Cuddy, R. F. Jarnot, B. W. Knosp, V. S. Perun, M. J. Schwartz, W. V. Snyder, P. C. Stek, R. P. Thurstans, P. A. Wagner, M. Allaart, S. B. Andersen, G. Bodeker, B. Calpini, H. Claude, G. Coetzee, J. Davies, H. De Backer, H. Dier, M. Fujiwara, B. Johnson, H. Kelder, N. P. Leme, G. Koenig-Langlo, E. Kyro, G. Laneve, L. S. Fook, J. Merrill, G. Morris, M. Newchurch, S. Oltmans, M. C. Parrondos, F. Posny, F. Schmidlin, P. Skrivankova, R. Stubi, D. Tarasick, A. Thompson, V. Thouret, P. Viatte, H. Vomel, P. von Der Gathen, M. Yela, and G. Zablocki. Validation of the Aura Microwave Limb Sounder ozone by ozonesonde and lidar measurements. *J. Geophys. Res.*, 112:D24S34, doi:10.1029/2007JD008776, 2007.

L. J. Kovalenko, N. J. Livesey, R. J. Salawitch, C. Camy-Peyret M. Dorf, D. J. Drouin, F. Goutail, K. Pfeilsticker, J.-P. Pommereau, W. G. Read, R. Stachnick, and J. W. Waters. Validation of Aura Microwave Limb Sounder BrO observations in the stratosphere. *J. Geophys. Res.*, 112:D24S41, doi:10.1029/2007JD008817, 2007.

A. Lambert, W. G. Read, N. J. Livesey, M. L. Santee, G. L. Manney, L. Froidevaux, D. L. Wu, M. J. Schwartz, H. C. Pumphrey, C. Jimenez, G. E. Nedoluha, R. E. Cofeld, D. T. Cuddy, W. H. Daffer, B. J. Drouin, R. A. Fuller, R. F. Jarnot, B. W. Knosp, H. M. Pickett, V. S. Perun, W. V. Snyder, P. C. Stek, R. P. Thurstans, P. A. Wagner, J. W. Waters, K. W. Jucks, G. C. Toon, R. A. Stachnik, P. F. Bernath, C. D. Boone, K. A. Walker, J. Urban, D. Murtagh, J. W. Elkins, and E. Atlas. Validation of the Aura Microwave Limb Sounder stratospheric water vapor and nitrous oxide measurements. *J. Geophys. Res.*, 112(D24): D24S36, doi:10.1029/2007JD008724, 2007.

N. J. Livesey and W. V. Snyder. EOS MLS retrieval processes algorithm theoretical basis. Technical report, Jet Propulsion Laboratory, 2004. D-16159, available on the MLS web site `http://mls.jpl.nasa.gov`.

N. J. Livesey, J. W. Waters, R. Khosravi, G. P. Brasseur, G. S. Tyndall, and W. G. Read. Stratospheric CH_3CN from the UARS Microwave Limb Sounder. *Geophys. Res. Lett.*, 28(5):779–782, 2001.

N. J. Livesey, W. G. Read, M. J. Filipiak, L. Froidevaux, R. S. Harwood, J. H. Jiang, C. Jiminez, H. M. Pickett, H. C. Pumphrey, M. L. Santee, M. J. Schwartz, J. W. Waters, and D. L. Wu. EOS MLS version 1.5 Level 2 data quality and description document. Technical report, Jet Propulsion Laboratory, 2005. D-32381.

N. J. Livesey, W. Van Snyder, W. G. Read, and P. A. Wagner. Retrieval algorithms for the EOS Microwave Limb Sounder (MLS). *IEEE Trans. Geosci. Remote Sens.*, 44(5):1144–1155, 2006.

N. J. Livesey, M. J. Filipiak, L. Froidevaux, W. G. Read, A. Lambert, M. L. Santee, J. H. Jiang, J. W. Waters, R. E. Cofeld, D. T. Cuddy, W. H. Daffer, B. J. Drouin, R. A. Fuller, R. F. Jarnot, Y. B. Jiang, B. W. Knosp, Q. B. Li, V. S. Perun, M. J. Schwartz, W. V. Snyder, P. C. Stek, R. P. Thurstans, P. A. Wagner, H. C. Pumphrey, M. Avery, E. V. Browell, J.-P. Cammas, L. E. Christensen, D. P. Edwards, L. K. Emmons, R.-S. Gao, H.-J. Jost, M. Loewenstein, J. D. Lopez, P. Nedelec, G. B. Osterman, G. W. Sachse, and C. R. Webster. Validation of Aura Microwave Limb Sounder O_3 and CO observations in the upper troposphere and lower stratosphere. *J. Geophys. Res.*, 113:D15S02, doi:10.1029/2007JD008805, 2008.

M. Mlynczak and J. M. Russell, III. An overview of the SABER experiment for the TIMED mission. *NASA Langley Research Center, Optical Remote Sensing of the Atmosphere*, 2, 1995.

D. Murtagh, U. Frisk, F. Merino, M. Ridal, A. Jonsson, J. Stegman, G. Witt, P. Eriksson, C. Jimenez, G. Mégie, J. de La Noëë, P. Ricaud, P. Baron, J.-R. Pardo, A. Hauchecorne, E. J. Llewellyn, D. A. Degenstein, R. L. Gattinger, N. D. Lloyd, W. F. J. Evans, I. C. McDade, C. Haley, C. Sioris, C. von Savigny, B. H. Solheim, J. C. McConnell, K. Strong, E. H. Richardson, G. W. Leppelmeier, E. Kyrölä, H. Auvinen, and L. Oikarinen. An overview of the Odin atmospheric mission. *Can. J. Phys.*, 80:309–319, 2002.

J. R. Pardo, E. Serabyn, and J. Cernicharo. Submillimeter atmospheric transmission measurements on Mauna Kea during extremely dry El Niño conditions: Implications for broadband opacity contributions. *J. Quant. Spectrosc. Radiat. Transfer*, 68:419–433, 2001.

H. M. Pickett. Microwave Limb Sounder THz Module on Aura. *IEEE Trans. Geosci. Remote Sens.*, 44(5): 1122–1130, 2006.

H. M. Pickett, B. J. Drouin, T. Canty, L. J. Kovalenko, R. J. Salawitch, N. J. Livesey, W. G. Read, J. W. Waters, K. W. Jucks, and W. A. Traub. Validation of Aura MLS HO_x measurements with remote-sensing balloon instruments. *Geophys. Res. Lett.*, 33(1):L01808, doi:10.1029/2005GL024442, 2006a.

H. M. Pickett, W. G. Read, K. K. Lee, and Y. L. Yung. Observation of night OH in the mesosphere. *Geophys. Res. Lett.*, page L19808 doi:10.1029/2006GL026910, 2006b.

H. M. Pickett, B. J. Drouin, T. Canty, R. J. Salawitch, R. A. Fuller, V. S. Perun, N. J. Livesey, J. W. Waters, R. A. Stachnik, S. P. Sander, W. A. Traub, K. W. Jucks, and K. Minschwaner. Validation of Aura Microwave Limb Sounder OH and HO_2 measurements. *J. Geophys. Res.*, 113(D16):D16S30, doi:10.1029/2007JD008775, 2008.

H. C. Pumphrey, M. J. Filipiak, N. J. Livesey, M. J. Schwartz, C. Boone, K. A. Walker, P. Bernath, P. Ricaud, B. Barret, C. Clerbaux, R. F. Jarnot, G. L. Manney, and J. W. Waters. Validation of middle-atmosphere carbon monoxide retrievals from the Microwave Limb Sounder on Aura. *J. Geophys. Res.*, 112:D24S38, doi:10.1029/2007JD008723, 2007.

H. C. Pumphrey, R. E. Cof eld, M. J. Filipiak, and N. J. Livesey. An all-sky survey at 230 GHz by MLS on Aura. *Adv. Space Res.*, 43:342–348, 2009.

Hugh C. Pumphrey, Carlos J. Jimenez, and Joe W. Waters. Measurement of HCN in the middle atmosphere by EOS MLS. *Geophys. Res. Lett.*, 33(8):L08804, doi:10.1029/2005GL025656, 2006.

W. G. Read, Z. Shippony, and W. V. Snyder. Microwave Limb Sounder forward model algorithm theoretical basis document. Technical report, Jet Propulsion Laboratory, 2004. JPL D-18130.

W. G. Read, Z. Shippony, M. J. Schwartz, N. J. Livesey, and W. V. Snyder. The clear-sky unpolarized forward model for the EOS Microwave Limb Sounder (MLS). *IEEE Trans. Geosci. Remote Sens.*, 44(5): 1367–1379, 2006.

W. G. Read, A. Lambert, J. Bacmeister, R. E. Cof eld, D. T. Cuddy, W. H. Daffer, B. J. Drouin, E. Fetzer, L. Froidevaux, R. Fuller, R. Herman, R. F. Jarnot, J. H. Jiang, Y. B. Jiang, K. Kelly, B. W. Knosp, L. J. Kovalenko, N. J. Livesey, H.-C. Liu, G. L. Manney, D. Miller, B. J. Mills, H. M. Pickett, H. C. Pumphrey, K. H. Rosenlof, X. Sabounchi, M. L. Santee, M. J. Schwartz, W. V. Snyder, P. C. Stek, H. Su, L. L. Takacs, R. P. Thurstans, H. Vömel, P. A. Wagner, J. W. Waters, C. R. Webster, E. M. Weinstock, and D. L. Wu. EOS Aura Microwave Limb Sounder upper tropospheric and lower stratospheric humidity validation. *J. Geophys. Res.*, 112:D24S35, doi:10.1029/2007JD008752, 2007.

M. M. Reinecker, M. J. Suarez, R. Todling, J. Bacmeister, L. Takacs, H.-C. Liu, W. Gu, M. Sienkiewicz, R. D. Koster, R. Gelaro, and I. Stajner. The GEOS-5 data assimilation system: A documentation of GEOS-5.0. Technical report, NASA, 2007. TM-104606, Tehcnical report series on Global Modeling and Data Assimilation.

C. D. Rodgers. *Inverse Methods for Atmospheric Science, Theory and Practice*. World Scientif c, 2000.

C. D. Rodgers. Retrieval of atmospheric temperature and composition from remote measurements of thermal radiation. *Rev. Geophys.*, 14(4):609–624, 1976.

C. D. Rodgers and B. J. Connor. Intercomparison of remote sounding instruments. *J. Geophys. Res.*, 108 (D3):4116, doi:10.1029/2002JD002299, 2003.

M. L. Santee, A. Lambert, W. G. Read, N. J. Livesey, R. E. Cof eld, D. T. Cuddy, W. H. Daffer, B. J. Drouin, L. Froidevaux, R. A. Fuller, R. F. Jarnot, B. W. Knosp, G. L. Manney, V. S. Perun, W. V. Snyder, P. C. Stek, R. P. Thurstans, P. A. Wagner, J. W. Waters, G. Muscari, R. L. de Zafra, J. E. Dibb, D. W. Fahey, P. J. Popp, T. P. Marcy, K. W. Jucks, G. C. Toon, R. A. Stachnik, P. F. Bernath, C. D. Boone, K. A. Walker, J. Urban, and D. Murtagh. Validation of the Aura Microwave Limb Sounder HNO_3 measurements. *J. Geophys. Res.*, 112:D24S40, doi:10.1029/2007JD008721, 2007.

M. L. Santee, A. Lambert, W. G. Read, N. J. Livesey, G. L. Manney, R. E. Cof eld, D. T. Cuddy, W. H. Daffer, B. J. Drouin, L. Froidevaux, R. A. Fuller, R. F. Jarnot, B. W. Knosp, V. S. Perun, W. V. Snyder, P. C. Stek, R. P. Thurstans, P. A. Wagner, J. W. Waters, B. Connor, J. Urban, D. Murtagh, P. Ricaud, B. Barret, A. Kleinboehl, J. Kuttippurath, H. Kuellmann, M. von Hobe, G. C. Toon, and R. A. Stachnik. Validation of the Aura Microwave Limb Sounder ClO measurements. *J. Geophys. Res.*, 113:D15S22, doi:10.1029/2007JD008762, 2008.

M. J. Schwartz, W. V. Synder, and W. G. Read. MLS mesosphere-specif c forward model algorithm theoretical basis document. Technical report, Jet Propulsion Laboratory, 2004. JPL D-28534.

M. J. Schwartz, W. G. Read, and W. V. Snyder. Polarized radiative transfer for Zeeman-split oxygen lines in the EOS MLS forward model. *IEEE Trans. Geosci. Remote Sens.*, 44(5):1182–1190, 2006.

M. J. Schwartz, A. Lambert, G. L. Manney, W. G. Read, N. J. Livesey, L. Froidevaux, C. O. Ao, P. F. Bernath, C. D. Boone, R. E. Cof eld, W. H. Daffer, B. J. Drouin, E. J. Fetzer, R. A. Fuller, R. F. Jarnot, J. H. Jiang, Y. B. Jiang, B. W. Knosp, K. Krüger, J.-L. F. Li, M. G. Mlynczak, J. M. Russell, III, M. L. Santee, W. V. Snyder, P. C. Stek, R. P. Thurstans, A. M. Tompkins, P. A. Wagner, K. A. Walker, J. W. Waters, and D. L. Wu. Validation of the Aura Microwave Limb Sounder temperature and geopotential height measurements. *J. Geophys. Res.*, 113:D15S11, doi:10.1029/2007JD008783, 2008.

A. Simmons, M. Hortal, G. Kelly, A. McNally, A. Untch, and S. Uppala. ECMWF analyses and forecasts of stratospheric winter polar vortex breakup: September 2002 in the southern hemisphere and related events. *J. Atmos. Sci.*, 62(3):668–689, 2005.

J. Urban, N. Lautié, E. Le Flochmoën, C. Jiméenz, P. Eriksson, J. de La Noë, E. Dupuy, M. Ekström, L. El Amraoui, U. Frisk, D. Murtagh, M. Olberg, and P. Ricaud. Odin/SMR limb observations of statospheric trace gases: Level 2 processing of ClO, N_2O, HNO_3 and O_3. *J. Geophys. Res.*, 110:D14307, doi:10.1029/2004JD005741, 2005.

J. Urban et al. Odin/SMR limb observations of trace gases in the polar lower stratosphere during 2004–2005. In H. Lacoste, editor, *Proceedings of the ESA First Atmospheric Science Conference, 8–12 May 2006, Frascati, Italy*. Eur. Space Agency Spec. Publ., ESA-SP-628, 2006.

T. von Clarmann, N. Glatthor, U. Grabowski, M. Höpfner, S. Kellmann, A. Linden, G. Mengistu Tsidu, M. Milz, T. Steck, G. P. Stiller, H. Fischer, and B. Funke. Global stratospheric HOCl distributions retrieved from infrared limb emission spectra recorded by the Michelson Interferometer for Passive Atmospheric Sounding (MIPAS). *J. Geophys. Res.*, 111:D05311, doi:10.1029/2005JD005939, 2006.

S. Wang, H. M. Pickett, T. J. Pongetti, R. Cheung, Y. L. Yung, C. Shim, Q. Li, T. Canty, R. J. Salawitch, K. W. Jucks, B. Drouin, and S. P. Sander. Validation of Aura Microwave Limb Sounder OH measurements with Fourier Transform Ultra-Violet Spectrometer total OH column measurements at Table Mountain, California. *J. Geophys. Res.*, 113:D22301, doi:10.1029/2008JD009883, 2008.

J. W. Waters, W. G. Read, L. Froidevaux, R. F. Jarnot, R. E. Cof eld, D. A. Flower, G. K. Lau, H. M. Pickett, M. L. Santee, D. L. Wu, M. A. Boyles, J. R. Burke, R. R. Lay, M. S. Loo, N. J. Livesey, T. A. Lungu, G. L. Manney, L. L. Nakamura, V. S. Perun, B. P. Ridenoure, Z. Shippony, P. H. Siegel, and R. P. Thurstans. The UARS and EOS Microwave Limb Sounder (MLS) experiments. *J. Atmos. Sci.*, 56:194–217, 1999.

J. W. Waters, L. Froidevaux, R. F. Jarnot, W. G. Read, H. M. Pickett, R. S. Harwood, R. E. Cof eld, M. J. Filipiak, D. A. Flower, N. J. Livesey, G. L. Manney, H. C. Pumphrey, M. L. Santee, P. H. Siegel, and D. L. Wu. An overview of the EOS MLS experiment. Technical report, Jet Propulsion Laboratory, 2004. D-15745.

J. W. Waters, L. Froidevaux, R. S. Harwood, R. F. Jarnot, H. M. Pickett, W. G. Read, P. H. Siegel, R. E. Cof eld, M. J. Filipiak, D. A. Flower, J. R. Holden, G. K. Lau, N. J. Livesey, G. L. Manney, H. C. Pumphrey, M. L. Santee, D. L. Wu, D. T. Cuddy, R. R. Lay, M. S. Loo, V. S. Perun., M. J. Schwartz, P. C. Stek, R. P. Thurstans, K. M. Chandra, M. C. Chavez, G. Chen, M.. A. Boyles, B. V. Chudasama, R. Dodge, R. A. Fuller, M. A. Girard, J. H. Jiang, Y. Jiang, B. W. Knosp, R. C. LaBelle, J. C. Lam, K.. A. Lee, D. Miller, J. E. Oswald, N. C. Patel, D. M. Pukala, O. Quintero, D. M. Scaff, W. V. Snyder, M. C. Tope, P. A. Wagner, and M. J. Walch. The Earth Observing System Microwave Limb Sounder (EOS MLS) on the Aura satellite. *IEEE Trans. Geosci. Remote Sens.*, 44(5):1075–1092, 2006.

J. Wickert, C. Reigber, G. Beyerle, R. Konig, C. Marquardt, T. Schmidt, L. Grunwaldt, R. Galas, T.K. Meehan, W.G. Melbourne, et al. Atmosphere sounding by GPS radio occultation: First results from CHAMP. *Geophys. Res. Lett.*, 28(17):3263–3266, 2001.

D. L. Wu and J. H. Jiang. EOS MLS algorithm theoretical basis for cloud measurements. Technical report, Jet Propulsion Laboratory, 2004. JPL D-19299.

D. L. Wu, J. H. Jiang, and C. P. Davis. Aura MLS cloud ice measurements and cloudy-sky radiative transfer model. *IEEE Trans. Geosci. Remote Sens.*, 44(5):1156–1165, 2006.

D. L. Wu, J. H. Jiang, W. G. Read, R. T. Austin, C. P. David, A. Lambert, G. L. Stephens, D. G. Vane, and J. W. Waters. Validation of Aura MLS cloud Ice Water Content (IWC) measurements. *J. Geophys. Res.*, 113:D15S10, doi:10.1029/2007LD008931, 2008.

D. L. Wu, R. Austin, S. Durden, A. Heymsf eld, J. H. Jiang, A. Lambert, J. Li, N. J. Livesey, G. McFarquhar, J. Pittman, G. Stephens, S. Tanelli, D. Vane, and D. Waliser. Comparison of global cloud ice from MLS, CloudSat and correlative data sets. *J. Geophys. Res.*, 113:D00A24 doi:10.1029/2008JD009946, 2009.